

# **Sensory and cognitive factors in multi-digit touch, and its integration with vision**

**Irena Arslanova**

Institute of Cognitive Neuroscience

University College London

Supervisor: Prof. Patrick Haggard

PhD thesis

2021

## Declaration

I, Irena Arslanova, confirm that the work presented in this thesis is my own<sup>1</sup>. Where information has been derived from other sources, I confirm that this has been indicated in the thesis.

Signed,

Irena Arslanova

06/03/2021

---

<sup>1</sup> Experiment reported in chapter 2 of this thesis has already been published as: Arslanova, I., Wang, K., Gomi, H., & Haggard, P. (2021). Somatosensory evoked potentials that index lateral inhibition are modulated according to the mode of perceptual processing: comparing or combining multi-digit tactile motion. *Cognitive Neuroscience*, 1-14.

## Abstract

*It is strange that the tactile sense, which is so infinitely less precious to men than sight, becomes at critical moment our main, if not only, handle to reality.*

– Vladimir Nabokov in *Lolita*

Every tactile sensation – an itch, a kiss, a hug, a pen gripped between fingers, a soft fabric brushing against the skin – is experienced in relation to the body. Normally, they occur somewhere on the body’s surface – they have *spatiality*. This sense of spatiality is what allows us to perceive a partner’s caress in terms of its changing location on the skin, its movement direction, speed, and extent. How this spatiality arises and how it is experienced is a thriving research topic, compelled by growing interest in the nature of tactile experiences from product design to brain-machine interfaces. The present thesis adds to this flourishing area of research by examining the *unified spatial quality* of touch. How does distinct spatial information *converge* from separate areas of the body surface to give rise to our normal unified experience of touch?

After explaining the importance of this question in **Chapter 1**, a novel paradigm to tackle this problem will be presented, whereby participants are asked to estimate the *average* direction of two stimuli that are simultaneously moved across two different fingerpads. This paradigm is a laboratory analogue of the more ecological task of representing the overall movement of an object held between multiple fingers. An EEG study in **Chapter 2** will reveal a brain mechanism that could facilitate such aggregated perception. Next, by characterising participants’ performance not just in terms of error rates, but by considering perceptual sensitivity, bias, precision, and signal weighting, a series of psychophysical experiments will show that this aggregation ability differs for within- and between-hand perception (**Chapter 3**), is independent from somatotopically-defined circuitry (**Chapter 4**) and arises after proprioceptive input about hand posture is accounted for (**Chapter 5**). Finally, inspired by the demand for integrated tactile and visual experience in virtual reality and the potential of tactile interface to aid navigation, **Chapter 6** will examine the contribution of tactile spatiality on visual spatial experience.

Ultimately, the present thesis will reveal sensory factors that limit precise representation of concurrently occurring dynamic tactile events. It will point to cognitive strategies the brain may employ to overcome those limitations to tactually perceive coherent objects. As such, this thesis advances somatosensory research beyond merely examining the selectivity to and discrimination between experienced tactile inputs, to considering the unified experience of touch despite distinct stimulus elements. The findings also have practical implications for the design of functional tactile interfaces.

## Impact Statement

We are well aware of the affective power of touch. The reassuring feeling when a close friend squeezes our hand. The instant alertness when a stranger accidentally touches us on a public transport. There is a good reason why museums have signs restraining people from touching the exhibits – it is often not enough for us to simply look; we also want to touch. Product designers have long understood the power of tactile experience. And creators of immersive virtual reality are looking for ways to incorporate tactile feedback.

However, what often gets overlooked, is that affective qualities of touch occur in relation to our body, they have *spatiality*. They normally occur at some location on the body surface. When something moves across our skin, like a partner's stroke, we experience it in terms of its changing location on the skin, its movement direction, speed, and extent. Restoring tactile spatiality is an ongoing challenge for brain-machine interfaces that could transform life for patients, who have lost limbs or suffered paralysis. Tactile interfaces are being designed that could produce spatial percepts from the skin in absence or as a supplement to vision. Progress on these endeavors needs a full characterisation of how spatiality of touched objects comes about. Because most tactile events occur by contacting multiple points along the skin surface (i.e., when we touch objects with multiple fingers), the main aim of this thesis is to examine how multiple spatiotemporal tactile inputs are processed and integrated to produce a coherent tactile spatial experience.

## Acknowledgements

I am immensely grateful to my supervisor, Patrick Haggard, who not only provided invaluable guidance for my PhD, but more importantly, instilled me with confidence and inspiration to pursue research and contribute to shared knowledge. Being exposed to so many diverse projects and ideas in the Action and Body lab has been the most exciting time of my life. I am truly grateful to all my colleagues for sustaining this stimulating environment and always providing constructive and helpful feedback, even when my work was not even close to their alley. I am especially grateful to students who assisted me with some of my projects: Keying Wang (Chapter 2) and Gertheeka Sritharan (Chapter 5). I am grateful to Shinya Takamuku, who found a way to advance my PhD, when testing was impossible due to the pandemic.

I am extremely thankful to Hiroaki Gomi, who hosted me as a visiting researcher at NTT in Japan. Without his team and support, the experiment in Chapter 6 would not have been possible. Having the opportunity to visit Japan was the most unforgettable experience for both developing my research, but also for meeting new friends. I cannot wait to cross paths again with Jackie and Loïc to have our 3 pm pick-me-up. I also wish to thank Kasia Bronk, who offered me a chance to engage with UCL as a whole and participate in exciting projects to improve PhD training. The final year of PhD is tough for everybody, but I was lucky to meet Silvia and Gulia, and share our pain and relief together. My PhD work would not have been possible without the generous funding from Medical Research Council in UK and from NTT in Japan.

If it wasn't for my dear friend Alex, I might not have had the courage to write my PhD proposal. Without the unceasing support of my parents, I wouldn't have kept my sanity. I am grateful for all the times they pretended to be interested in my experiments as I struggled to translate the scientific terms into Russian. PhD should not be an isolating and lonely endeavor. I realised how important it is to have people in life, who can put work struggles into perspective and bring one back to normality. Michael taught me how to laugh it off and keep going. My high school friends have always been there to offer a non-academic support. I need to thank them individually, because this is how far they will read this thesis: Kadri-Ann, Anne-Mari, Maarja, Deivi, and Inge-Marie – thank you for the endless friendship in its truest form.

# Contents

<b>Chapter 1: From motion at separate fingers to overall object movement .....</b>	<b>11</b>
1.1. <i>Spatiality in touch</i> .....	12
1.1.1. Stimuli to probe the spatiality in touch.....	13
1.1.2. Is the somatosensory system enough to encode the spatiality of tactile motion? .....	15
1.1.3. What can a single tactile sensor do?.....	18
1.1.4. How can information be combined across multiple sensors? .....	20
1.1.5. Skin structures perception .....	22
1.1.6. Gestalt principles operate in touch.....	22
1.1.7. Interim summary .....	22
1.2. <i>Integration between multiple touches</i> .....	23
1.2.1. Importance of processing capacity .....	24
1.2.2. Two stimuli, one hand: Physiological mechanisms of multi-touch integration on one side of the body .....	27
1.2.3. Two stimuli, two hands: Physiological mechanisms of multi-touch integration across two sides of the body .....	30
1.2.4. Beyond S1: Neurons that do not care about touched digits .....	32
1.2.5. Beyond S1: Contribution of proprioceptive information .....	33
1.2.6. Cognitive models of multi-touch integration .....	34
1.2.7. Interim summary .....	36
1.3. <i>Beyond touch: interaction between touch and vision</i> .....	37
1.4. <i>Summary and thesis overview</i> .....	39
<b>Chapter 2: Brain mechanism of multi-touch aggregation .....</b>	<b>41</b>
2.1. <i>Introduction</i> .....	42
2.1.1. Measuring lateral inhibitory process non-invasively in touch .....	44
2.1.2. Experiment 1: Aims and hypothesis.....	45
2.2. <i>Methods</i> .....	46
2.2.1. Participants .....	46
2.2.2. Perceptual multi-touch motion task .....	46
2.2.3. Apparatus and tactile motion stimuli.....	47
2.2.4. Digital nerve stimulation to evoke somatosensory activity.....	48
2.2.5. Electroencephalographic (EEG) recording and pre-processing .....	49
2.2.6. Statistical analysis .....	50
2.3. <i>Results</i> .....	51
2.3.1. Behavioural analysis .....	51
2.3.2. EEG results .....	53
2.3.3. EEG results without low-pass filter to identify earlier components .....	55
2.3.4. Relationship between EEG activity and response accuracy .....	57
2.4. <i>Discussion</i> .....	58
2.4.1. Considerations for the task design .....	58
2.4.2. Control mechanism that enables multi-touch integration .....	60
2.4.3. The control mechanism affects early somatosensory cortex.....	61
2.5. <i>Conclusions</i> .....	63
<b>Chapter 3: Multi-touch aggregation within- and between-hands.....</b>	<b>64</b>
3.1. <i>Introduction</i> .....	65
3.2. <i>Methods</i> .....	66
3.2.1. Participants .....	66
3.2.2. Tactile apparatus and experimental set-up.....	66
3.2.3. Tactile stimuli .....	67
3.2.4. Task design and procedure .....	68
3.2.5. Main measures: sensitivity, bias, precision, and weighting .....	69
3.2.6. Statistical analysis.....	71
3.3. <i>Results</i> .....	72
3.3.1. Analysis of single-finger conditions .....	72
3.3.2. Does perception benefit from averaging component directions? .....	74
3.3.3. Is averaging ability constrained by directional discrepancy? .....	77
3.3.4. Weight assignment across component stimuli during the averaging task. ....	79

3.3.5. Extra: sensory weighting model based on ‘virtual-leading-finger’ (VLF) predicts discrepancy-dependent sensitivity, but not precision .....	79
3.3.6. Extra: can participants perceive discrepancy?.....	83
3.4. Discussion .....	84
3.4.1. Averaging benefitted in a more precise estimate but only when components were delivered bimanually .....	85
3.4.2. VLF-based model accounts for the biases in unimanual inter-digit weights and discrepancy-dependent sensitivity results.....	87
3.5. Conclusions.....	88
<b>Chapter 4: Multi-touch aggregation beyond somatotopy.....</b>	<b>89</b>
4.1. Introduction .....	90
4.2. Methods .....	91
4.2.1. Participants .....	91
4.2.2. Task design.....	91
4.2.3. Main measures and statistical analysis .....	92
4.3. Results.....	93
4.3.1. Analysis of single-finger conditions .....	93
4.3.2. Double-finger conditions: t-tests on slope and intercept values.....	95
4.3.3. Experiment 4: averaging performance was not influenced by finger adjacency.....	96
4.3.4. Experiment 4: discrepancy-dependent effect on averaging regardless of adjacency between component directions .....	97
4.3.5. Experiment 4: biased weighting regardless of adjacency .....	98
4.3.6. Experiment 5: averaging performance was not influenced by bimanual finger homology.....	99
4.3.7. Experiment 5: no discrepancy-dependent effects.....	100
4.4. Discussion .....	101
4.4.1. Precision: bimanual averaging benefit extends to non-homologous fingers .....	102
4.4.2. Sensitivity and weight allocation: strategic weighting during unimanual aggregation to overcome unimanual limitation.....	104
4.5. Conclusions.....	106
<b>Chapter 5: Effect of posture on bimanual multi-touch perception .....</b>	<b>107</b>
5.1. Introduction .....	108
5.1.1. Compulsory remapping of touch into external space .....	108
5.1.2. Evidence against compulsory remapping.....	109
5.1.3. Tactile motion perception as a better test for remapping processes .....	110
5.2. Methods .....	112
5.2.1. Participants .....	112
5.2.2. Task design.....	113
5.2.3. Analysis .....	113
5.3. Results.....	115
5.3.1. Analysis of single-finger conditions: posture elicits a significant attracting effect .....	115
5.3.2. Double vs. mean of single-finger conditions: bias during averaging is equivalent to a linear combination of biased component estimates .....	116
5.3.3. Effect of directional discrepancy on averaging performance, and weight assignment across fingers.....	119
5.4. Discussion .....	121
5.4.1. Remapping coupled with insufficient postural compensation .....	121
5.4.2. Averaging is independent from remapping.....	122
5.4.3. Bias in aggregation arose from components that were less discrepant .....	124
5.5. Conclusion.....	125
<b>Chapter 6: Integrating directional information between touch and vision .....</b>	<b>126</b>
6.1. Introduction .....	127
6.1.1. Encoding translational force.....	127
6.1.2. Experience of heading.....	128
6.1.3. Contribution of tactually acquired input on visual perception.....	129
6.2. Methods .....	131
6.2.1. Participants .....	131
6.2.2. Apparatus and experimental set-up .....	131
6.2.3. Task design.....	133

6.2.4. Behavioral analysis .....	135
6.2.5. Body sway analysis .....	137
<b>6.3. Results .....</b>	<b>141</b>
6.3.1. Can people perceive direction from force and optical flow? .....	141
6.3.2. Is there integration at the level of explicit perception? .....	146
6.3.3. Is there integration at the level of implicit postural response? .....	148
6.3.4. Does extent of body sway contribute to explicit perception? .....	149
<b>6.4. Discussion .....</b>	<b>151</b>
6.4.1. Reliable touch improves explicit perception of 'heading' .....	151
6.4.2. Noisy tactile input interferes with perception of 'heading' .....	153
6.4.3. Implicit postural response mainly arises due to tactile input.....	154
<b>6.5. Conclusion.....</b>	<b>156</b>
<b>Chapter 7: Final discussion .....</b>	<b>158</b>
7.1. <i>Task context shapes somatosensory processing to allow for convergence of inputs for multi-touch perception .....</i>	159
7.2. <i>Multi-touch integration is shaped by cognitive rather than somatotopy-based factors .....</i>	161
7.3. <i>Multi-touch integration occurs on "remapped" component representations.....</i>	165
7.4. <i>Limitations and future directions of the current multi-touch paradigm.....</i>	166
7.5. <i>Reliability of tactile spatial input affects visual-tactile integration.....</i>	168
7.6. <i>Final conclusion and practical implications .....</i>	169
<b>References .....</b>	<b>172</b>
<b>Appendix A: Supplementary material for Chapter 6.....</b>	<b>191</b>



## List of figures

<b>Figure 1.1.</b> Different types of tactile stimuli to probe spatiality of the skin.....	14
<b>Figure 1.2.</b> Can somatosensory cortex convey spatiality? .....	16
<b>Figure 1.3.</b> Two forms of spatial complexity in tactile perception. ....	18
<b>Figure 1.4.</b> Somatosensory processing pathway .....	20
<b>Figure 1.5.</b> Processing differences between unimanual and bimanual touch.....	26
<b>Figure 1.6.</b> Relationship between lateral inhibition and multi-touch segregation, interaction, discrimination, and integration. ....	29
<b>Figure 1.7.</b> Differences between optimal cue integration and ensemble perception. ....	35
<b>Figure 2.1.</b> Experiment 1: paradigm, tactile stimuli, and apparatus.....	47
<b>Figure 2.2.</b> Experiment 1: behavioural results.....	52
<b>Figure 2.3.</b> Experiment 1: EEG results.....	54
<b>Figure 2.4.</b> Experiment 1: EEG result without low-pass filter.....	56
<b>Figure 2.5.</b> Experiment 1: EEG result according to response accuracy.....	58
<b>Figure 3.1.</b> Experiments 2 and 3: paradigm and stimuli.....	67
<b>Figure 3.2.</b> Experiment 2 and 3: main measures. ....	69
<b>Figure 3.3.</b> Experiments 2 and 3: results for single-finger conditions.....	74
<b>Figure 3.4.</b> Experiments 2 and 3: regression fits. ....	75
<b>Figure 3.5.</b> Experiments 2 and 3: main measures.....	77
<b>Figure 3.6.</b> Experiments 2 and 3: effect of discrepancy on averaging performance and weighting of component directions during averaging. ....	78
<b>Figure 3.7.</b> VLF-based model: relationship between sensitivity and component discrepancy.....	82
<b>Figure 3.8.</b> Experiments 2b and 3b: results of additional discrimination task. ....	84
<b>Figure 4.1.</b> Experiments 4 and 5: results for single-finger conditions.....	94
<b>Figure 4.2.</b> Experiments 4 and 5: regression fits. ....	95
<b>Figure 4.3.</b> Experiment 4: main measures.....	97
<b>Figure 4.4.</b> Experiment 4: effect of discrepancy on averaging performance and weighting of component directions during averaging. ....	98
<b>Figure 4.5.</b> Experiment 5: main measures.....	99
<b>Figure 4.6.</b> Experiment 5: effect of discrepancy on averaging performance and weighting of component directions during averaging. ....	101
<b>Figure 4.7.</b> Precision across Experiments 2 to 5. ....	102
<b>Figure 5.1.</b> Predictions on how postural information is integrated with skin-based directional representation.....	112
<b>Figure 5.2.</b> Experiment 6: results for single-finger conditions.....	116
<b>Figure 5.3.</b> Experiment 6: main measures.....	118
<b>Figure 5.4.</b> Experiment 6: effect of discrepancy on averaging performance and weighting of component directions during averaging.....	120
<b>Figure 5.5.</b> Schematic illustration of multi-touch integration given conflicting spatial frame of reference. ....	124
<b>Figure 6.1.</b> Illustration of the COP as a function of a stimulus direction.....	129
<b>Figure 6.2.</b> Experiment 7: methods. ....	132
<b>Figure 6.3.</b> Experiment 7: body sway data from one representative participant.....	139
<b>Figure 6.4.</b> Experiment 7: mean forward-backward COP across trials as a participant progressed though the experimental blocks, along with the outcome of the trial. ....	141
<b>Figure 6.5.</b> Experiment 7: unisensory behavioural performance. ....	142
<b>Figure 6.6.</b> Experiment 7: group-level body sway data.....	144
<b>Figure 6.7.</b> Experiment 7: mean COP displacement in all conditions. ....	146
<b>Figure 6.8.</b> Experiment 7: multisensory behavioural results and predictions for integration.....	148
<b>Figure 6.9.</b> Experiment 7: mean COP displacement as a function of trial outcome. ....	150
<b>Figure 6.10.</b> Experiment 7: individual JNDs.....	152
<b>Figure 7.1.</b> Processing differences between discrimination and integration. ....	161
<b>Figure 7.2.</b> Sensory and cognitive factors that were predicted to affect multi-touch processing.....	163

## List of tables

<b>Table 3.1:</b> Experiments 2 and 3: main measures for single-finger conditions.....	74
<b>Table 3.2:</b> Overview of the main measures for all conditions in Experiments 2 and 3 .....	75
<b>Table 4.1:</b> Experiments 4 and 5: main measures for single-finger conditions.....	95
<b>Table 4.2:</b> Experiments 4 and 5: main measures for all conditions .....	96
<b>Table 5.1:</b> Experiment 6: main measures for single-finger conditions .....	116
<b>Table 5.2:</b> Experiment 6: main measures in all conditions.....	118
<b>Table 6.1:</b> Experiment 7: measures from psychometric fits.....	136
<b>Table 6.2:</b> Experiment 7: mean COP displacement .....	145

## Chapter 1: From motion at separate fingers to overall object movement

The process of integrating multiple dynamic tactile signals across separate locations of the skin surface encompasses two main steps: (1) perception of a spatiotemporal tactile signal at one skin location; and (2) integration of two or more such signals across distinct skin regions. In daily life, tactile events are rarely contained within a single point of contact. Rather, we often need to perceive the movement of an object sliding across multiple fingers. During such manual manipulation, each finger receives distinct tactile motion input, and the overall object motion percept arises from convergence of activation across separate sensory afferents in the skin. This convergence differs with proximity between the inputs. Specifically, integration of inputs between fingers on the same hand implies close proximity in space, spread of excitation, and often redundant input. In contrast, fingers on different hands are farther away in space and more independent. Yet, in many daily activities we integrate tactile information across bimanual fingers with ease. Imagine driving a car and after a steep turn releasing your grip on the steering wheel and letting it slide to its starting position. The movement of the wheel gliding against the skin of the two hands feels unified, despite the input being received at non-adjacent body locations. Such multi-touch perception must be a computationally demanding process, yet our conscious experience of a unified tactile environment is seamless. This thesis attempts to show how this process occurs in the brain and establish a paradigm for studying perceptual integration of multiple tactile elements.

This introductory chapter is divided into two parts. Before describing multi-touch perception (**section 1.2**), a slight detour to a historical matter concerning the nature of spatiality in touch is required. Namely, it is not obvious that the system that supports the integrated tactile spatial percept, which will be studied in this thesis, is tactile at all (**section 1.1**). Historically, the somatosensory system has been considered inadequate for supporting perception of space. Consequently, by probing tactile spatial perception, one may actually be probing an external system (e.g., visual, motor, proprioceptive) that merely receives its sensory content via touch. We hope to show that despite tactile spatial perception being undeniably multisensory, somatosensory system is capable of giving rise to spatiality in relation to the skin itself, just like vision gives rise to spatiality in relation to the retina.

## 1.1. Spatiality in touch

Historically, touch has been considered as mainly an intensive sense (i.e., a sense that primarily provides information about amplitude and variation in intensity of a tactile contact) rather than a spatial sense (i.e., a sense that primarily provides information about location of tactile contact). This idea has been sustained to some extent by ‘modality-appropriateness’ accounts of sensory dominance during multisensory interactions (e.g., Freides, 1974; Welch & Warren, 1980). For example, when participants have been asked to judge spatial properties, experiments have shown a consistent visual dominance over touch (Cho et al., 2016; Bensmaia, Killebrew, & Craig, 2006; Wani, Convento, & Yau, 2020). For example, Cho and colleagues (2016) equated the peripheral input received by touch and vision by filtering visually presented patterns to mimic the spatial filtering done by the skin. Yet, even then, vision consistently outperformed touch in pattern discrimination. Indeed, after a tactile contact, the intensity of that touch is usually felt almost immediately, before a clear representation of the sensation's exact location is known. This has led some to question whether skin is an adequate sensory organ to convey spatial qualities of tactile events (Fulkerson, 2014).

That said, spatial information must be obtained via touch, otherwise Braille readers would not be able to understand the patterns they scan with their fingertips. Numerous experiments on human tactile perception have shown that spatial properties such as orientation (Bensmaia et al., 2008), motion direction (Pei & Bensmaia, 2014; Amemiya et al., 2017) and even more complex stimulus movement trajectories (Fardo et al., 2018; Perquin et al., 2020) can be accurately estimated. Anyone who has ever had letters spelt out on their back knows that, while the task can be difficult, it can be performed. In fact, such graphesthesia (Bender, Stacy, & Cohen, 1982) is a widely used method of communication for individuals with little or no sight nor hearing (Deafblind, n.d.). Moreover, Pruszynski, Flanagan, and Johansson (2018) demonstrated that when participants are intentionally touching a stimulus, its orientation can be extracted very rapidly and with similarly high accuracy as in an equivalent task that relies on vision. To appreciate the necessity of recognising minute spatial details purely by touch, imagine fastening a necklace behind your neck by holding a tiny clasp while aligning it with a ring. It is hard to picture how such a fine manipulation task can be completed without a fine-grained spatial capacity that must exist in the skin.

However, the fact that spatial properties can be estimated by touch does not necessarily mean that spatial capacity arises from the processing within the somatosensory system *per se*. It might be that while peripheral input is skin-based, the spatial aspect is derived by an external system. For example, active touch relies heavily on proprioceptive input and motor commands (Gibson, 1962). Considering that perception through active touch is superior to passive delivery

of tactile stimuli (Lederman & Klatzky, 1993; 2004), one might wonder whether the motor system is responsible for the observed precision in fine manipulation tasks described by Pruszynski et al. (2018). Even the classic demonstration that when skin surface is anaesthetised people cannot successfully perform the most mundane manipulation tasks like lighting a match (Sainburg et al., 1995), could be partially explained by disruptions to proprioceptive signals that inform the brain about the position of the fingers relative to one another. Thus, to reveal whether skin alone is capable of decoding space, one should consider examples that do not involve active motor command or proprioceptive feedback.

### *1.1.1. Stimuli to probe the spatiality in touch*

Scientific understanding about tactile sensation inevitably depends on the ability to produce well-controlled tactile stimuli to elicit those sensations. **Figure 1.1** illustrates the major different types of tactile spatial stimuli and examples of perceptual judgements for which each is suitable. This list is not exhaustive, but it illustrates the main differences between the types of stimuli. First, there is a difference in the spatial extent these stimuli can cover in terms of how many skin receptors and corresponding peripheral afferents they activate. This is crucial because localising a single-point stimulation requires a much different spatial representation than distinguishing between complex patterns created by multiple tactile contact points in Braille-like arrays. Imagine detecting a mosquito landing on one's arm against a Braille reader comprehending words through the minute patterns applied to their fingertips. Indeed, the ability to represent spatial relations between multiple stimuli requires a common perceptual space, which is one of the requirements for a sensory system to be able to convey spatiality (Haggard & Giovagnoli, 2011).

A second distinction lies in the temporal aspect of the stimulation. Namely, some stimuli are stationary while others produce motion on or across the skin. For example, we can judge the *orientation* of a static bar pressed against the skin, but when the bar is moved across the skin, we can also judge its movement *direction*. Encoding a moving stimulus implies that the system is able to track the activation pattern across sequentially activated peripheral fibers and retain such representation long enough for an agent to be able to judge motion's speed, extent and direction. Here, three main types of stimuli have been used: (1) rotating drum-like stimuli, (2) apparent motion created with a Braille-like array, and (3) a stimulus that is moved across the skin. Although all these produce a temporally extended stimulation, it remains to be seen whether they produce an equivalent spatial percept.

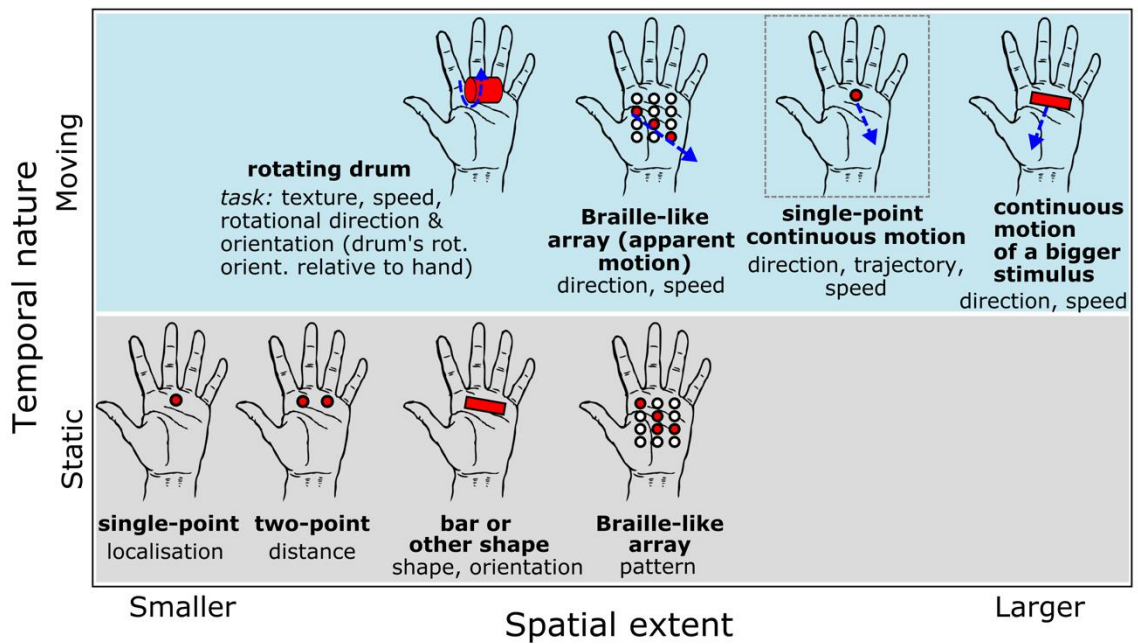


**Figure 1.1. Different types of tactile stimuli to probe spatiality of the skin.** The stimuli can be categorised based on their temporal nature. Namely, based on whether they result in a static contact or induce a motion on or across the skin. They can also be distinguished based on the spatial extent of their stimulation. In particular, how many skin receptors and the corresponding peripheral afferents they activate. Red colour indicates the stimulation. Blue arrow represents the temporality of that stimulation. For example, to create apparent motion, dots in the Braille-like array indent the skin sequentially to create a sensation of a discrete wave travelling in a specific direction. In contrast, in continuous motion, a stimulus moves ceaselessly across the skin. The grey dashed outline indicates the type of stimulus used in the present thesis to probe tactile spatial processing.

The rotating drum or cylinder has been successfully used to replicate the experience of having a texture scanned across a restricted area of the skin (Lieber & Bensmaia, 2019). The drum can be rotated at different *orientations* and speeds, thus allowing examination of the encoding of speed and scanning direction (Delhaye et al., 2019; Pei et al., 2014; Chen et al., 2020). However, the cylinder itself cannot be moved across the skin. So, detecting the direction of rotation could, in principle, be performed by encoding temporal cues in a restricted afferent fibers, rather than relying on an extended set of several adjacent afferents that would be activated in a systematic spatiotemporal order, when a stimulus moves across the skin. Imagine placing a hand on a linen tablecloth and moving it across the table to feel the roughness of the cloth *versus* feeling the path of a tiny bug who lands on your ankle and swiftly runs across the skin. Depending on what information needs to be extracted - texture vs. movement trajectory - one or the other stimulus might be more appropriate.

In Braille-based displays, a set of pins sequentially indents the skin, creating a sensation of a discrete wave travelling in a specific direction. If the pin arrays are dense, they can produce very realistic sensation of complex spatiotemporal patterns like dynamic plaid patterns and randomly moving dots (e.g., Killebrew et al., 2007; Pei et al., 2008; 2010; 2011). A consideration for such displays is the resolution of spatial activation they can produce. Pruszinsky and

Johansson (2014) stimulated fingertips with a bar at different orientations. They found that an individual peripheral receptive field (RF) can contain a local pattern of complex deformations that produce numerous peaks of sensitivity as tiny as a fraction of a millimetre. This means that a stimulus that moves *continuously* across the skin would produce a very elaborate set of changes in neural activity, even as it moves across a single RF. Consequently, for Braille-like displays, where individual pins are not denser than one RF, it would be difficult to produce such complex patterns of activity. This does not seem to be a problem for the dense array used by Killebrew et al. (2007), as the distance between individual pins is 0.5 mm. So, if an average diameter of peripheral RF is approximately 4 mm (Valbo & Johansson, 1984), apparent motion created with their array may produce the complex patterns mentioned above. In addition, Pei et al. (2010) showed that responses of cortical neurons to the moving patterns that were created with pins approximately 5 mm apart were similar to the response to a bar scanned across the fingerpad, although they did not show the activation maps of the peripheral afferents.

While dense Braille-like arrays seem to produce a convincing illusory percept of smooth motion, in this thesis, an actual single-point continuous motion was used. Whether such stimulus differs from Braille-type stimulation is unknown, as no single-unit recordings have been conducted. Yet, continuous displacement of an object across the skin ensures a successive stimulation of afferent fibres in a systematic spatial path, which captures everyday tactile motion processing. A controlled single-point stimulus has been previously used to probe motion processing by Keyson and Houtsma (1995), Amemiya et al. (2017) and Fardo et al. (2018). Another imperative for using single-point moving stimuli is the ease of creating distinct motion paths across separate skin regions to investigate the spatial integration across larger distances than Braille-like arrays allow. Using single-point stimuli, instead of larger objects (e.g., a bar), allows more fine-grained control over the properties of the concurrent stimulus trajectories. For example, discrepancy between the direction of two stimuli can be easily modulated to examine how integration is constrained by how discrepant the to-be-integrated inputs are.

### *1.1.2. Is the somatosensory system enough to encode the spatiality of tactile motion?*

The motion percept of a continuously moving stimulus can arise if the brain can track its movement across a broad range of sensory receptors. The question is whether this tracking process occurs in the somatosensory system. That is, can the percept of a stimulus path be computed from the skin itself, just like visual motion is based on the organisation of the retina? Or does it arise from a system that tracks motion in some other external rather than skin-based space? This may seem like an obvious question and, naturally, one would consider skin capable

of conveying spatiality similarly to retina. Yet, as we will show, it can be legitimately argued that while the input comes from touch, the spatiality comes from another system (see **Figure 1.2**).

## Tactile spatiality is hypothesised to arise from:

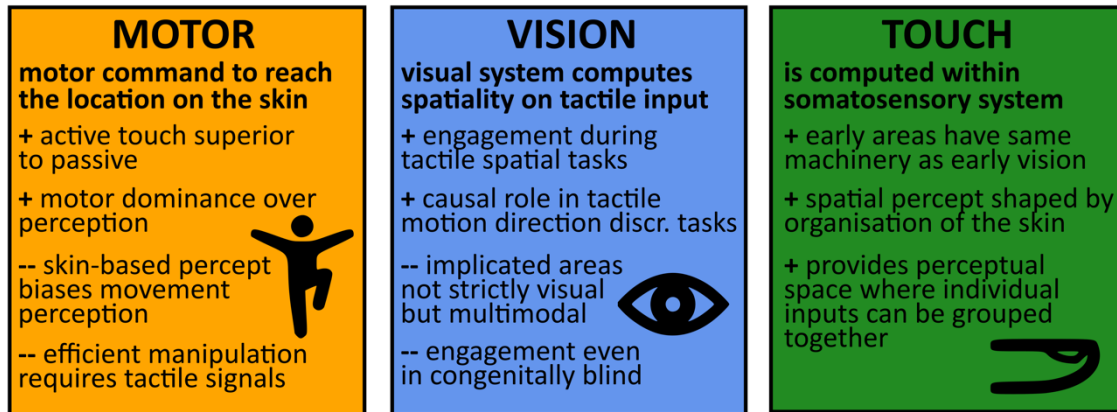


**Figure 1.2. Can somatosensory cortex convey spatiality?** Summary of the evidence for (+) and against (-) based on this chapter.

In terms of movement, Lotze (1885) argued that spatiality in touch is derived from the motor system, whereby touched location can be encoded directly from orienting commands that would be required for eye movement, pointing or spatial attention to orient to the touched locations on the skin. In that way, the extent of movement across the skin would be based on the extent of muscular contraction necessary to saccade or reach from the start to the end of the stimulus path. Indeed, motor dominance over perception has been widely demonstrated (Bays et al., 2005; Blakemore et al., 1999; Kilteni et al., 2019), providing some support for the theory that perceptual spatiality is derived from motor experience.

However, in a recent study, Cataldo and colleagues (2020) were able to decouple motor and tactile signals to investigate their contribution, when participants judged the spatial extent of either a tactile stimulus moving across the skin or a performed motor movement. They designed a self-touch paradigm, where one mechanical arm produced tactile motion along the participant's arm, when the participant moved a second mechanical arm. Importantly, while in some trials the mechanical arms mirrored each other's movement, the extent of tactile stimulation was controlled by the experimenter, so it could be either longer or shorter than the actual movement made by the participant. The authors found that while participants' judgements of the extent of tactile stimuli were biased by the movement they made; this bias was smaller than the prediction of motor dominance theory. In addition, when participants were judging the extent of the motor movement, tactile stimulation itself had a significant biasing effect. Thus, while one cannot deny the contribution of motor signals to spatial perception, there



must be some spatiality intrinsic to touch that could have influenced the spatial experience of the motor movement.

An alternative way spatiality of tactile percepts might arise without implicating the somatosensory system is if tactile peripheral input is translated into a visual code. This suggestion is supported by studies that have reported engagement of visual brain regions during encoding of tactile spatial features, such as orientation and tactile motion (Zangaladze et al., 1999; Wacker et al., 2011; van Kemenade et al., 2014; Hagen et al., 2002). However, it is questionable whether this engagement reflects the use of a visual code or visual imagery, because this activation is present even in congenitally blind individuals (Matteau et al., 2010). Amemiya and colleagues (2017) found that disrupting activity within a visual motion area, MT, disrupted participants' ability to discriminate direction of a moving tactile stimulus, providing evidence for MT's causal role in tactile motion processing. Yet, this result does not necessarily mean that the tactile motion task was performed by translating the tactile path into a visual code. Namely, MT may contain a subpopulation of neurons that are specialised to process motion in different modalities, so it may be a multimodal rather than a visual area (van Kemenade et al., 2014, Matteau et al., 2010, Ricciardi et al., 2007). Furthermore, Amemiya et al. also found an equivalent drop in performance when activity within the primary somatosensory cortex (S1) was disrupted. However, disruption to S1 could have merely degraded a common early tactile processing stage, and not the spatial aspect of that tactile information. Although the functional significance of engagement of visual areas during tactile perception remains unresolved, one explanation is that perception of any stimuli engages multi-modal resources (Yau et al., 2015; Konkle et al., 2009), and that MT engagement reflects such multi-modal processing, rather than automatic conversion of tactile information into a visual code.

Considering that external systems (i.e., proprioceptive, motor, or visual) could give rise to a spatial percept that seems to be somatosensory in nature, what evidence could be provided to reassure that the somatosensory system alone is capable of providing us with spatial qualities of touched objects? In the following sections, three lines of evidence will be outline:

- (1) The skin and the somatosensory system seem to have a dedicated machinery to process tactile motion, and it does so similarly to the early visual system.
- (2) The spatial organisation of the receptors in the skin structures spatial perception.
- (3) Multiple tactile stimuli seem to be automatically grouped based on well-known Gestalt principles that also operate in vision.

Points (2) and (3) will be only briefly described as these have been mainly examined for stationary tactile stimuli. Point (1) gives this chapter an opportunity to outline the physiological mechanisms that support tactile spatiotemporal processing. The main question is whether the

trajectory of a continuous tactile motion percept can be computed with a single sensor or whether multiple sensors are necessary (see **Figure 1.3**). If multiple sensors are necessary, then it is important to know whether the somatosensory system houses a necessary mechanism to track motion information across multiple adjacent sensors, similarly to visual motion area MT, as well as whether it houses a representation of the spatial layout of RFs across the skin enabling perception of motion in relation to one's body.

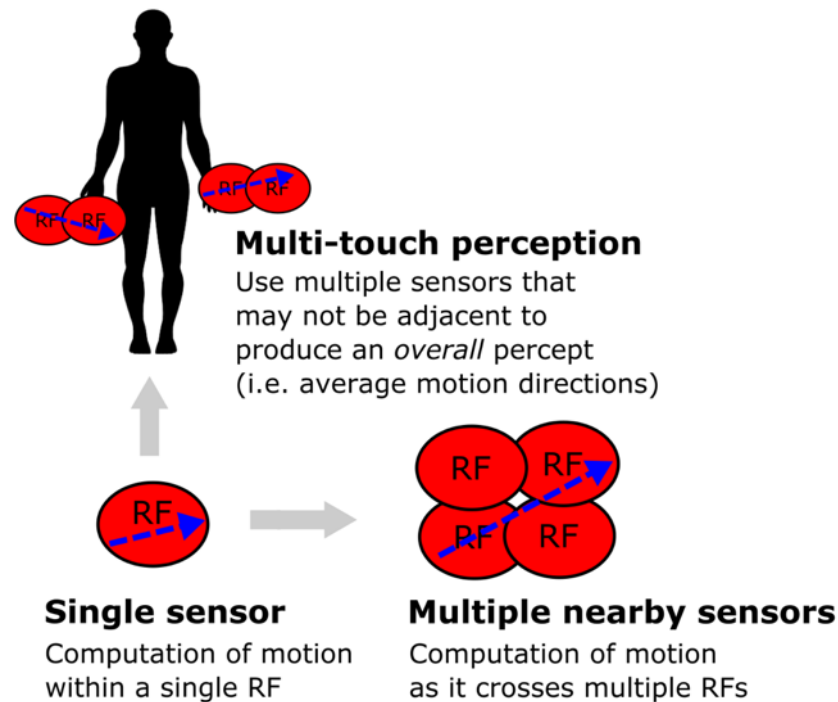


**Figure 1.3. Two forms of spatial complexity in tactile perception.** First, there is a problem of spatiality. This reflects the transition between having a single RF to having two or more adjacent RFs that can compute motion trajectory. Second, there is an integration problem. This concerns the experience of having disjointed sets of RFs on different parts of the skin which are all getting stimulated at once.

### 1.1.3. What can a single tactile sensor do?

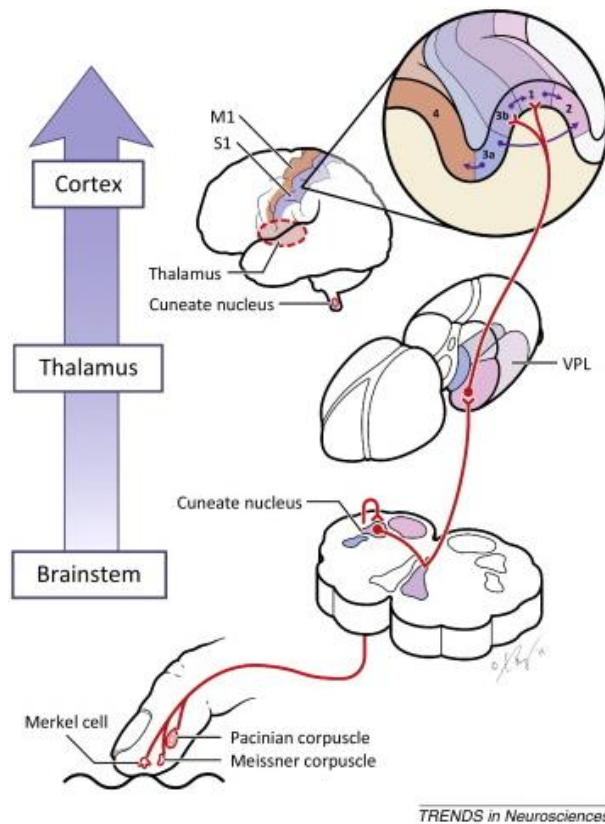
Perception of tactile motion (and other tactile qualities) begins in the skin, where specialised mechanoreceptor cells convert the deformations of the skin into neural signals. Beginning with the pioneering work of Vernon Mountcastle in the 70s, psychophysical and neurophysiological studies have demonstrated that there are four kinds of mechanoreceptive peripheral afferent fibers that are selectively sensitive to different aspects of cutaneous stimuli. A comprehensive overview of the afferent fibers is provided elsewhere (see Delhaye, Long, & Bensmaia, 2011; Johansson & Flanagan, 2009; Saal & Bensmaia, 2014). Briefly, four groups of afferents are: slowly adapting type 1 (SA1), rapidly adapting type 1 (RA), slowly adapting type 2 (SA2), and Pacinian (PC) afferents. SA1 and RA terminate superficially in the skin, with high density in the fingertips. RAs are sensitive to high frequency skin deformations, remaining

unresponsive to static force. As a result, RAs signal local spatial discontinuities such as edge contours and Braille-like stimuli. SA1s, on the other hand, show sensitivity to low frequency dynamics and remain active during sustained force. Therefore, SA1s are believed to convey the most acute spatial information. SA2s and PCs terminate in deeper tissues and have large, obscure RFs. PCs respond to high-frequency vibrations propagating through tissues and are implicated in signalling distant tactile events from hand-held tools (Miller et al., 2018). SA2s have low dynamic sensitivity and fire in response to skin stretch that occurs during object manipulation, as such, they seem to encode hand conformation. Tactile motion perception is mainly mediated by converging input from RA and SA1 afferents (Saal & Bensmaia, 2014).

A long-standing tradition in somatosensory research has been to target each afferent fibre in isolation to reveal the tuning properties of individual somatosensory units. In fact, Pruszynski and Johansson (2014) showed that stimulus *orientation* could be encoded by single afferent fibres thanks to their non-uniform RFs. However, most motion stimuli in natural life, such as a stimulus moving along the skin, would activate a succession of receptors and their corresponding afferent fibers according to its path. Because the RF sizes of peripheral RFs are small, they can accurately signal the location and position of a small stimulus, but they are too small to establish any direction selectivity of a moving stimulus. Indeed, Pei and colleagues (2010) found only a weak direction tuning in peripheral neurons for a tactile motion stimulus, which was either a sliding bar or apparent motion of dots in a dense array. This suggests that a stimulus path must be computed more centrally from peripheral signals.

Peripheral afferent signals are transmitted centrally via spinal cord and thalamus, to the somatosensory cortex (**Figure 1.4**). At the cortical level, tactile signals are processed in a hierarchical manner: neurons at successive levels of somatosensory neuroaxis have progressively larger RFs and progressively more complex feature selectivity. The primary somatosensory cortex (S1) consists of four areas: Brodmann's areas 3a, 3b, 1 and 2. Each area of S1 is organised in cortical columns that receive projections for a restricted population of afferent fibers. Thus, each column has a well-defined RF. It also means that nearby neurons respond to similar stimulus features (i.e., similar orientation or direction). The columnar organisation is widespread across neocortex, which has led to the notion that all sensory systems perform similar canonical computations. In this sense, while peripheral receptors that acquire the input are different across sensory systems, the further processing of that input is highly similar across modalities (Yau et al., 2009; Pack & Bensmaia, 2015). The columnar organisation also ensures that afferent projections that reach S1 retain the spatial layout of receptors in the skin. This means that S1 contains a complete topographically organised representation of the contralateral side of the body (Penfield and Boldrey, 1937), including

fingers (Merzenich et al., 1978). So, adjacent fingers tend to project to adjacent cortical columns of S1 (Blankenburg et al., 2003).



TRENDS in Neurosciences

**Figure 1.4. Somatosensory processing pathway.** The dorsal column-medial lemniscus pathway conveys tactile signals from the skin to the somatosensory cortex and mediates tactile perception. The pathway receives information from the mechanoreceptors in the skin and carries it through the dorsal columns of the spinal cord to the cuneate nucleus in the brain stem. From there tactile signals cross over to the other side of the body and synapse on the contralateral ventroposterior lateral nucleus of the thalamus (VPL). Axons from VPL are then relayed to areas 3b and 1 of the primary somatosensory cortex. Reproduced with permission from Saal and Bensmaia (2014).

#### 1.1.4. How can information be combined across multiple sensors?

The earliest area in S1 is area 3b, which sends projections to area 1, where RFs grow in size. Pei and colleagues (2011) created a sensation of plaid patterns moving across monkeys' fingerpads while recording activity from areas 3b and 1. The plaid pattern motion was created by superimposing two different components (multiple bars moving in the same direction) – each component could move in a different direction with different speed. Importantly, the resulting plaid pattern moved in a direction that was the weighted average between the component directions (weight was determined by the component speed). They showed that while neurons in 3b responded to different component directions, neurons in area 1 were only selective to the resulting plaid direction. Thus, area 1 neurons seem to be able to integrate individual direction cues from 3b into a more global motion percept. The specific computations area 1 conducts

seem to be analogous to the ones that occur for similar visual stimuli in MT (Pack & Benmaia, 2015), suggesting that area 1 is able to perform motion direction processing. This might occur without implicating MT itself, although it would have been interesting to record from MT during their task to ascertain that MT was not participating in the computation.

Pei et al.'s study was mainly looking at area 1's capacity to integrate across different spatial features within a single RF, but what if a stimulus moves across a larger area of the skin (see **Figure 1.3**)? Neurons in area 1 exhibit larger RFs, some of which encompass adjacent digits (Iwamura et al., 1993). This means that area 1 could integrate across "end-stop" RFs in 3b that reflect the appearance or end of a stimulus contour (Pack et al., 2003) or it could track the delay between successive activations in nearby 3b RFs (similarly to Reichardt detectors in vision) in order to compute the stimulus trajectory as it crosses nearby sensors.

However, one question remains: how does the brain know that firing in specific cortical neurons refers to adjacent locations on the skin? Namely, to benefit from multiple RFs in spatial perception, an agent needs to have some notion of where the RFs are relative to one another. As mentioned earlier, there is a somatotopically organised mapping between peripheral afferents and S1 neurons, and indeed, textbook explanations assume that such mapping is sufficient to localise and track activations on the skin surface. However, somatotopic mapping is malleable. Plastic reorganisation in the map occurs after loss of peripheral input (Feldman & Brecht, 2005) and as a result of learning (Pascual-Leone & Torred, 1993). Yet, these changes do not translate into tactile performance as predicted by direct mapping (Makin & Bensmaia, 2017), meaning that perception might be retained despite changes to the somatotopic mapping. Moreover, the representation of skin regions in the somatosensory map does not reflect the actual size of the skin surface, but rather the receptor density.

Therefore, there needs to be an additional level of representation that provides a link between cortical neurons and the location of their RFs on the skin, and that link needs to be updated to reflect the changes in the somatotopic map. This representation – classically called superficial schema (Head & Holmes, 1911; Longo et al., 2010; Medina & Coslett, 2010; Tamè, Azañón, & Longo, 2019) – needs to be acquired through natural interactions with the environment (Haggard et al., 2017). The consistent patterns of stimulation via natural interactions, such a parent stroking the arm of their infant or a leaf brushing against the skin while walking, ensure that neurons with adjacent RFs will fire in an ordered fashion. Because neurons with adjacent RFs fire in close proximity, the synaptic weights between the corresponding neurons are strengthened via Hebbian learning (Hebb, 1949). Thus, when a stimulus moves across the skin, the pattern of information across multiple afferent neurons allows the spatial path of the stimulus to be perceived. This is conceptually similar to the

observation that visual perception of length, for example, is shaped by the statistics of natural visual inputs (Howe & Purves, 2002).

#### *1.1.5. Skin structures perception*

Nevertheless, the actual organisation of the RFs on the skin has been shown to affect perception. For example, in a classical Weber illusion, the distance between two touches is perceived as larger on more sensitive skin surfaces (Weber, 1996) and also across the width of the limbs than along the length of the limb (Green, 1982; Longo & Haggard, 2011), mirroring anisotropies in the shape of tactile receptive fields (Alloway, Rosenthal, & Burton, 1989). Fiori and Longo (2018) demonstrated that this distance illusion can be explained with a model of simple stretch of tactile space. If spatial relationships between tactile stimuli were determined solely by an external system, then the local distortions in the receptor surface structure should not affect those relationships.

#### *1.1.6. Gestalt principles operate in touch*

Finally, by investigating how people perceive patterns composed of multiple tactile stimuli, several studies have revealed that pattern perception in touch is governed by Gestalt principles, which describe how distinct stimuli across sensory receptor surfaces are grouped together into a unified whole (Koffka, 1922; Wertheimer, 1923; Breidbach & Jost, 2006). Although originally and extensively described in vision, Gestalt grouping principles have been also revealed in touch (Gallace & Spence, 2011; Overvliet et al., 2012; Serino et al., 2008). For example, Serino et al. (2008) demonstrated that two tactile stimuli are automatically organised into a perceptual line, which then structures the perception of succeeding tactile stimuli. The findings that Gestalt principles affect tactile pattern perception has been taken as evidence for the existence of a *tactile field*. This is because to group multiple distinct stimuli into a coherent spatial pattern, one needs a common perceptual space (Gallace & Spence, 2011). The existence of such organising principles of large-scale spatial perception presupposes that the somatosensory system includes, or has access to, some process that locates signals in each peripheral afferent within this larger organisation.

#### *1.1.7. Interim summary*

This section has shown that the skin with embedded sensory receptors and corresponding peripheral afferents provides a perceptual space that can convey spatial and temporal qualities that give rise to perception of a moving stimulus. It can do so by dedicated areas in somatosensory neocortex (area 1) that possibly represent the temporal order of activation across multiple peripheral RFs to convey the direction of a moving stimulus. Studies

have shown that organisation of peripheral RFs shapes spatial perception, indicating that spatiality arises from the skin rather than some external system (see **Figure 1.2**). However, considering that the topographic maps in somatosensory cortex do not always reflect the true organisation of the skin, additional mental representations may be necessary to represent true spatial properties of external touched objects. Where such secondary representation is located and how it influences spatial processing is a topic of ongoing debate and out of scope for this thesis (see Serino & Haggard, 2010), but its influence could manifest as a feedback signal to area 1.

Having established the spatiality in touch and how it arises, one can approach the second problem: multi-touch integration (see **Figure 1.3**). The multi-touch integration problem represents the fact that our skin covers the whole of our body, yet different parts of the body are represented in the brain as segregated columns that share some neural representation with nearby parts via horizontal connection. In situations, where one needs to focus on one site of stimulation (e.g., feeling a mosquito suddenly land on your arm), this segregation is beneficial. However, there are also situations, whereby instead of segregation of inputs, one needs to integrate them. Object manipulation involves motion between the object and the surface of multiple fingers. If you are lifting a box with both of your hands, but it starts slipping, distinct motion signals will affect fingers on both hands. An overall percept of the object's movement, thus, must emerge from an integration of disparate motion signals at different fingers that are spatially separated. Ultimately, our normal somatosensory experience, despite being incessantly bombarded with discrepant tactile signals, does not consist of fragmented sensations, but rather a combined overall experience of a single overall perceptual quality (Martin, 1992). Seemingly, only a few studies have investigated the integrative process that makes this possible.

## **1.2. Integration between multiple touches**

Multi-touch motion perception raises an additional computational problem. It requires the brain to combine distinct motion cues across spatially separated skin regions. For example, a hand-held object that begins to move may be sensed by multiple digits, crossing a succession of RFs on each digit. The brain must produce an overall representation of the spatial path of stimulation across the spatial array of RFs on each digit, in order to produce a single, coherent description of the object as a whole. So far, most studies on multi-touch integration have been concerned with frequency- and intensity-based signals (Ho et al., 2011; Walsh et al., 2016; Kuroki, Watanabe, & Nishida, 2017; Cataldo et al., 2019). For example, in thermal referral illusions, when warm or cold thermal stimulators are applied to the ring and index fingers, a neutral temperature stimulator at the middle finger suddenly feels also warm or cold (Ho et al., 2011). This illusion arises due to a convergence mechanism operating across stimulated fingers

(Fardo et al., 2020). In another example, Walsh and colleagues (2016) and Cataldo and colleagues (2016) described an aggregation mechanism that gave rise to a total intensity of tactile stimulation across different fingers. Finally, Kuroki and colleagues (2017) demonstrated a similar multi-digit mechanism for overall frequency estimation. However, as the previous section of spatiality showed, extracting spatial aspects of touch, particularly tactile motion, may involve a level beyond the peripheral receptors and may additionally engage secondary representations of the body (Longo, Azañón, & Haggard, 2010). Indeed, Li Hegner et al. (2010) found greater brain activation in somatosensory regions when participants were judging spatial information of tactile patterns than when they were judging frequency-based information, suggesting additional requirements for spatial processing.

### *1.2.1. Importance of processing capacity*

The main problem for successful integration is limited sensory capacity to divide attention and process multiple stimuli in parallel (e.g., Desimone & Duncan, 1995; Huang, Treisman, & Pashler, 2007). An important debate in the literature concerns the role of attentional selection in multi-sensory integration. Specifically, whether integration is automatic and pre-attentive (*early selection view*; Bertelson et al., 2000; Driver, 1996; Van Der Burg et al., 2008; Vroomen, Bertelson, & de Gelder, 2001) or whether attention is a prerequisite for successful integration (*late selection view*; Alsius et al., 2005; Duncan, Martens, & Ward, 1997; Talsma & Woldorff, 2005). The early selection view predicts that integration should always happen seamlessly even with complex input, whereas the late selection view predicts that complex conditions may impose limitations on the integration process. Research has shown that both views are valid. In some cases, integration can occur in a stimulus-driven bottom-up automatic processes. For example, some inputs, which are usually more salient, can be integrated even under high perceptual load conditions or when attention is diverted elsewhere, while other inputs can be integrated only after top-down selection process (for an extensive discussion see Soto-Faraco et al., 2019).

It is generally accepted that processing capacity in touch is limited (Driver & Grossenbacher, 1996; Gallace, Tan, & Spence, 2006; Spence & Gallace, 2007; Riggs et al., 2006). For example, Gallace et al. (2006) found that when people need to count simultaneous brief tactile stimuli distributed across the body surface, the error rates increase rapidly (>30%) whenever more than two tactile stimuli are presented at once. This capacity limit may be more severe for processing complex dynamic tactile stimuli, such as motion, as even in visual motion literature a strict three-signal capacity limit has been observed (Greenwood & Edwards, 2009). Going back to the aforementioned studies on combining intensive tactile properties, Walsh and colleagues (2016) found that when participants had to estimate the total intensity of discrepant



tactile stimulus pairs, their judgements were biased towards the more intense stimulus. Importantly, the weaker stimulus was not completely extinguished and still contributed to the ultimate percept, indicating a mechanism that attempts to aggregate multiple inputs, but does so in a manner biased towards the stronger stimulus. Similarly, Kuroki and colleagues (2017) instructed participants to estimate the total frequency of two dissimilar vibro-tactile stimuli and found that final responses could be characterised by the arithmetic average of two frequencies, but with considerably more weight assigned to the more intense stimulus, resulting in overestimation. Such biases in sensory weighting could arise due to attentional limitations, which in general enforces us to allocate available resources to more relevant stimuli. Such resource allocation can be based on input salience as in Walsh et al. (2016), or on the reliabilities of individual cues as in optimal cue integration framework (Ernst & Banks 2002; Oruç, Maloney, & Landy, 2003; Ernst & Bühlhoff, 2004; Alais & Burr, 2004), which will be discussed later, or even on the novelty of given information (Yang, Wolpert, & Lengyel, 2018) to maximise information gain (Friston et al., 2015; Itti & Baldi, 2009; Vergassola et al., 2007).

In sum, previous studies on multi-touch perception point to the importance of attentional capacity, which is relatively poor in the tactile modality, and thus may give rise to biased multi-touch percepts. Importantly, participants still experience a unified sensation despite multiple tactile events, implying that the brain must employ strategies to overcome limited processing capacity. In this section, the physiological mechanisms within the somatosensory system that may support multi-touch spatial integration will be described. It will, first, show that mechanisms that support attentional selection in terms of input segregation seems to constrain multi-touch integration. Second, cognitive models of integration that may facilitate integration despite physiological limitations will be outlined. Humans have almost a unique ability to perform a large repertoire of fine motor actions with both hands. Relative to other body parts, hands can be moved freely in space around the body. They can interact directly with one another to perform coordinated actions or manipulate the same object, or to perform completely independent actions and manipulate remote objects. Consequently, multi-touch integration will be described separately for unimanual and bimanual multi-touch perception (**Figure 1.5**).

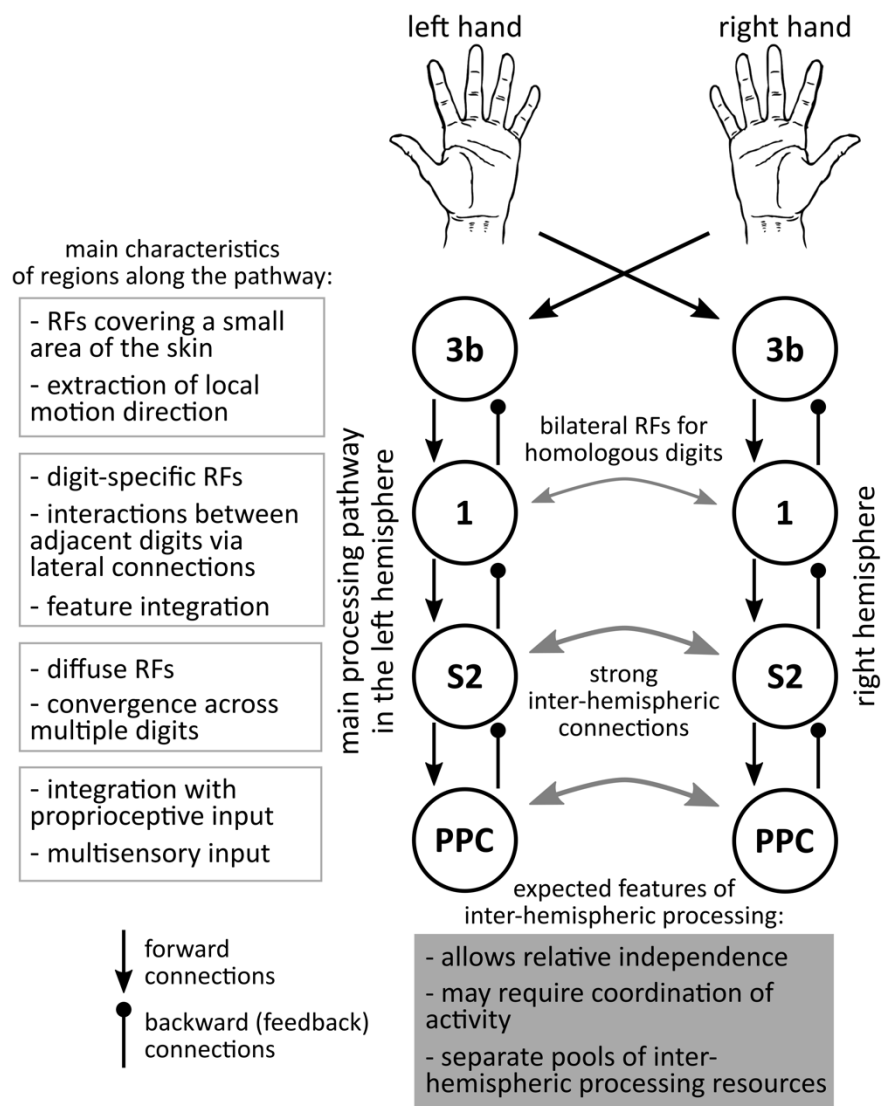


**Figure 1.5. Processing differences between unimanual and bimanual touch.** Simplistic representation of the main tactile motion direction processing pathway and inter-hemispheric connections. Input from each hand is received by area 3b in the contralateral S1 (primary somatosensory cortex). In 3b, receptive fields (RFs) code for small portions of the skin, but can extract tactile motion direction (Pei et al., 2011). Inter-hemispheric connections at the level of 3b are sparse, and bilateral interactions are mainly due to feedback (point arrow) from higher areas (Reed et al., 2011). Area 1 shows larger RFs that encompass a whole digit. Importantly some RFs include homologous bilateral digit (Iwamura et al., 2002), implying early inter-hemispheric interactions. Digit representations tend to be connected via lateral connections that may mediate suppressive interactions between digits (i.e., those that give rise to masking effects; Reed et al., 2008). Area 1 has been shown to extract global motion between two discrepant component directions (i.e., plaid motion; Pei et al., 2011). Areas of S1 project further to S2, where RFs are more diffuse and respond to stimulus features regardless of stimulated digits (Fitzgerald et al., 2006a,b), suggesting a possible convergence mechanism between input delivered to multiple digits. S2 contains bilateral excitatory connections (Iwamura et al., 2002), suggesting possible convergence pathway for inputs across hands. Finally, PPC is considered a largely multi-sensory area that may be responsible for multisensory interactions, but also for integration of skin-based representation with the movement and posture of the body. The dark grey box highlights that the activity within each hemisphere tends to be relatively independent (i.e., mono-hemispheric fluctuations), but needs to be coordinated for integrated perception and action. However, inter-hemispheric processing may benefit from separate pools of processing resources. Note that, for brevity, some area like area 3a and 2 have not been included.

### *1.2.2. Two stimuli, one hand: Physiological mechanisms of multi-touch integration on one side of the body*

As described above, the somatosensory system, just like the visual system, seems to process tactile input in a hierarchical fashion with each stage extracting increasingly complex stimulus features and incorporating larger areas of the skin (see **Figure 1.5**). For example, area 1 seems to integrate features extracted by area 3b, and it does so over larger regions of the skin. It was briefly mentioned that S1 is organised in columns that represent peripheral afferent projections from different body regions. This columnar organisation becomes essential when considering multi-touch integration across adjacent skin regions. This is because the cortical columns are interconnected by horizontal or lateral connections (Reed et al., 2008). At first sight, such lateral connections would seem to facilitate spread of information as they could represent spread of excitation between adjacent body regions (i.e., adjacent fingers). However, in the literature, these connections are mainly described as inhibitory. Therefore, when neighbouring columns are stimulated, the resulting activation is suppressed rather than increased (Biermann et al., 1998; Forss et al., 1995). This phenomenon is called lateral inhibition (von Bekesy, 1967) – an ubiquitous neuroanatomical principle of sensory system organisation found in visual (Blakemore & Tobin, 1972; DeAngelis et al., 1992; Angelucci et al., 2017), olfactory (Urban, 2002), auditory (Foeller et al., 2001; Wehr & Zodor, 2003; Kato et al., 2017), and somatosensory (Laskin & Spencer, 1979; Brumberg et al., 1996; Dykes et al. 1984; DiCarlo et al. 1998; Brown et al., 2004; Mirabella et al., 2001; Sachdev et al., 2012) cortices.

Lateral inhibition in S1 is believed to shape RFs and maintain topographic organisation of cortical maps. For example, it has been shown that weakening lateral inhibition may underlie the very rapid spread of adjacent body RFs to another body part's RF, when that original body part is surgically amputated (Calford & Tweedale, 1991; Kelly et al., 1999; Foeller et al., 2005). Lateral inhibition has been also shown to manifest in tactile judgements. Namely, lateral connections follow a strict somatotopic spatial gradient (Merzenich et al., 1978; Ishibashi et al., 2000). Meaning that lateral inhibition is strongest between adjacent body regions and it weakens as a function of distance between two skin regions in the somatotopic map. Consistently, Wilimzig and colleagues (2012) showed that reaction times to detect a stimulus on fingers within a hand follow an inverted U-shape function, whereby reactions are slowest for middle fingers. Strikingly, after a co-activation protocol, that is believed to reduce lateral inhibition between digit representations, this U-shape curve was flattened, indicating the importance of lateral inhibition in shaping perceptual performance.

Lateral inhibition, in principle, should facilitate segregation (or selectivity) between concurrent tactile inputs on skin regions that project to adjacent columns of S1 to maintain the

somatotopic organisation of the body (see **Figure 1.6**). Indeed, attending to a stimulus on one finger suppresses the activity related to processing the adjacent finger (Iguchi et al., 2001; 2005; Braun et al. 2002), potentially via lateral inhibitory mechanism. The failure of *perfect* segregation is evidenced by masking effects, whereby a distractor stimulus interferes with a target (von Békésy, 1967; Gilson, 1969). Interestingly, the strength of masking effects decreases not just as a function of spatial distance between the target and the distractor, but also as a function of somatotopic proximity according to the organisation of the S1, with stronger masking occurring for somatotopically adjacent body parts (Harris et al., 2001a; Tamè et al., 2014; Gilson, 1969). This means that some spread of information along with at least some suppression is required for masking effects to occur. However, in some cases, a tactile distractor stimulus not merely inhibits the target, but biases the estimates towards itself (Kuroki et al., 2017; Rahman & Yau, 2019). Kuroki et al. observed this assimilative effect when stimuli were applied to adjacent unimanual fingers, meaning that compulsory interactions can arise despite possible inter-digit suppression. These interactions can be characterised by normalization models (Rahman & Yau, 2019; Brouwer et al., 2015), whereby the response of a single unit is divided by the response of a population, which, in turn, can be modulated by the strength of attention (Rahman & Yau, 2019). This has a similar net effect to lateral inhibition, but it does not involve the explicit mechanism of inhibitory lateral connections.

An important distinction between previous studies on multi-touch *interactions* and multi-touch *integration* is that multi-touch integration requires attentional selection of information on both stimulated digits (see **Figure 1.6**). In the literature on multisensory integration (Soto-Faraco et al., 2019), *interaction* refers to the process, whereby information in one modality influences (or interferes with) the information in the other. For example, as I am trying to type this sentence, my partner is giving a virtual seminar in the same room. The auditory cues from his talk, which are clearly unrelated to the letters I type, interact with my visual, tactile, and motor signals of pressing each keyboard key, but are not integrated. In contrast, *integration* refers to an aggregation mechanism, whereby two inputs in two modalities are both selected and brought together. For instance, every time I press and tactually feel a key on my keyboard, a letter appears on this document. The motor, tactile, and visual signals are all related to the same sensory outcome, and thus are integrated into a unified perceptual event. Similarly, estimation of average or total quality between two tactile inputs requires *integration*. Although in the multisensory context, integration occurs between multisensory signals that provide redundant information to improve an integrated percept, perception of an average tactile feature involves integration across unisensory inputs with each providing distinct information about the overall percept (more in **section 1.2.6**). The predicted relationship

between attention, lateral inhibition (or inter-cortical suppression), and cognitive processes of selectivity, interaction, and integration are shown in **Figure 1.6**.

While interactions suggest a failure of segregation, and some leakage between adjacent cortical representations, they are problematic for integration. This is because interactions may lead to a distortion of the representation of stimuli at each stimulation site, thus resulting in biased aggregated final percept. This raises an interesting, but slightly unintuitive prediction, whereby more optimal integration would occur between stimuli delivered to non-adjacent body parts. Accordingly, integrating tactile inputs from adjacent fingers of the same hand would be distorted due to suppressive interactions, while aggregating inputs across skin regions that are far apart, like fingers on different hands, would be easier due to lesser interactions (more on lateral inhibition and its role in **Chapters 2, 3 and 4**). However, it needs to be noted that interaction and integration processes likely arise from a competition between spread of neural activation and suppression.

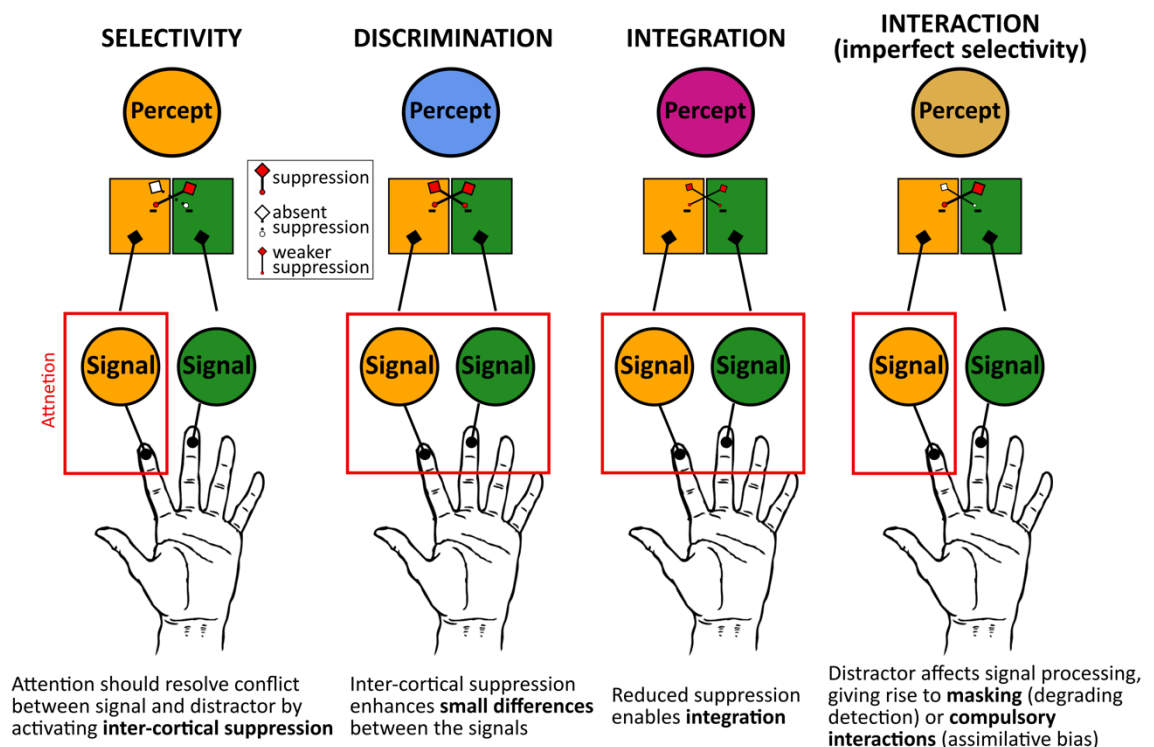


**Figure 1.6. Relationship between inter-cortical suppression and multi-touch segregation, discrimination, integration, and interaction.** Illustration of the role of inter-cortical lateral suppression. Most studies have focussed on the role of selective attention (conceptualized by a red box around the to-be-attended finger) to a localized target signal (orange), when a distractor (green) is presented simultaneously to another finger. Attention to a target stimulus can activate inter-digit suppression between corresponding representations. If that suppression is stronger than the suppression from the distractor signal (green), two signals are perfectly distinguishable, giving rise to perfect segregation or selectivity. However, research shows that distracting signal (green) can interact with the target signal either by masking or biasing it. Importantly, the work in this thesis will focus on the processes that take place when **both** signals are task-relevant and **both** need to be attended to. In **Chapter 2**, discrimination

will be considered, whereby attention is divided between both stimuli in order to discriminate between them. In this case, local lateral suppression enhances the differences between the two stimuli, making them easier to discriminate. Finally, integration also requires divided attention to both stimuli, but instead of contrasting the two stimuli, the two stimuli need to be combined. This is easiest when local lateral suppression is reduced, and convergence between the signals is strong.

Support for better integration across somatotopically distant body parts comes from studies that have found improvements in multi-touch integration when stimuli were delivered to fingers on different hands (Craig, 1985; Walsh et al., 2016; Overvliet, Smeets, & Brenner, 2007; Plaisier, Tiest, & Kappers, 2010). For instance, Craig (1985) obtained greater spatial integration of two halves of vibrotactile patterns presented to two fingers on separate (versus the same) hands. Yet, whether such performance improvement is due to reduced suppressive interactions remains unclear, as it could also be due to an increase in the ability to allocate attentional resources to each stimulus. The beneficial effect on performance when using two hands remains controversial, as other studies characterise bimanual interactions as mainly inhibitory (Palmer et al., 2012; Tommerdahl et al., 2005), which incur performance costs for judging tactile stimuli (Nguyen et al., 2014; Nguyen et al., 2020; Braun et al., 2005). In addition, interfering interactions occur for bimanually presented stimuli (Kuroki et al., 2017; Rahman & Yau, 2019; Wani et al., 2020; but see Evans & Craig, 1991 - show a reduced distractor effect).

### *1.2.3. Two stimuli, two hands: Physiological mechanisms of multi-touch integration across two sides of the body*

Generally, S1 is believed to receive input strictly from the contralateral side of the body (Hari et al. 1984; Hämäläinen et al., 1990; Hoshiyama et al., 1997; Jones & Powell, 1970; Kaas, et al., 1984). This means that bilateral multi-touch integration tasks would require transferring the tactile input between the two cerebral hemispheres before integration. This signal exchange could occur through several channels, but most prominently, through corpus callosum (CC). Inter-hemispheric neural transfer via CC may incur delays (Berardi et al., 1988) and other costs associated with coordination of activity between the hemispheres (Banich & Belger, 1990). But to appreciate the importance of such inter-hemispheric exchange one should consider split-brain patients, whose CC has been completely severed. The brain of these patients behaves as if it is two separate entities. The experience of one such patient has been described as if the two hands are repelling magnets: “I'd reach with my right for the thing I wanted, but the left would come in and they'd kind of fight. Almost like repelling magnets.” (Wolman, 2012).

Given the demands of transferring information across hemispheres, integrating stimuli delivered to the same side of the body should lead to better performance. That said, bilateral presentation of stimuli may allow better division of attention between the inputs, as some point out the possibility for parallel processing (Overvliet et al., 2007; Plaisier et al., 2010). This idea is

consistent with general hemispheric models (Friedman & Polsen, 1981), according to which each hemisphere has mutually inaccessible pools of processing resources. To make the most optimal use of processing resources, tasks may be shared between the hemispheres. The relative advantage of interhemispheric transmission will depend on the difficulty and processing load of the experimental task. In particular, inter-hemispheric processing advantage has been generally observed for more difficult tasks (Banich & Belger, 1990; Norman et al., 1992). This is because task difficulty is related to the trade-off between the costs of coordinating activity between hemispheres and the advantage of parallel processing between the hemispheres (Banich & Belger, 1990). Studies that have not found inter-hemispheric advantage may, thus, be simply less demanding, whereby the costs associated with transmitting and coordinating activity between the hemispheres exceed the benefits associated with inter-hemispheric processing.

However, a competing view argues that some bilateral tasks in tactile modality may be completed more efficiently by engaging bilateral interactions at the early stages of somatosensory pathway (see **Figure 1.5**). Challenging the strict laterality of S1, studies have observed activation of ipsilateral S1 following unilateral stimulation, primarily in areas 1 and 2 (Iwamura, Iriki, & Tanaka, 1994; Schnitzler et al. 1995; Hansson & Brismar, 1999; Shuler et al., 2001; Iwamura et al., 2002; Reed, Qi, & Kaas, 2011), suggesting existence of RFs that encompass homologous fingers of both hands and that do not distinguish between body sides. This view is corroborated by psychophysical studies that have found that the masking effects for bimanual stimuli are digit-specific. For example, Harris and colleagues (2001a) asked participants to compare the frequency of two vibration stimuli applied to two different fingers. When the vibrations were on homologous fingers on opposite hands, performance was as good as when the vibrations were presented to a single finger. Performance worsened, however, when the fingers were no longer homologous. Similar results were obtained with a masking paradigm - a distractor stimulus on the other hand disrupted the discrimination of two vibrations on one finger, but its effect weakened when it was delivered to non-homologous bilateral fingers. Digit-specific bilateral interference was also reported by Tamè et al. (2011).

In addition, Braun et al. (2005) found that participants tended to mislocalise tactile targets to the homologous finger on the other hand. Because mislocalisation is believed to occur due to overlapping RFs or lateral connections, these results support the view that bilateral representation of homologous fingers must be integrated at the early stage of somatosensory processing. Moreover, studies looking at perceptual transfer of learning have found that learning transfers to homologous fingers on the opposite hand, but not to the non-homologous fingers (Dempsey-Jones et al., 2016; 2019; Harrar, Spence, & Makin, 2014; Harris et al., 2001b). Finally, Tamè and colleagues (2015) used MEG to show that interactions between bilateral

tactile stimuli in S1 occurred at early rather than late stages of processing. In sum, this line of work suggests that while laterality is maintained in areas 3b and 3a, signals from homologous bilateral body parts are integrated in areas 1 and 2. Indeed, maintaining double representation along the whole tactile processing pathway may be inefficient, when the brain can use a single body model, which does not distinguish between the left and right body side (Tamè et al., 2019). Importantly, this view suggests that multi-touch integration across fingers on opposite hands may occur at the same level of processing as multi-touch integration across fingers of the same hand. Therefore, the same somatotopically organised masking effects may limit bimanual multi-touch integration. One way to behaviorally test this idea is to modulate the homology between to-be-integrated bimanual fingers (more in **Chapter 4**).

#### *1.2.4. Beyond S1: Neurons that do not care about touched digits*

All areas of S1 project further to the secondary somatosensory cortex (S2; see **Figure 1.5**), where RFs are more complex and diffuse. S2 is less topographically organised than S1 (Ruben et al., 2001) and respond bilaterally to stimuli applied to either hand (Iwamura et al., 1994). If only some neurons in areas 1 and 2 of S1 had multi-digit RFs, the majority of S2 neurons have RFs that encompass multiple digits (Burton & Carlson, 1986; Fitzgerald et al., 2006a,b). In landmark studies by Fitzgerald and colleagues (2006a,b), monkey pads were sequentially stimulated with stationary bars at different orientations, while activity of S2 neurons was recorded. The authors found that S2 neurons were selective to specific bar orientations regardless of which specific pad was stimulated. Interestingly, the preferred orientation tended to be similar across different pads, meaning that tuning of S2 neurons formed an oriented line across multiple pads. This suggests that S2 could represent large-scale spatial features encompassing multiple digits even if they are non-adjacent. Therefore, while S1 may serve the perception of spatial features on a single digit or represent interactions between stimuli on adjacent fingers, integration of inputs into a coherent representation of a hand-held tactile object may arise from computations in S2 (Haggard, 2006; Serino et al., 2008).

Yet, there are two important aspects of multi-touch perception missing from the paradigm employed by Fitzgerald et al. (2006). First, the pads were stimulated one at a time rather than all at once. While sequential stimulation still allowed the authors to build up a description of each neuron's response profile across stimulation on different pads, one could wonder whether tuned neurons' response profiles would have shown more complex interactions if multiple pads felt the stimulus concurrently. As mentioned above, simultaneous stimulation of different fingers produces mainly inhibitory interactions between finger representations in S1, which may arise due to topographic lateral connections. Given that RFs in



S2 are more diffuse, one may wonder whether the interaction for concurrent stimuli on multiple pads are excitatory instead, reflecting a stronger basis for integration.

The second limitation concerns the fact that limbs and fingers can move in space relative to one another when objects are touched. To illustrate this, consider integration of visual scenes across the two eyes. If we leave the changing posture of fingers and limbs aside, then similarly to integration across discontinuous regions of the skin, experience of unified vision comes from integration across discontinuous receptive surfaces of the two eyes. Binocular vision allows us to have a single visual percept despite having two eyes. Accordingly, a similar process must occur in touch, whereby a single tactile percept arises despite two separate touches. However, in vision, the receptor surface (retina) itself is not deformable in the same way as the skin. In touch, receptors in the skin move relative to one another as hand posture changes and as the hand is placed into different locations around the body, constrained by agent's flexibility (e.g., touching something on its back; Hsiao, 2008). Although eyes can be moved to look at different parts of the external environment, they cannot be moved independently from each other (at least in humans). In addition, eyes stay in one specific place on the body at a fixed distance from each other. Therefore, in order to truly account for multi-touch perception across separate body regions that can move independently from each other (e.g., fingers of opposite hands), proprioceptive information about body posture needs to be eventually integrated with the purely tactile signal arising from the skin.

#### *1.2.5. Beyond S1: Contribution of proprioceptive information*

Extensive research has shown that the position of our limbs and fingers influences tactile spatial perception (Pei et al., 2014; Kuroki et al., 2012; Rinker & Craig, 1994; Yamamoto & Kitazawa, 2001; Craig, 2003). Therefore, to determine stimulus movement across a limb or across multiple fingers that change position, the brain must integrate the skin location with current body posture. Neurons in area 3a and 2 of S1 primarily encode information about joint kinematics from muscle and tendon-associated receptors, but even areas 3b and 1 have been found to encode some proprioceptive signals along with purely tactile signals (Yau et al., 2016). A recent study by Goodman and colleagues (2019) found that RFs of area 3a neurons encode several joints spanning the entire hand and thus can convey the configuration of the fingers relative to one another. This may underlie stereognosis or the ability to perceive the shape of held 3D-objects (for review see Yau et al., 2016). Yet, how this proprioceptive information from 3a and area 2 is integrated with cutaneous information remains to be explored.

It is known that areas 3a and 2 project to the posterior parietal cortex (PPC; see **Figure 1.5**), which comprises two major areas originally described by Brodmann's areas 5 and 7. PPC

compromises strong interhemispheric connections as well as many connections with premotor regions (Caminiti et al., 2017). Crucially, PPC responds both to cutaneous stimulation and joint movement. However, unlike S1 and S2, it responds to other sensory modalities (Cohen et al., 2004), has the strongest response when an animal is awake and behaving (Seelke et al., 2012), and is involved in motor functions such as planning to reach and grasping (Kalaska et al., 1997). As a result, PPC is considered to play a critical role in multisensory integration and sensorimotor planning, especially for upper limbs (Snyder, Batista, & Andersen, 1997).

Indeed, disrupting neural activity within PPC has been shown to disrupt performance on a tactile localisation task that required consideration of body position (Azañón et al., 2010). Furthermore, it takes time for tactile-proprioceptive integration to occur (Soto-Faraco & Azañón, 2013). This suggests that PPC might be the site of tactile-proprioceptive integration that enables perception of tactile spatial properties in external space. In monkeys, Sakata et al. (1973) found that neurons in area 5 of PPC responded preferentially to tactile stimulation only when the stimulated body part was in a specific location in space. For example, one neuron in area 5 responded preferentially when the forearm was stimulated, while the arm was drawn towards the body, but did not respond to the same forearm stimulation, when the arm was positioned away from the body. The role of body posture in multi-touch spatial integration will be discussed in more detail in **Chapter 5**.

### *1.2.6. Cognitive models of multi-touch integration*

Having described the physiological processes that underlie multi-touch integration, one needs to also consider the cognitive processes that facilitate integration between multiple sources of information (i.e., multiple touches). Namely, when an agent receives tactile stimuli on separate regions of the skin, there are two main things that the agent could be doing with the received inputs. First, the agent may be trying to get an optimal estimate of a “single object” (optimal cue integration), or second, the agent could be trying to get a general “gist” of what is happening without necessarily assuming that the sensations arise for a single object (ensemble perception). A form of ‘gist’ between multiple distinct tactile stimuli is when a person holds a bunch of coins and can immediately extract the overall number of coins (e.g., Plaisier, Tiest, & Kappers, 2009). The crucial distinction between these two models is whether the agent decides *a priori* that there is one object of which it has two estimates or whether it has got multiple signals that are not bound to a single thing, but that still produce an ensemble (see **Figure 1.7**).

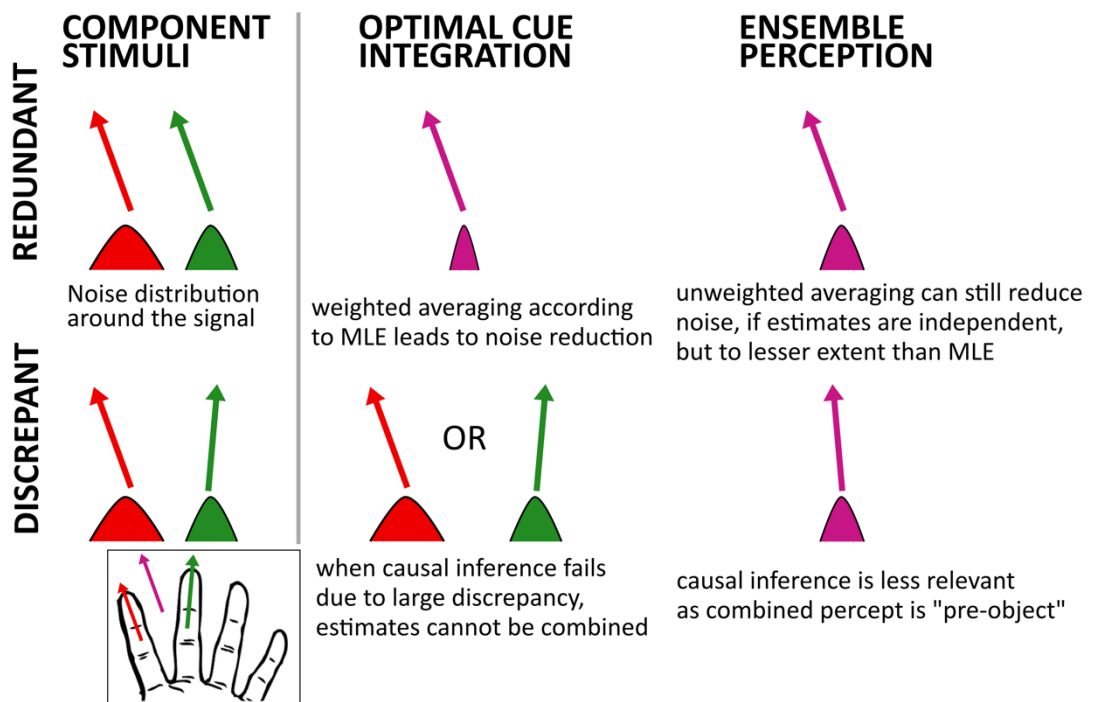


**Figure 1.7. Differences between optimal cue integration and ensemble perception.** Two component motion directions are delivered to index and middle finger (red and green). The precision of the two components varies (noise distributions). The task is to combine them into an overall direction (purple). Optimal cue integration operates on redundant signals only (i.e., ones that come from a common source). Signals that are too discrepant would not be integrated due to a failure of causal inference and result in selectivity. Noise in a new integrated input follows a maximum likelihood estimate (MLE) rule, where more precise component receives a greater sensory weighting. Thus, the noise in the overall percept is reduced below the noise in both component inputs. Ensemble perception gives rise to an average percept even when components are discrepant. Noise reduction could follow noise summation theory, whereby averaging reduces noise, given that components are independent.

In optimal cue integration (Ernst & Bühlhoff, 2004) participants are asked to report some property of an object that depends on two separate but redundant signals. The main aim of optimal cue integration is to combine the two signals to form a maximally reliable new percept about the object property. As such, cue integration describes integration between redundant signals, whereby individual signals are weighted depending on their precision, so that the precision of the final estimate is enhanced as much as possible or at least above that of the individual estimates (Ernst & Banks, 2002; Oruç et al., 2003, Alais & Burr, 2004). To illustrate, if participants are touching a moving object, and motion on one finger is more reliable than motion on another finger, the more reliable motion cue will receive higher weighting during integration, resulting in a more precise estimate of overall object motion. This weighting process would help the agent overcome attentional and physiological limitations to process both signals in parallel while still producing a highly reliable percept. Importantly, such reliability-based integration is useful only when the signals refer to the same object. If signals are too discrepant to refer to a common object, the brain would selectively attend to one of the signals without attempting to integrate (Cao et al., 2019).

However, even when individual sensory signals are highly discrepant, people can still access an overall synthesis of these individual signals. Imagine a flock of birds with each bird moving in a slightly different direction. While an observer can isolate one particular bird's movement, the observer is also able to perceive the average movement of the flock as a whole. This is possible thanks to a process called ensemble perception (Alvarez, 2011; Whitney & Yamanashi Leib, 2018). The main function of ensemble perception is to overcome brain's limited processing capacity by representing the overall gist information across multiple regions of the sensory surface, each of which may individually receive varying stimulation. For example, in vision it has been shown that participants can extract overall or average motion information from simultaneous discrepant motion cues (Watamaniuk et al., 1989; Watamaniuk and McKee, 1998). An equivalent process in touch has not been yet directly investigated.

Although integration of multiple cues is required for ensemble perception, the main aim of ensemble perception is to extract the aggregate signal from multiple regions of a receptor surface, rather than to combine multiple signals into a single, new, more reliable percept. Such aggregate information can be successfully extracted from even very discrepant stimuli (Whitney & Yamanashi Leib, 2018). Importantly, in ensemble perception, averaging can also improve precision by cancelling uncorrelated noise across different components of the overall stimulus. In contrast, if noise across different components of the overall stimulus is correlated, averaging will not improve precision. Ensemble perception shares some resemblance with Gestalt grouping, whereby multiple signals across separate regions of receptor surface are grouped into a unified whole. However, in ensemble perception, the main objective is to extract the aggregate across multiple stimuli to best represent the group despite limited attentional resources (e.g., average motion across separate motion trajectories). This is a different conceptualisation from that in Gestalt grouping, where there is less focus on aggregation and more focus on representing all the separate signals as part of a bigger whole.

### *1.2.7. Interim summary*

If an agent wants to combine two tactile spatial cues across separate regions of the skin, it will need to first overcome physiological constraints such as interactions between adjacent skin locations and limited attentional resources to process multiple tactile stimuli in parallel. These constraints will give rise to cognitive processes that will attempt to overcome these limitations while producing a reliable estimate of multiple touches. The agent could either weigh and combine cues based on each signal's reliability, if it believes the signals to arise from a common source, or it may extract an aggregate sensation between even highly discrepant signals. In the experimental chapters that follow, we will try to tap into these cognitive models of multi-touch integration by asking participants to combine two continuous motion trajectories

along two different fingertips to estimate the *average* motion between the two separate signals. The capacity to average two concurrent inputs delivered to adjacent skin surfaces means that participants can perceive integrated ensemble despite inhibitory interactions between concurrent inputs and limited attentional resources. If the capacity extends to remote non-homologous body parts, this ability may rely on higher levels of somatosensory processing described in the **Beyond S1 sections**. But before proceeding to the experimental testing of multi-touch spatial integration, there is one last section that requires attention. Namely, what happens when vision is added to disentangle the spatiality of touch. This last section will set the stage for the work in the final experimental chapter of this thesis (**Chapter 6**).

### **1.3. Beyond touch: interaction between touch and vision**

For people, who are not congenitally blind, vision, either at some point in their life (for late blind individuals) or continuously throughout the life, guides haptic processing by providing predictions about tactile events (Jenmalm and Johansson, 1997). However, note that during fine object manipulations, vision is not sufficient, and haptic predications may be based on tactile information itself (Johansson and Flanagan, 2009). Nevertheless, vision undeniably aids a lot of haptic interactions. When visual and tactile signals are believed to arise from the same sensory event, they can aid perception and enhance the perceptual quality of that event.

Whether the two multisensory signals are integrated can be shown by adjusting the noise level of a sensory cue and examining whether the brain can balance that noise when it is combined with another redundant cue, producing a more reliable integrated percept. According to the optimal cue integration framework described above (**Section 1.2.6**), reduction of noise in the final percept provides evidence for integration and not just augmentation (Ernst & Bühlhoff, 2004; Green & Angelaki, 2010). The majority of multi-sensory integration studies, however, rarely focus specifically on touch. For example, Ernst and Banks (2002) demonstrated that visual and tactile cues are integrated optimally by adjusting noise in the visual stimulus, and showed that participants down-weighted vision, when it was noisy, but not when it was reliable. However, reliability of tactile cue was never directly modulated. Thus, the authors did not examine the extent to which touch itself influenced the combined tactile-visual percept. Yet, there is already some evidence that vision can be augmented by tactile information. For example, Pérez -Bellido, Pappal, and Yau (2018) showed that concurrent spatial information from touch and vision enhance a visual illusion, while Gray and Tan (2002) showed that motion information acquired through touch can aid visual perception.

There is an urgent need for studies tapping into touch's role in augmenting visual experience, but also into how touch is integrated with visual signals to maximise the

augmentation (for more discussion on tactile-based technologies see Gallace & Spence, 2014, chapter 9). The difference between augmentation and integration lies in a distinct perceptual experience of the event. Adding a background music when playing on a PlayStation may enhance the experience of gaming, but when specific sounds are tied to visual events that happen in the game, the perceptual boundary between sounds and visual events blurs (like when watching a movie), giving rise to a truly integrated experience. Imagine, a character from the game reaches out to you on the screen and you feel a concurrent tactile sensation on your shoulder as the character “touches” it. Acquiring such integrated experience in gaming and virtual reality, similar to that depicted in *Ready Player One* (Cline, 2011), is still a distant dream for developers. However, steps to augment visual experience in gaming (e.g., Rubin, 2019 on PlayStation and Stowe, 2017 on Nintendo) and virtual reality (Culbertson et al., 2018) are slowly being accomplished. Tactile feedback devices aimed to enhance visual experience are also being rapidly developed for improving driving (Harrington et al., 2018; Meng & Spence, 2015; Gallace & Spence, 2014) and surgery (Okamaru, 2009; Gallace & Spence, 2014).

However, because seemingly no study has examined what happens to visual-tactile integration when reliability of touch is varied, we do not have a clear idea of the consequences of artificially adding tactile information to visual perception. Optimal cue integration and visual dominance theories would predict that participants should be able to down-weight tactile signals to produce a precise combined estimate. However, touch has been considered to be qualitatively different from vision. Philosophers like Descartes had already noted that touch gives us the most direct contact with reality (Descartes, 1998; Fulkerson, 2020). This belief may stem from the fact that the sense of touch is ultimately linked to our bodily awareness (O’Shaughnessy, 1989). Vladimir Nabokov (1955) wrote in *Lolita*, “It is strange that the tactile sense, which is so infinitely less precious to men than sight, becomes at critical moment our main, if not only, handle to reality.” (p. 398).

Although, the fallibility of tactile perception has been established (Badde, Röder, & Heed, 2019) and a lot of studies demonstrate visual dominance over touch when both signals are competing (e.g., Suzuishi, Hidaka, & Kuroki, 2020; Craig, 2006; Bensmaia et al., 2006), a recent study has revealed a more complex picture. Fairhurst et al. (2018) found that while judging an object's length by touch was less accurate than by vision, touch provided a greater feeling of certainty even when participants were merely guessing. Given the claims of tactile superiority in providing a stronger sense of confidence, the predictions of optimal integration might not stand when the reliability of touch is carefully considered (more in **Chapter 6**).

## 1.4. Summary and thesis overview

In this Chapter we addressed two problems of multi-touch spatial integration. First, we described how somatosensory systems can extract motion information from the skin and represent not only intensive qualities of touched objects, but also their spatiality. Second, we laid the ground to the processes that may underpin the ability to produce an overall description of tactile events that may occur on discontinuous parts of the skin. What is striking is that the columnar organisation of the early levels somatosensory system, which at first glance should support multi-touch integration, instead seems to be limiting optimal integration due to lateral inhibitory mechanisms.

In the next chapter (**Chapter 2: Brain mechanism of multi-touch aggregation**), we will show that this rigid view of lateral suppression, according to which two concurrent stimuli should always inhibit one another, may be an unjustified remnant of the field's historic focus on tactile acuity. Instead, we will show that inter-digit suppression, as measured with electroencephalogram (EEG), can be reduced when people attempt to aggregate multiple adjacent touches. That is, given that the task context is to extract the synthesis of concurrent stimuli, somatosensory circuitry is tuned to inter-digit convergence rather than inter-digit suppression.

After suggesting that early somatosensory cortex can be tuned to multi-touch integration, we will explore how individual spatiotemporal inputs are integrated in multi-touch and tactile-visual perception to produce a coherent percept of direction. For multi-touch spatiotemporal integration, we will present a novel paradigm, whereby participants are asked to estimate the *average* direction between two tactile motion trajectories delivered simultaneously to two different fingerpads. This task will serve as an example of ensemble perception in tactile spatial processing and may underpin how motion of a touched object is integrated. However, instead of using a unified tactile object, our paradigm allows manipulation of the discrepancy between the component tactile motion inputs. This allows us to see how discrepancy between individual inputs constrains integration. In **Chapter 3 (Multi-touch aggregation within- and between-hands)** by comparing averaging ability in within-hand and between-hand integration, we will show that factors related to processing tactile stimuli within each hand limit this aggregation mechanism.

Next, by manipulating the somatotopic relationship between stimulated fingers for both within-hand and between-hand integration (**Chapter 4: Multi-touch aggregation beyond somatotopy**) we will argue that the aforementioned limits are likely of hemispheric origin. Our findings will show that somatotopic distance between stimulated fingers does not explain the aggregation performance. This result is consistent with studies that suggest that bimanual tasks

benefit from better division of attention that is hemispheric in nature. In other words, sharing processing between two hands may result in more optimal integration performance.

Further, we examine the influence of proprioceptive input on multi-digit motion integration by changing the posture of one the hands that receives tactile input (**Chapter 5: Effect of posture on bimanual multi-touch perception**). We show that while proprioceptive input seems to be incorporated during tactile motion perception, it has an attracting effect of directional judgements, suggesting that it is not fully compensated for. Importantly, we will show that aggregation process occurs after proprioceptive input of each hand is incorporated, suggesting an independent and serial process.

Finally, with a rapid growth in demand for tactile feedback devices that could compensate, but also enhance visual experience, there is an urgent need for research that investigates how paired tactile and visual stimuli can contribute to spatial perception. The important consideration here is that, while vision might provide more accurate spatial cues, touch may be an inherently more “engaging” sense. This could lead to unexpected effects of tactile input not accounted for by theories that have solely focussed on modulating the visual input. To investigate tactile-visual integration (**Chapter 6: Integrating directional information between touch and vision**), we ask participants to combine the direction of tactile pulling force and direction of visual optical flow, and to report the direction of overall heading. Our findings show that when touch is corrupted by noise, it can degrade overall performance, in contrast to predictions of visual dominance theories.

Overall, the present thesis demonstrates across six experiments that participants can perceive the movement direction of two discrepant tactile stimuli presented to different non-adjacent and even bimanual fingers, in order to average them into their overall direction. This aggregation can occur despite the “severe” limitations of tactile processing capacity. We show that this aggregation process incorporates proprioceptive input, is unconstrained by somatotopic mechanism, and general discrepancy between the component inputs, but it is modulated by a hemispheric factor. The final experiment of this thesis emphasises the importance of the reliability of tactile input over and above the reliability of visually acquired information in visual-tactile integration. All this strongly suggests that inclusion of models of multi-touch integration into the classical models of tactile acuity and selective attention have both theoretical implications for somatosensory processing and practical implications for tactile interface design.



## **Chapter 2: Brain mechanism of multi-touch aggregation**

The previous chapter introduced the concept of long-range lateral inhibition that operates between the cortical columns of the primary somatosensory cortex (S1) and described how it is dysfunctional when sensory inputs delivered to adjacent body regions need to be integrated rather than segregated. Based on a previous study that showed that a suppressive interaction between adjacent fingers akin to lateral inhibition can be increased to facilitate tactile acuity (Cardini, Longo, & Haggard, 2011), we reasoned that the same mechanism may be decreased to facilitate multi-touch integration. Thus, we contrasted the ability to average two tactile trajectories with the ability to discriminate between them. To probe the lateral inhibitory process between the stimulated fingers, we used an established event-related potential design that measured the interaction between cortical representations evoked by digital nerve shocks immediately before each pair of tactile stimuli. We found a suppressive interaction between cortical activations, when participants were instructed to discriminate or compare the tactile motion directions. This reflects the role of lateral inhibition in enhancing local spatial differences between sensory inputs from nearby regions of the receptor surface. Importantly, this suppressive interaction was reduced when participants had to average or combine the same stimuli. This suggests that the brain can strategically switch between a comparative and a combinative mode of somatosensory processing, according to the perceptual goal, by preparatorily adjusting the strength of a process akin to lateral inhibition.

## 2.1. Introduction

Functional perception involves at least two modes of perceptual processing: discrimination and integration. Sometimes we need to discriminate between stimuli based on specific details. For example, if you are an animal, being able to differentiate a predator from a tree trunk can be a matter of life and death. However, our normal experience of the world is not limited to merely contrasting one sensory input against another. Often our sensory experience consists of the synthesis of multiple inputs in a unified percept. Yet, historically, the starting point for describing sensory systems have generally been acuity and discrimination thresholds. While integration describes the maximal information that can be processed at a given time, acuity reflects the minimal units of sensory information required to identify a sensory input. Outside the tradition of Gestalt psychology (Gallace & Spence, 2011), where the focus is on how separate signals are represented as a part of a bigger whole, and multisensory integration (Ernst & Bühlhoff, 2004; Coa et al., 2019), where the focus is on integrating redundant sensory cues, the ability to combine distinct sensory cues into a unified event has remained relatively neglected.

Specifically, in touch, research has tended to focus on performance limits for perceiving a single stimulus (Weinstein, 1968; Mancini et al., 2014) and on the ability to discriminate between stimuli (Sherrick, 1964; Evans & Craig, 1991; Driver & Grossenbacher, 1996; Soto-Faraco et al., 2004; Tamè, Farnè, & Pavani, 2011; Rahman & Yau, 2019; Halfen et al., 2020). Considering that our everyday haptic experience involves dynamic interactions with objects and perception of a single object through multiple skin contacts, there is now a growing interest in the mechanisms that support the brain's capacity to combine multiple tactile inputs (Walsh et al., 2016; Kuroki et al., 2017; Cataldo et al., 2019), despite a limited processing capacity (Broadbent, 1958; Luck & Vogel, 1997; Gallace et al., 2006; Spence & Gallace, 2007).

In Chapter 1, we introduced the concept of long-range lateral inhibition between the cortical columns of the primary somatosensory cortex (S1) and how it may underlie masking effects that result in mutual inhibition between concurrently presented stimuli to adjacent regions of the skin (von Békésy, 1967). Although such a lateral inhibitory mechanism can be related to masking, it also should promote acuity and contrast detection. Classically, lateral inhibition between sensory neurons means that the firing of one cortical neuron tends to lead to inhibition of its neighbours. This arrangement makes neurons more sensitive to local variations in the stimulus than to uniformity in the stimulus, since the former results in less inhibition than the latter (Bakshi & Ghosh, 2017). For example, in a study of a drosophila visual system, Keleş and Frye (2017) found that blocking GABAergic inhibition resulted in reduced visual responses to a single moving object, and increased responses to a wide-field pattern

motion. In another study on a mouse olfactory system, Yokoi et al. (1995) showed that lateral inhibition facilitates odour discrimination by providing enhanced pattern separation for specific molecules within complex mixtures. However, even at higher levels in the brain, inhibition-like process can occur between similar semantic concepts so one will easily detect a difference between “astronomy” and “astrology” (Baars & Gage, 2010).

In the somatosensory system, Brumberg, Pinto, and Simons (1996) showed that lateral inhibition within the mouse barrel cortex served as a contrast enhancement mechanism, which during multi-whisker touch identified the principal whisker (i.e., the one with the strongest response). In a behavioral study of tactile acuity, Haggard, Christakou, and Serino (2007) found that viewing a task-irrelevant body part during location discrimination (whether tactile stimulus was more proximal or distal) not only improved discrimination performance, but also seemed to shrink the RFs that subserved the discrimination. That is, when participants were viewing a body part, distractors that were presented close to the tactile target become more effective, while distractors presented farther away become less effective, compared to when participants were viewing an object. This suggests that a spatial mechanism akin to lateral inhibition seemed to be driving the effect of vision on the body. Importantly, such a facilitatory effect of vision has been shown to spread to body parts that have adjacent representations in S1 (Serino et al., 2009), confirming that a lateral inhibition-like mechanism may act beyond individual neurons and function across cortical columns in S1. Consistently, if inhibitory interneurons extend to the level of cortical columns, they may represent the suppressive interactions between individual fingers (Forss, Jousmäki, & Hari, 1995), which is strongest for adjacent finger representations (Merzenich et al., 1978; Ishibashi et al., 2000). For example, Cardini, Longo, and Haggard (2011) found that viewing the body modulated the ERP measure of suppressive interaction between adjacent finger representations in early somatosensory cortex, and that the amount of suppression was predictive of tactile acuity.

In the visual system, lateral inhibition is one of the mechanisms that could contribute to a visual phenomenon called “repulsion”, which manifests as an exaggeration of contrast between two visual stimuli (Solomon, 2020). For instance, in a classical tilt illusion (Gibson, 1937; Clifford, 2014), “repulsive bias” reflects the exaggeration of the difference between the orientations of neighbouring Gabor patches, so that the target Gabor’s tilt is biased away from the orientation of flanker Gabors. Interestingly, Mareschal, Morgan, and Solomon (2010) showed that such repulsion occurs even when the distance between target and flankers exceeds the size of individual RFs, suggesting that lateral inhibitory process can spread across neighbouring RFs, exerting inhibitory influence on more distant neurons.

Based on these findings, it seemed reasonable to expect that lateral inhibition, or a suppressive mechanism between finger representation akin to lateral inhibition, would be particularly relevant for tasks requiring detection of contrast between tactile stimuli that are delivered concurrently to adjacent fingers. In contrast, as highlighted in Chapter 1, such inhibition would seem dysfunctional when concurrent sensory inputs from adjacent digits need to be combined to compute a synthesis of these inputs. This is because adjacent representations will tend to inhibit or interfere with one another, making it difficult to form precise and accurate representations of each stimulus, and thus distorting the aggregated percept. In fact, some researchers studying sensory processing in autism have noted that excessive lateral inhibition may hinder integrative processing leading to high sensitivity to details at the expense of an ability to integrate those details (e.g., Bertone et al., 2005; Gustafsson, 1997).

### *2.1.1. Measuring lateral inhibitory processes non-invasively in touch*

Lateral inhibition was traditionally demonstrated by a visual phenomenon such as Mach bands by Ernst Mach. In Mach bands continuous visual gradients are perceived as discontinuous due to the enhancement of contrast by lateral inhibition. In touch, masking effects are often taken as a demonstration of lateral inhibition mechanism (von Békésy, 1967; Haggard et al., 2007). It has been shown that an irrelevant stimulus (a masker) impairs perception of a target stimulus only if it falls within the neuron's RF that represents that target stimulus (Laskin & Spencer, 1979). In touch, masking occurs when a masker and a target are delivered to adjacent fingers (von Békésy, 1967; Harris *et al.*, 2001a; Tamè *et al.*, 2014). However, apart from direct neurophysiological recording studies (Laskin & Spencer, 1979; Dykes et al. 1984; DiCarlo et al. 1998; Brown et al., 2004; Mirabella et al., 2001) and behavioral approximations, non-invasive studies of lateral inhibition in humans are scarce.

Touch has provided a good model to index lateral inhibitory processes between S1 cortical columns non-invasively with EEG. Specifically, Gandevia, Burke, and McKeon (1983) found that the cortical potentials evoked by simultaneous stimulation of two adjacent digits had lower amplitude than the sum of potentials evoked by stimulating each digit individually. This underadditive aggregation of evoked responses was linked to (lateral) inhibitory processing (Gandevia et al., 1983; Hsieh et al., 1995; Ishibashi et al., 2000). Moreover, this suppressive interaction follows the somatotopic columnar organisation within S1 (i.e., underadditivity is stronger when stimulation is applied to adjacent skin regions such as index and middle finger relative to index and ring finger; Ishibashi et al. 2000; Ferrè, Sahani, & Haggard, 2016) and thus cannot be explained solely by response saturation (Severens et al., 2010).

In addition, this suppression has been found in several regions along the somatosensory pathway, with stronger interactions in the cortex than in brainstem or thalamus (Hsieh et al., 1995). Furthermore, such suppressive interactions have been found to vary with the functional state of the sensorimotor system (i.e., following the alteration to the boundaries of cortical sensory maps; Haavik-Taylor & Murphy, 2007; Cardini & Longo, 2016). Finally, Cardini and colleagues (2011) showed that the degree of suppression is not fixed but can be modulated by multisensory context. They observed stronger suppression when viewing one's own body than when viewing a neutral object in the same location. However, the tactile task they used was not varied in their study, and always involved acuity judgements for stimuli delivered to the index or middle finger. Thus, to our knowledge, the wider question of how tactile task requirements might influence suppressive somatosensory interactions has not previously been considered.

### *2.1.2. Experiment 1: Aims and hypothesis*

In this chapter we present the first experiment of this thesis, which investigated whether the EEG measure of somatosensory suppression (Gandevia et al., 1983; Hsieh et al., 1995; Ishibashi et al., 2000) was modulated as a function of the requirements of a perceptual task. Specifically, we predicted that switching from comparing inputs to combining them will require neural control over the strength of lateral inhibition. To examine this possibility, we developed a completely novel tactile perception task that allowed us to probe combine vs. compare modes in the somatosensory system. Namely, we asked participants to judge the *average* motion direction of tactile motion trajectories delivered simultaneously to index and middle fingertips. To contrast the neural mechanisms engaged during unified perception to those engaged during more widely researched acuity-focussed perception, the same participants were asked, in a separate task, to compare the same tactile stimuli to identify differences between the tactile motion directions.

Averaging two distinct sensory cues is a form of cue integration. However, while the main aim of cue integration is to form a maximally reliable new percept (Ernst & Bühlhoff, 2004), the main aim of averaging is to extract overall gist information (Whitney & Yamanashi Leib, 2018; see **section 1.2.6**). In an averaging task, optimal performance requires participants to allocate equal weights to both cues. Suppressive interactions between finger representations would not be functional for averaging as these may induce biases in the weighting process. In contrast, because lateral inhibitory mechanisms have been suggested to amplify differences (Solomon, 2020), it would be beneficial for detecting small differences between stimuli.

The interaction between cortical representations of the stimulated digits was measured immediately before presentation of tactile stimuli that participants either compared or

combined. This allowed probing the preparatory tuning of the inhibitory mechanism. Our hypothesis was that the task instruction would lead to strategic top-down modulation of the state of suppressive interactions, in expectation of either comparing stimuli, or combining them. In other words, the brain might prepare the appropriate mode of processing in advance of stimulation, by tuning circuits in somatosensory cortex accordingly.

## **2.2. Methods**

### *2.2.1. Participants*

We could not perform a formal power calculation as there have been no studies that have reported an effect size for the effect of tactile task on EEG measures of somatosensory suppression. Cardini et al.'s (2011) study has been the only one looking at the modulation of EEG measures of somatosensory suppression, but from a multisensory perspective. They obtained a large effect size ( $d = .86$ ) with  $n = 15$ . Therefore, we considered it to be reasonable to use the same sample size as Cardini et al.'s study. Of the 15 volunteers (aged 20 to 39 years with mean age of 24.5) 9 were women. All participants were reportedly right-handed and reported normal or corrected-to-normal vision and no abnormalities of touch. They all provided a written consent. Procedures were approved by the University College London (UCL) research ethics committee and were in accordance with the principles of the Declaration of Helsinki.

### *2.2.2. Perceptual multi-touch motion task*

Participants were asked to either discriminate or compare the directions of the two stimuli, by reporting the magnitude of the directional discrepancy between them (comparison task), or to average or combine the two stimuli by reporting their average direction (combination task; see **Figure 2.1A**). Importantly, the tactile stimuli were identical in both tasks and different task instructions were used to make participants adapt the two modes of processing. The tasks were performed in alternating counter-balanced blocks, four blocks per task.

In each trial, after the electrical stimulation, both probes were moved simultaneously along both right index and middle fingertips in pre-specified directions. In the comparison task, participants had to identify whether the discrepancy was zero ( $0^\circ$ ), moderate ( $10^\circ$ ), or large ( $20^\circ$ ). In the combination task, participants were required to report whether the average direction was more to the left from straight ahead ( $-10^\circ$ ), straight ahead ( $0^\circ$ ), or more to the right from straight ahead ( $10^\circ$ ). The response was given after tactile motion stimulation by pressing a corresponding key with their left hand. Responses were unspeeded, and no feedback was given. In total, participants completed 180 trials per task.

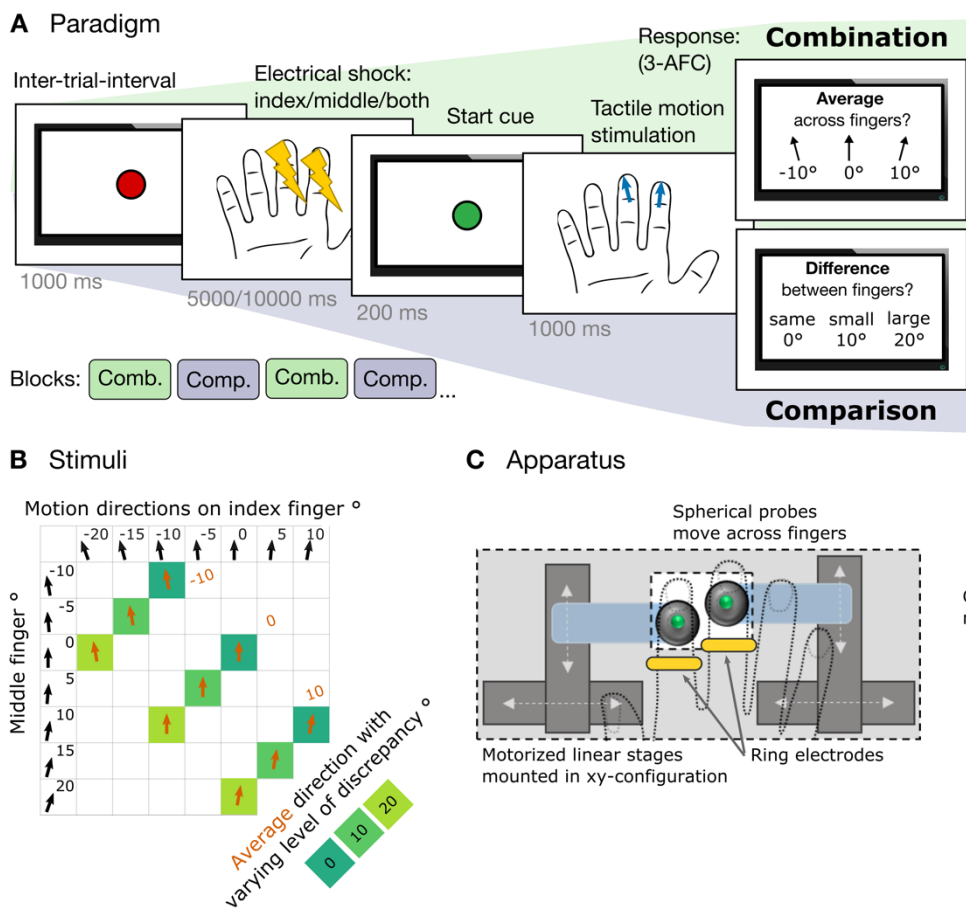


**Figure 2.1. Experiment 1: paradigm, tactile stimuli, and apparatus.** **A)** Combination and comparison tasks were performed in alternating blocks. In the combination task, participants averaged two tactile motion trajectories, whereas in the comparison task, they discriminated between the trajectories. Prior to tactile motion stimuli, mild digital nerve shocks were delivered to the to-be-stimulated fingers to reveal preparatory somatosensory-evoked activity. **B)** Nine different pairs of tactile motion stimuli produced three average direction patterns ( $-10^\circ$ ,  $0^\circ$ ,  $10^\circ$ ) with three levels of discrepancy ( $0^\circ$ ,  $10^\circ$ ,  $20^\circ$ ). Stimuli were identical in both tasks. **C)** Motorised linear stages produced continuous tactile motion along the fingertips. The apparatus was covered by a box with a small aperture. To-be-stimulated fingertips were positioned over the aperture, and secured with foam padding. The aperture and the hand were then covered with a computer screen. Digital nerve stimulation was delivered via a pair of ring electrodes.

### 2.2.3. Apparatus and tactile motion stimuli

The tactile apparatus consisted of two spherical probes (4 mm diameter) attached to two stepper linear actuators (Haydon Kerk Motion Solutions 15000 series, model LC1574W-04) that were fixed to two motorised linear stages (Zaber X-LSM100B, Zaber Technologies Inc., Canada) mounted in an XY configuration (**Figure 2.1C**). The actuators were controlled by a microcontroller (Arduino) and were moved up and down to let the probe make static contact with the skin at the start of tactile stimulation and retract after the end of stimulation. The linear stages were controlled by custom Matlab scripts that allowed the probe to be moved in predefined trajectories. The apparatus was covered by a box with a small aperture. The to-be-stimulated right index and middle fingertips were positioned over the aperture, and secured

with foam padding. Participants rested their right hand in a fixed palm-down position, so that, through the aperture, the probes lightly touched the centre of their index and middle fingertips.

The force with which the probes touched the fingers was equal to the weight of the resting finger. For a typical participant this was approximately  $8.4 \pm 0.6$  g (mean  $\pm$  SD; measured outside of the experiment, SD refers to variation between 4 measuring sessions). Although we did not employ an automated force control mechanism, a webcam was placed under the apparatus to have a continuous observation over the finger placement and contact. The distance between the fingers was approximately 25 mm. The hand was then covered with a screen, so that the probes could not be seen.

Continuous motion along the fingertips was created by moving the probes at preselected angles ranging from -25 to 25 degrees to the distal-proximal finger axis in 5° steps, at a constant speed of 10 mm/s. The movement of each probe was controlled individually allowing for delivery of trajectories with varying discrepancy simultaneously along both fingertips. **Figure 2.1B** shows 9 possible combinations of 7 individual directions delivered simultaneously to two fingers. The combinations produced three different average motion patterns (-10°, 0°, or 10° from straight ahead), with varying levels of discrepancy (0°, 10°, or 20°) between the two stimuli. The duration of each trajectory was approximately 1 s and the distance travelled was 10 mm.

At the beginning of each trial, the probe was advanced to make a static contact with the fingertip. The initial position of the probe was jittered across trials (-2.0, 0.0, or 2.0 mm from the centre of the fingertip) to discourage using memory for locations as a proxy for direction. After each trajectory, the probe was immediately retracted and returned to its starting position. The sound made by the apparatus was masked with white noise continuously playing over headphones. Note that the same apparatus and tactile motion stimulation was used through the experiments presented in Chapters 2 to 5, but with a larger repertoire of trajectories, and a different way participants responded to the stimuli.

#### *2.2.4. Digital nerve stimulation to evoke somatosensory activity*

To elicit somatosensory-evoked activity electrical stimulation was delivered via a pair of ring electrodes placed over the distal phalanges of the right index and middle fingers with a cathode 1 cm proximal to the anode, at a rate of 2 Hz. Individual sensory detection thresholds for electrical shocks were determined prior to the main experiment with a method of limits. Reversals occurred after participants detected the stimulus twice in a row, resulting in stimulus intensity that corresponded to a 70% detection. Stimulation was delivered with a neurophysiological stimulator (Digitimer DS5 stimulator) as a square-wave pulse current, each



pulse lasting 0.2 ms. In the main experiment, stimulation was produced at intensity 1.4 times higher than the individual sensory threshold. In each trial either the index finger, the middle finger, or both fingers were randomly stimulated. Brain activity elicited by stimulating index and middle finger in isolation provided a predicted sum of activity (index + middle) under the assumption of no suppression. If suppression occurred, actual activity during double-stimulation (both) would be reduced compared to the sum of individual stimulations. The electrical stimulation occurred before the tactile motion stimuli to reveal the preparatory tuning of somatosensory cortex. The number of electrical pulses was randomly varied (10 or 20) to make the timing of tactile motion onset partly unpredictable, thereby encouraging participants to maintain preparedness for the tactile motion task. In total, there were 900 electrical stimuli delivered for each stimulation condition (index, middle, or both) per task.

### *2.2.5. Electroencephalographic (EEG) recording and pre-processing*

EEG was recorded from 17 scalp electrodes (Fp1, Fp2, AFz, F3, F4, C5, C3, Cz, C4, C6, CP5, CP3, CPz, CP4, CP6, O1, O2) using a BioSemi ActiveTwo system. Horizontal electro-oculogram (EOG) recordings were made using external bipolar channels positioned on the outer canthi of each eye. Reference electrodes were positioned on the right and left mastoids. EEG signals were recorded at a sampling rate of 2048 Hz. A trigger channel was used to mark the timing of electrical shocks. Data were preprocessed in Matlab with EEGLAB toolbox (Delorme & Makeig, 2004) and ERPLAB toolbox (Lopez-Calderon & Luck, 2014). Data were re-referenced to the average of the mastoid electrodes, subjected to high-pass (0.5 Hz) and low-pass (30 Hz) filtering. A short baseline (50ms) was used because the electrical pulse occurred every 500ms. Thus, a longer baseline may have contained late ERP components from the previous pulse. A high-pass filter of 0.5 Hz was used because the main focus of the study was the neural response to each pulse, and the pulses occurred at 2 Hz. Any lower frequency components would represent drift from one pulse to another.

Epochs of 250 ms were extracted spanning from 50 ms before each shock to 200 ms after shock onset. For each epoch, signal between -1 and 8 ms relative to electric shock onset was linearly interpolated in order to remove electrical artifact (Cardini et al., 2011; Cardini and Longo, 2016). Epochs were then baseline corrected to the first 50 ms. Trials with eyeblinks (HEOG left and right channels exceeding  $\pm 80$  mV) or with voltage exceeding  $\pm 120$  mV at any channel between -50 and 200 ms relative to each shock were eliminated. The mean percentage of trials rejected was  $24.1\% \pm 11.5\%$  (mean  $\pm$  SD) in the combination task and  $23.8\% \pm 10.9\%$  in the comparison task. There were no significant differences in the number of rejected trials between tasks ( $p = .70$ ) nor between stimulation conditions ( $p = .88$ ). Grand average SEPs were

computed separately for the two tasks (comparison and combination) and electrical stimulation conditions (index-alone, middle-alone, both).

### 2.2.6. Statistical analysis

We expected the suppressive effect to arise within the P40 component (Biermann et al., 1998; Ishibashi et al., 2000; Cardini et al., 2011), which reflects the afferent volley and first processing wave within somatosensory cortex. Scalp topographies of P40 showed a positive parietal peak and a reversed polarity over frontal channels (**Figure 2.3A**). This reversal across the central sulcus is consistent with prior reports of this component (e.g., Cardini et al., 2011), and is a marker of SI processing (Allison et al., 1989). Accordingly, we analysed the mean SEP amplitudes between 20 to 60 ms following digital shock onset. The time-window was chosen after visual inspection of grand-averaged waveform pooled across all stimulation conditions. Previous studies have tended to see a slightly later onset of the P40 component, starting at 40 ms after stimulation (Cardini et al., 2011; Cardini & Longo, 2016; Gillmeister & Forster, 2012). In the present study, the component started slightly earlier around 20 ms after stimulation. We ended our time-window at 60 ms, because from there P40 started to overlap with N70. Thus, we chose the 20 to 60 ms time-window that encompassed the whole component around the peak at 45 ms. The mean SEP amplitudes between 20 to 60 ms were acquired per participant ( $n = 15$ ) for each stimulation condition (index, middle, both), separately for combination and comparison tasks.

Based on index and middle SEP amplitudes, we calculated the predicted sum under the assumption of no suppression (index + middle). If suppression occurred, SEP amplitudes during double-stimulation (both) would be significantly reduced compared to predicted sum of individual stimulations (under-additivity). Shapiro-Wilk test of normality indicated that all measures did not significantly deviate from a normal distribution (all  $p$  values were  $.12 < p < .96$ ). Thus, the amplitudes were fit into a repeated-measures ANOVA with factors task (combination vs. comparison) and stimulation (both vs. index + middle). Significant interaction would indicate differential somatosensory activation between tasks. The interaction would be followed-up by simple effects analysis comparing stimulation condition across tasks.

To compare suppression between tasks, we calculated a “Somatosensory Suppression Index” (SSI), defined as the difference in amplitude between the arithmetic sum of potentials evoked by two individually stimulated fingers and the potentials evoked by simultaneous stimulation of two fingers (Cardini *et al.*, 2011). The SSI was calculated with the following equation:  $SSI = \text{Index alone} + \text{Middle alone} - \text{Combined}$ . Higher values of SSI indicate stronger suppression within the somatosensory system. A paired- sample t-test was employed to

compare SSI between comparison and combination tasks, because there was no significant deviation from normality (Shapiro-Wilk test:  $p = .81$ ).

Behavioural performance was quantified as the accuracy to choose the correct average (in combination task) or correct difference (in comparison task) from three options. Accuracy was then compared across tasks with paired-sample t-test, because there was no significant deviation from normality (Shapiro-Wilk test:  $p = .52$ ).

## 2.3. Results

### 2.3.1. Behavioural analysis

**Figure 2.2A** shows a confusion matrix with the mean proportion of each response as a function of the actual directional difference (comparison task) or average direction (combination task). Overall accuracy was greater in the combination task (56% correct, SD= 9%) relative to the comparison task (47% correct, SD = 8%). Because the task involved 3-alternative forced choices, participants performance was well above chance level in both tasks (33%). However, the difference between performance on the two tasks was significant (paired-sample t-test:  $t(14) = 3.5$ ,  $p = .004$ ,  $d = .90$ ). Previous studies have also found that somatosensory aggregation tends to produce better performance than discrimination (Cataldo et al., 2019), possibly reflecting that the aggregate can be derived even when discrepancy between stimuli is unclear. Performance between the tasks was not correlated across participants ( $r = .20$ ,  $p = .47$ ), showing no evidence for a common computational factor underlying individual differences in performance.

We also wished to ensure that in the combination task, participants actually attempted to average the two tactile motion trajectories instead of using some strategic rules, such as “one stimulus left, and one straight: therefore left”. If they did use such a rule, then their performance should have been near perfect. Also, participants would have needed to learn such a strategy as they progressed through the experiment, so performance should have gotten better as the experiment progressed. Thus, we examined performance as a function of block with a linear contrast analysis (**Figure 2.2B**). The analysis yielded a non-significant effect in the combination task ( $t(42) = 1.77$ ,  $p = .08$ ), but a significant effect in the comparison task ( $t(42) = -5.8$ ,  $p < .001$ ). However, in the comparison task, instead of increasing, performance seemed to drop in the 3rd block, which is inconsistent with participants learning a strategy. Thus, this block-by-block performance analysis suggests that it is unlikely that participants were using learned strategies.

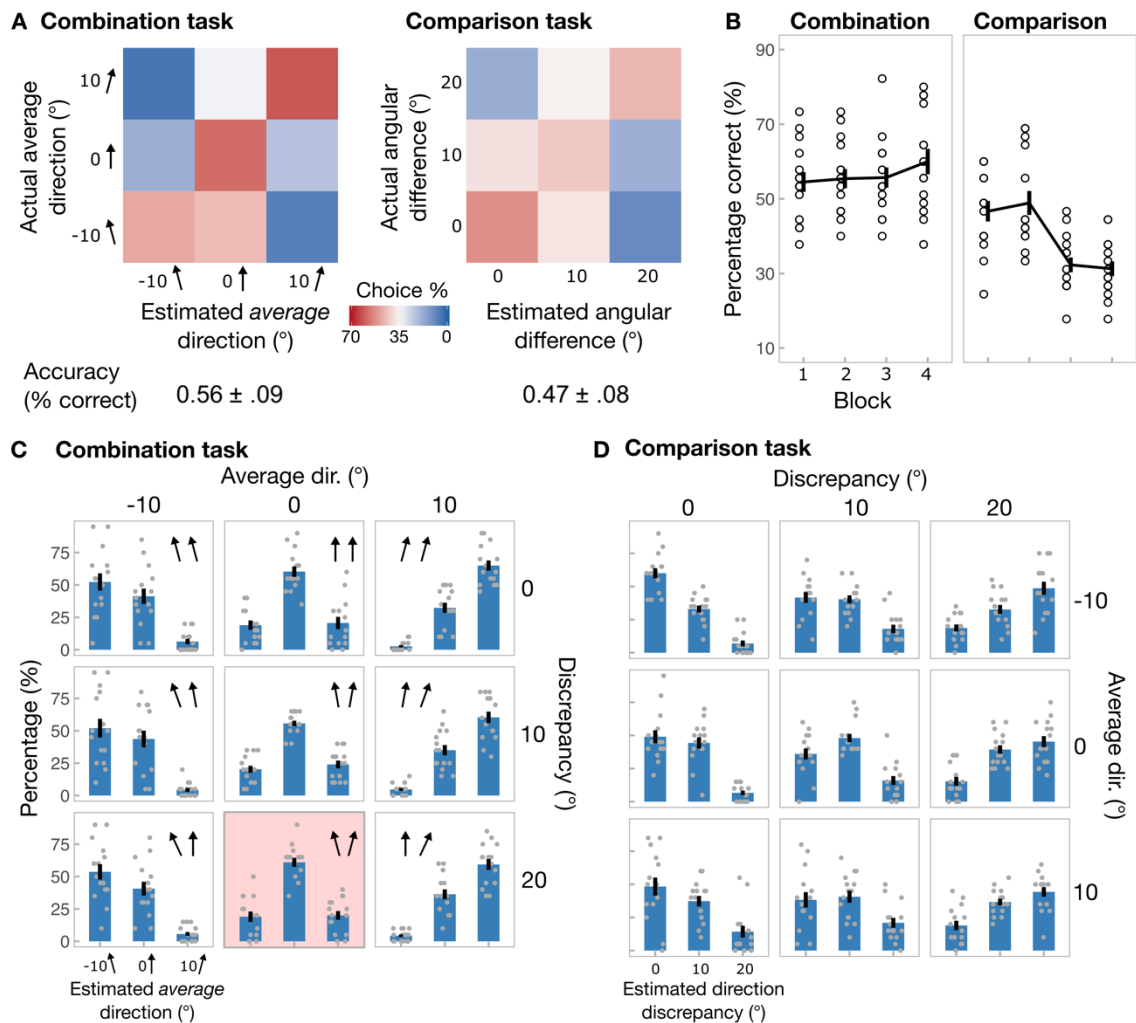


**Figure 2.2. Experiment 1: behavioural results.** **A)** Confusion matrices illustrate the group-mean percentage of choosing one of three response choices as a function of correct response. Participants were more accurate in combination task (right panel) compared to comparison task (left panel;  $p = .004$ ). **B)** Accuracy as a function of task block. Dots represent each participant's data and error bars represent SEM. **C)** Response distribution in the combination task for each combination. The highlighted cell shows the combination where stimuli on both fingers could be "correct" if participants just selectively attended to either finger instead of averaging them. Dots represent each participant's data and error bars represent SEM. **D)** Response distribution in the comparison task for each combination.

Furthermore, we inspected the errors in participants' judgements more closely. **Figure 2.2C** shows the distribution of responses in the combination task for each combination. First, we looked at the combination where the true average direction was straight ahead ( $0^\circ$ ), but direction on the index finger was to the left ( $-10^\circ$ ) and direction on the middle finger was to the right ( $10^\circ$ ) (the highlighted cell on **Fig. 2.2C**). This is an important combination, because stimuli on both fingers could be "correct" if participants just selectively attended to either finger instead of averaging them. If that was the case, they would have been as likely to choose the left ( $-10^\circ$ ) or the right ( $10^\circ$ ) as the correct straight ahead ( $0^\circ$ ) direction. Yet, most responses were correct, indicating that participants were not merely selecting either finger, but considering both stimuli during their averaging judgements.

Moreover, by looking at the errors in trials where the actual average was either left or right, it is apparent that most errors on these trials were largely due to confusion with straight ahead average direction. Interestingly, this confusion was similar across all discrepancy levels. Meaning that participants were as likely to confuse  $-10^\circ$  with  $0^\circ$  when discrepancy was  $10^\circ$  as when it was  $20^\circ$ . Yet when discrepancy was  $10^\circ$  both stimuli were tilted towards the correct response. Thus, if participants were using strategic rules mentioned above, they had more evidence on these  $10^\circ$  discrepancy trials for a left response. However, it seems that participants, if anything, tended to under-weight the more eccentric stimulus. Overall, these patterns of responses are inconsistent with the use of some simple strategy and, thus, give us more confidence that participants were attempting to combine the two directions, although in a slightly biased manner.

Lastly, **Figure 2.2D** shows the response distributions in the comparison task for each combination. Considering the frequency of choosing  $0^\circ$  discrepancy even when the actual discrepancy was  $20^\circ$ , it seems that the errors occurred due to a difficulty in detecting discrepancy between the directions. Although participants seemed to be better at identifying the similarity between the directions (mean % correct for discrepancy  $0^\circ = 52$ ,  $SD = 21$ ) rather than the difference (mean % correct for discrepancies  $10^\circ = 43$ ,  $SD = 14$ , and  $20^\circ = 46$ ,  $SD = 16$ ), the accuracy (% of choosing the correct response) was similar across different combinations both in terms of average direction ( $F(2,28) = 1.23$ ,  $p = .31$ ,  $np^2 = .08$ ) and discrepancy ( $F(2,28) = 2.24$ ,  $p = .23$ ,  $np^2 = .14$ ). This means that task difficulty did not significantly differ across different discrepancies and thus errors in the comparison task were not solely due to an inability to detect stimulus discrepancy.

### 2.3.2. EEG results

We analysed EEG data time-locked to digital nerve shocks, which were delivered immediately before tactile motion stimuli to reveal the somatosensory activity during preparation to either combine or compare the tactile stimuli. **Figure 2.3A** shows the grand mean EEG response (somatosensory-evoked potentials; SEPs) pooled across electrodes that lay over contralateral somatosensory cortex (C3, C5, CP3, and CP5). Our main interest was the suppressive interaction between digit representation within the P40 component, which is accurately reflected on scalp topographies as a positive parietal peak with a reversed polarity over frontal channels (**Figure 2.3A** lower panels). Suppressive interaction is defined as the amplitude reduction for combined stimulation relative to the sum of the amplitudes for individual finger stimulation. To investigate this suppression quantitatively, we first summed the amplitudes for individual index and middle finger stimulations (purple line on **Figure 2.3A**). This

effectively provides a prediction of the amplitude for combined stimulation under a hypothesis of no somatosensory suppression (i.e., perfect additivity).

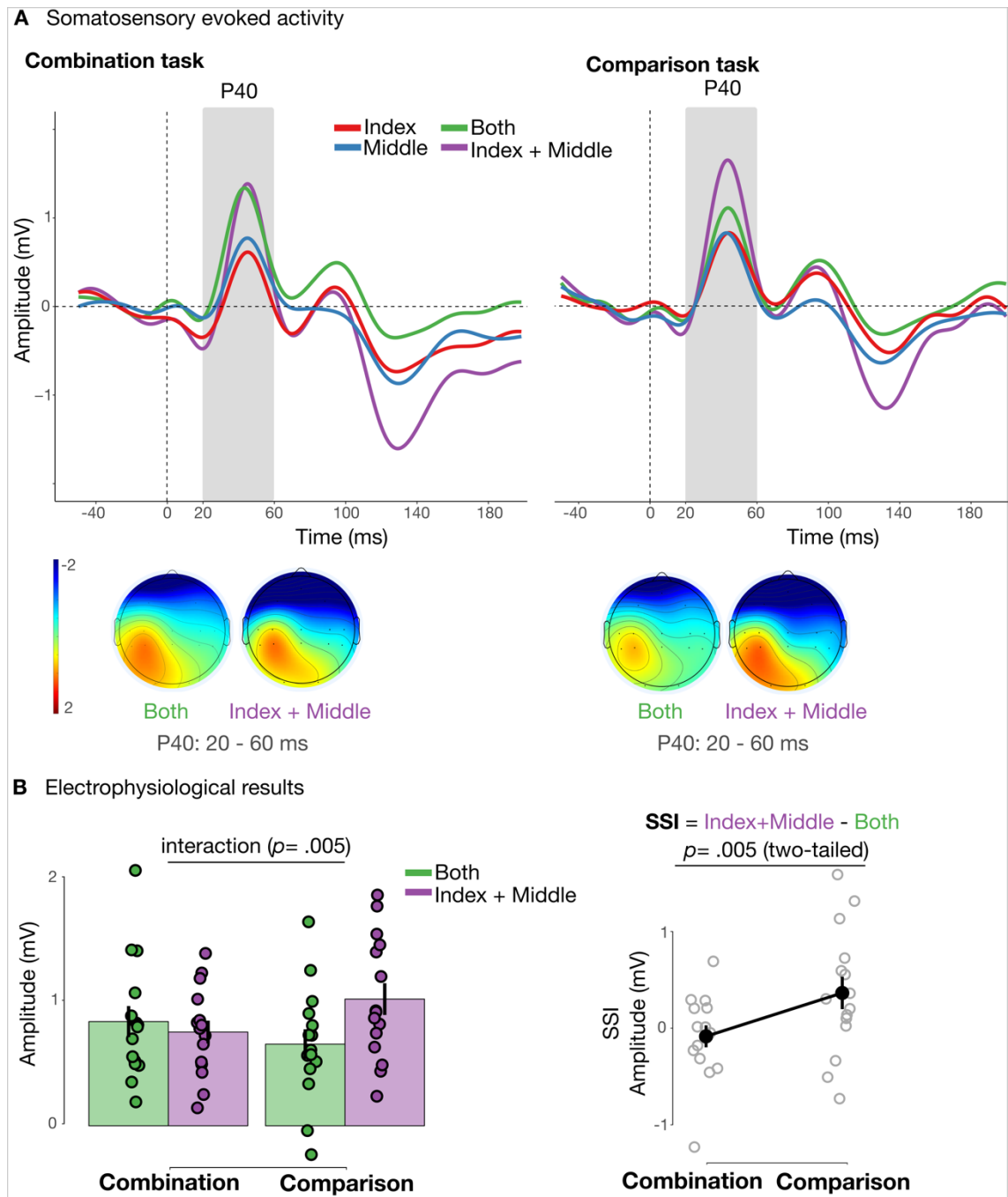


**Figure 2.3. Experiment 1: EEG results.** **A**) ERP waveforms show grand averaged SEPs separately when shocking index finger (red), middle finger (blue), and both (green) fingers simultaneously. In addition, it shows the sum of individual stimulations (purple) that reflects the predicted amplitude for double-stimulation under the assumption of no suppression. The waveforms represent pooled activity across contralateral somatosensory electrodes (C5, C3, CP5, CP3). The grey shaded area shows the analysis time-window that corresponds to P40 component (20 to 60 ms relative to shock onset). Topographic maps show mean activity in the P40 component. **B**) Right panel shows mean amplitudes for actual double-shock stimulation (green) and predicted double-shock stimulation under assumption of no suppression (purple) separately for combination and comparison tasks. Dots are single participants' amplitudes and error bars represent SEM. Left panel shows mean calculated SSI (index + middle - both) and its difference between tasks. Grey dots are single participants' SSI with error bars representing SEM.

We then performed a 2-by-2 repeated measures ANOVA with factors task (combination vs. comparison) and stimulation (both vs. summed-index-and-middle) on the mean amplitudes within the 20 to 60 ms time-window (**Figure 2.3B** left-side panel). The main effects of task ( $F(1, 14) = .45, p = .52, \eta^2 = .03$ ) and stimulation ( $F(1, 14) = 1.23, p = .29, \eta^2 = .08$ ) were not significant. As predicted, the analysis yielded a significant interaction ( $F(1, 14) = 10.78, p = .005, \eta^2 = .44$ ), indicating that the degree of under-additivity varied between the tasks. Importantly, the interaction remained significant after controlling for differences in behavioural performance between the tasks ( $F(1, 13) = 13.34, p = .003, \eta^2 = .51$ ), suggesting that the differences in underadditivity between tasks were not simply due to differences in task difficulty. Indeed, given the assumption of a linear relation between performance and S1 responses, the true effect of task on somatosensory underadditivity may be *larger* than suggested by the uncorrected means data shown in **Figure 2.3B**.

We further explored the significant interaction using simple effects analysis. It showed that in the combination task, amplitudes to double-stimulation were similar to amplitude to summed-index-and-middle stimulation ( $F(1) = .55, p = .47$ ), whereas in comparison the task, the difference between amplitudes to double-stimulation relative to summed-index-and-middle stimulation became larger ( $F(1) = 1.0, p = .05$ ). This supported the predicted shape of the interaction. Simple effects analysis was not Bonferroni-corrected, because it was not used to draw any additional inferences, but merely to describe the shape of the significant interaction.

To compare the magnitude of underadditivity between tasks, we calculated the SSI (index + middle – both) separately for the comparison and combination task (**Figure 2.3B** right-side panel). A paired-sample t-test revealed greater SSI in the comparison task (mean SSI = 0.36, SD = 0.65 mV) than in combination task (mean SSI = -0.08, SD = 0.44 mV) ( $t(14) = 3.28, p = .005, d = .85$ ; **Figure 2.3B**). Thus, somatosensory suppressive interactions between stimulated digits were modulated according to the specific perceptual task.

### 2.3.3. EEG results without low-pass filter to identify earlier components

Although the focus of our analysis was the P40 component, because inter-finger suppression has not been found to affect earlier components such as N20 (Forss et al., 1995; but see Ishibashi et al., 2000), a recent study showed that important trial-by-trial dynamics can occur as early as 20 ms after tactile stimulus onset (Stephani et al., 2020). Our 30 Hz low-pass filter could have concealed the rapid early components. Therefore, we re-ran our EEG preprocessing without any low-pass filter to maximise the opportunity of detecting early components. **Figure 2.4** shows the resultant waveforms, which clearly demonstrate an early component in the 20 – 25 ms time-window with a peak at 23ms (-.35 mV at the peak, when data was pooled across

tasks). We ran a similar 2 x 2 rmANOVA analysis on this N23 component as for the P40 component to identify whether the task-related modulation occurred at this earlier time-window. However, the task by stimulation interaction was not significant ( $F(1, 14) = .55, p = .47, \eta^2 = .04$ ). The main effects of task and stimulation remained non-significant as well ( $F(1, 14) = 3.7, p = .07, \eta^2 = .21$  and  $F(1, 14) = .25, p = .62, \eta^2 = .02$ , respectively). For consistency, we also analysed the unfiltered P40 component, but starting from 25 ms rather than 20 ms to not overlap with the N23 component. The analysis yielded a significant interaction ( $F(1, 14) = 6.7, p = .02, \eta^2 = .32$ ) with simple effects showing a significant suppression in comparison ( $F(1) = 13.6, p = .002$ ), but not in combination task ( $F(1) = 0.14, p = .72$ ). The main effects of task and stimulation were not significant ( $F(1, 14) = 1.5, p = .25, \eta^2 = .10$  and  $F(1, 14) = 3.3, p = .09, \eta^2 = .19$ , respectively).

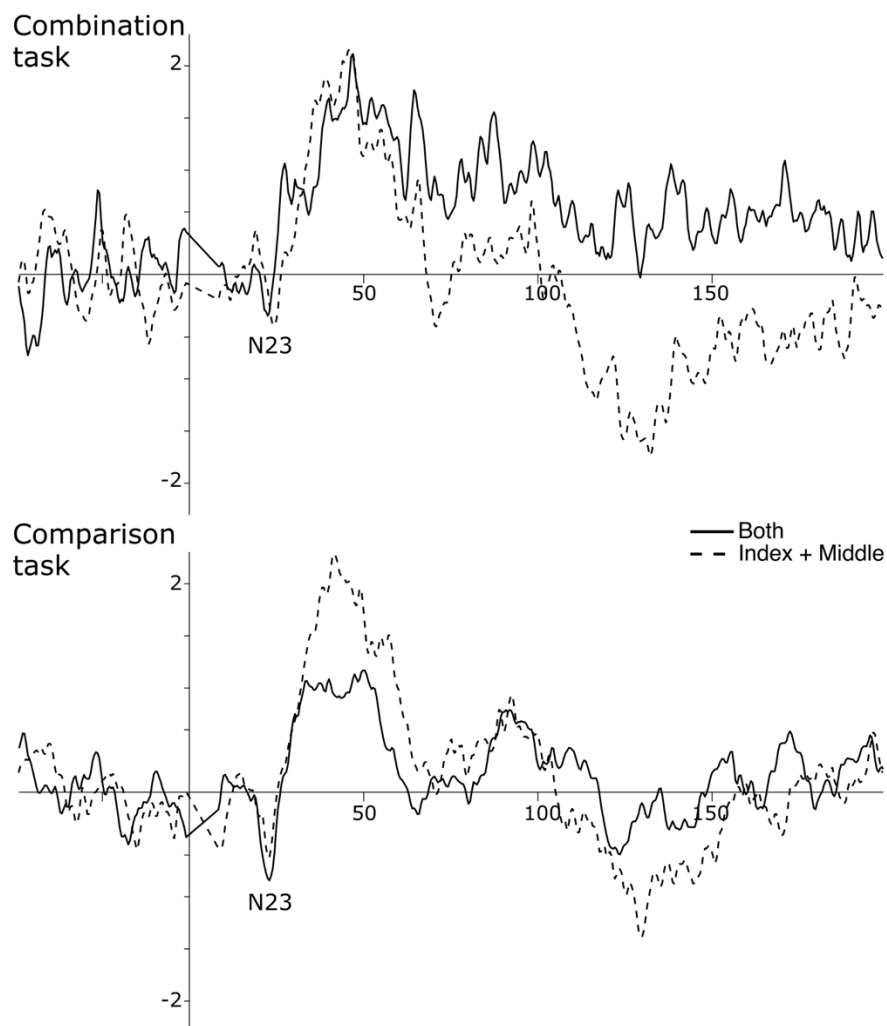


**Figure 2.4. Experiment 1: EEG result without low-pass filter.** Upper panel displays combination task while lower panel displays comparison task. Solid line represents the grand-average of trials, where both fingers (index & middle) were simulated simultaneously. Dashed line shows the grand average of the sum of individual simulations, which represent the predicted amplitude under the assumption of no suppression. The waveforms represent pooled activity across contralateral somatosensory electrodes (C5, C3, CP5, CP3).



### 2.3.4. Relationship between EEG activity and response accuracy

One could expect the magnitude of suppressive interaction between index and middle fingers to predict the performance on the tasks. Specifically, in the comparison task greater SSI should precede correct responses, whereas in the combination task, the opposite could be true – lesser SSI should precede correct responses. To examine these predictions, we divided the EEG trials that were used in the main analysis (i.e., with the 30 Hz low-pass filter) based on whether they preceded a correct or incorrect response (**Figure 2.5**). We then analysed the magnitude of SSI as a function of task and accuracy with a 2x2 rmANOVA. This analysis yielded a main effect of task ( $F(1, 14) = 28.5, p < .001, \eta^2 = .67$ ), which shows the difference of SSI between tasks, and a main effect of accuracy ( $F(1, 14) = 6.3, p = .03, \eta^2 = .31$ ), indicating that SSI varied depending on whether it led to a correct or incorrect response. We also found a significant interaction ( $F(1, 14) = 14.1, p = .002, \eta^2 = .50$ ), suggesting that the effect of accuracy on SSI was modulated according to the task. However, the direction of that interaction was inconsistent with our hypothesis. In particular, simple main effects analysis showed that while in the comparison task, SSI remained constant between correct and incorrect responses ( $F(1) = .14, p = .71$ ), in the combination task, greater SSI led to correct responses (mean SSI =  $-.02, SD = .60$  mV vs. mean SSI =  $-1.7, SD = 1.1$  mV;  $F(1) = 11.7, p = .003$ ). However, because of unequal number of trials between and incorrect responses across comparison and combination tasks, the number of correct trials in the combination task was greater than that in the comparison task.

When we pooled the data across the tasks the waveform showed possible differences between correct and incorrect responses in later time windows following P40. Therefore, we ran a similar but purely exploratory analysis on the following time windows: 60 - 80 ms, 80 - 100 ms, 100 - 150 ms. None showed any significant main effects of task ( $p$  values  $.13 < p < .42$ ), accuracy ( $p$  values  $.37 < p < .90$ ) or significant interaction ( $p$  values  $.10 < p < .92$ ). The difference in the double-shock response preceding either correct or incorrect response also did not reveal any significant effects.

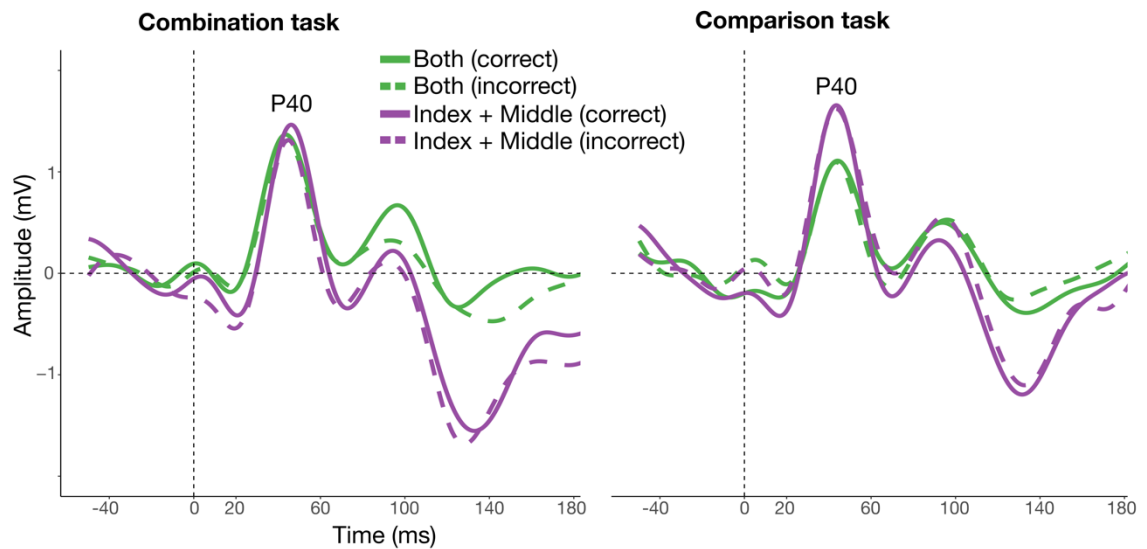


**Figure 2.5. Experiment 1: EEG result according to response accuracy.** The left-side panel displays the combination task while the right-side panel displays the comparison task. Purple lines show the sum of individual stimulations that reflect the predicted amplitude for double-stimulation under the assumption of no suppression. Green lines show the actual response to double-stimulation. Solid lines represent EEG response that preceded correct responses, while dashed lines show the response preceding the incorrect response. The waveforms represent pooled activity across contralateral somatosensory electrodes (C5, C3, CP5, CP3).

## 2.4. Discussion

The present EEG study was conducted to examine a probable mechanism that might switch between two distinct perceptual modes of tactile sensory processing: integration and discrimination. Based on previous literature pointing to a relationship between tactile acuity and inhibitory process within somatosensory cortex (Haggard et al., 2007; Cardini et al., 2011), we focussed on the EEG measure of this inhibitory mechanism. Specifically, we hypothesised that this suppressive mechanism might not be fixed but could be strategically adjusted when the task requires integration instead of discrimination. Our results supported that prediction. When participants compared stimuli on the two fingers, suppressive interaction between neural digit representations was stronger relative to when they combined stimuli across both fingers to extract an average. Importantly, both comparing and combining required processing information from both digits, so the difference between tasks is not merely in attentional selection. Rather, the tasks differed in their post-selection processing. Our results suggest that the neural circuitry of sensory systems may be tuned to extract differences in comparison mode, or to extract consistent overall features in combination mode. Switching between these processing modes may involve adjusting the gain of local inhibitory circuits.

### 2.4.1. Considerations for the task design

We believe that the underadditivity between EEG responses to double-digit stimulation found in the present study reflects the lateral inhibitory mechanism in early somatosensory

cortex. However, a common criticism of the underadditive EEG interaction is that, in principle, it may simply reflect a ceiling effect, rather than a specific inhibitory process. Suppressive interaction between digits is defined as the underadditive difference between the EEG response to double-digit stimulation and the summed response of individual digit stimulations. However, this underadditivity may arise due to increased stimulus energy in the double-shock condition. To avoid this, we used very mild electrical stimulation just above detection threshold.

Moreover, Severens and colleagues (2010) reported the same underadditive interaction using a frequency-tagging method, which may avoid some of the interpretational concerns regarding ceiling effects. Importantly, they also found that the strength of that subadditivity was lower when double-shock was applied to non-adjacent fingers. A similar spatial gradient of EEG suppression was found by Hsieh et al. (1995) and Ishibashi et al. (2000). Ferrè et al. (2016) showed a similar somatotopic gradient for suppression arising from a subliminal stimulation. These results are consistent with the findings that lateral inhibitory connections have weaker influence with increasing somatotopic distance within S1 (Merzenich et al., 1978). Here, we did not test the spatial gradient of the suppressive interaction as we only stimulated adjacent fingers. However, even if some saturation similar to a ceiling effect were to be present in our data, we still observed a significant difference between two perceptual tasks in scalp responses evoked by identical stimuli. Thus, ceiling effects alone cannot readily explain our results.

We did find a significant difference in task difficulty, despite designing the tasks to have comparable levels of performance based on pilot testing. We do not believe the performance difference could have been the sole driver for the difference found in the underadditive EEG interaction, since including performance as a covariate did not abolish (and in fact strengthened) the difference between tasks. To avoid performance difference future studies should use an adaptive design, where stimuli is adjusted to balance the performance across tasks for each participant. Here, however, we wished to keep the stimuli identical across the tasks, so the difference in ERP response was purely due to task instructions and not different tactile stimuli.

We probed the inhibitory interaction occurring before participants felt the tactile stimulus as we wanted to reveal the preparatory tuning of somatosensory cortex in preparation for the tactile task. Another line of literature has focussed on the pre-stimulus neuronal states in terms of brain-wide oscillations. This extensive research has shown that pre-stimulus states affect stimulus-evoked activity (Pleger & Villringer, 2013; Reinacher et al., 2009; Iemi et al., 2019) and subsequent tactile processing (Craddock et al., 2017; Haegens, Händel, & Jensen, 2011). The reason we did not examine pre-stimulus state was because our pre-stimulus period (i.e., the period before the tactile motion stimuli) was occupied with a train of electrical stimulation. Therefore, our current design would have not allowed measuring pre-stimulus state

independently, because we were already probing the pre-stimulus activity with electrical stimulation. Moreover, although the magnitude of lateralisation of pre-stimulus alpha could have, in principle, showed us whether participants remained in a preparatory state prior to tactile motion stimuli (Heagens et al., 2011), we were not sure whether pre-stimulus oscillations could be shaped by task-specific modulations. In particular, it is questionable whether pre-stimulus frequency bands could distinguish unimanual inter-finger suppression. However, future studies should attempt to re-design the current paradigm into a bimanual design, which could allow using alpha lateralisation to predict the relative weighting of stimuli on either finger during combination or comparison. Yet, that would reflect a different type of process, not a lateral inhibitory mechanism, that was the main focus of the present study.

#### *2.4.2. The control mechanism that enables multi-touch integration*

In a recent study, Canales-Johnson and colleagues (2020) found that whether participants perceived bistable auditory streams as one integrated stream or two distinct streams was reflected in the coherence of the neural activity within frontoparietal cortices. Their results showed that integration vs. differentiation might be a global mode of coordination in fronto-parietal networks. Our study suggests that these putative modes are associated with different states of early cortical circuitry. Canales-Johnson *et al.*'s study relied on uncontrolled endogenous fluctuations in a bistable percept to switch between integrative/combining and distinct/comparison modes. Our study instead relies on strategic shifting, according to the current perceptual task. Together, our study and the result of Canales-Johnson et al. (2020) reveal that the higher cortical areas, such as frontoparietal networks, may be the source of the strategic signal that modulates early somatosensory cortical processing, adjusting the degree of inhibition, and thus the extent of observed underadditivity. In this view frontoparietal signal can act as a control mechanism over the sensory cortex and allows the switching between discrimination and integration.

Our concept of distinct perceptual modes for integrative vs. discriminative processing recalls similar distinctions in the visual attention literature. For instance, Baek and Chong (2020) recently proposed two modes of processing in visual perception: ensemble perception, whereby observers extract a combined quality across multiple stimuli, and selectivity, whereby observers discriminate a specific stimulus among others. They explained the difference between these perceptual modes using a mechanistic model of selective attention. Distributed attention allows the brain to extract the mean activity across a population of sensory neurons, whereas focussed attention narrows the activity profile down to a smaller population. Focussed attention might achieve this selection of a smaller subset of sensory neurons by increasing lateral inhibition to provide tighter tuning. However, it is important to note that our study was designed to keep the

attentional focus equal across the tasks. That is, our tasks always required processing information from both digits. In the comparison task, participants had to report the *exact* difference between the stimuli, whereas in the combination task they had to report the *exact* average between the stimuli. The pattern of results in the combination task confirmed that participants did successfully divide their attention between digits, rather than merely attending selectively to one digit. What differed between the tasks was the way in which information from one digit was related to information from another. Therefore, our discrimination/integration distinction cannot be explained by distinct attentional mechanisms. Instead, we believe that our tasks reflect different perceptual modes applied to attentionally selected tactile information.

We focussed specifically on lateral inhibition as the putative mechanism that enables the sensory system to be tuned to one of the processing modes. However, another mechanism that may regulate the balance between integration and discrimination is divisive normalization, which has been also considered a canonical neural computation (Carandini & Heeger, 2012; Rahman & Yau, 2019; Brouwer *et al.*, 2015). During divisive normalization, the response of a single unit is divided by the response of a population. This has a similar net effect to lateral inhibition, since it again emphasises local departures from the population mean, but it does not involve the explicit mechanism of inhibitory interneurons associated with lateral inhibition in the visual system. Several studies have shown that the brain can exert cognitive control over the parameters of divisive normalisation (Reynolds & Heeger, 2009), but these studies again suggest that this control is enabled via engagement of attentional mechanisms rather than distinct processing modes. We believe that selecting which processing mode is performed may involve adjusting inhibitory links, normalization pools, or both.

#### *2.4.3. The control mechanism affects early somatosensory cortex*

The focus of the current study was the P40 component, because it is considered a marker of S1 processing (Allison *et al.*, 1989). In a previous study on inter-digit EEG suppressive index, Cardini *et al.* (2011) did not observe a significant suppression at later components, such as the N140, which might be generated in more frontal areas (Allison *et al.*, 1989). In addition, in a slightly different paradigm, Forss *et al.* (1995) showed that the suppression from sequentially presented distractor stimulus did not affect earlier components, such as the N20. However, because N20 is also believed to originate from S1 (Allison *et al.*, 1989) and has been shown to be important for tactile processing (Stephani *et al.*, 2020), we analysed the suppression for N20 in unfiltered EEG data. Nevertheless, our analysis did not detect any task-specific modulations of somatosensory suppression in the N20 time-window that were found for the P40. A potential explanation could be that task information is processed at the later processing stage. Indeed, the N20 is believed to reflect the arrival of the thalamocortical volley into the area

of 3b, whereas P40 reflects the slightly later processing wave in area 1 (Allison et al., 1989), which may be more influenced by task information.

Interestingly, previous studies have found that suppressive mechanisms can occur already at the level of the thalamus and the brainstem, albeit to a lesser magnitude compared to the suppression in the cortex (Hsieh et al., 1995). The increasing strength of suppression along the somatosensory processing pathway could be related to larger convergence between the finger representations (e.g., restricted RFs in 3b vs. larger RFs in area 1; Iwamura et al., 1993). Although, in some situations, suppression as low as the spinal cord can modulate perception, for example in perception of pain (Melzack & Wall, 1965). Our study was concerned with suppression in relation to task-context, and task-dependent information may require slightly higher cortical processing.

One previous study reported multisensory modulation of somatosensory suppressive interactions within the P40 time-window by simply viewing one's own body (Cardini *et al.*, 2011). That finding already suggested that the strength of subadditivity that indexes lateral inhibition may not be constant but can be modified by other factors. However, to our knowledge, the wider question of how and why lateral interactions might be adjusted has rarely been considered. Studies of olfactory processing in animals assume that such interactions always aim at maximum acuity (Yokoi *et al.*, 1995), providing enhanced pattern separation for specific molecules within complex mixtures. However, one recent study suggests that the circuitry underlying pattern separation is plastic, and shaped by experience of perceptual discrimination (Chu, Li, & Komiyama, 2016). Our study goes further, in suggesting that the degree of suppressive interactions can be strategically engaged, as a distinct mode of perceptual processing, according to the requirements of a task. When participants need to favour differentiation based on specific details, increased inhibition may amplify small local differences. When participants are preparing to access an overall synthesis of complex inputs, reduced inhibition may facilitate aggregation and generalisation.

We note that caution is required in asserting that the modulation of suppressive interaction between digit representations *facilitated* or *promoted* performance on either task, as we did not find a clear relationship between magnitude of suppression and task performance. This could simply be due to limitations of that analysis, as our task was not designed to use EEG response to predict trial outcomes, and as such it may have not had enough sensitivity to detect such differences. It could also mean that while top-down modulation occurs at early inter-digit interactions to tune the S1 for either discriminative or integrative processing mode, it does not directly influence discrimination or integration performance.

## 2.5. Conclusions

To our knowledge, this has been the first study that has attempted to directly examine ensemble perception of tactile *spatial* information, such as motion direction. By employing a completely novel tactile perception task, where participants had to either average or compare tactile motion directions presented simultaneously to two fingers, we could probe neural mechanisms that could allow participants to engage in different cognitive computations on identical stimuli. Our results suggest that there exists a top-down control mechanism, which can regulate multi-finger interactions to allow ensemble perception. In the next chapters, the factors that shape this ensemble perception will be characterised.

### Chapter 3: Multi-touch aggregation within- and between-hands

The previous chapter revealed that the somatosensory system houses a mechanism that enables integration of two distinct tactile motion stimuli. Here, this aggregation ability will be further characterised in two experiments. Participants were asked to report the *average* motion direction, when the component directions were delivered either to adjacent fingers of the same hand (Exp. 2) or homologous fingers of the opposite hands (Exp. 3). A method of adjustment was employed, whereby participants adjusted a visual arrow to indicate the perceived direction. This method allowed the characterisation of aggregation performance beyond simple error rates, by also considering sensitivity, bias, precision, and relative weighting of component directions. The results revealed different performance between unimanual (Exp. 2) and bimanual (Exp. 3) experiments in terms of sensitivity, weighting, and precision. First, the sensitivity to the average direction was influenced by the discrepancy between component motion signals, but only in the unimanual experiment. This was explained by a model, in which the ‘virtually leading finger’ (VLF) received a higher perceptual weighting. The model was designed by Shinya Takamuku after the data was already analysed. While the model could explain differences in sensitivity, we also found differences in precision, whereby averaging improved signal precision, but only in the bimanual case. Precision differences could not be explained by the VLF model, implying additional sensory limitations during within-hand integration. These additional limitations will be discussed in a greater detail.



### 3.1. Introduction

Chapter 1 (**section 1.2**) described the possible limitations of aggregating multiple tactile stimuli across separate regions of the skin. First, inhibitory interactions between concurrent stimuli have been shown to occur, when those stimuli are delivered to adjacent skin regions that are laterally connected. The findings of Experiment 1 (**Chapter 2**) showed that such inter-digit suppressive interactions may be relieved, when participants are intentionally trying to integrate two tactile inputs. Nevertheless, multi-touch integration can still be restricted by attentional resources required to process multiple tactile stimuli in parallel (Driver & Grossenbacher, 1996; Gallace, Tan, & Spence, 2006). Previous studies that have focussed on aggregation of intensive tactile features have shown that attentional limits may explain the inability to assign equal weight to component tactile inputs producing biased aggregation (Walsh et al., 2016; Cataldo et al., 2019; Kuroki et al., 2017).

Importantly, the demands of multi-touch integration could either diminish or increase when component stimuli are delivered to opposite hands, depending on the neural circuitry underlying somatosensory integration. Some studies on multi-touch perception have found perceptual benefits for bimanual stimulus presentation (Craig, 1985; Walsh et al., 2016). For example, in Walsh et al.'s study, biased integration was abolished when total intensity judgements were made about bimanually delivered tactile stimuli. This benefit could arise because, first, somatotopically organised inter-digit interactions should be lessened between fingers on the opposite hands, and second, because two hands may engage separate pools of processing due to engagement of respective cerebral hemispheres.

However, a different line of work suggests that information from homologous bimanual fingers may be processed by engaging bilateral RFs at the level of S1 (Iwamura et al. 2002; see **section 1.2.3**). In that case, integration across homologous bimanual fingers should resemble integration across adjacent unimanual fingers. That said, even on the assumption that bimanual aggregation occurs by engaging separate hemispheres, performance could still worsen as inter-hemispheric exchange may incur costs in terms of signal delay and coordination of neural resources. Because the early processing of bimanual inputs (Tamè et al., 2016; 2019) and the relative advantage of inter-hemispheric processing (Banich & Belger, 1990; Norman et al., 1992) depends on the specific task performed, we sought to elucidate the performance difference between unimanual and bimanual tactile stimulus delivery in the context of tactile motion direction averaging.

As in Experiment 1, we delivered two tactile motion stimuli (point stimulus movement across the skin) simultaneously to two fingerpads. However, to describe the aggregation performance in more detail and ensure that participants truly aggregate the directions, we

employed a method of adjustment with a wider range of stimuli. Specifically, we asked participants to estimate the *average* direction by adjusting the orientation of a visual arrow on a computer monitor placed directly above the stimulated hand(s) until it matched the perceived direction. This way we were able to extract two main measures of aggregation performance: sensitivity and precision. If participants were able to combine two discrepant motion cues and perceive the average motion direction, they should exhibit a positive relationship between the actual and estimated directions (indicating high sensitivity). Further, if participants averaged the two trajectories in an efficient manner, they should show consistency in their estimates as indicated by small standard deviations across repeated trials (indicating high precision). We also manipulated the discrepancy between the component directions to examine how averaging ability is constrained by the distribution of component inputs. This allowed us to examine the weight assignment between individual directions during aggregation. Finally, the stimulated digits varied across experiments to examine within- and between-hand aggregation. In Experiment 2, participants had to average component trajectories across index and middle fingerpads of the same hand, whereas in Experiment 3, participants averaged the same trajectories across index fingers of different hands.

## **3.2. Methods**

### **3.2.1. Participants**

A separate group of 15 participants took part in each of the two experiments. All participants gave informed consent prior to participation, in accordance with the declaration of Helsinki. The study was approved by the University College London Research Ethics Committee. Five participants were excluded from analysis (four in Exp. 2; one in Exp. 3), because they had estimation errors exceeding 20 degrees in more than 50% of trials in at least one single-finger condition. Excluded participants were replaced with others. The demographics of the final sample were as follows: Experiment 2 (age range: 21 – 39; mean: 27.07; 10 women, 5 men; all but one reportedly right-handed) and Experiment 3 (age range: 22 – 40; mean: 25.87; 9 women, 6 men; all reportedly right-handed). A sample size of 15 was estimated using G\*Power 3.1 (Faul et al., 2009), based on desired power of 0.80 and an effect size of 0.68 for aggregated versus single-digit motion perception precision (unpublished pilot study).

### **3.2.2. Tactile apparatus and experimental set-up**

The apparatus is shown in **Figure 3.1C** together with the set-up. It was the same as for Experiment 1 (apart from the ring electrodes, which were absent in the current set-up). In both experiments, participants rested their hand(s) in a fixed palm-down position over the aperture; the hand(s) was secured with a foam padding. In Experiment 2, the probes, through the

aperture, lightly touched the centre of right index and middle fingertips, whereas in Experiment 3, the probes touched the right index and left index fingertips (**Fig. 3.1B**). The distance between fingers and corresponding width between probes was held fixed across experiments in order to minimise the effects of spatial distance between fingers. Thus, in both experiments the distance between fingers was fixed to approximately 25 mm.

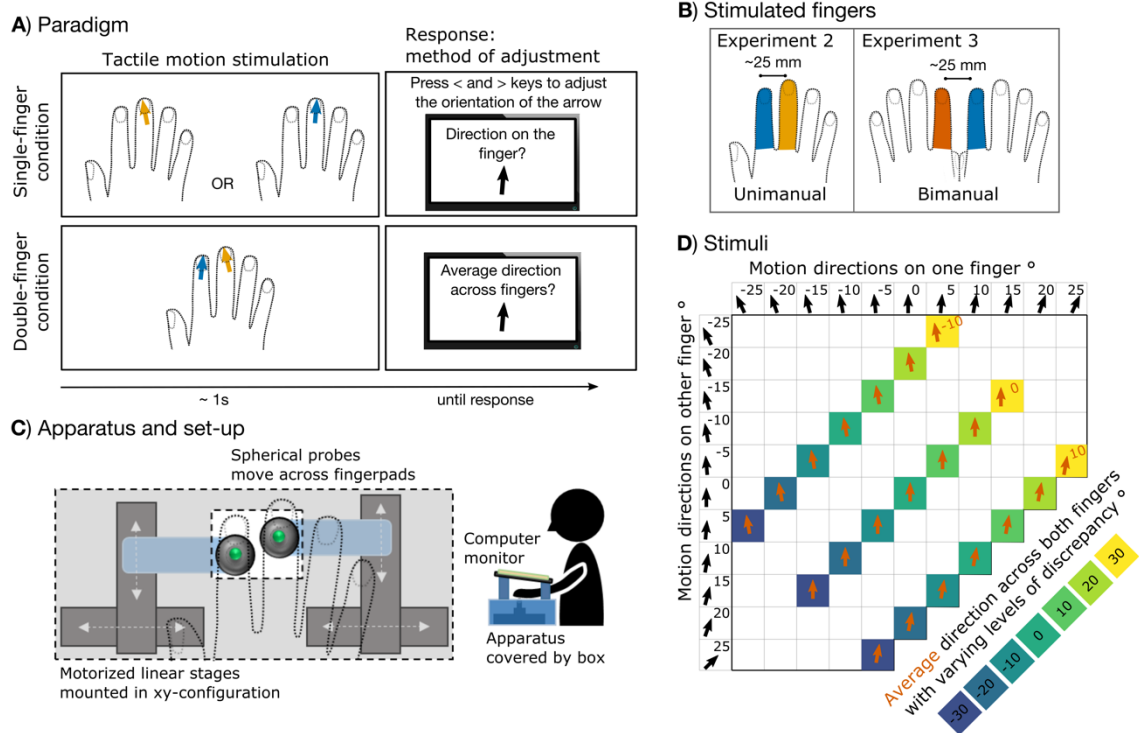


**Figure 3.1. Experiments 2 and 3: paradigm and stimuli.** **A)** Paradigm and trial example from Experiment 2. Fingers were stimulated in two main conditions: single-finger condition and double-finger condition. In the single-finger condition, in different blocks, just the index or just the middle finger was stimulated. Participants reported the direction of the stimulus' movement across their fingerpad. To do so, they adjusted a visual pointer on the screen after each trial (by pressing left and right keys or left and right foot pedals). In the double-finger condition, both component fingers were stimulated simultaneously, and participants had to judge the average direction between the two component directions. **B)** Stimulated fingers in each experiment. **C)** Tactile motion apparatus and set-up. The tactile apparatus consisted of two spherical probes (4 mm diameter) attached to two motorized linear stages mounted in a XY-axis configuration. The apparatus was covered by a wooden box with a rectangular gap, which was used to guide finger placement and secure the hand position. A computer screen, where participants indicated their response, was placed above the hand. **D)** Tactile stimuli. Eleven component single-finger directions were combined into 3 average directions with 7 levels of discrepancy. The sign of discrepancy reflects whether the component directions tended to converge (negative discrepancy) towards the inner edges of fingertips or diverge (positive discrepancy) towards the outer edges of fingertips.

### 3.2.3. Tactile stimuli

Continuous motion along the fingertips was created in the same way as in Experiment 1 (**Chapter 2**). However, we used a much wider range of possible combinations to probe the tactile aggregation mechanism in more detail. Specifically, **Figure 3.1D** shows the 21 possible combinations of 11 individual directions delivered simultaneously to two fingers. The

combinations produced three different average motion patterns, with varying levels of discrepancy between the two stimuli. The sign of discrepancy reflects whether the component directions tended to converge towards the inner edges of fingertips (negative discrepancy) or diverge towards the outer edges of fingertips (positive discrepancy). Other features of the tactile stimuli such as contact force, duration, distance, and jitter in probes' starting positions were identical to that in Experiment 1.

### 3.2.4. *Task design and procedure*

To characterise perception of the *average* motion pattern from two separate trajectories, we compared perception of the average direction to perception of the two individual component stimuli presented alone. Accordingly, both experiments contrasted double-finger stimulations with the single-finger stimulations of which they were composed (**Figure 3.1A**). In single-finger conditions, only one probe was moved, touching only one fingertip, and participants had to estimate the direction of its movement. Single-finger conditions were repeated for each finger (e.g., in Experiment 2 participants performed estimation on index finger and separately on middle finger). The single-finger conditions for each finger were then averaged to obtain one measure characterising mean single-finger perception (**Figure 3.2C**).

In double-finger conditions, both probes were moved simultaneously along both fingertips, and participants had to estimate the average direction of the two trajectories. In all conditions, participants gave their response after the motion stimuli ended, by adjusting the orientation of a visual arrow that appeared on the computer screen placed immediately above their fingertips. They had to adjust the arrow's orientation to the perceived single-finger direction (single-finger condition) or average direction (double-finger condition). The adjustment was made either by pressing left and right arrow keys (and enter key to record their final response) with their (unstimulated) left hand in Experiment 2, or by pressing anticlockwise and clockwise rotator pedals with the left foot (and a third pedal with the right foot to record their response) in Experiments 3. Responses were unspeeded, and no feedback was given. After the response, the arrow disappeared, and the probes moved to their starting positions.

All conditions were blocked. The order of finger conditions was counterbalanced across participants. In double-finger conditions, the 21 stimulus combinations were repeated 7 times. In single-finger conditions, the number of repetitions of each direction was matched to that in the double-finger condition. The total number of trials was 168 per condition. Experiments lasted approximately 1.5 hours.

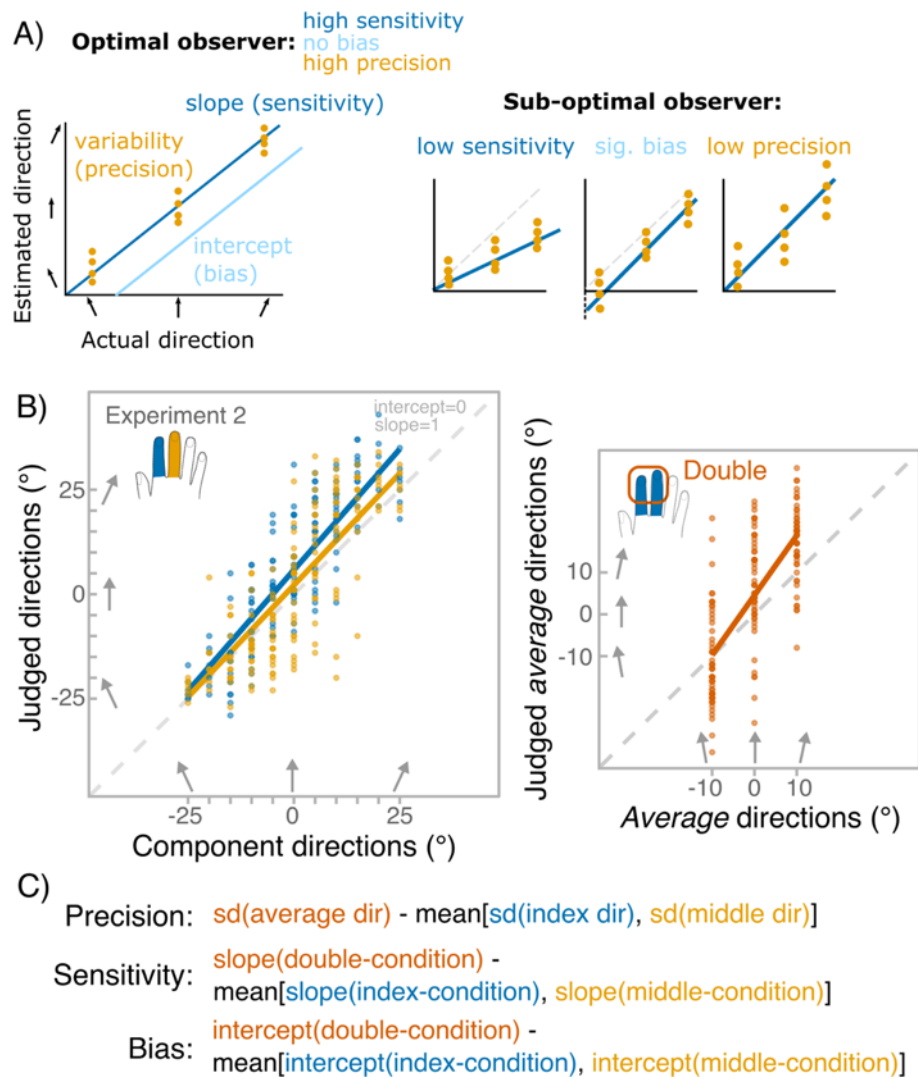


**Figure 3.2. Experiment 2 and 3: main measures.** **A)** Measures used to characterise tactile motion perception: sensitivity, bias and precision. Sensitivity quantifies the ability to perceive differences between motion directions. Bias reflects the shift of the perceived 0° motion, in our case corresponding to the midline of the finger. Precision measures the consistency of a direction percept elicited by repetitions of the same stimuli. The schematic panels show that these three measures are independent. **B)** Data from an example participant in Experiment 2. Linear regression was fit to the data separately for the two single-finger conditions (left panel) and the double-finger condition (right panel). Slope and intercept values reflecting sensitivity and bias, respectively, were estimated from the regression fit. The dots indicate repeated judgements of each direction. Unbiased standard deviations (SDs) were calculated for each direction reflecting the precision. Note that each average direction was composed of one component direction delivered to the index finger and another delivered to the middle finger resulting in 21 combinations: 7 discrepancy levels for a given average direction. In the right panel plot, the discrepancy has been pooled together. **C)** We were interested in the contrast between perceiving the average direction versus estimating individual component directions. For precision we contrasted SD for average direction to the mean SDs for corresponding component directions, while for sensitivity and bias, we contrasted slope and intercept of double-finger condition to the mean slope and intercept value of both single-finger conditions.

### 3.2.5. Main measures: sensitivity, bias, precision, and weighting

Tactile motion processing was characterised in terms of sensitivity to changes in stimulus direction, bias of direction judgments, and precision of repeated estimates of direction for the same stimulus (**Figure 3.2A**). **Figure 3.2B** shows the fitted linear regression to a

representative participant in Experiment 2. The slope reflects the relationship between perceived direction and actual tactile direction, while the intercept reflects the perceptual shift of the perceived midline of a given finger. We expected the slope to be greater than 0 and close to 1, reflecting participants' ability to perceive spatiotemporal information from the skin. Because we did not manipulate finger posture, and always aligned the finger long axis with the 0° stimulus direction, we expected intercept values to be close to 0 reflecting unbiased perception. Slope and intercept values were estimated by fitting linear regressions to each participant's data separately in each condition. Group-level adjusted R<sup>2</sup>s for linear fits for single-finger conditions were as follows: .61 ± .07 in Exp. 2, .57 ± .11 in Exp. 3, and for double-finger conditions: .28 ± .12 in Exp. 2, .42 ± .11 in Exp. 3 (Fig 3.3A).

A perceiver with a given level of sensitivity or bias may be more or less precise (Fig. 3.2A). We used unbiased standard deviation (SD) over repeated different tactile motion stimuli as a measure of precision. That is, in single-finger conditions, SDs were measured for each angle. The mean of this value reflects the inverse precision for single-finger condition. Strictly speaking, precision is traditionally characterised as an inverse of variance (Ernst and Banks, 2002), however we wished to avoid squaring the terms and keep the values in interpretable units. In double-finger condition, SDs were measured for each combination. The mean of this value reflects inverse precision for the double-finger condition. Because we wanted to keep the stimuli in single-finger conditions identical to the ones in the double-finger conditions, the number of trials for each single-finger angle varied (i.e., 0° was used 28 times, whereas 25° only 7 times) to match the number of times each was used in double-finger combinations. However, normal sample SD is a biased estimate of the population SD – the smaller the sample the more likely it will underestimate the population SD (Montgomery and Runger, 2010, section 7.3). Therefore, to account for different number of trials in each angle, we used an unbiased SD to calculate precision over angles and combinations with the following equation:

$$\sigma_{unbiased} = \sqrt{\frac{n-1}{2} \times \frac{\Gamma(\frac{n-1}{2})}{\Gamma(\frac{n}{2})}} \times s \quad (3.1)$$

where  $\Gamma(\cdot)$  is the Gamma function and  $s$  represents the usual SD.

Furthermore, we wished to infer the relative contribution of each finger in making the aggregated direction judgments. Thus, we estimated the weight given to the spatially left-most finger (index finger of the right hand in unimanual experiments and left index finger in bimanual experiment) using the following equation:

$$w_{left} = \frac{\theta_{jud} - \theta_{right}}{\theta_{left} - \theta_{right}} \quad (3.2)$$

where  $\theta_{jud}$  represents the judged *average* direction, and  $\theta_{left}$  and  $\theta_{right}$  represent the direction of the component stimuli. The decision to focus on the finger on the left side of space is arbitrary, as the weight given to right-most finger is simply:  $1 - w_{left}$ . It was assumed that the judgements were based on weighted averaging of the individual angles as follows:

$$\theta_{jud} = w_{left} \times \theta_{left} + (1 - w_{left}) \times \theta_{right} \quad (3.3)$$

Participants engaged in unbiased averaging if  $w_{left} = 0.5$ , reflecting perfect divided attentional processing of each component direction. We estimated the weight for all the stimulus combinations except for those in which the discrepancy of the directions was  $0^\circ$ , as weight calculation is impossible in this case.

### 3.2.6. Statistical analysis

For the statistical analyses, we first used one-sample t-tests on slope and intercept values to see whether participants could perceive probes' directions (slopes greater than 0 and not different than 1) and whether their perception was unbiased (intercepts no different than 0). When the dependent variable violated the normal distribution, checked with Shapiro-Wilk test, we used a sign test instead.

For the main analysis, we were interested whether the aggregation process differed according to whether component directions were combined within- or between hands. Thus, we carried out a mixed ANOVA with within-subjects factor number-of-fingers (single-finger vs. double-finger condition) and between-subject factor experiment (Experiment 2: unimanual vs. Experiment 3: bimanual) separately on slope, intercept and unbiased SD values. For linear models such as ANOVA, the normality assumption should be checked not against raw dependent variable but on the residuals (or errors) from the fitted model (Kozak & Piepho, 2017). However, ANOVA with a balanced design is considered robust even with normality violations, thus, violations of parametric assumptions were unlikely to majorly influence Type I and Type II errors (Boneau, 1960; Glass et al., 1972). In addition, alternative non-parametric Friedman test cannot be done for factorial designs. For these reasons, parametric ANOVA was used throughout. Residuals of the ANOVA model did not violate normality assumption when modelling the slopes ( $p = .93$ ), intercepts ( $p = .43$ ), and SDs ( $p = .97$ ). When sphericity assumption was violated Greenhouse correction was applied.

In addition to the main analysis, we explored whether averaging ability varied as a function of discrepancy between the component directions. Therefore, we fitted separate linear

regressions to the double-finger data for each discrepancy level and extracted the slope and intercept values for each discrepancy. Discrepancy of 0, when component directions were identical, was excluded from the analyses, as those stimuli did not have two signs of direction. For precision, unbiased SDs were calculated to each pair of stimuli (3 average directions by 6 levels of discrepancy). We, again, used a mixed ANOVA with within-subjects factors sign of discrepancy (negative or diverging vs. positive or converging) and level of discrepancy (30° vs. 20° vs. 10°) and between-subjects factor experiment (unimanual vs. bimanual). When modelling precision, average direction (-10° vs. 0° vs. 10°) was added as an additional within-subject factor to reveal any direction-specific differences.

Finally, analysed whether the relative weighting varied across the direction of the average and whether it was modulated by experiment. Thus, we ran another mixed ANOVA on  $w_{left}$  with within-subject factors: average direction (-10°, 0°, 10°), direction of discrepancy (diverging, converging) and level of discrepancy (30°, 20°, 10°), and between-subject factor experiment (unimanual vs. bimanual).

Lastly, support for the null hypothesis could be scientifically informative, as well as support for the experimental hypothesis. Therefore, we used Bayes Factors (Jeffreys, 1961; Rouder et al., 2012; Wagenmaker et al., 2018a, 2018b) to assess support for the null hypotheses, in appropriate cases.  $BF^{01}$  was used to indicate the strength of evidence for the absence of an effect/interaction over a model that did not contain that specific effect/interaction, while  $BF_{inclusion}$  was used to reflect the strength of evidence for including a particular effect/interaction against all other models. Following the guidelines by Kass and Raftery (1995) we considered  $BF > 3$  and  $BF < 0.33$  showing sufficient evidence, while  $0.33 < BF < 3$  showing inconclusive evidence.

### 3.3. Results

#### 3.3.1. Analysis of single-finger conditions

We conducted preliminary analyses on single-finger conditions separately to establish whether participants were able to perceive component directions and whether perception was similar across individual fingers. **Figure 3.3A** shows individual linear regressions fit for each single-finger condition separately in each experiment. The slope and intercept values from those regressions are shown in **Figure 3.1B,D**. Unbiased SDs for repeated judgments of repeated component direction are shown in **Figure 3.1C**. **Table 3.1** shows the summary of the main measures (slope, intercept, and SD) as well as the t-test results. The slopes were significantly above 0 in both experiments indicating that the component directions could be successfully perceived. In fact, in all experiments, slopes were either not significantly different from 1, indicating perfect sensitivity, or greater than 1, showing overestimation. We also compared



sensitivity between fingers, which did not differ in either experiment (paired-sample t-test:  $t(14) = -0.64$ ,  $p = .53$ ,  $d = -.17$  and  $t(14) = 1.89$ ,  $p = .08$ ,  $d = .49$  for Exp.2 and Exp.3, respectively).

Except for the intercept for index finger in Experiment 2, all other intercept values did not significantly differ from 0, indicating an absence of bias. Judgments on index finger in Exp. 2 showed a positive bias of  $\sim 4^\circ$ , meaning that the perceived midline of the finger was shifted slightly rightwards. Indeed, there was a significant difference between single-finger intercepts in Exp. 2 (sign test due to non-normality:  $V = 99$ ,  $p = .03$ ,  $d = 0.66$ ). There was no such difference between fingers in Exp. 3 (paired-sample t-test:  $t(14) = -.19$ ,  $p = .85$ ,  $d = -.05$ ). The shift in intercept might have arisen due to slight shifts in how participant's fingers were placed on the apparatus across the two experiments, or in how the different parts of the apparatus were assembled for each experiment. What is important, however, is that even in conditions where perception was biased, participants retained near-optimal sensitivity.

For precision, we calculated unbiased SDs for each component direction separately for each finger and ran a repeated-measures ANOVA with factors finger (stimulated fingers in the particular experiment), overall direction (leftward vs. rightward) and specific angle ( $25^\circ$ ,  $20^\circ$ ,  $15^\circ$ ,  $10^\circ$ ,  $5^\circ$ ). We excluded the component direction  $0^\circ$  from this analysis, as it could not be divided into leftward vs. rightward direction. In Experiment 2, there was no significant effect of finger ( $F(1, 14) = .18$ ,  $p = .68$ ,  $\eta^2 = .01$ ). The effects of overall direction and specific direction were also non-significant ( $F(1, 14) = .31$ ,  $p = .58$ ,  $\eta^2 = .02$  and  $F(4, 56) = .43$ ,  $p = .78$ ,  $\eta^2 = .02$ , respectively). All interactions were non-significant as well ( $p$  values:  $.16 > p > .90$ ). Similarly, no effect of finger ( $F(1, 14) = .27$ ,  $p = .61$ ,  $\eta^2 = .02$ ) was revealed in Experiment 3, and all other main effects and interactions also remained non-significant (all other  $p$  values:  $.08 > p > .79$ ).

In summary, participants could successfully extract component directions in both experiments and their judgments seemed to be generally unbiased (except in Exp.2 index finger). In addition, both fingers within each experiment seemed to provide equally precise input, which was similar across individual component directions.

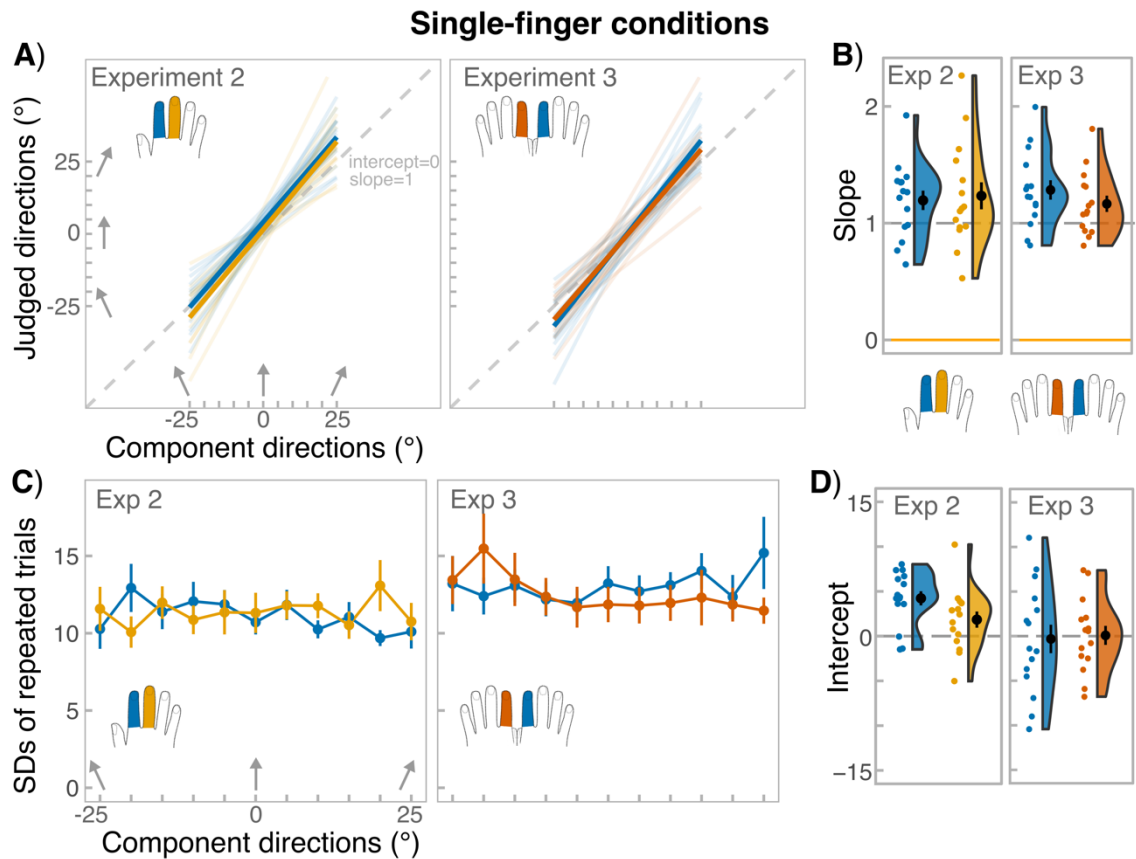


**Figure 3.3. Experiments 2 and 3: results for single-finger conditions.** **A)** Individual fitted linear regressions (transparent lines) and group-level regressions (thick lines) for each finger, separately for experiments 2 and 3. The grey dashed line represents the equality line of slope 1 and intercept 0. **B)** Individual slope values (coloured dots) derived from linear regressions in **A**, together with the group-level means (black dots). Raincloud plots (Allen et al., 2019) represent data distribution and error bars represent standard error from the mean. Colours on the plots correspond to the finger-conditions in **A**. **C)** Group-level unbiased standard deviations (SDs) for repeated trials for each component direction. Error bars represent SEM. **D)** Individual intercept values derived from linear regressions in **A**, together with the group-level means, annotations same as in **B**.

**Table 3.1:** Experiments 2 and 3: main measures for single-finger conditions

Condition	Slope		Intercept		SD	
	mean $\pm$ SD	t-test against 0: $t(d)$	t-test against 1: $t(d)$	mean $\pm$ SD	t-test against 0: $t(d)$	mean $\pm$ SD
Exp. 2:						
Index	1.2 $\pm$ .3	14.39(3.72)**	2.35(.61)*	4.22 $\pm$ 3.1	5.35(1.38)**	11.1 $\pm$ 4.1
Middle	1.2 $\pm$ .5	10.66(2.75)**	2.02(.52)	1.84 $\pm$ 3.5	2.04(.53)	11.4 $\pm$ 4.5
Exp. 3:						
Left index	1.3 $\pm$ .3	16.70(4.31)**	2.37(.61)*	.09 $\pm$ 4.1	.08(.02)	13.0 $\pm$ 5.1
Right index	1.2 $\pm$ .3	15.43(3.98)**	3.42(.88)*	-.3 $\pm$ 6.2	-.20(-.05)	12.5 $\pm$ 5.5

*Note:* \* $p < .05$ , \*\* $p < .001$ . Same group of 15 participants performed under all single-finger conditions within a single experiment, but each experiment had a new group of 15 participants.

### 3.3.2. Does perception benefit from averaging component directions?

Having established that participants were able to perceive component direction, we examined their ability to combine the component directions of varying discrepancy applied simultaneously to two fingers into their average direction. We compared the ability to average (double-finger condition) against the mean perception of corresponding component directions

(single-finger condition). **Figure 3.4** shows the fitted linear regressions that were used to derive slope and intercept values. **Table 3.2** gives an overview and t-test results for the intercept and slope values. In both experiments, participants showed slope values to average direction (double-finger condition) that were significantly higher than 0 and close to 1, and except in Exp.2, perception was unbiased (intercept values not different from 0).

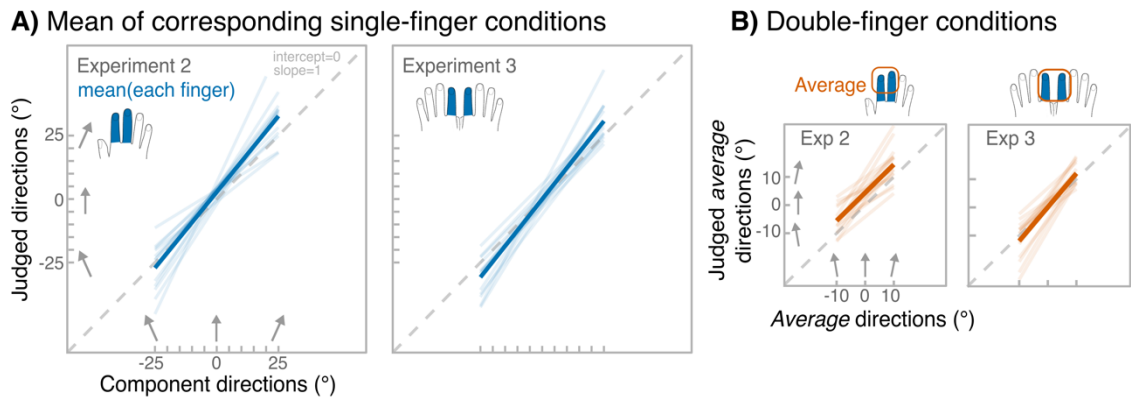


**Figure 3.4. Experiments 2 and 3: regression fits.** Individual fitted linear regressions (transparent lines) and group-level regressions (thick lines) in experiment 2 and 3, separately for the mean of single-finger conditions (A), and for double-finger condition, when participants were estimating the average between the individual component directions (B). The grey dashed line represents the equality line of slope 1 and intercept 0.

**Table 3.2:** Experiments 2 and 3: main measures for all conditions in Experiments 2 and 3

Condition	Slope		Intercept		SD	
	mean $\pm$ SD	t-test against 0: $t(d)$	t-test against 1: $t(d)$	mean $\pm$ SD		t-test against 0: $t(d)$
<b>Exp. 2:</b>						
Single	1.2 $\pm$ .4	12.64(3.26)**	2.24(.58)*	3.03 $\pm$ 2.8	4.27(1.10)*	11.2 $\pm$ 2.1
Double	1.0 $\pm$ .4	9.76(2.52)**	-.1(-.00)	4.42 $\pm$ 4.4	3.92(1.01)*	12.5 $\pm$ 3.4
<b>Exp. 3:</b>						
Single	1.2 $\pm$ .3	120 <sup>†</sup> (4.51)**	108 <sup>†</sup> (.83)*	-.12 $\pm$ 3.3	-.14(-.04)	12.8 $\pm$ 2.4
Double	1.2 $\pm$ .4	13.09(3.38)**	2.19(.57)	.08 $\pm$ 4.1	.07(.02)	10.9 $\pm$ 2.5

Note: \* $p < .05$ , \*\* $p < .001$ .  $x^{\dagger}$  indicate the sign test (V), which was used instead of t-test, due to non-normality. Each condition contains  $n = 15$ ; different group of 15 participants performed in each experiment

To quantify averaging ability, the double-finger condition was contrasted against single-finger condition. We modelled the experiment (Exp.2 unimanual vs. Exp.3 bimanual) as a between-subjects factor to examine whether averaging ability differed depending on whether participants had to average component directions from the fingers on the same or on different hands. Specifically, we were interested in the statistical significance of the interaction between experiment and number-of-finger condition (double vs. single), which would indicate whether perception benefitted from averaging differently across unimanual and bimanual experiments.

**Figure 3.5A** shows the results for the slope values or the sensitivity to directional input. We did not find a significant interaction for sensitivity ( $F(1, 28) = 2.24, p = .15, \eta^2 = .07, BF^{01} = 1.2 \pm 2.3\%, BF_{incl} = .6$ ). The main effects of experiment ( $F(1, 28) = .90, p = .35, \eta^2 = .03, BF^{01} = 2.0 \pm 1.7\%, BF_{incl} = .5$ ) and number-of-finger condition ( $F(1, 28) = 3.5, p = .08, \eta^2 = .11, BF^{01} = .5 \pm 1.4\%, BF_{incl} = .9$ ) were also non-significant. **Figure 3.5B** shows the intercept values, which reflect bias in direction estimation. Again, no significant interaction was found ( $F(1, 28) = .55, p = .46, \eta^2 = .02, BF^{01} = 2.3 \pm 3.7\%, BF_{incl} = .5$ ) and no effect of number-of-finger condition ( $F(1, 28) = .96, p = .34, \eta^2 = .03, BF^{01} = 44.7 \pm 1.8\%, BF_{incl} = .4$ ). However, we did observe a significant effect of experiment ( $F(1, 28) = 12.1, p = .002, \eta^2 = .30, BF^{01} = .02 \pm 1.9\%, BF_{incl} = 13.7$ ) with judgments being tilted clockwise relative to actual stimuli in Experiment 2. This was likely due to biased perception on the right index finger (see **Table 3.1**).

Lastly, **Figure 3.5C** shows the unbiased SDs averaged across individual directions; these reflect mean precision in estimating repeated trials. Importantly, the interaction for precision was statistically significant ( $F(1, 28) = 11.6, p = .002, \eta^2 = .29, BF^{01} = .05 \pm 8.4\%, BF_{incl} = 5.0$ ). When directions had to be aggregated across hands, the averaging process resulted in a more precise average estimate (mean SD = 10.9, sd = 2.5) compared to the mean estimate of the component directions (mean SD = 12.8, sd = 2.4; paired-sample t-test:  $t(14) = 4.1, p = .001, d = 1.1$ ). In contrast, when the same directions were delivered to the fingers of the same hand, aggregation did not lead to significant benefit (paired-sample t-test:  $t(14) = -1.59, p = .13, d = -.41$ ). The main effects of experiment and number-of-finger condition were both non-significant ( $F(1, 28) < .001, p = 1.0, \eta^2 < .001, BF^{01} = 2.7 \pm .6\%, BF_{incl} = 1.4$  and  $F(1, 28) = .43, p = .51, \eta^2 = .02, BF^{01} = 3.3 \pm 2.2\%, BF_{incl} = 1.3$ , respectively).

In sum, sensitivity was as high to average directions as it was to component directions, and it was not modulated by whether averaging was performed on unimanual or bimanual fingers. Interestingly, averaging led to an increase in precision over mean precision of estimating each of the component direction but only when components were delivered bimanually.

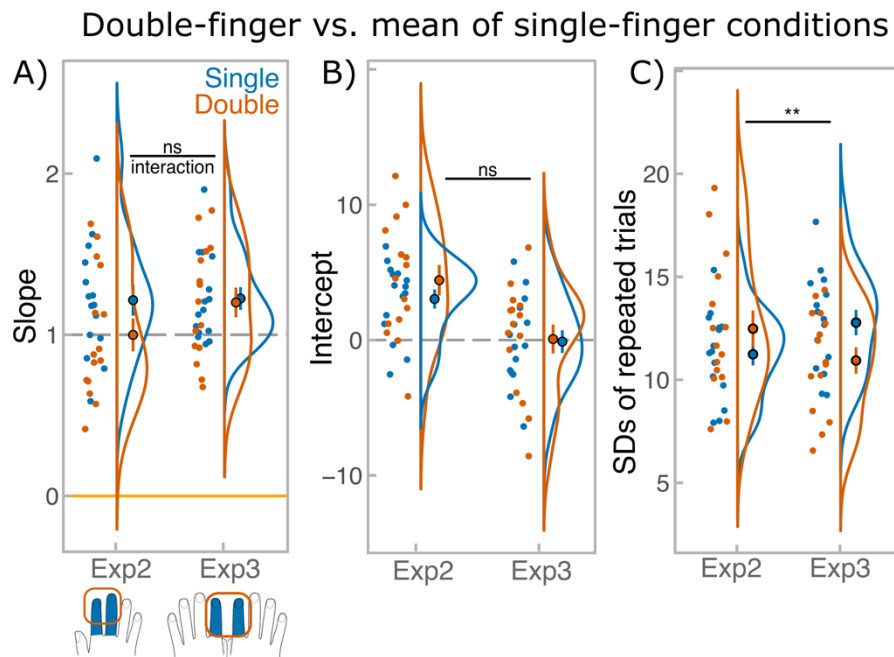


**Figure 3.5. Experiments 2 and 3: main measures.** **A)** Slope values estimated from single-subject regressions, corresponding to the sensitivity. **B)** Intercept values also estimated from single-subject regressions, corresponding to the bias. **C)** Unbiased SD values for repeated estimation of identical directions. SDs were calculated separately for each repeated stimulus; for simplicity, data was averaged across repeated stimuli to show the mean SDs for single-finger (blue) and double-finger (orange) conditions. In all panels, points with error bars reflect group-level means and SEM. Raincloud plots (Allen et al., 2019) show the distribution of the data. Upper black annotation shows statistical significance of number of fingers (single vs. double) by experiment (unimanual vs. bimanual) interaction. The data includes two independent groups of 15 participants per experiment.

### 3.3.3. Is averaging ability constrained by directional discrepancy?

We next explored averaging ability more closely, specifically whether averaging was modulated by the discrepancy between component directions. **Figure 3.6A** shows the sensitivity to average direction as a function of discrepancy. While sensitivity was not affected by discrepancy itself (main effect of level of discrepancy:  $F(2, 56) = .48, p = .62, \eta^2 = .02, BF^{01} = 13.8 \pm 1.7\%, BF_{incl} = .03$ ; level of discrepancy by experiment interaction:  $F(2, 56) = .21, p = .81, \eta^2 = .007, BF^{01} = 9.4 \pm 3.7\%, BF_{incl} = .02$ ), sign of discrepancy had a differential effect depending on whether aggregation was unimanual or bimanual (sign of discrepancy by experiment interaction:  $F(1, 28) = 11.5, p = .002, \eta^2 = .29, BF^{01} = .01 \pm 5.6\%, BF_{incl} = 92.2$ ; main effect of sign of discrepancy:  $F(1, 28) = 6.1, p = .02, \eta^2 = .18, BF^{01} = .42 \pm 1.0\%, BF_{incl} = 64.5$ ). Specifically, during unimanual averaging the sensitivity dropped when component directions diverged to the outer corners of the fingertips (Bonferroni-corrected pairwise test:  $p < .001$ ; mean slope = 1.19,  $SD = .56$  for converging vs. mean slope = .79,  $SD = .44$  for diverging). No such effect was found during bimanual averaging (Bonferroni-corrected pairwise test:  $p = .45$ ).

In terms of intercept values (**Figure 3.6B**) averaging was in general more biased in the unimanual than bimanual experiment (main effect of experiment:  $F(1, 28) = 12.1, p = .001, \eta^2$

= .30,  $BF^{01} = .06 \pm 1.6\%$ ,  $BF_{incl} = .4$ ), but was not influenced by discrepancy-related effects and did not show any significant interactions (all other  $p$  values:  $.06 < p < .28$ ). **Figure 3.6C** shows the mean unbiased SDs averaged across average directions, reflecting the mean precision to average directions as a function of discrepancy. For the analysis, unbiased SDs were calculated for each average direction ( $-10^\circ, 0^\circ, 10^\circ$ ), and average direction was added as an additional within-subject factor. The analysis yielded a significant interaction between discrepancy level and average direction ( $F(4, 112) = 3.6$ ,  $p = .008$ ,  $\eta^2 = .11$ ), Bonferroni-corrected pairwise tests showed that precision was higher during low discrepancy ( $10^\circ$ ) compared to discrepancy of  $20^\circ$  ( $p = .001$ ) and discrepancy of  $30^\circ$  ( $p < .001$ ), but this effect persisted only when average direction was  $10^\circ$ . No other effects or interaction reached significance.

In sum, how dissimilar the component directions were to each other did not clearly influence the averaging performance (lack of discrepancy level effect). However, whether the component directions were converging or diverging had a large effect on averaging sensitivity in the unimanual experiment.

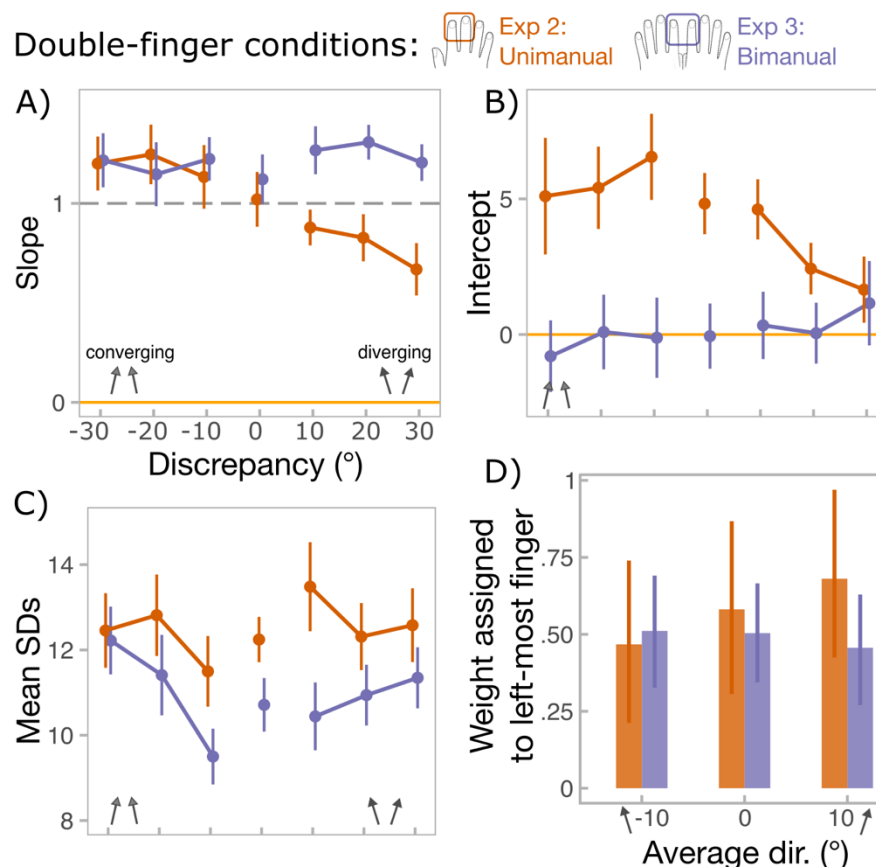


**Figure 3.6. Experiments 2 and 3: effect of discrepancy on averaging performance and weighting of component directions during averaging.** A) slope values as a function of discrepancy. The points correspond to group-level slope values, estimated from single-subject regressions fit to double-finger conditions, but separately to each discrepancy level (x axis). Error bars correspond to SEM. Discrepancy of 0 (when component directions were identical) is included in the plots for illustrative purposes, but was

not included in the analysis, because discrepancy was factored into sign of discrepancy (negative discrepancy, when directions converged vs. positive discrepancy, when directions diverged) and level of discrepancy (30° vs. 20° vs. 10°). **B**) intercept values as a function of discrepancy; annotations are the same as for panel **A**. **C**) unbiased SD values for repeated estimations of identical trials as a function of discrepancy (x axis). SDs were calculated for each average direction separately, but for simplicity data was pooled across average directions to show the mean SDs for each discrepancy. Annotations same as for panel **A**. **D**) weight assigned to the left-most finger during averaging (right index in unimanual experiment and left index in bimanual experiment) as a function of average direction. Weight of 0.5 meant that the directional information from both fingers was weighted equally. In all panels, orange traces reflect unimanual averaging, while purple traces reflect bimanual averaging.

### 3.3.4. *Weight assignment across component stimuli during the averaging task.*

Unbiased averaging implies that the component directions were equally weighted (see equation 3.3. **Figure 3.6D** shows the relative weight assigned to the left-most finger (right index in Exp. 2 and left index in Exp. 3) across the three average directions. The analysis yielded a significant average direction by experiment interaction ( $F(2, 56) = 6.1, p = .005, \eta p^2 = .18$  -  $p$  value Greenhouse corrected). Bonferroni-corrected pairwise tests showed that while in the bimanual experiment weighting was similar across average directions (all  $p$  values = 1), in the unimanual experiment the left-most finger received a higher perceptual weight when average direction was rightward (10°; mean weight = 0.68, SD = 0.6) compared to when the average direction was leftward (-10°; mean weight = 0.47, SD = 0.6;  $p = .01$ ). This suggests that during unimanual averaging a shift in relative weights was evident, whereby left component received more weight when the overall direction was towards right. The question is whether this shift to biased weights could explain the deteriorated sensitivity in diverging components (**Figure 3.6A**) and the lack of precision benefit (**Figure 3.5C**) in the unimanual condition.

### 3.3.5. *Extra: sensory weighting model based on ‘virtual-leading-finger’ (VLF) predicts discrepancy-dependent sensitivity, but not precision*

In this section, a model developed by Shinya Takamuku will be briefly described (for full details see Arslanova and Takamuku et al., 2021, unpublished pre-print). The main purpose of this section is not the treatment of the model, but rather the illustration that VLF-based biased weighting model, which was designed based on the weighting results above, could account for the sensitivity results, but could not explain the precision difference between the experiments.

In natural hand-object interactions different fingers of the *same hand* often receive redundant information. For instance, when an object slides across multiple fingers, one of the fingers will receive a novel stimulus event, such as an edge of the object or a surface texture change, first (we call this the ‘*virtually leading finger*’, VLF). The remaining finger(s) would then receive similar stimulation, but with a slight temporal delay. If the brain prioritises *novel* information, the virtual leading finger will attract more attention and have a greater impact on

the overall perception. We term this *virtual-leading-finger priority (VLF-priority)*. Although, VLF would be normally defined based on temporal priority, temporal sequence of finger stimulation in natural interactions is tightly coupled with the *geometric* relationship between the fingers and the relative motion of the touched object. Therefore, even when fingers are stimulated synchronously, without any phase difference between stimulations, VLF can still be defined by considering the direction of motion of an implied virtual object that causes the stimulations.

The finding that relative weighting changed as a function of average motion direction supports VLF-priority. However, it is unlikely that the weight assignment depended on the process of specifying the VLF because this essentially requires estimating the average angle. Therefore, a mathematical model was designed that estimates the average direction by integrating distorted estimates of the component directions without explicitly specifying the VLF. In that model (*biased-integration model*) estimates for each component direction were calculated considering the sensitivity ( $a$ ) and bias ( $b$ ) linked to the individual fingers:

$$\hat{\theta}_i = a \times \theta_i + b \quad (3.4)$$

Then, an estimate of the average angle was given as a weighted average of the individual estimates:

$$\hat{\theta}_{avr} = \sum_{i=1}^2 w_i \times \hat{\theta}_i \quad (3.5)$$

$$\sum_{i=1}^2 w_i = 1 \quad (3.6)$$

The index  $i=1,2$  corresponds to the left-most and right-most fingers, respectively. Equations 3.5 and 3.6 are equivalent to equation 3.3 except for the fact that the integrated information is now based on biased (in terms of intercept that deviate from 0) estimates of the individual fingers. The unbiased-integration model then assumes that weights are allocated equally to the two fingers, whereas biased-integration included a *gain factor* for each finger and the condition that determined the *strength* to which the finger attracted the weight (equation 3.7) depending on the direction of stimulus delivered to that finger:

$$g_i = C + c_i \tilde{\theta}_i \quad (3.7)$$

$c_i$  ( $i=1,2$ ) are finger- and context-specific gain factors which allow the different fingers to have different direction-dependencies in different contexts (unimanual/bimanual).  $C$  is a constant



which can be any positive real number (in our analysis, it was set to 1/2 to ease interpretation). The weights allocated to the fingers are calculated by normalizing the strengths as follows:

$$w_i = \frac{g_i}{\sum_{i=1}^2 g_i} \quad (3.8)$$

The weights were constrained to have a value between 0 and 1. The model had four parameters in total ( $a, b, c_1, c_2$ ) and the parameters were determined by fitting the model to the judgements. The model can assign the weights to the fingers in various ways depending on the gain factors. When there are two fingers, as was the case in our study, the condition for the biased integration model to always assign more weight to the leading finger (defined by average angle) is given as follows:

$$\bar{c} = \frac{c_1 + c_2}{2} = 0 \quad (3.9)$$

$$\Delta c = (c_1 - c_2) > 0 \quad (3.10)$$

A possible neural implementation of the biased model is the normalization model of attention (Reynolds and Heeger, 2009). Accordingly, the stimuli delivered to the two fingers cause the initial sensory responses (stimulus drive) that correspond to  $\hat{\theta}_i$  in equation 3.4. The saliencies of each stimulus depend both on the motion directions and the context. This results in different levels of attentional gain on each stimulus, the gain represented as  $g_i$  in equation 3.7. The final population response to the stimulus results from divisive normalization (equation 3.8) of the attention-modulated sensory drive. The percept reflects the biased and normalized population response averaged across the RFs.

Importantly, fitting the model to the data accounted for the discrepancy-dependent changes in sensitivity. Namely, in combinations with negative discrepancy the VLF, which receives the higher weighting, also receives a larger angle (i.e., it deviates more away from 0°; see **Figure 3.7A**). Thus, the percept of the average directions is overestimated during negative discrepancy, resulting in slopes larger than one. Conversely, when discrepancy was positive, the VLF received a smaller angle, resulting in underestimation of the average direction. Because no such prioritisation occurs in the bimanual experiment, there is no discrepancy-related changes in average direction estimation that would be reflected in changes of slope values.

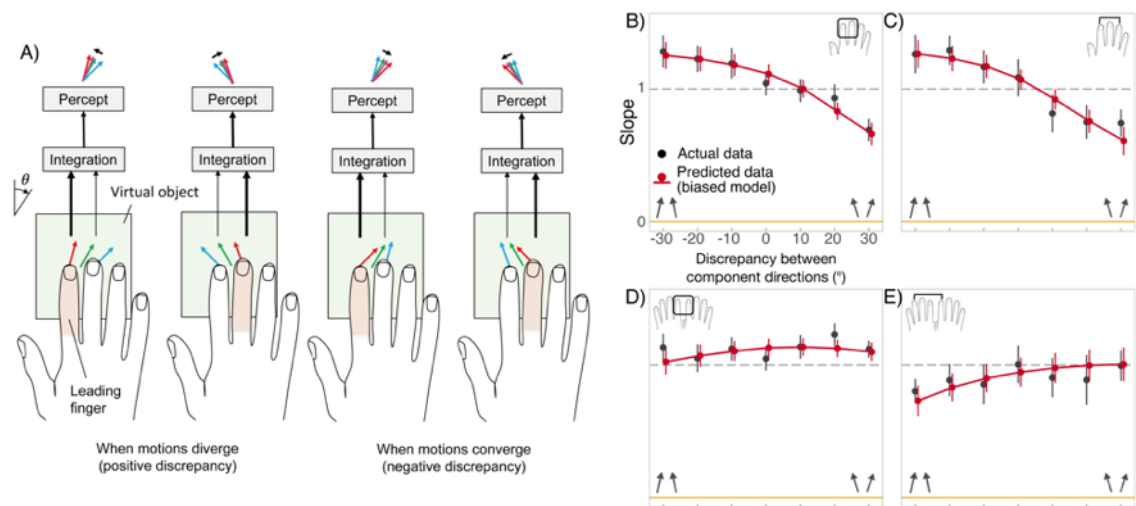


**Figure 3.7. VLF-based model: relationship between sensitivity and component discrepancy.** **A)** How VLF-theory explains the effect of angular discrepancy. Red and blue arrows indicate motions delivered to the *leading* and *following* fingers, respectively. The VLF is defined by assuming a virtual object (shown as a green box) moving in the direction of the averaged motion direction (green arrow). The theory assumes that the VLF would have a larger influence (indicated as thicker arrows) on perception than the non-leading finger. Importantly, when the discrepancy of the motion direction between the two stimuli is positive (left panel), the motion on the VLF would have an equal or smaller absolute angle ( $|\theta_i|$ ) than that of the other finger. Therefore, the theory predicts that the perception (shown as purple arrow on top) would underestimate the size of the average angle ( $|\theta_{avr}|$ ). When the discrepancy is negative (right panel), the size would be overestimated. Thus, the VLF-hypothesis predicts that the sensitivity to the average angle would be larger when the discrepancy is negative. Panels **B**, **C**, **D**, and **E** show actual data (black dots) and model fit (red dots and overlays) to average angle slope as a function of discrepancy. Dots show group-level slope and error bar SEM. The red overlays show group-level interpolation of biased model predictions. Note that the panels include data from this and next chapter, so panel **B** comprises pooled data from unimanual adjacent conditions ( $N = 30$ ; Exp. 2 and Exp. 4 adjacent), panel **C** represents data from non-adjacent condition ( $N = 15$ ; Exp. 4 non-adjacent), panel **D** contains pooled data from bimanual homologous condition ( $N = 30$ ; Exp. 3 and Exp. 5 homologous) and panel **E** represents data from non-homologous condition ( $N = 15$ ; Exp. 5 non-homologous).

It was then examined whether the VLF-based model could also predict the changes in precision between unimanual and bimanual experiments. Since precision of integrated estimate decreases as the weights become biased, the model did predict lower precision in the unimanual condition. The question was whether this quantitatively explained the data. We predicted the unbiased SDs in double-finger conditions relative to those in single-finger conditions from the weights of the models. This suggested that the ratio between SDs of unimanual and bimanual averaging would be 1.04 at the largest (when noise in individual estimates is completely independent). The actual ratio ( $1.09 / 0.91 = 1.2$ ) was larger. This suggested that the difference in precision between the unimanual and bimanual experiments cannot be explained solely on the bias of the sensory weighting. Moreover, the degree of sensitivity reduction between converging vs. diverging component directions in unimanual experiment (Exp. 2) did not correlate with the difference in precision between average vs. component direction estimation ( $r = .44, p = .10$ ). This implies not sufficient evidence for a shared factor underlying the decrease in sensitivity and in precision under unimanual averaging.

### 3.3.6. *Extra: can participants perceive discrepancy?*

We did not find that averaging ability was constrained by the level of discrepancy between the component directions. We reasoned that if averaging is similar to integration in a multi-sensory context, lower discrepancy should lead to better averaging performance as more similar components may be referred to a ‘common object’ (Coa et al., 2019). However, we saw a trend in bimanual experiment (**Figure 3.6C**), this effect was not statistically significant. To ensure that the lack of discrepancy level effect was not due to inability to perceive discrepancy between the two component directions, we asked participants to perform an additional task.

We used exactly the same stimuli as in the main experiment’s double-finger condition, but after each stimulus, participants had to report whether the two component directions were the same or different. **Figure 3.8** shows the results from tasks in unimanual and bimanual case. For each task, we fit two psychometric functions; one for when the discrepancy between directions was negative (directions were converging) and the other when it was positive (directions were diverging). The data from some participants (dashed line in **Figure 3.8**) produced very poor fits (adjusted  $R^2 < .50$ ), so we had to exclude those participants from further analysis (three in Exp. 2b and five in Exp. 3b). From the remaining participants we estimated (1) JND (“just noticeable difference”), which reflects the steepness of the psychometric curve and can be considered as a measure of the sensitivity to discrepancy, and (2) PSE (“point of subjective equality”) that reflects the discrepancy at which discrepancy detection ability is at the chance level (50%). Overall, the psychometric function provided a reasonable fit to the data of the remaining participants (mean adjusted  $R^2 = .84$ ,  $SD = .20$  and  $.83$ ,  $SD = .15$  for Exp. 2b and Exp. 3b, respectively). The mean JND was 10.8 ( $SD = 6.4$ ) in unimanual and 14.0 ( $SD = 4.9$ ) in bimanual experiment. The mean PSE was 11.1 ( $SD = 6.8$ ) in unimanual and 12.5 ( $SD = 7.7$ ) in bimanual experiment. This suggests that combinations with 20° discrepancy were clearly perceived as discrepant.

We also analysed whether the measures differed between the sign of discrepancy. In the unimanual experiment, there was no significant difference in JNDs (sign test due to violation of normality:  $p = .15$ ), but there was for PSEs ( $t(11) = 3.0$ ,  $p = .01$ ,  $d = 0.9$ ) with PSE reached with smaller discrepancy when it was positive (mean PSE = 7.4,  $SD = 4.0$ ) compared to when it was negative (mean PSE = 14.8,  $SD = 7.0$ ). This means that when component directions were diverging, discrepancy detection was easier. This may be because when diverging, the trajectories tended to reach end locations that were further away in space (i.e., outer edges of the fingers). In the bimanual experiment, there was no difference in PSEs ( $t(9) = -.20$ ,  $p = .85$ ,  $d = -.06$ ) nor in JNDs ( $t(9) = -.10$ ,  $p = .92$ ,  $d = -.03$ ).

Whether the greater PSE in unimanual experiment for diverging directions is related to the drop in sensitivity for average directions (see **Figure 3.6** and **Figure 3.7**) is unclear. It could be that because trajectories ended further away, the sensitivity for average direction was distorted. However, the space between the fingers was exactly the same in the bimanual experiment, yet none of the effects were observed. Thus, the drop in sensitivity seems to be better explained by the VLF-model that could account for differences between unimanual and bimanual averaging. In sum, this additional task showed that most participants did perceive discrepancy between the two directions (at least at 20°), and that they perceived the directions as progressively different as a function of level of discrepancy. Therefore, the lack of level of discrepancy effect in the main analysis is unlikely due to participants' inability to detect any discrepancy between the component directions.

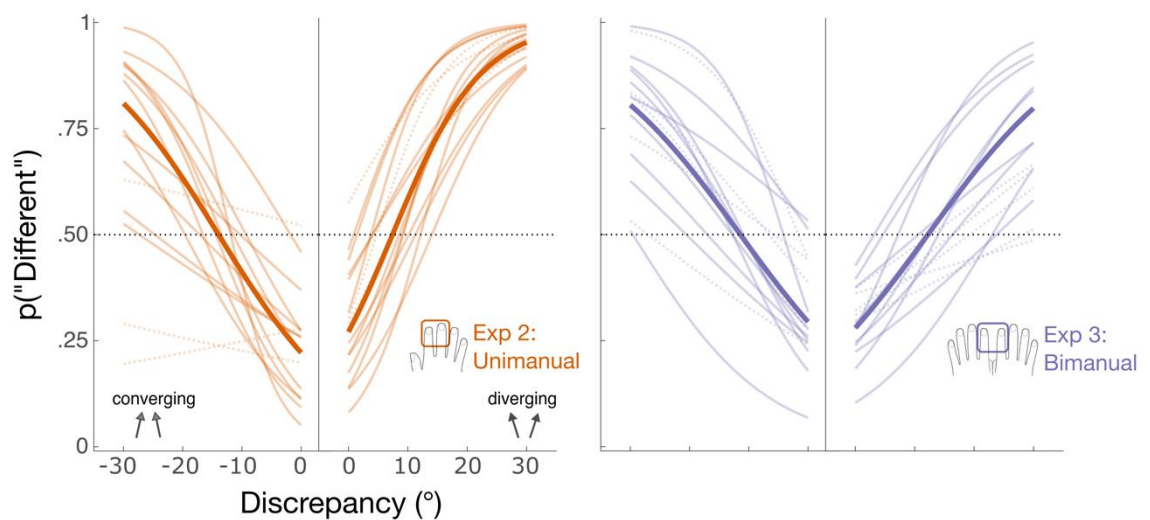


**Figure 3.8. Experiments 2b and 3b: results of additional discrimination task.** Individual psychometric functions (transparent solid lines) along with group-level functions (thick lines) for unimanual (orange) and bimanual (purple) experiments. Dashed individual lines show fits of excluded participants.

### 3.4. Discussion

The aim of the two experiments presented in this chapter was to examine people's ability to combine discrepant spatiotemporal motion trajectories from different fingers on either the same hand or across different hands. To characterise averaging performance sensitivity, bias, and precision for the average direction judgements were compared to the judgements of either single trajectory that compromised the average. Averaging itself was then analysed as a function of discrepancy between single trajectories along with the relative weighting assigned to each single trajectory. The results showed strong integration between spatiotemporal inputs, but subject to possible limitations for stimuli delivered within a hand.

### *3.4.1. Averaging benefitted in a more precise estimate but only when components were delivered bimanually*

An interesting finding of the present chapter is that averaging directions bimanually led to increased precision as compared to estimating each direction in isolation. This precision benefit did not occur for unimanual stimuli. Successful averaging implied that participants had to first form reliable representations of tactile motion direction at each stimulation site and then mentally aggregate them with equal weights. As mentioned in Chapter 1 (see **section 1.2.1**) performance on such a task may be restricted by limited processing bandwidth. Namely, limited attentional capacity to attend to two digits may prevent the parallel processing of two trajectories and thus result in imperfect perception of the whole somatosensory scene. Our weighting results showed biased weighting during unimanual averaging, but they did not find total selectivity, in which signals from one finger would be entirely ignored. This suggests that information from both fingers was processed.

However, the reduction in precision during unimanual averaging compared to estimating each component in isolation suggests that the two signals were compromised when presented simultaneously. The improved relative precision in bimanual task implies improved ability to process the two signals in parallel. This could be due to the engagement of two separate pools of processing resources corresponding to each hand. Although some authors find performance costs for bimanual tasks (Nguyen et al., 2020), the idea that perception can benefit from distributing resources across hemispheres is well documented (Friedman & Polsen, 1981). Moreover, Craig (1985) and Overvliet, Smeets, & Brenner (2007) both showed that participants were better at identifying tactile patterns when the pattern components were presented bimanually rather than unimanually.

Because precision ultimately indicates the noise in the system, another explanation for the precision difference could be based on theories of noise summation. Classically, when multiple signals are each affected by an independent source of noise, then averaging those signals leads to increased precision (Zohary, Shadlen, & Newsome, 1994; Averbeck, Latham, & Pouget, 2006; Alvarez, 2011). Accordingly, two noisy inputs should produce a less noisy average, but only if the inputs are independent. As the correlation between the two noise sources increases, this reduction in noise should diminish. Thus, the finding that there is no such reduction in noise after averaging unimanually presented trajectories could mean that multiple stimuli processed within the same hemisphere are affected by some shared sensory noise, whereas stimuli processed in different hemispheres might be affected by relatively independent noise. Consistent with this view, Cohen and Maunsell (2009) found that variability in individual

neurons' firing rates were positively correlated within a hemisphere, indicating a shared variability throughout the neural population. In contrast, noise correlations for pairs of neurons in different hemispheres were close to zero, suggesting that sensory noise between the two hemispheres remained independent. We speculate that a potential source of noise interdependence for stimuli encoded from the same hand could be fluctuations in the mono-hemispheric somatosensory rhythms. Recordings of cortical sensorimotor oscillatory activity in humans have demonstrated a lack of phase coherence and coupling between the two hemispheres (Andrew and Pfurtscheller, 1999; Kilner et al., 2003). Thus, mono-hemispheric oscillations could manifest as noise in the neural response that is correlated across all stimulated fingers on one hand, yet remain independent in each hemisphere. The independent hemispheric sensorimotor rhythms can be then coordinated as required (e.g., during bimanual skill acquisition; Anders et al., 1999).

Since our study was purely behavioural, we cannot draw strong conclusions regarding the neural basis of our participants' percepts. As mentioned in Chapter 1 (see **section 1.2.3**), unilateral tactile stimuli can engage both hemispheres, in stark contrast to textbook descriptions of strict laterality in S1 (for review see Tamè et al., 2016; 2019). Thus, one could argue that it is beneficial for bimanual aggregation to occur within S1 of a single hemisphere as to not incur the delay and coordination of inter-hemispheric transfer. Yet, our results show that within-hand and between-hand aggregation are likely engaging distinct processes. Whether this distinction is the difference between intra-hemispheric and inter-hemispheric processing remains unknown.

However, Sutherland and Tang (2006) found that while unimanual stimulation activated both contralateral and ipsilateral S1, the ipsilateral activation was significantly less than its contralateral counterpart, and presumably still arises via transcallosal input from the contralateral S1. Therefore, even if unimanual stimulation engages processing in the ipsilateral hemisphere, it would do so to a lesser extent than in the contralateral hemisphere. Further, bilateral activation would always be stronger, and more symmetric, for bimanual than for unimanual stimuli. Thus, we assume that differences between averaging unimanual and bimanual stimuli correspond to predominantly intra-hemispheric vs. inter-hemispheric processing of tactile information. Still, additional neuroimaging or EEG methods are necessary to confirm the hemispheric lateralisation of our stimuli, and to provide direct support for this conclusion. In terms of behavioral studies that can give us more evidence for hemisphere-specific effect, in Chapter 4, bimanual averaging as a function of finger homology will be examined. The effect of homology has been taken as evidence that a bimanual task can occur at the early somatotopically organised levels of somatosensory processing (Tamè et al., 2016;

2019; see **section 1.2.3**). The absence of the digit-specific effect could indicate that averaging performance is more strongly constrained by the hand rather than specific digits.

Yet, another possibility for improved precision in bimanual averaging condition might be reduced or absent inter-digit interactions that can cause sensory interference between concurrent tactile stimuli. Importantly, the strength of inter-digit inhibitory interactions follows a somatotopic organisation. Meaning that interactions will be the strongest for adjacent fingers and will decrease as a function of somatotopic separation. Chapter 2 showed that suppressive interactions between adjacent digits were reduced when participants were instructed to report average directions, as opposed to direction discrepancies. Thus, somatotopic effects might have been attenuated in our averaging conditions. However, the act of attenuation may already have incurred some performance costs, in which case, precision of averaging across non-adjacent digits may have been better to begin with. For that reason, in the next chapter, we also examined unimanual averaging as a function of adjacency.

#### *3.4.2. VLF-based model accounts for the biases in unimanual inter-digit weights and discrepancy-dependent sensitivity results*

Although, our weighting results did not reveal total selectivity of one or the other finger, indicating that information from both fingers were considered, it did reveal idiosyncratic pattern of relative weighting in the unimanual experiment. The finding that relative weighting was modulated by average direction, but only in the unimanual case, inspired an integration model that is based on a specific “object-prior” in the unimanual case, but not in the bimanual case. Specifically, if we think about our normal tactile experience, we usually touch one object with one hand and different objects with the two hands. This means that the tactile inputs we receive at the fingers of the same hand tend to be similar and often redundant. Importantly, the present task resembles a physical situation where the hand(s) moves sideways across “an object”. In this situation, one of the fingers touches the object first (“the leading finger”, VLF). Given that the inputs received from “a single object” are typically similar, the following fingers would receive redundant information about the object's motion direction. In this case, because of limited processing resources, it would be more efficient to allocate resources to the leading finger as it would provide the novel information (Yang et al., 2018), which may maximise information gain (Friston et al. 2015; Itti & Baldi 2009; Vergassola et al. 2007).

The idea of a leading finger in humans or of a leading whisker in rats has been shown in previous research (Ziat et al., 2010; Drew & Feldman, 2007). Indeed, the weighting results point to the possibility that when the “virtual object” moved to the right (average direction is to the right), the left-most finger received the directional information first and thus also received a

higher weighting. Importantly, the VLF-based model explained the under- and over-estimation of average direction depending on the discrepancy between component directions. However, because VLF-based model was a post-hoc explanation for the data, future experiments should be designed to target the theoretical constructs of the object-prior theory. For instance, such experiments might specifically manipulate the 'single object' prior (e.g., by visually showing either one or two moving objects during tactile stimulation) and examining whether this leads to changes in relative weighting.

### **3.5. Conclusions**

In conclusion, the previous chapter (**Chapter 2**) showed that the intention to combine two distinct motion stimuli to extract their average motion direction was a distinct process from their comparison that occurred by modulations in somatosensory brain regions. However, the averaging task itself was relatively rudimentary (3-forced-choice response) and did not ensure that information from both fingers was truly processed and averaged. This chapter represents an important improvement in the task design. By asking participants to *estimate* the average directions, we could characterise averaging performance in terms of sensitivity to gradual changes in motion directions, bias in the perceived reference for the directional judgements, noise in directional estimation, and relative weighting of component directions during averaging. The results of the two experiments showed distinctive features of tactile within-hand and between-hand motion integration. First, we identified a process of biased sensory weighting, which operates for the digits within one hand. This pattern of weighting may point to an existence of a prior belief based on natural tactile interactions that dictates the weight assignment during the aggregation process. Second, analysis of precision showed that bimanual aggregation led to a reduction of noise, but unimanual aggregation did not. This difference could be related to limited processing resources or shared noise between fingers of the same hand. As a result, bimanual touch may have a perceptual advantage in terms of precision. However, whether the effects described in this chapter are hand- or hemisphere-specific, or whether they could be ascribed to digit-specific interactions, is still under question, and will be investigated further in the following chapter.



## Chapter 4: Multi-touch aggregation beyond somatotopy

The previous chapter found that while unimanual aggregation exhibited idiosyncratic biases, whereby one component direction got upweighted depending on the motion direction, bimanual aggregation seemed to escape such bias and produced a more precise average motion estimate. We speculated that bimanual advantage arose due to a hand- or hemisphere-specific effect. Namely, noise between fingers on one hand could be inter-dependent, or bimanual aggregation could benefit from redistributed attentional resources. However, the potential effect of somatotopic inter-digit interactions was not examined in the previous chapter. Yet, such an effect could help us disentangle the factors that constrain or support multi-touch spatiotemporal aggregation. For this reason, in this chapter, we present two additional experiments, where in addition to manipulating whether aggregation had to occur across fingers of the same hand or opposite hands, we also manipulated the somatotopic relationship between stimulated fingers. In the first experiment (Exp. 4), we examined averaging across either adjacent (right index and right middle) or non-adjacent (right index and right ring) fingers. In the second experiment (Exp. 5), stimulated fingers were either bimanually homologous (right index and left index) or non-homologous (right ring, left index). Neither experiment exhibited a significant somatotopic influence on averaging performance, suggesting that spatiotemporal aggregation might occur at a level of processing, where tactile information has been abstracted away from the detailed information about which precise skin receptors are stimulated. Thus, distinctive features between unimanual and bimanual multi-touch aggregation may be attributed to a hand- or hemisphere-specific mechanism rather than a digit-specific mechanism.

## 4.1. Introduction

In line with an earlier study on combining intensity-based tactile signals (Walsh et al., 2016), **Chapter 3** found that biases in relative weighting of component directional stimuli observed for unimanual integration disappeared, when stimuli had to be aggregated across fingers on opposite hands. This result was corroborated with the finding of increased precision for aggregated direction estimate in the bimanual case. This chapter further investigated whether the observed effects could be replicated, and whether performance was modulated by the somatotopic relationship between stimulated fingers.

As described in Chapter 1 (see **section 1.2.2**) adjacent fingers are represented in adjacent portions of S1, which are connected with lateral and horizontal connections (Reed et al., 2008). Those give rise to masking effects, whereby concurrently presented stimuli inhibit one another (von Békésy, 1967). In **Chapter 2**, we showed that such inhibitory interactions between adjacent digit representation can be attenuated, given that participants intentionally prepare to combine two tactile stimuli delivered to adjacent fingers. Yet, we did not modulate the somatotopic distance between the stimulated fingers. Inter-digit interactions follow a spatial gradient, where they decrease with somatotopic distance (Ishibashi et al., 2000; Severens et al., 2010). The spatial gradient of inter-digit interactions has been demonstrated in behavioral experiments (Harris et al., 2001a; Tamè et al., 2011; Schweizer et al., 2000). For example, Harris and colleagues (2001a) showed that while participants were discriminating the frequency of two vibrations delivered sequentially to the same finger, a distractor stimulus interfered with discrimination accuracy depending on its somatotopic distance from the target finger. In addition, transfer of learning has been found between adjacent fingers, but not non-adjacent fingers, suggesting some overlapping representation (Dempsey-Jones et al., 2015; Harrar et al., 2013; Harris et al., 2001b). Thus, if topographically-organised lateral connections indeed contribute to averaging ability, one would expect performance to change when the somatotopic distance between component directions is increased.

Strikingly, the same somatotopically-organised effects observed for unimanual touch have been extended for bimanual touch (Harris et al., 2001a,b; Tamè et al., 2011; Dempsey-Jones et al., 2015; Harrar et al., 2013), suggesting that at least some tactile tasks that engage both hands occur at the same processing level of unimanual tasks. For example, the interference effect shown by Harris et al. (2001a) extended to the other hand and was strongest when the distractor was delivered to the homologous bilateral finger compared to non-homologous finger. In addition, learning has been shown to transfer to the homologous bilateral finger from the finger that originally received the training, but not the non-homologous finger (Harris et al., 2001b; Dempsey-Jones et al., 2015; Harrar et al., 2013).

This suggests that homologous bimanual fingers may be treated by S1 as adjacent unimanual fingers, while processing from a non-homologous bimanual finger may resemble that from a non-adjacent unimanual finger. These results suggest that multi-touch tasks are constrained by a digit-specific mechanism, which does not consider the body side or exact hemisphere as an important factor. Our finding from Chapter 3 that averaging tactile information across adjacent unimanual fingers seems different compared to averaging across homologous bimanual fingers, is already in disagreement with a digit-specific somatotopic mechanism. Nevertheless, we wished to examine whether homology between bimanual fingers could have some further modulating effect on bimanual aggregation.

## 4.2. Methods

### 4.2.1. Participants

To acquire comparable data to that in **Chapter 3**, we used the same sample size of 15 participants for each experiment. Thus, a group of 15 new participants took part in each of the two experiments. All participants gave informed consent prior to participation, in accordance with the declaration of Helsinki. The study was approved by the University College London Research Ethics Committee. Two participants were excluded from analysis (one in Exp. 4; one in Exp. 5) because of poor tactile perceptual performance (estimation errors exceeding 20° in more than 50% of trials in at least one single-finger condition). Excluded participants were replaced with others. The demographics of the final sample were as follows: Experiment 4 (age range: 18 – 30; mean: 23.47; 11 women, 4 men; all but one reportedly right-handed); Experiment 5 (age range: 18 – 34; mean: 22.20; 10 women, 5 men; all reportedly right-handed).

### 4.2.2. Task design

The tactile apparatus, experimental set-up, paradigm and tactile stimuli were identical to those used in **Chapter 3** (see **section 3.2**). The only difference was in the fingers that were stimulated (see **Figure 4.1A**). In Experiment 4, the adjacent condition was identical to Experiment 2 (stimulated fingers were right index and middle fingers). An additional condition was a non-adjacent condition, in which the probes touched the right index and right ring fingers. In Experiment 4, the homologous condition was identical to Experiment 3 (the stimulated fingers were right index and left index fingers). An additional condition was non-homologous condition, in which the probes touched the left index and right ring fingers. In Experiment 4, fingers in the adjacent condition remained at ~25 mm; in the non-adjacent condition, the distance between index and ring finger was ~45 mm. In Experiment 6, the distance between bimanual fingers was fixed to ~65 mm in order to make homologous and non-homologous conditions comparable without the confounding effects of spatial separation. The order of somatotopy conditions

(adjacency or homology) was counterbalanced across participants, and number-of-finger condition (single-finger or double-finger condition) was counterbalanced within each somatotopy condition. In double-finger conditions, the 21 stimulus combinations were repeated 5 times in Experiment 4 and 6 times in Experiment 5. In single-finger conditions, the number of repetitions of each direction was matched to that in the double-finger condition. The total number of trials was 105 per condition in Experiment 4 and 120 per condition in Experiment 5. Both experiments lasted approximately 2 hours and were performed across two 1-hour sessions on separate days.

#### *4.2.3. Main measures and statistical analysis*

Main measures were the same as in Chapter 3 (see **section 3.2.5**). Motion processing was described in terms of sensitivity to changes in stimulus direction, bias of direction judgments, precision of repeated estimates of direction for the same stimulus, and relative weighting between component directions. Slope and intercept values were estimated by fitting linear regressions to each participant's data separately in each condition. Group-level adjusted  $r^2$  values for linear fits for single-finger conditions were as follows:  $.65 \pm .09$  in Exp4 (adjacent),  $.62 \pm .09$  in Exp4 (non-adjacent),  $.57 \pm .15$  in Exp5 (homologous), and  $.55 \pm .17$  in Exp5 (non-homologous). For double-finger conditions:  $.34 \pm .11$  in Exp4 (adj),  $.28 \pm .13$  in Exp4 (non-adj),  $.42 \pm .17$  in Exp5 (hom), and  $.37 \pm .18$  in Exp5 (non-hom). Precision was derived as the inverse of unbiased SDs that were measured over repeated different tactile motion stimuli. Lastly, weight given to the spatially left-most finger (index finger of the right hand in unimanual experiments and left index finger in bimanual experiment) was estimated. For discrepancy-dependent effects the measures were derived during averaging task for each discrepancy separately.

For the statistical analyses, we again first used one-sample t-tests on slope and intercept values to see whether participants could perceive probes' directions and whether their perception was unbiased. When normality was violated, we used a sign test instead. For the main analysis, we were interested whether the aggregation process was influenced by somatotopy. In Experiment 4, the main interest was whether within-hand averaging ability depended on the somatotopic distance between fingers. A repeated-measures ANOVA (rmANOVA) was employed with factors number of fingers (single-finger vs. double-finger condition) and adjacency (adjacent vs. non-adjacent fingers) on the three measures. In Experiment 5, the main interest was whether the putative somatotopic mechanism extends to between-hands averaging. Here, similarly to Experiment 4, rmANOVA was employed with factors number of fingers (single-finger vs. double-finger condition) and homology (homologous vs. non-homologous fingers). To check the normality assumption, Shapiro-Wilk test was run on the residuals of the ANOVA. No significant deviations were found in Experiment 4. In Experiment

5, a slight deviation was found for the interaction in slope values ( $p = .03$ ), no other significant deviations were found. Modulations of weights and discrepancy-dependent effects during averaging were analysed by adding adjacency or homology as a within-subjects factor.

### 4.3. Results

#### 4.3.1. Analysis of single-finger conditions

**Figure 4.1B** shows the individual linear regressions fit for each single-finger condition separately in each experiment. **Table 4.1** shows the summary of the main measures (slope, intercept, and unbiased SD) as well as the t-test results. The slopes, shown in **Figure 4.1C**, were significantly above 0 in both experiments, indicating that the component directions could be successfully perceived. We compared the sensitivity across fingers in each experiment with a three-level one-way ANOVA that had finger as a factor. In Experiment 4, the effect of finger was significant ( $F(2, 28) = 3.33, p = .05, \eta^2 = .19$ ). We expected perception to be possibly worse on the ring finger compared to index and middle fingers. However, contrast analysis showed that the ring finger did not differ from index and middle fingers ( $t(28) = 1.03, p = .31$ ). Rather, the slope for index finger was higher than that for middle finger ( $t(28) = 2.37, p = .03$ ). Yet, the effect was marginal, and all fingers yielded slope values greater than 1. In Experiment 5, there was no significant effect of finger ( $F(2, 28) = .54, p = .59, \eta^2 = .14$ ). In terms of intercepts, shown in **Figure 4.1D**, none deviated from 0 and no significant difference between fingers was observed either in Experiment 4 ( $F(2, 28) = 1.50, p = .24, \eta^2 = .10$ ) or Experiment 5 ( $F(2, 28) = .71, p = .50, \eta^2 = .05$ ).

Unbiased SDs for each trajectory are shown in **Figure 4.1E**. We calculated unbiased SDs for each component direction separately for each finger and ran a rmANOVA with factors finger (stimulated fingers in the particular experiment), overall direction (leftward vs. rightward) and specific angle ( $25^\circ, 20^\circ, 15^\circ, 10^\circ, 5^\circ$ ). We excluded the component direction  $0^\circ$  from this analysis, as it could not be divided into leftward vs. rightward direction. In Experiment 4, the effect of finger was non-significant ( $F(2, 28) = 1.53, p = .23, \eta^2 = .10$ ), but there was a significant effect of overall direction ( $F(1, 14) = 9.29, p = .009, \eta^2 = .40$ ), with participants being more precise judging leftward (mean SD = 12) relative to rightward (mean SD = 14) directions. In Experiment 5, we observed a significant effect of finger ( $F(2, 28) = 6.1, p = .007, \eta^2 = .30$ ) with judgments from left index finger being more variable (mean SD = 13) than both right index (mean SD = 11) and right ring (mean SD = 11). In addition, the effect of specific angle was also significant ( $F(4, 56) = 3.1, p = .015, \eta^2 = .18$  - Greenhouse-corrected p-value), but Bonferroni-corrected pairwise tests indicated a significant difference only between  $5^\circ$  and  $15^\circ$  as well as  $5^\circ$  and  $25^\circ$  with judgements about  $5^\circ$  being more precise (mean SD = 11) than for  $15^\circ$  (mean SD = 12) and  $25^\circ$

(mean SD= 12). Note that 0° was excluded from analysis, but its mean SD was also low (mean SD = 10). This suggests that precision might have been higher, when estimating directions that were around the midline of the finger relative to the ones that deviated away from the midline. But this effect was only present in Experiment 5.

In sum, participants could successfully estimate component directions in both experiments and their judgments seemed unbiased. Some inter-finger differences in terms of precision could be observed, specifically reduced precision on the left index finger in Exp. 5. In addition, there were a few direction-specific precision effects, however due to exploratory and unpredicted nature of these, they will not be discussed.

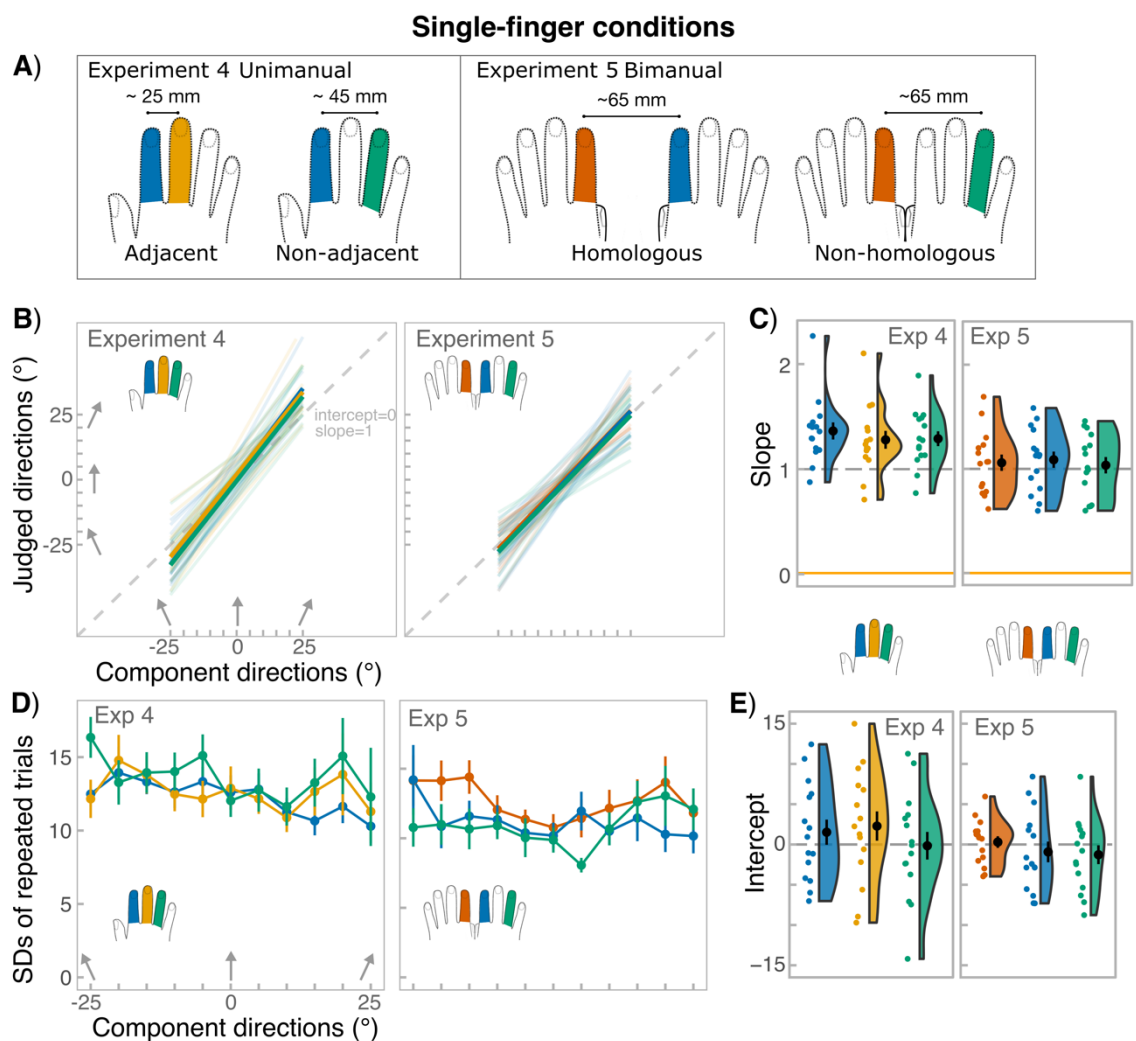


**Figure 4.1. Experiments 4 and 5: results for single-finger conditions.** **A)** Stimulated fingers in each condition. **B)** Individual fitted linear regressions (transparent lines) and group-level regressions (thick lines) for each finger, separately for experiments 4 and 5. The grey dashed line represents the equality line of slope 1 and intercept 0. **C)** Individual slope values (colored dots) derived from linear regressions in **B**, together with the group-level means (black dots). Raincloud plots (Allen et al., 2019) represent data distribution and error bars represent SEM. Colors on the plots correspond to the finger-conditions in **B**. **D)** Group-level unbiased standard deviations (SDs) for repeated trials for each component direction. Error bars represent SEM. **E)** Individual intercept values derived from linear regressions in **B**, together with the group-level means; annotations same as in **C**.

**Table 4.1:** Experiments 4 and 5: main measures for single-finger conditions

Condition	Slope			Intercept		SD
	mean $\pm$ SD	t-test against 0: $t(d)$	t-test against 1: $t(d)$	mean $\pm$ SD	t-test against 0: $t(d)$	mean $\pm$ SD
<b>Exp. 4:</b>						
Index	1.4 $\pm$ .3	120 <sup>†</sup> (4.32)**	118 <sup>†</sup> (1.15)**	1.5 $\pm$ 6.1	.97(.25)	12.3 $\pm$ 4.3
Middle	1.3 $\pm$ .3	15.02(3.88)**	3.28(0.85)*	2.3 $\pm$ 7.0	1.26(.33)	12.6 $\pm$ 6.1
Ring	1.3 $\pm$ .3	16.26(4.20)**	4.11(1.06)*	-0.2 $\pm$ 6.6	-.09(-.02)	13.6 $\pm$ 6.9
<b>Exp. 5:</b>						
Left index	1.1 $\pm$ .3	13.49(3.5)**	.75(.19)	0.3 $\pm$ 2.8	.41(.11)	12.6 $\pm$ 5.4
Right index	1.1 $\pm$ .3	13.91(3.6)**	1.12(.29)	-0.9 $\pm$ 5.0	-.72(-.19)	11.2 $\pm$ 5.3
Right ring	1.0 $\pm$ .3	13.16(3.4)**	.45(.12)	-1.3 $\pm$ 4.5	-1.09(-.28)	10.9 $\pm$ 5.3

Note: \* $p < .05$ , \*\* $p < .001$ .  $x^{\dagger}$  indicate the sign test (V), which was used instead of t-test, due to non-normality. Same group of 15 participants performed under all single-finger conditions within a single experiment, but each experiment had a new group of 15 participants.

#### 4.3.2. Double-finger conditions: t-tests on slope and intercept values

Next, we looked at the sensitivity and bias in all conditions to ensure that participants could perceive the average directions and that their perception was not biased. **Figure 4.2** shows the fitted linear regressions that were used to derive slope and intercept values for each condition. **Table 4.2** gives an overview and t-test results for the intercept and slope values. In both experiments and in all conditions, slope values were significantly higher than 0 and close to 1 in all double-finger conditions. Looking at the intercept values, perception was generally unbiased except in the homologous condition of Experiment 5, where we observed a consistent shift of approximately 2°.

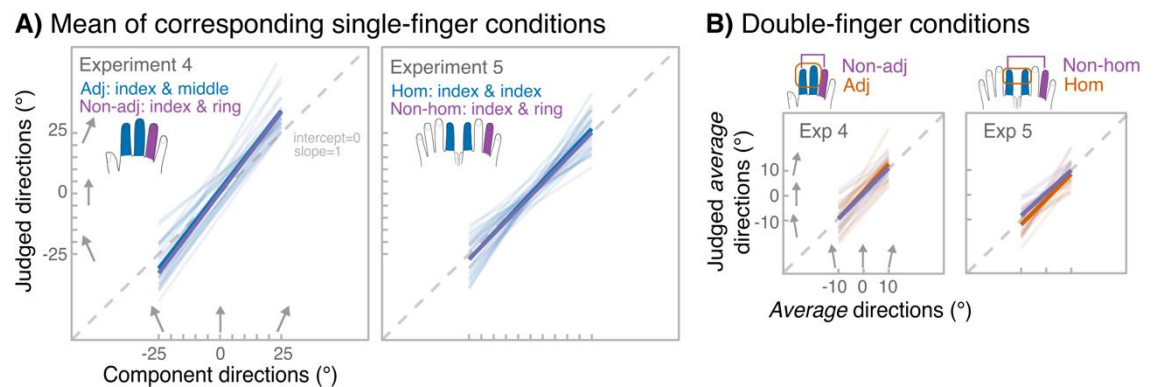


**Figure 4.2. Experiments 4 and 5: regression fits.** Individual fitted linear regressions (transparent lines) and group-level regressions (thick lines) in experiment 4 and 5, separately for the mean of single-finger conditions (A), and for double-finger condition, when participants were estimating the average between the individual component directions (B). The grey dashed line represents the equality line of slope 1 and intercept 0.

**Table 4.2:** Experiments 4 and 5: main measures for all conditions

Condition	Slope		Intercept		SD	
	mean $\pm$ SD	t-test against 0: $t(d)$	t-test against 1: $t(d)$	mean $\pm$ SD	t-test against 0: $t(d)$	mean $\pm$ SD
<b>Exp. 4:</b>						
A. S	1.3 $\pm$ .3	120 <sup>†</sup> (4.17)**	116 <sup>†</sup> (.99)**	1.9 $\pm$ 5.9	1.23(.32)	12.4 $\pm$ 3.5
A. D	1.1 $\pm$ .4	11.81(3.05)**	1.14(0.29)	1.7 $\pm$ 5.2	1.26(.33)	11.5 $\pm$ 3.2
N. S	1.3 $\pm$ .3	17.66(4.56)**	4.45(1.15)*	.72 $\pm$ 6.3	.44(.11)	13.0 $\pm$ 3.2
N. D	1.0 $\pm$ .3	13.75(3.55)**	.23(.06)	.95 $\pm$ 4.6	.81(.21)	12.7 $\pm$ 2.8
<b>Exp. 5:</b>						
H. S	1.1 $\pm$ .3	14.39(3.72)**	1.03(.27)	-.2 $\pm$ 3.0	-.27(-.07)	11.5 $\pm$ 3.2
H. D	1.0 $\pm$ .4	10.15(2.62)**	.22(.06)	-1.8 $\pm$ 2.8	-2.48(-.64)*	9.7 $\pm$ 3.5
N. S	1.0 $\pm$ .3	13.37(3.45)**	.88(.14)	-.6 $\pm$ 3.2	-0.70(-.18)	12.1 $\pm$ 4.3
N. D	.9 $\pm$ .4	8.54(2.21)**	-.76(.20)	.7 $\pm$ 3.0	.95, (.25)	10.3 $\pm$ 4.5

Note: \* $p < .05$ , \*\* $p < .001$ .  $x^{\dagger}$  indicate the sign test (V), which was used instead of t-test, due to non-normality. Each condition contains  $n = 15$ ; different group of 15 participants performed in each experiment. A. S (adjacent single); A. D (adjacent double); N. S (non-adjacent single); N. D (non-adjacent double); H (homologous)

#### 4.3.3. Experiment 4: averaging performance was not influenced by finger adjacency

The main interest was whether averaging was modulated by somatotopic distance, thus we looked at the statistical significance of adjacency by number-of-finger interaction. The interaction was not significant for slope values (**Figure 4.3A**;  $F(1, 14) = 1.5$ ,  $p = .24$ ,  $\eta^2 = .10$ ,  $BF^{01} = 1.9 \pm 3.3\%$ ,  $BF_{incl} = .5$ ). There was also no main effect of either adjacency ( $F(1, 14) = .45$ ,  $p = .51$ ,  $\eta^2 = .03$ ,  $BF^{01} = 3.5 \pm 1.0\%$ ,  $BF_{incl} = .3$ ). But the main effect of number-of-finger was significant ( $F(1, 14) = 16.5$ ,  $p = .001$ ,  $\eta^2 = .54$ ,  $BF^{01} < .001 \pm 2.0\%$ ,  $BF_{incl} = 984.5$ ) with sensitivity being higher in single-finger conditions (mean slope =  $1.3 \pm .3$ ) relative to double-finger condition (mean slope =  $1 \pm .4$ ). However, it is notable that the slope values in double-finger condition were close to 1, whereas slope values were exceeding 1 in single-finger conditions, indicating overestimation of component directions. Intercept values (**Figure 4.3B**) did not exhibit a significant interaction ( $F(1, 14) = .16$ ,  $p = .69$ ,  $\eta^2 = .01$ ,  $BF^{01} = 2.8 \pm 3.1\%$ ,  $BF_{incl} = .1$ ). Both main effects were also non-significant (adjacency:  $F(1, 14) = 1.4$ ,  $p = .26$ ,  $\eta^2 = .08$ ,  $BF^{01} = 2.0 \pm 1.0\%$ ,  $BF_{incl} = .4$ ; and number-of-finger:  $F(1, 14) = .001$ ,  $p = .97$ ,  $\eta^2 = .001$ ,  $BF^{01} = 3.8 \pm 3.0\%$ ,  $BF_{incl} = .2$ ).

**Figure 4.3C** illustrates the SD values, which again did not show a statistically significant interaction ( $F(1, 14) = .48$ ,  $p = .50$ ,  $\eta^2 = .03$ ,  $BF^{01} = 2.8 \pm 4.9\%$ ,  $BF_{incl} = .2$ ). The main effects were also non-significant (adjacency:  $F(1, 14) = 3.7$ ,  $p = .07$ ,  $\eta^2 = .21$ ,  $BF^{01} = 1.2 \pm .9\%$ ,  $BF_{incl} = .7$ ; and number-of-fingers:  $F(1, 14) = .73$ ,  $p = .41$ ,  $\eta^2 = .05$ ,  $BF^{01} = 2.3 \pm .8\%$ ,  $BF_{incl} = .3$ ). Importantly, the non-significance of number-of-finger condition shows that, similarly to Experiment 2, there was no precision benefit during averaging two component directions within the same hand. Overall, these results suggest no evidence that aggregation performance was affected by somatotopic distance between the stimulated fingers.



## Double-finger vs. mean of single-finger conditions

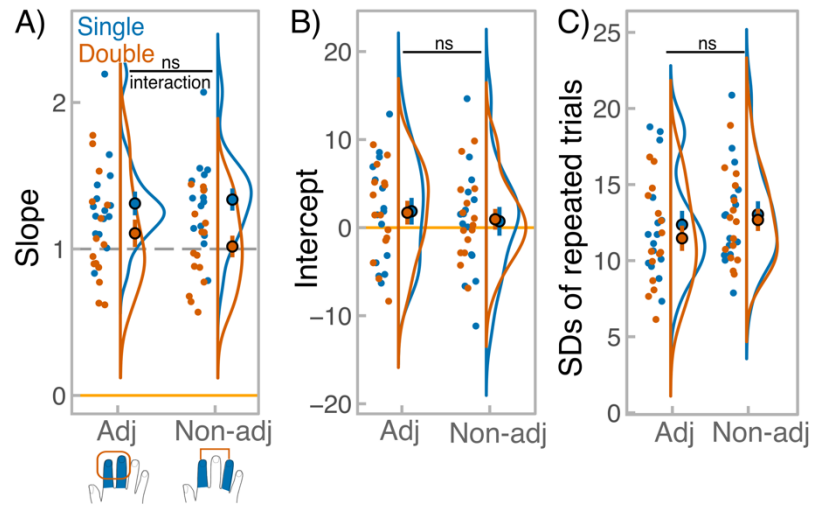


**Figure 4.3. Experiment 4: main measures.** **A)** slope values estimated from single-subject regressions, corresponding to the sensitivity. **B)** intercept values also estimated from single-subject regressions, corresponding to the bias. **C)** unbiased SD values for repeated estimation of identical directions. SDs were calculated separately for each repeated stimuli; for simplicity, data was averaged across repeated stimuli to show the mean SDs for single-finger (blue) and double-finger (orange) conditions. In all panels, points with error bars reflect group-level means and SEM. Raincloud plots (Allen et al., 2019) show the distribution of the data. Upper black annotation shows statistical significance of number-of-fingers (single vs. double) by adjacency (adjacent vs. non-adjacent) interaction. Each condition (number-of-fingers and adjacency) was performed by the same group of 15 participants.

### 4.3.4. Experiment 4: discrepancy-dependent effect on averaging regardless of adjacency between component directions

The averaging performance broken down by discrepancy showed, similarly to Experiment 2, that sensitivity to average direction dropped when directions started to diverge (main effect of sign of discrepancy:  $F(1, 14) = 12.7$ ,  $p = .004$ ,  $\eta p^2 = .48$ ,  $BF^{01} < .001 \pm 1.2\%$ ,  $BF_{incl} = > 20000$ ; mean slope = .86,  $SD = .52$  for diverging vs. mean slope = 1.26,  $SD = .58$  for converging; see **Figure 4.4A**). This effect was present regardless of the adjacency between the stimuli (sign of discrepancy by adjacency interaction:  $F(1, 14) = 1.4$ ,  $p = .25$ ,  $\eta p^2 = .09$ ,  $BF^{01} = 3.1 \pm 4.1\%$ ,  $BF_{incl} = .2$ ). The level of discrepancy itself did not influence averaging ( $F(2, 28) = .45$ ,  $p = .64$ ,  $\eta p^2 = .03$ ,  $BF^{01} = 114.8 \pm .9\%$ ,  $BF_{incl} = .04$ ), regardless of finger adjacency ( $F(2, 28) = .40$ ,  $p = .62$ ,  $\eta p^2 = .03$ ,  $BF^{01} = 7.2 \pm 6.6\%$ ,  $BF_{incl} = .01$ ). There were no discrepancy-related effects for intercept values (all  $p$  values:  $.43 < p < .95$ ; see **Figure 4.4B**) or SDs (all  $p$  values:  $.18 < p < .81$ ; see **Figure 4.4C**). Overall, these results replicate the sensitivity drop when components were diverging seen in the unimanual experiment in the previous chapter but add that this effect is present both when components were adjacent and non-adjacent.

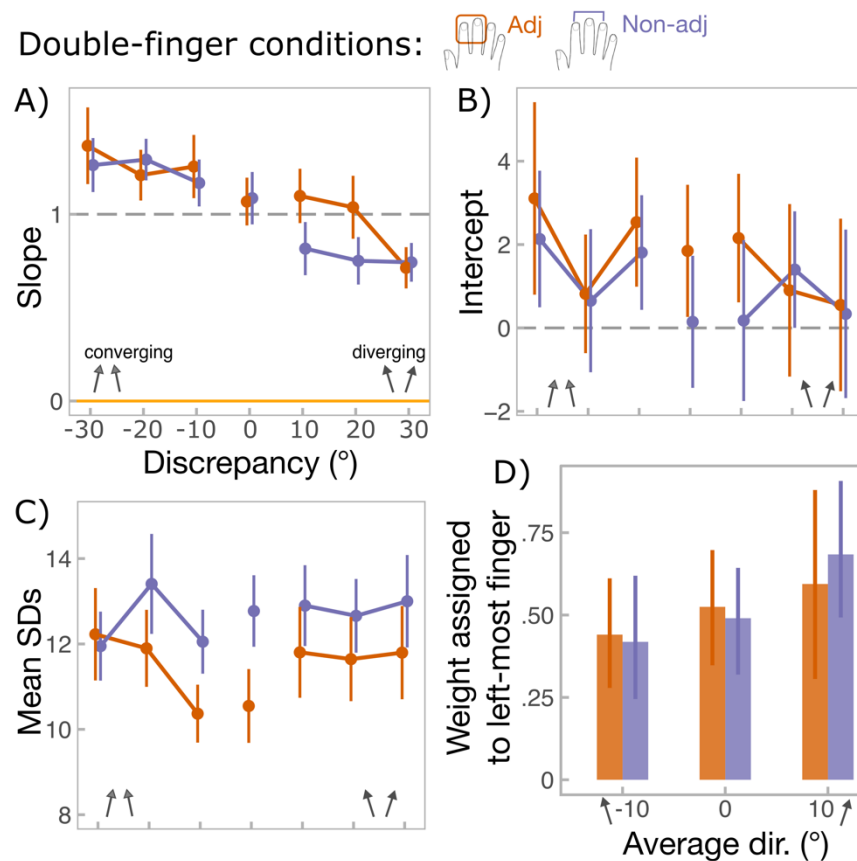


**Figure 4.4. Experiment 4: effect of discrepancy on averaging performance and weighting of component directions during averaging.** **A)** Slope values as a function of discrepancy. The points correspond to group-level slope values, estimated from single-subject regressions fit to double-finger conditions, but separately to each discrepancy level (x axis). Error bars correspond to SEM. Discrepancy of 0 (when component directions were identical) is included in the plots for illustrative purposes, but was not included in the analysis, because discrepancy was factored into sign of discrepancy (negative discrepancy, when directions converged vs. positive discrepancy, when directions diverged) and level of discrepancy (30° vs. 20° vs. 10°). **B)** Intercept values as a function of discrepancy; annotations are the same as for panel **A**. **C)** Unbiased SD values for repeated estimations of identical trials as a function of discrepancy (x axis). SDs were calculated for each average direction separately, but for simplicity data was pooled across average directions to show the mean SDs for each discrepancy. Annotations same as for panel **A**. **D)** the weight assigned to the left-most finger during averaging (right index in unimanual experiment and left index in bimanual experiment) as a function of average direction. Weight of 0.5 meant that the directional information from both fingers was weighted equally. In all panels, orange traces reflect averaging across adjacent fingers, while purple traces reflect averaging across non-adjacent fingers.

#### 4.3.5. Experiment 4: biased weighting regardless of adjacency

**Figure 4.4D** shows the weight assignment to the left-most finger as a function as a function of average direction. Consistently with the weighting pattern found in Experiment 2, the weight shifted as a function of average direction ( $F(2, 28) = 7.60, p = .008, \eta p^2 = .35$ , Greenhouse corrected p value). Bonferroni-corrected pairwise tests showed that the left-most finger received a higher perceptual weight when average direction was rightward (10°; mean weight = .64, SD = .7) compared to when the average direction was leftward (10°; mean weight = .43, SD = .5;  $p = .001$  Bonferroni-corrected test). This shift in weights was similar across adjacency conditions (interaction by adjacency:  $F(2, 28) = 1.2, p = .30, \eta p^2 = .08$ ).

#### 4.3.6. Experiment 5: averaging performance was not influenced by bimanual finger homology

Here, the main interest laid in the statistical significance of homology by number-of-finger condition interaction. In terms of slope values (**Figure 4.5A**), the interaction was not significant ( $F(1, 14) = .70, p = .42, \eta^2 = .002, BF^{01} = 2.1 \pm 9.2\%, BF_{incl} = .4$ ). Both main effects were also non-significant (homology:  $F(1, 14) = 4.3, p = .06, \eta^2 = .23, BF^{01} = 1.7 \pm 1.7\%, BF_{incl} = .5$ ; and number-of-fingers:  $F(1, 14) = 2.0, p = .18, \eta^2 = .13, BF^{01} = .9 \pm .9\%, BF_{incl} = .9$ ). In terms of intercept values (**Figure 4.5B**), the interaction was significant ( $F(1, 14) = 6.44, p = .02, \eta^2 = .32, BF^{01} = .5 \pm 2.2\%, BF_{incl} = .8$ ). Follow-up paired-sample t-tests showed that in homologous condition there was a greater bias in the double-finger condition (mean intercept =  $-1.8, SD = 2.8$ ) compared to the single-finger condition (mean intercept =  $-.2, SD = 3.0; t(14) = 2.9, p = .01, d = .75$ ). No such difference was found in the non-homologous condition ( $t(14) = -1.3, p = .20, d = -.34$ ). This reflects the significant bias during the homologous double-finger condition. For SDs (**Figure 4.5C**), the interaction was not significant ( $F(1, 14) = .002, p = .96, \eta^2 < .001, BF^{01} = 2.7 \pm 2.8\%, BF_{incl} = .4$ ). The main effect of homology was also not significant ( $F(1, 14) = 1.3, p = .27, \eta^2 = .09, BF^{01} = 2.4 \pm 2.6\%, BF_{incl} = .4$ ). Importantly, consistent with Experiment 3, SDs were reduced when estimating the average (mean  $SD = 10, sd = 4$ ) in contrast to estimating the component directions in isolation (mean  $SD = 11.8, sd = 3.8; F(1, 14) = 9.0, p = .01, \eta^2 = .39, BF^{01} = .03 \pm 1.8\%, BF_{incl} = 24.4$ ). Overall, these results suggest no evidence that aggregation performance was affected by whether the bimanual fingers were homologous or not (except for intercept values).

Double-finger vs. mean of single-finger conditions

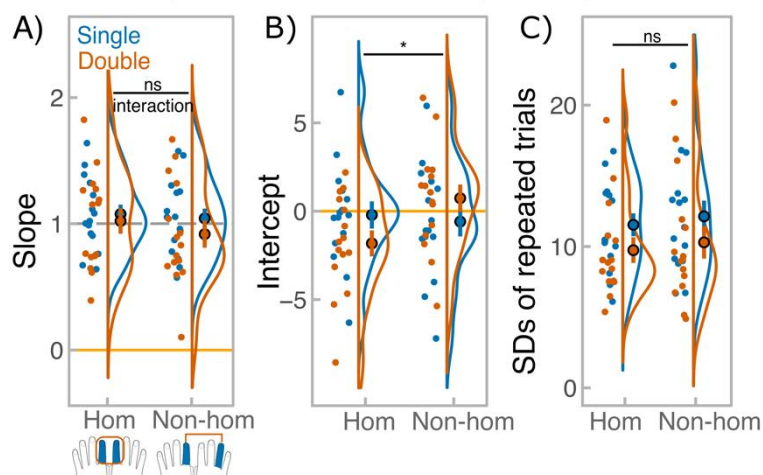


**Figure 4.5. Experiment 5: main measures.** **A)** Slope values estimated from single-subject regressions, corresponding to the sensitivity. **B)** Intercept values also estimated from single-subject regressions, corresponding to the bias. **C)** Unbiased SD values for repeated estimation of identical directions. SDs were calculated separately for each repeated stimuli; for simplicity, data was pooled across repeated stimuli to show the mean SDs for single-finger (blue) and double-finger (orange) conditions. In all panels, points with error bars reflect group-level means and SEM. Raincloud plots (Allen et al., 2019) show the distribution of

the data. Upper black annotation shows statistical significance of number-of-fingers (single vs. double) by homology (homologous vs. non-homologous) interaction. Each condition (number-of-fingers and adjacency) was performed by the same group of 15 participants.

#### 4.3.7. Experiment 5: no discrepancy-dependent effects

Discrepancy-related effects are shown in **Figure 4.6**. There were no discrepancy-related effects for slope values (main effect of discrepancy level:  $F(2, 28) = .08$ ,  $p = .92$ ,  $\eta^2 = .006$ ,  $BF^{01} = 16.8 \pm 1.0\%$ ,  $BF_{incl} = .02$ ; main effect of discrepancy sign:  $F(1, 14) = .81$ ,  $p = .38$ ,  $\eta^2 = .05$ ,  $BF^{01} = 3.2 \pm 2.9\%$ ,  $BF_{incl} = .13$ ), and neither were modulated by homology (both interactions have  $p$  values of .96 for level and .81 for sign). For intercept values, only the main effect of homology was significant ( $F(1, 14) = 5.3$ ,  $p = .04$ ,  $\eta^2 = .27$ ,  $BF^{01} = .34 \pm 2.6\%$ ,  $BF_{incl} = 1.1$ ), none of the other effects or interactions reached significance (all other  $p$  values:  $.38 < p < .92$ ). For SDs, the interaction between average direction and sign of discrepancy reached statistical significance ( $F(2, 28) = 3.8$ ,  $p = .03$ ,  $\eta^2 = .21$ ), but follow-up Bonferroni-corrected tests did not show any significant differences due to correction for multiple comparisons. None of the other effects or interactions reached significance level (all other  $p$  values:  $.22 < p < .89$ ). In terms of weight allocation across component directions (**Figure 4.6D**), there was no systematic shift in weighting as a function of average direction ( $F(2, 28) = .18$ ,  $p = .84$ ,  $\eta^2 = .01$ ), regardless of homology ( $F(2, 28) = .87$ ,  $p = .43$ ,  $\eta^2 = .06$ ).

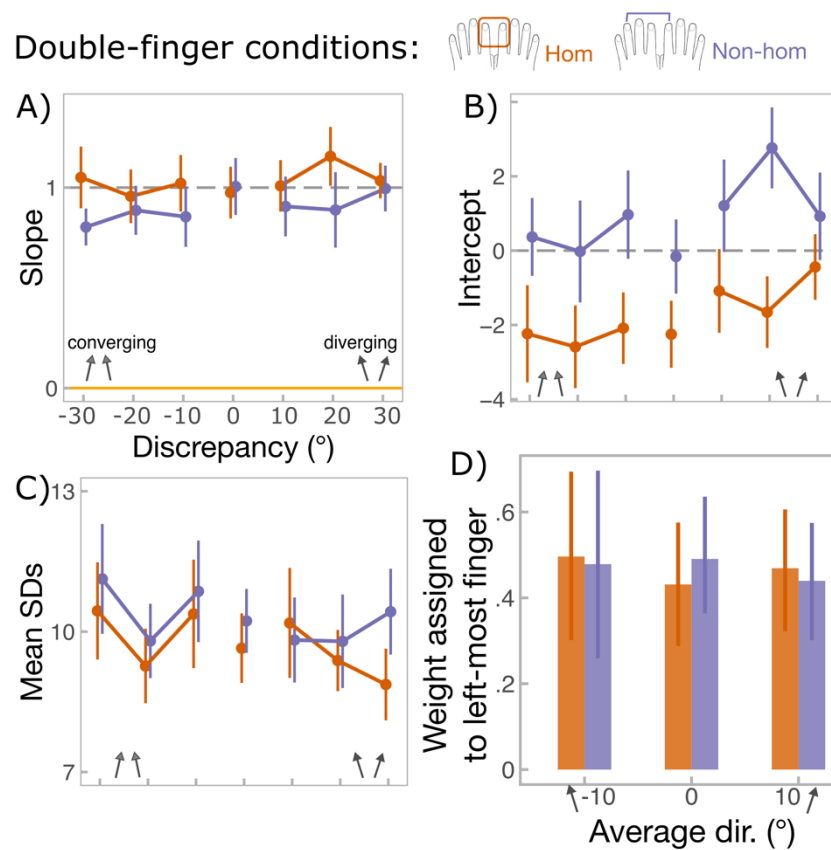


**Figure 4.6. Experiment 5: effect of discrepancy on averaging performance and weighting of component directions during averaging.** **A)** Slope values as a function of discrepancy. The points correspond to group-level slope values, estimated from single-subject regressions fit to double-finger conditions, but separately to each discrepancy level (x axis). Error bars correspond to SEM. Discrepancy of 0 (when component directions were identical) is included in the plots for illustrative purposes, but was not included in the analysis, because discrepancy was factored into sign of discrepancy (negative discrepancy, when directions converged vs. positive discrepancy, when directions diverged) and level of discrepancy (30° vs. 20° vs. 10°). **B)** Intercept values as a function of discrepancy; annotations are the same as for panel **A**. **C)** unbiased SD values for repeated estimations of identical trials as a function of discrepancy (x axis). SDs were calculated for each average direction separately, but for simplicity data was averaged across average directions to show the mean SDs for each discrepancy. Annotations same as for panel **A**. **D)** the weight assigned to the left-most finger during averaging (right index in unimanual experiment and left index in bimanual experiment) as a function of average direction. Weight of 0.5 meant that the directional information from both fingers was weighted equally. In all panels, orange traces reflect averaging across homologous fingers, while purple traces reflect averaging across non-homologous fingers.

#### 4.4. Discussion

The aim of the two experiments presented in this chapter was to elucidate the mechanisms that may underlie the ability to aggregate spatiotemporal tactile input across multiple different fingers. Specifically, we wanted to find out whether changing the somatotopic relationship between stimulated fingers would affect averaging ability. Overall, our findings suggest that somatotopic organisation does not affect aggregation, at least in our task, where participants intentionally combine two spatiotemporal trajectories to represent their average motion direction.

#### 4.4.1. Precision: bimanual averaging benefit extends to non-homologous fingers

Experiment 5 again demonstrated that when component directions were combined across fingers on different hands, aggregation benefitted from multiple inputs. Such benefit did not occur for unimanual aggregation. Importantly, neither adjacency between fingers on the same hand nor homology between bimanual fingers affected the contrast in precision between averaging and perceiving component direction alone. That is, the factors affecting precision of tactile perception when averaging across multiple digits were not significantly affected by whether those digits were adjacent or not in the case of unimanual case, nor by whether the digits were homologous or not in the bimanual case. **Figure 4.7** illustrates this difference when data was pooled across adjacency and homology conditions. This result substantiates our finding that bimanual multi-touch perception produces a more precise aggregated representation than unimanual multi-touch perception. The lack of adjacency and homology effect suggests that this precision effect likely arises from a hand- or hemisphere-specific mechanism rather than somatotopic or digit-specific mechanism.

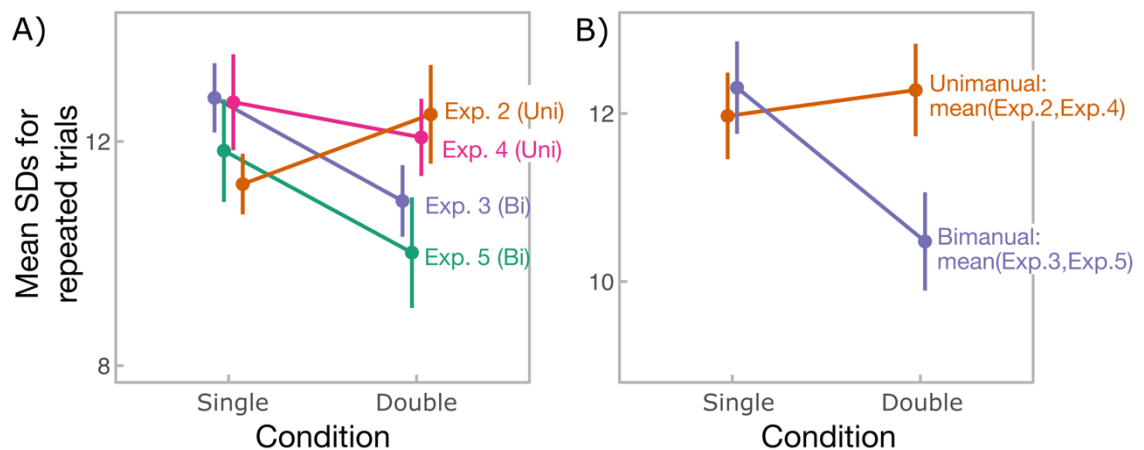


**Figure 4.7. Precision across Experiments 2 to 5.** Precision difference between averaging (double-finger condition) and perceiving components directions in isolation (single-finger conditions). Precision is measured as unbiased standard deviations (SDs) for repeated identical trials, separately for each experiment (A) and averaged across unimanual and bimanual experiments (B). Error bars represent SEM.

In terms of adjacency during unimanual aggregation, Bayesian analysis tended to show support for the lack of effect based on adjacency ( $BF^{01} = 2.8$ , which is very close to 3), indicating that the null result was not simply due to lack of statistical power. Similarly, Bayesian analysis supported the null result for lack of homology during bimanual aggregation ( $BF^{01} = 2.7$ ). A recent paper by Kusnir, Pesin, and Landau (2020) also failed to find digit-specific effects during a bimanual vibration discrimination task, where participants were asked to detect a brief intensity change within an ongoing vibration on one finger while a distractor vibration was applied to different fingers on the other hand. Similarly, Tamè et al. (2014) showed that tactile interference

in bimanual context was the same regardless of the stimulated fingers of the two hands. In their task, participants had to choose in which of the two intervals a target finger was stimulated while a distractor was applied to another finger.

Tamè et al. (2016) emphasise that the presence or absence of finger-specific interaction for tactile stimuli delivered to opposite hands can depend on the task demands. Specifically, they suggest that tasks that have stronger demand on working memory (i.e., tactile detection in a go-no-go context, tactile localization, and discrimination), but not in simpler tasks without a memory demand (tactile detection in a two-intervals force choice design). This may be related to the criticality of S1 involvement in the given task. For example, Tamè and Holmes (2016) showed that TMS over S1 disrupted performance on a one-interval forced-choice detection task, where participants have to continuously retain the target stimulus in memory, but not in two-interval forced-choice detection task, where participants are reminded of the target stimulus on every trial. This may explain why Tamè et al. (2014) did not observe a digit-specific effect, however, it cannot fully explain why neither us nor Kusnir et al. (2020) failed to find such somatotopic performance influence, as both tasks had a considerable memory component. In our study participants had to presumably retain the trajectories in memory to estimate their average direction. To make matters worse, Reed et al. (2011) found that the bilateral RFs in S1 tend to be more diffuse than the respective unilateral RFs, suggesting that they may encompass skin areas of non-homologous fingers. Thus, absence of homology effect on behavioral performance may not invalidate the engagement of early bilateral RFs in S1. However, this would still not explain why bimanual averaging, regardless of specific fingers stimulated, led to greater precision.

Previous studies have focussed on the ability to localise a stimulus or segregate two tactile stimuli (i.e., ignore a distractor stimulus on one finger, and selectively attend to a target stimulus on another finger), whereas in our tasks the focus was on the ability to combine two tactile stimuli across different fingers to extract some common tactile property (i.e., average motion direction). One could argue that such aggregation should require the brain to abstract away from the detailed information about which precise skin receptors happen to have been stimulated, in order to recover a representation of the stimulating object. In vision, such abstraction away from the contingent details of viewpoint is considered a crucial precursor for visual object and event perception (Marr, 1982). The absence of somatotopic effects fits well with findings of Fitzgerald et al. (2006a,b) who showed that neurons in S2 (secondary somatosensory cortex) could encode stimulus properties encompassing multiple digits (orientation of a bar) without being contingent upon exact digit stimulated.

In addition, the absence of somatotopic effects during averaging may be related to the findings of Experiment 1 (**Chapter 2**), whereby suppressive inter-digit interactions were attenuated when participants were instructed to report average directions, as opposed to direction discrepancies. Thus, any somatotopic effects might be attenuated in our averaging conditions. In agreement with our results, Walsh and colleagues (2016) showed that biased aggregation of tactile *intensity* inputs occurred regardless of adjacency between unimanual fingers, yet participants' performance improved during bimanual aggregation (however, those authors did not examine homology effects). The authors of that study also argued that judgements about total intensity depend on a processing level that is hemisphere-specific rather than digit-specific.

For these reasons, we believe that the performance limits in our tactile motion aggregation task also arise from hemisphere-specific constraints. As speculated in **Chapter 3**, these could be either related to attentional resources that cannot perfectly retain two concurrent moving stimuli within the same hand but can be divided between the processing related to each hand, resulting in the ability to attend to two stimuli in parallel when these are presented between hands. One way to test this explanation further would be to present the component directions with a temporal delay, which should relieve the demands on attentional resources. However, such design could incur demands on working memory (Harris et al., 2001a). Another way to explain the precision-specific effect is through noise independence theory, whereby non-independent noise sources do not decrease in noise following aggregation (Zohary et al., 1994; Averbeck et al., 2006; Alvarez, 2011). Accordingly, two fingers on the same hand may be affected by non-independent noise, whereas noise affecting fingers on opposite hands may be relatively independent. The lack of digit-specificity fits well with findings of Cohen and Maunsell (2009), who found that noise correlations between pairs of individual neurons tended to extend across the whole hemisphere, but not to the opposite hemisphere. Such intra-hemispheric noise correlations could arise via fluctuations in the mono-hemispheric somatosensory rhythms (Andrew & Pfurtscheller, 1999; Kilner et al., 2003). Further EEG studies could help to illuminate this explanation.

#### ***4.4.2. Sensitivity and weight allocation: strategic weighting during unimanual aggregation to overcome unimanual limitation***

Another important finding of Experiment 4 was the replication of Experiment 2 in terms of the pattern on sensory weighting and the deterioration of sensitivity when component directions started to diverge. Importantly, these effects were not observed in Experiment 5 and Experiment 3, which used the same component directions, but delivered them bimanually. Thus, we can ascertain that these effects are specific for unimanual aggregation. Furthermore, the fact



that we found that the same effects extend to non-adjacent unimanual fingers suggests that what is important is the use of either a single hand or two different hands. As a consequence, our results fit with the proposed model of hand-specific heuristic, where a “virtually leading finger” (VLF) attracts more weight due to information novelty, and thus biases the estimation of the average.

The VLF-based theory assumes that participants have pre-existing priors (or beliefs) about the statistics of the natural stimuli, particularly for coherent object motion across the multiple fingers of one hand. For such coherent object motions, one finger can be designated as the “virtually leading finger”, which first encounters a given tactile stimulus feature. Other fingers encounter the same features after a delay – the information they provide may therefore be redundant and less important. Strikingly, in our tasks, the tactile stimuli were two probes that moved across the static fingertips, in independent directions. The stimulus directions were generally discrepant, and thus incompatible with a coherent object motion. Nevertheless, the distinctive VLF bias associated with coherent object motion was present in the data. This suggests that participants could not avoid averaging the stimuli in a way that expresses a strong prior reflecting situation of coherent motion of an object with respect to the hand. In natural tactile tasks, such ‘object-motion’ priors could serve as a cognitive heuristic to overcome the limited physiological resources for optimal integration in unimanual touch. However, in our task that involved discrepant motion directions, such prior led to a biased, and suboptimal weighting, which in turn led to under- or over-estimation of the average direction.

From Gestalt theory we know that “single object” beliefs can shape sensory processing. In vision, a bar interrupted by an occluder evokes a qualitatively similar, but weaker, neuronal response as if the bar was continuous (Baumgartner et al., 1984). This means that given a strong object-prior a neuron will respond even if its RF was never stimulated by the traversing stimulus. In other words, the sensory system cannot help but to try to restore an incomplete object percept. The power of object-priors has been also exhibited in tactile “funneling” illusion, where a simultaneous presentation of brief tactile stimuli at multiple points on the skin produces a single focal sensation at the centre of the stimulus pattern, even when no physical stimulus occurs at that site (e.g., Sherrick, 1964). Chen, Friedman, and Roe (2003) showed that brain response to the funneling stimuli represents a single focal cortical activation within an area of the somatosensory cortex that lies between the regions that were actually stimulated. Spence and Gallace (2011) review numerous examples of “filling in” phenomenon in tactile modality grounded by a strong belief that given tactile information must arise from a single object. Although these are not directly relevant for our aggregation task, they still illustrate that power

perceptual coherent object priors that in our case did not lead to “filling in” of tactile information but biased the average motion estimation.

#### **4.5. Conclusions**

The findings in this chapter extend those in **Chapter 3**, by showing that distinctive features of tactile within-hand and between-hand motion integration are in fact hand-specific, but not finger-specific. That is, the ability to average the direction of two tactile motions depended on whether they were delivered to the same hand, or different hands, but did not depend on whether they were delivered to adjacent or non-adjacent fingers unimanually, nor on whether they were delivered to homologous or non-homologous fingers bimanually. The precision data could speculatively be explained in terms of a limitation on the amount of tactile spatial information that could be represented in each hemisphere. One possible reason for the capacity limitation could be that neural noise from multiple tactile signals within a single hemisphere may be correlated, reducing the expected benefit of averaging multiple signals. Indeed, when signals from opposite hands are combined, the expected benefit of averaging is indeed present. One solution for multi-digit touch with limited capacity would be to weight signals from the most important digit more than signals from a less important digit. Although in our task both digits were important, participants seemed to employ some sort of biased weighting. Specifically, the sensitivity data could be explained in terms of a prior leading to increased weighting for one finger, based on it providing more important, and less redundant information than the other finger. This prior-based weighting is consistent with representing an object interacting with one hand, but it does apply when stimuli were delivered to two hands.

## Chapter 5: Effect of posture on bimanual multi-touch perception

This chapter investigated how proprioceptive input is integrated with skin-based representation of stimulus direction. In addition to a parallel condition, when both hands were pointing straight away from the body midline, the right hand was rotated by 45°. In this case, participants needed to integrate skin-based spatiotemporal information with the information about postural change of one of the hands in order to derive the veridical average direction. A process that is often called *remapping*. The present experiment showed that the hand posture had an attracting effect on tactile direction judgements, yet the resulting bias seemed considerably weaker than the actual hand rotation – an outcome that suggests a remapping process coupled with over-compensation for the posture. Further, when participants averaged motion directions across a parallel and a rotated finger, their biases were equivalent to the arithmetic mean of the biases that arose from estimating the component directions in isolation. This suggests that averaging might be an independent process occurring *after* remapping. Strikingly, the bias in the averaging task depended on the discrepancy between the direction of the component trajectories. In addition, hand rotation induced additional noise into the estimation process both during single-finger estimation and averaging. Overall, our findings suggests that multi-touch aggregation occurs on ‘remapped’ representations of component directions.

## 5.1. Introduction

So far, it could be assumed that it has been enough for the brain to determine the movement of the probe by encoding the successive activation of multiple receptive fields (RFs) on the skin - a process that we believe may occur at the level of area 1 in S1. In order to then estimate the overall movement across the two probes, **Chapter 2** showed that the brain can aggregate the spatially separated component inputs by modulating inter-finger interactions that are evident at the earlier levels of somatosensory processing (i.e., at P40 component). However, as mentioned already in **Chapter 1**, one difference between multi-touch integration and the integration of visual information between two eyes, is that the skin is deformable, and moves as the body moves. Thus, touch locations can change in external space relative to one another (see **section 1.2.5**). In contrast, eyes remain at fixed locations on the body and at a fixed distance from each other. What this means for multi-touch perception is that when the touched locations move in external space, as in when body posture changes, the information about the movement and posture of the body needs to be considered if multiple tactile signals are to be aggregated accurately. The process of transforming skin-based spatial information (i.e., motion direction as a successive activation of skin RFs) into an external reference frame, where changes in the body posture are accounted for, is called *tactile remapping* (Driver & Spence, 1998; Heed et al., 2015).

### 5.1.1. Compulsory remapping of touch into external space

To examine tactile remapping, the skin-based and external reference frames can be brought into conflict by changing limb posture. Most previous studies have mainly focussed on perception of stationary stimulus location and relied on the effect of limb crossing, where a right hand (skin-based reference frame) is crossed over the body midline and is then located in left space (external reference frame). Azañón and Soto-Faraco (2008) asked participants to discriminate the location of a visual flash presented on either hand as fast as possible. They found that a tactile cue presented shortly before the visual flash (60 ms before) enhanced performance on the hand defined by a skin-based reference frame. Meaning that tactile cue delivered to a right hand improved visual discrimination in the right space, even when the right hand was in the left space due to crossing. In contrast, when the time between the tactile cue and visual flash was extended (more than 180 ms), the facilitation effect occurred on the basis of external space. In other words, now touch on the right hand that was placed in left space enhanced visual perception in the left space. Similar shifts between skin-based and external frames of reference in a cross-hand paradigm have been found for saccades (Overvliet, Azañón, & Soto-Faraco, 2011). These findings suggest that touch is first represented in skin-based space, and subsequently via a remapping process automatically represented in external space.

Another line of studies has combined the cross-hand paradigm with judgements about the order of tactile taps delivered to the hands and has shown a persistent dominance of external over skin-based reference frame (e.g., Azañón, Mihaljevic, & Longo, 2016; Heed & Azañón, 2014). A prominent example is a study by Yamamoto and Kitazawa (2001). In their study, participants became significantly worse in crossed-hand condition, when the interval between taps was less than 300 ms. At longer intervals (> 1s) performance improved. Importantly, this cross-arm effect was not extended to visual stimuli attached to the hands – participants could perform the visual task with high accuracy at all inter-flash intervals. The drop in performance during medium-length intervals is believed to reflect the period where remapping is occurring but is not yet complete. This is consistent with curved saccade trajectories during crossed condition, whereby participants initially aim their saccades to the incorrect hand but then correct it (Overvliet et al., 2011). Crucially, the task could be performed successfully if the posture was discounted, and participants relied completely on skin-based information. The finding that, instead, posture exerted significant and detrimental influence suggests that remapping happens automatically and dominates perception.

### *5.1.2. Evidence against compulsory remapping*

However, there is also evidence to suggest that in some contexts tactile perception retains the skin-based representation even when posture is changed. For example, the masking effect for concurrent stimulations to adjacent fingers disappears when fingers of two hands are intertwined and the new stimulated finger is spatially, but not somatotopically, adjacent (Röder, Spence, & Rösler, 2002). Thus, at least inter-digit interactions depend on skin-based space. In addition, the mapping between hands and corresponding feet are not affected by crossing the hands (Medina et al., 2014). Furthermore, Kuroki et al. (2010) showed that temporal order judgments between tactile stimulation of separate fingers was affected by somatotopic distance between the finger representations, but not by spatial separation between fingers. However, Kuroki et al.'s study used ipsilateral adjacent versus bilateral non-homologous fingers to examine the somatotopic effect and found worse performance in the bilateral condition. Yet, the performance deficit in bilateral conditions could be due to a delay in information transfer between the two hemispheres rather than digit-specific effect *per se*. Nevertheless, the important result was that the separation between bilateral fingers did not exert any further effects on performance.

Similarly, Kuroki et al. (2017) found no modulation of hand separation on frequency discrimination. However, Rahman and Yau (2019) did observe performance modulations as a function of separation between hands in external space. Yet, these separation effects could be accounted for by considering the effect of spatial attention, whose gain on the distractor

stimulus weakened as it was moved away from the target, reducing the target-distractor interactions (Forster and Eimer, 2004). The idea that skin-based and external reference frames both contribute to tactile spatial perception was proposed by Heed et al. (2015) and Badde & Heed (2016). They argue that performance deficits in hand crossing occur due to suboptimal weighting of the skin-based and external reference frames. Specifically, they claim that while crossing effects indicate that remapping must have taken place (otherwise external spatial information would not be available), they do not characterise the remapping process *per se*, but rather arise as an integration of spatial information anchored to different frames.

### 5.1.3. Tactile motion perception as a better test for remapping processes

The reason why tactile motion estimation tasks are particularly useful in examining the remapping processes is because they allow one to examine the systematic bias in motion direction estimation as a function of body posture. Earlier studies on tactile motion have focussed on judgements of the angle between two motion stimuli as a function of finger rotation (Rinker & Craig, 1995; Pei et al., 2014). A recent study by Chen and colleagues (2020) went a step further and employed a method of adjustment to systematically predict estimates of tactile direction based on the rotation of the finger and of the head. They found that finger rotation biased the direction judgements, but opposite to the rotation of the finger. The opposite pattern could be due to the type of tactile stimulus they employed. Specifically, they used a rotating drum that rotated in different directions on a finger. Thus, in contrast to continuous movement of a stimulus across the fingertip, the rotating drum may not have a clear external principal axis. Indeed, in the condition where the finger was straight, participants still exhibited considerable bias. In addition, because Chen and colleagues used the mean error rate as a measure of accuracy, their measure did not distinguish between directional sensitivity and directional bias.

Here, we extended our previous studies to consider the effect of posture on motion direction judgements in terms of sensitivity, bias, and precision. Moreover, we sought to contribute to the aforementioned fruitful literature by examining how postural change affects multi-touch integration. **Figure 5.1** illustrates two situations, where a big object held between both hands begins to slide. In one situation (**Figure 5.1A**) the hands remain parallel to each other (as in previous experiments). In this case, veridical object's direction can be successfully inferred by merely considering the activation across receptive fields (RFs) of the skin. However, if one hand is rotated relative to the other hand (**Figure 5.1B**), a conflict is induced between skin-based and object-based frames of reference. A veridical representation of the object's motion can be then derived by successfully accounting for the postural change and transforming perception into the object-based reference frame (*perfect remapping*). Such coordinate transformation is common in visual modality, where the position of a viewed stimulus can be also coded relative

to different frames of reference. For instance, a stimulus location can be defined in an eye-centered or gaze-centered frame (i.e., based on activation on the retina) or it can be defined in body-centered frames (i.e., based on the position of the stimuli in external space with reference to the observer's body midline or a hand that is executing an action). If no remapping occurs, the brain will not have access to postural information, and it will compute object's motion based on the new activation across RF's. Without knowing that the hand was rotated, it will lead to biased perception (*postural under-compensation*). However, even if remapping occurs and the integration process has access to postural information, the brain can over-compensate for postural change leading to perception that is biased by posture (*postural over-compensation*).

Importantly, our measure of bias (intercept) can dissociate between these three possible predictions (**Figure 5.1C**). Specifically, intercept values reflect the perceived axis to which a probe's movement is anchored. Thus, in case of a hand rotation, intercept values close to 0 would indicate a perfect remapping, whereby skin-based reference frame is integrated with posture and transformed to probe's frame of reference. Positive intercept values (opposite hand rotation) would indicate reliance of RF-based frame of references, while negative values (towards hand rotation) would indicate over-compensation of posture.

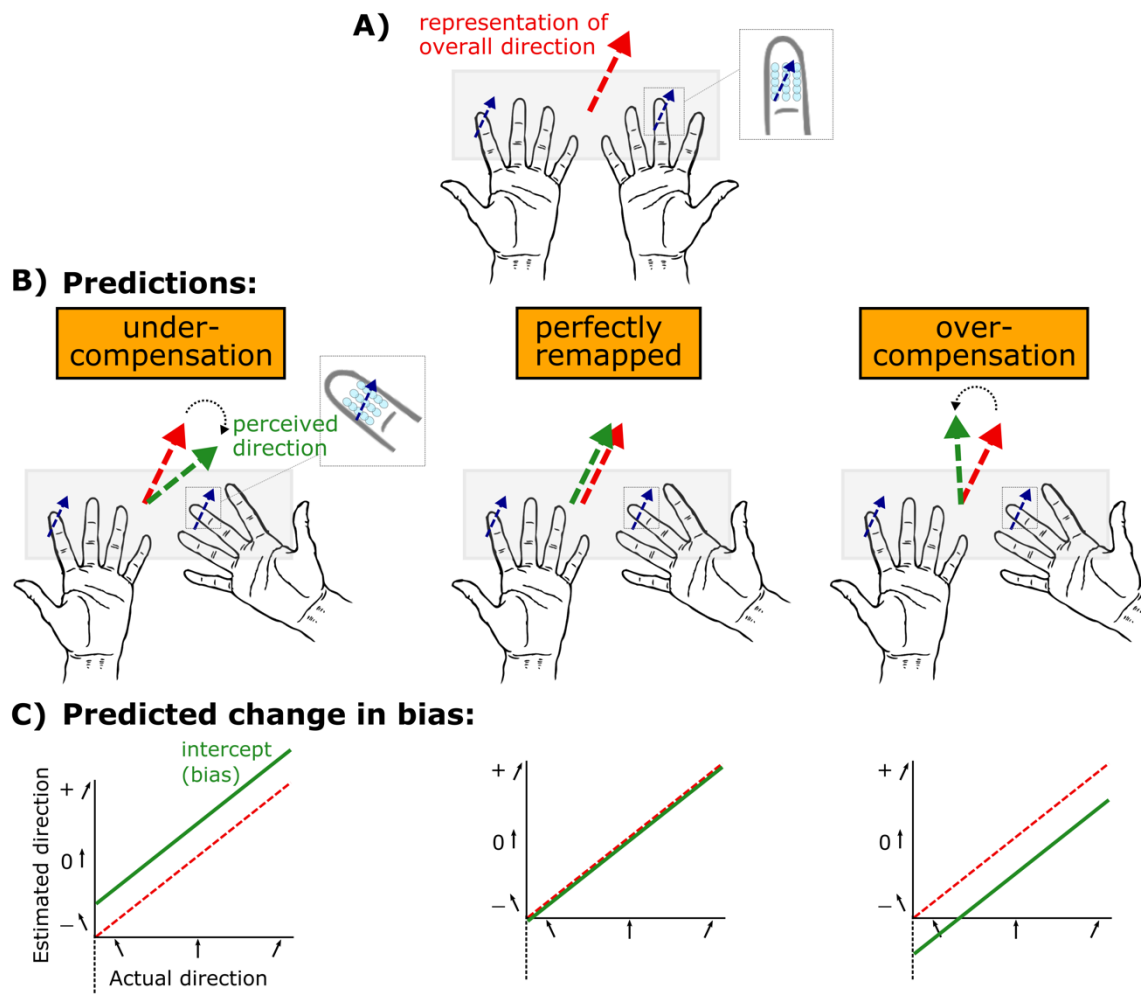


**Figure 5.1. Predictions on how postural information is integrated with skin-based directional representation.** The figure depicts an object moving across fingers of both hands. The perceptual representation of the object's movement is the *average* between the motion direction components at each finger (red arrow). **A)** Both hands are in the same orientation (or posture). The inset shows one of the motion components as it crosses the receptive fields (RFs) on one of the fingertips. **B)** The same situation as in **A)**, but the right hand is rotated relative to the left hand. The small inset shows how the motion component on the finger of the rotated hand crosses different RFs. The three panels illustrate the possible outcomes for perceiving the overall object's direction (green arrow). Central panel shows the perfectly remapped representation. In that case postural and skin-based information are perfectly integrated. The left-side panel shows postural under-compensation, whereby the brain seems unaware of the postural change and attempts to perceive direction solely based on the new skin-based or RF-based representation. The right-side panel shows postural over-compensation, whereby postural information is considered, but rather than accounting for the postural change, the new direction estimate is biased by the rotation. **C)** Corresponding changes to intercept values that reflect the biases in directional estimations. Note that in the experiment the hands were palm down as in previous experiments.

## 5.2. Methods

### 5.2.1. Participants

To acquire comparable data to previous experiments, a new sample of 15 volunteers took part in the experiment (10 females, 5 males, aged 20 – 35 years with mean age of 25.3, all but two reportedly right-handed). All participants gave informed consent prior to experiments,



in accordance with the declaration of Helsinki. The study was approved by the University College London Research Ethics Committee.

### *5.2.2. Task design*

The tactile apparatus, experimental set-up, paradigm and tactile stimuli were identical to those used in **Chapter 3** and **4**. The stimulated fingers were bimanual homologous right and left index fingers. Participants performed the tasks in two conditions: parallel and rotated. In the parallel condition, both hands were positioned fingertips pointing straight away from the body (just like in the previous bimanual experiments 3 and 5). In the rotated condition, the right hand was rotated 45° towards the left hand (similarly to the illustration in **Figure 5.1**). The distance between stimulated fingers (the centre of the fingertip) was kept fixed to approximately 45 mm in both conditions.

All conditions were blocked. The order of posture conditions (parallel vs. rotated) was counterbalanced across participants, and number-of-finger conditions (single vs. double) was counterbalanced within each posture condition. In double-finger conditions, the 21 stimulus combinations were repeated 5 times (the combinations where both directions were the same was repeated twice), resulting in 120 trials per condition. In single-finger conditions, the number of repetitions of each direction was matched to that in the double-finger condition. The experimental session lasted approximately 2 hours and was performed across two 1-hour sessions on separate days.

### *5.2.3. Analysis*

In previous chapters 3 and 4, the main measures of interest were sensitivity (slope) and precision (inverse unbiased SDs), while the measures of directional bias (intercept) were included only to check that no substantial biases were present in the data as the fingers were always aligned antero-posteriorly. Here, we wished to assess the effect of changing finger posture on direction estimation. When a hand was straight, the finger midline was aligned with the principal axis of the motion of the probe (0°). In other words, the skin-based reference frame was aligned with the object-based reference frame, and direction judgement could, in principle, be successfully derived using either frame of reference. When the hand was rotated the skin-based reference frame was put into conflict with the object's frame. If participants were able to account for postural change and transform skin-based activation (activation across skin RFs) into object's frame of reference, intercept values should not have significantly deviated from 0°, which is the principal axis of the object's movement. In contrast, if intercept values started shifting towards the rotation of the hand, it can be assumed that participants were unable to account for the postural change and misaligned object's movement axis to hand's new axis (-

45°). Furthermore, if participants were completely oblivious of any postural change and their directional judgements remained anchored to skin-based activation, their intercept values would shift opposite the hand rotation (45°). Moreover, by asking participants to average the probe's directions across a parallel and a rotated hand, we examined whether postural change further affected the multi-touch integration. Thus, directional bias (intercept) was the main measure of interest in this chapter.

As before, linear regressions were fit to each participant's data (judged direction as a function of actual direction), separately for each single-finger condition and to each double-finger condition. Intercept and slope values were then estimated from the fits. Unbiased SDs were calculated in the same way as in the previous chapters; over identical angles in single-finger conditions and over repeated combinations (average direction at different discrepancies) in double-finger conditions.

We first looked at the single-finger conditions. Specifically, we were interested whether the rotated right index finger induced systematic shifts in participants' judgements of the probe's direction. We used one-sample t-tests on intercept and slope values to see whether those significantly deviated from 0, and 0 and 1, respectively. When normality was violated, we used a sign test instead. We then used a one-way repeated-measures ANOVA with *finger* as a factor (parallel left index, parallel right index, rotated right index) to see whether all of the measures (including SDs) varied across fingers. We were particularly interested in the planned contrast between rotated right index and the mean of parallel fingers.

For the main analysis, we reasoned that averaging the directions of the two probes should be at least as good as the mean performance across single-finger conditions. For this reason, just as before, we averaged the data from the two single-finger conditions and ran a repeated-measures ANOVA with factors number-of-finger condition (single-finger vs. double-finger condition) and posture (both hands parallel vs. right hand rotated). Separate ANOVAs were conducted for intercept, slope, and unbiased SD values. The normality assumption was checked with Shapiro-Wilk test on residuals of ANOVA's effects and interactions. A slight deviation was found for the main effect of posture in SD values ( $p = .03$ ), no other significant deviations were found. In addition to the main analysis, the same steps were taken as in the previous chapter to examine the degree to which averaging ability varied as a function of discrepancy, and how the weights were allocated across fingers.

## 5.3. Results

### 5.3.1. Analysis of single-finger conditions: posture elicits a significant attracting effect

In this experiment, analysis of single-finger conditions was important, because it provided an insight into whether rotation of the right index finger influenced directional judgements relative to the unrotated fingers. **Figure 5.2A** shows the regression fits for each single-finger condition. Note that the parallel left finger was stimulated in both parallel and rotated condition blocks to avoid the reusing of the same single-finger data in the main analysis. In these single-finger analyses, however, the data was pooled to acquire a single measure of left finger perception. **Figure 5.2B** illustrates the slope values between the three single-finger conditions. **Table 5.1** shows that slope values were both significantly greater than 0 and greater than 1, suggesting that directions on all fingers were overestimated. ANOVA did not yield any significant difference between fingers ( $F(2,39) = .44$ ,  $p = .65$ ,  $np^2 = .02$ ).

**Figure 5.2C** shows the intercept values and **Table 5.1** indicates that while both parallel fingers produced intercept values that were close to 0, the rotated right index finger produced intercept values that showed a significant anticlockwise bias in direction judgements. Indeed, ANOVA yielded a significant effect of finger ( $F(2,39) = 3.85$ ,  $p = .03$ ,  $np^2 = .16$ ). Planned contrasts showed a significant difference between rotated finger versus mean of parallel fingers ( $p = .01$ ), but not between parallel fingers ( $p = .99$ ). This indicates that postural change induced an postural over-compensation. However, that bias was much smaller than the actual rotation of the hand ( $-8^\circ$  vs.  $-45^\circ$ ).

Lastly, **Figure 5.2D** shows unbiased SD values for each component direction. Although **Table 5.1** suggests that judgements from the rotated finger were slightly more variable, ANOVA with factors finger, overall direction (leftward, rightward) and angle ( $10^\circ$ ,  $0^\circ$ ,  $10^\circ$ ) did not yield any significant effects or interactions (all  $p$  values:  $.07 < p < .97$ ). Yet, the planned contrasts did reveal a significant difference between the rotated finger against the mean of parallel fingers ( $p = .04$ ), suggesting that variability was higher for judgements made on the rotated finger.

## Single-finger conditions

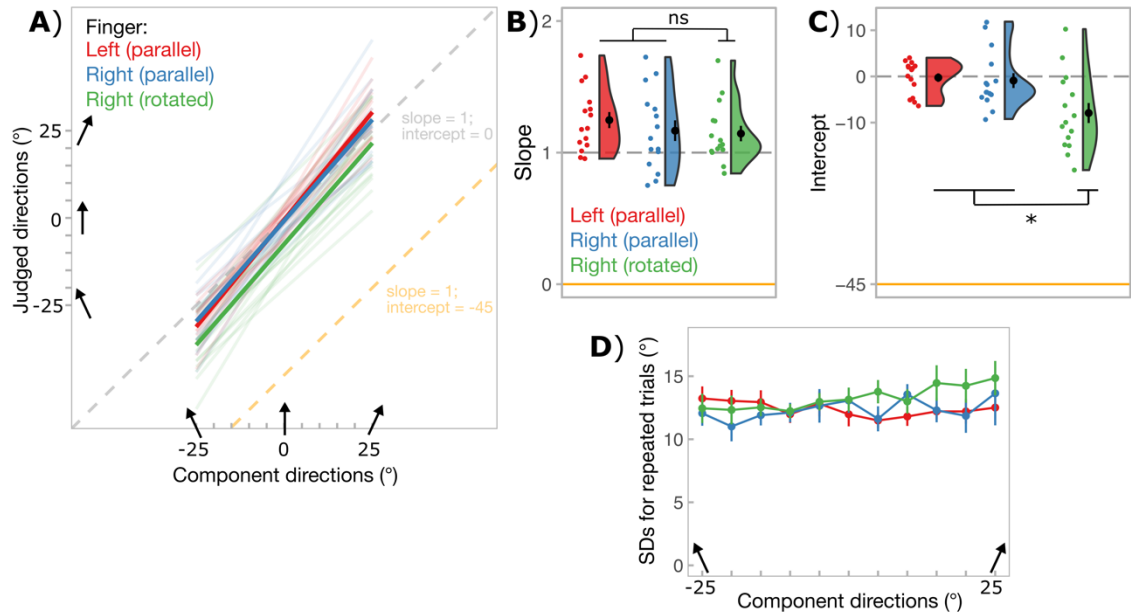


**Figure 5.2. Experiment 6: results for single-finger conditions.** **A)** Individual fitted linear regressions (transparent lines) and group-level regressions (thick lines) for each finger. The grey dashed line represents the slope 1 and intercept 0; the yellow line shows the predicted results with full posture-based bias (intercept -45). **B)** Individual slope values (colored dots) derived from linear regressions in **A**, together with the group-level means (black dots). Raincloud plots (Allen et al., 2019) represent data distribution and error bars represent SEM. **C)** Individual intercept values derived from linear regressions in **A**, together with the group-level means; annotations same as in **C**. **D)** shows group-level unbiased standard deviations (SDs) for repeated trials for each component direction. Error bars represent SEM.

**Table 5.1:** Experiment 6: main measures for single-finger conditions

Condition	Slope			Intercept		SD
	mean $\pm$ SD	t-test against 0: $t(d)$	t-test against 1: $t(d)$	mean $\pm$ SD	t-test against 0: $t(d)$	mean $\pm$ SD
Par. Left	1.2 $\pm$ .2	20.41(5.27)**	4.04(1.04)*	-0.3 $\pm$ 3.6	60 <sup>†</sup> (-.07)	12.4 $\pm$ 3.2
Par. Right	1.2 $\pm$ .3	14.87(3.84)**	2.12(0.55)	-0.9 $\pm$ 6.2	-.56(-.14)	12.3 $\pm$ 4.8
Rot. Right	1.1 $\pm$ .2	19.46(5.02)**	2.46(0.63)*	-7.9 $\pm$ 8.4	-3.66(-.94)*	13.3 $\pm$ 4.1

Note: \* $p < .05$ , \*\* $p < .001$ .  $x^{\dagger}$  indicate the sign test (V), which was used instead of t-test, due to non-normality.  $n = 15$

### 5.3.2. Double vs. mean of single-finger conditions: bias during averaging is equivalent to a linear combination of biased component estimates

**Figure 5.3A** shows the linear fits for double-finger conditions (left panel) and corresponding mean of single-finger conditions. The group-level adjusted  $r^2$  were for single-finger conditions:  $.56 \pm .09$  (parallel) and  $.59 \pm .07$  (rotated), and for double-finger conditions:  $.45 \pm .07$  (parallel) and  $.40 \pm .12$  (rotated).

The most important result concerns the intercept values shown in **Figure 5.3B** and summarised in **Table 5.2**. It seems that while estimating the average direction of two component motions (double-finger conditions) that were delivered to parallel fingers produced unbiased intercepts, when the right hand was rotated, average estimates shifted anti-clockwise and

towards the rotation of the hand. Indeed, rmANOVA yielded a significant main effect of posture ( $F(1,14) = 20.5$ ,  $p < .001$ ,  $np^2 = .59$ ;  $BF^{01} = .001 \pm 1.0\%$ ,  $BF_{incl} = 713$ ) indicating that overall hand rotation had an attracting influence on intercept values. The main effect of number-of-fingers conditions was non-significant ( $F(1,14) = .55$ ,  $p = .47$ ,  $np^2 = .04$ ;  $BF^{01} = 3.1 \pm 1.2\%$ ,  $BF_{incl} = .3$ ). Importantly, the interaction between posture and number-of-fingers condition was also not significant ( $F(1,14) = 1.3$ ,  $p = .28$ ,  $np^2 = .08$ ;  $BF^{01} = 2.3 \pm 2.6\%$ ,  $BF_{incl} = .5$ ). This means that the bias during averaging was not statistically different from the arithmetic mean of biases across to-be-averaged fingers. Thus, while postural influence extends from independent directional judgements to estimation of average direction, the magnitude of that effect during average is less than that on the single rotated hand ( $-8^\circ$  vs.  $-3^\circ$ ). In fact, it is equivalent to the arithmetic average of the two direction inputs; one from rotated and the other from parallel hand.

In terms of slope values (shown in **Figure 5.3B** middle panel), **Table 5.2** indicates that average direction estimates produced slopes exceeding both 0 and 1 in both posture conditions. ANOVA yielded an overall effect of hand ( $F(1,14) = 6.05$ ,  $p = .03$ ,  $np^2 = .30$ ;  $BF^{01} = .30 \pm 1.3\%$ ,  $BF_{incl} = 2.0$ ) with slopes being higher during averaging (mean slope = 1.3,  $SD = .3$ ) compared to estimating the component directions in isolation (mean slope = 1.2,  $SD = .3$ ). The effect of posture was non-significant ( $F(1,14) = .12$ ,  $p = .73$ ,  $np^2 = .01$ ;  $BF^{01} = 3.6 \pm 1.5\%$ ,  $BF_{incl} = .2$ ) and there was no interaction ( $F(1,14) = .32$ ,  $p = .58$ ,  $np^2 = .02$ ;  $BF^{01} = 2.4 \pm 7.5\%$ ,  $BF_{incl} = .3$ ), suggesting that the sensitivity to directions was unaffected by postural change.

Finally, SDs were analysed by first taking the mean of unbiased SDs across separate component directions in single-finger condition and across separate combinations in double-finger condition. This way we had a single measure of precision per each condition (**Figure 5.3B** last panel). rmANOVA produced a significant effect of posture ( $F(1,14) = 7.8$ ,  $p = .01$ ,  $np^2 = .36$ ;  $BF^{01} = 3.5 \pm 3.7\%$ ,  $BF_{incl} = .2$ ), with larger overall variability in rotated (mean  $SD = 12.9$ ,  $sd = 2.5$ ) compared to parallel (mean  $SD = 12.1$ ,  $sd = 2.5$ ) conditions. Although in the parallel condition, variability was reduced in double-finger condition compared to single-finger condition, there was no effect of number-of-fingers ( $F(1,14) = .10$ ,  $p = .80$ ,  $np^2 = .005$ ;  $BF^{01} = .3 \pm 1.7\%$ ,  $BF_{incl} = 2.4$ ) and no statistically significant interaction ( $F(1,14) = 1.2$ ,  $p = .26$ ,  $np^2 = .08$ ;  $BF^{01} = 2.6 \pm 4.2\%$ ,  $BF_{incl} = .3$ ). The lack of precision benefit for averaging is inconsistent with results from bimanual experiments in previous chapters. This could be due to the data for parallel double-finger condition showing almost a bimodal distribution with a group of participants producing much higher variability than the rest (**Figure 5.3B** last panel).

## Double-finger vs. mean of single-finger conditions

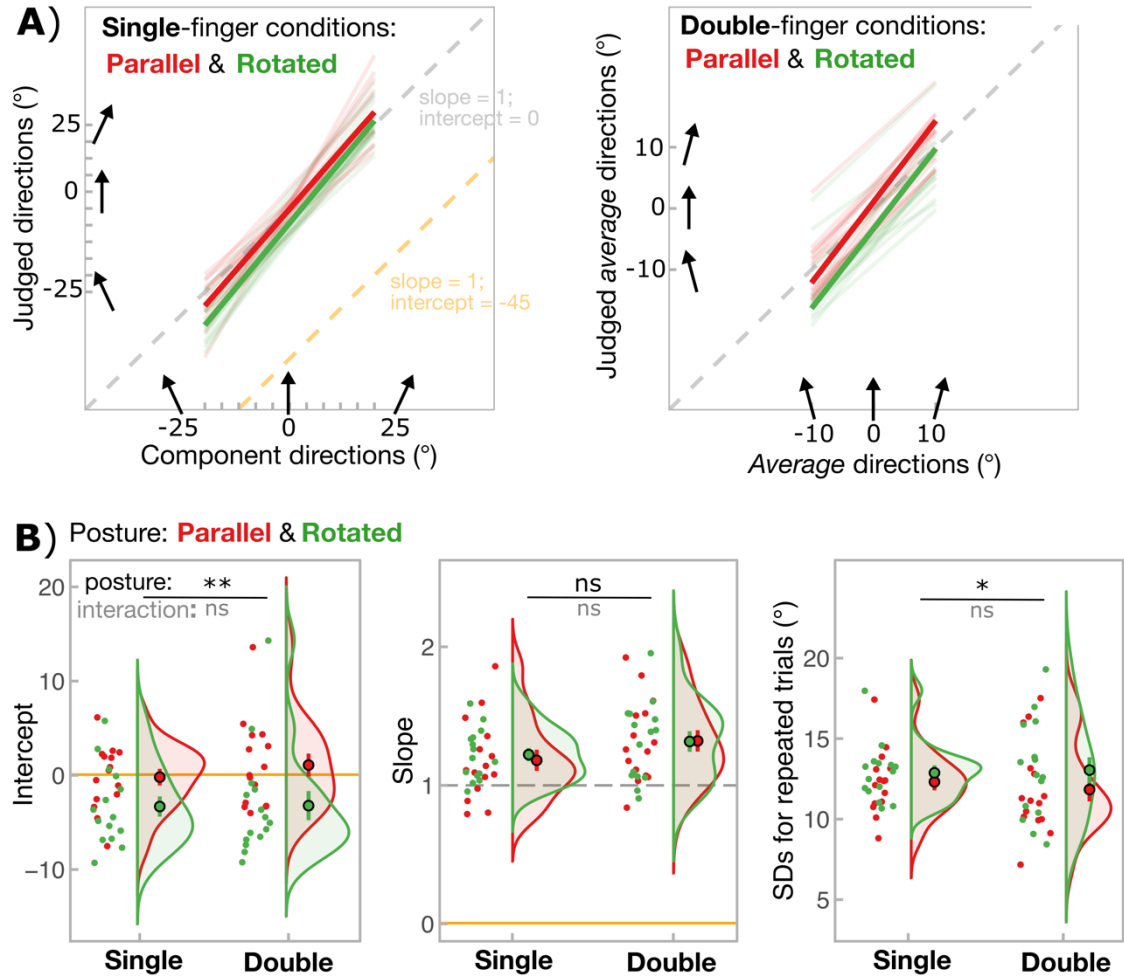


**Figure 5.3. Experiment 6: main measures.** **A)** Individual fitted regressions (transparent lines) and group-level regressions (thick lines), separately for the mean of single-finger conditions (left panel), and for double-finger condition (right panel). **B)** shows the main measures, from left: slope values reflecting sensitivity, intercept values reflecting bias, and unbiased SD reflecting inverse precision. SDs were calculated separately for each repeated stimuli; for simplicity, data was averaged across repeated stimuli to show the mean SDs for single- and double-finger conditions. In all panels, points with error bars reflect group-level means and SEM. Raincloud plots (Allen et al., 2019) show the distribution of the data. Upper black annotation shows statistical significance of the main effect of posture (parallel vs. rotated), whereas lower gray annotation shows statistical significance of number-of-fingers (single vs. double) by posture interaction. Each condition was performed by the same group of 15 participants.

**Table 5.2: Experiment 6: main measures in all conditions**

Condition	Slope			Intercept		SD
	Mean $\pm$ SD	t-test against 0: $t(d)$	t-test against 1: $t(d)$	Mean $\pm$ SD	t-test against 0: $t(d)$	Mean $\pm$ SD
Par. Single	1.2 $\pm$ .3	15.45(3.99)**	2.37(.61)*	-0.2 $\pm$ 3.4	-0.22(-.06)	12.3 $\pm$ 2.0
Par. Double	1.3 $\pm$ .3	17.02(4.39)**	4.14(1.07)*	1.1 $\pm$ 4.7	70 <sup>†</sup> (.23)	11.8 $\pm$ 2.9
Rot. Single	1.2 $\pm$ .2	25.72(6.64)**	4.67(1.21)**	-3.3 $\pm$ 4.2	-3.08(-.79)*	12.9 $\pm$ 1.8
Rot. Double	1.3 $\pm$ .3	17.74(4.58)**	4.26(1.10)**	-3.2 $\pm$ 6.0	21 <sup>†</sup> (-.54)*	13.0 $\pm$ 3.1

Note: \* $p < .05$ , \*\* $p < .001$ .  $x^\dagger$  indicate the sign test (V), which was used instead of t-test, due to non-normality.  $n = 15$

### 5.3.3. Effect of directional discrepancy on averaging performance, and weight assignment across fingers

All measures were analysed with a three-factor model of posture (parallel vs. rotated), sign of discrepancy (negative - converging vs. positive - diverging) and level of discrepancy (30°, 20°, 10°). The discrepancy of 0° was not included in the analysis as it did not have a specific sign, and because the weight could not be calculated for average directions with 0 discrepancy. For SDs and weights, average direction was added as an additional factor (-10°, 0°, 10°). We only report results that were related to the effect of posture.

**Figure 5.4A** shows the intercept values. Analysis yielded a main effect of posture ( $F(1,14) = 16.7, p = .002, \eta^2 = .36$ ), reflecting the significant bias during the rotated condition. There was also a significant interaction between posture and level of discrepancy ( $F(2,28) = 5.4, p = .02, \eta^2 = .28$  –  $p$  value Greenhouse-corrected). The significant interaction was followed-up by Bonferroni-corrected pairwise tests separately for each posture condition. When hands were parallel, there was no significant difference between any discrepancies ( $p$  values: 1.0, 1.0, and .31). In contrast, when the right hand was rotated, there was a significant difference between smallest (10° and -10°) and largest (30° and -30°) discrepancies ( $p = .01$ ), with bias being larger at the smaller discrepancies, while at the bigger discrepancies the intercept values were close to 0, indicating no bias. These results suggest that the bias observed during averaging when one hand was rotated largely resulted from component directions that were similar to each other. In terms of slope values (**Figure 5.4B**), none of the effects or interactions were statistically significant (all  $p$  values:  $.21 < p < .98$ ).

**Figure 5.4C** shows SDs averaged across average directions. Consistent with the main analysis above, the main effect of posture was significant ( $F(1,14) = 5.0, p = .04, \eta^2 = .26$ ) with less variability in parallel (mean SD = 11.9, sd = 5.9) compared to rotated (mean SD = 13.3, sd = 6.4) condition. Again, effect of posture seemed to interact with level of discrepancy ( $F(2,28) = 5.4, p = .02, \eta^2 = .28$  –  $p$  value Greenhouse-corrected). Furthermore, there was a significant three-way interaction between posture, level of discrepancy and sign of discrepancy ( $F(2,28) = 4.4, p = .02, \eta^2 = .24$ ). To break down this interaction, we examined the effects of level and sign of discrepancy separately across posture conditions. However, neither for parallel nor for rotated conditions did the effects reach significance ( $p$  values were .09 & .84 for level and sign, respectively when hands were parallel; and .62 & .50 when one hand was rotated).

Finally, we examined the change of relative weight assigned to the left index finger (which maintained the same posture whether the right hand was parallel or rotated) as a function of average direction. **Figure 5.4D** shows that at least when the average direction was straight, the rotated hand attracted more weight than the parallel hand (green bar). However,

the analysis did not yield a significant effect of posture ( $F(1,14) = 1.5, p = .24, np^2 = .10$ ) nor posture by average directions interaction ( $F(2,28) = 1.4, p = .27, np^2 = .10$ ).

In sum, the main results from this analysis are that the bias observed during averaging mainly arose from component directions that were less discrepant, and that there was no clear evidence that rotated hand attracted more or less weight than the parallel hand.

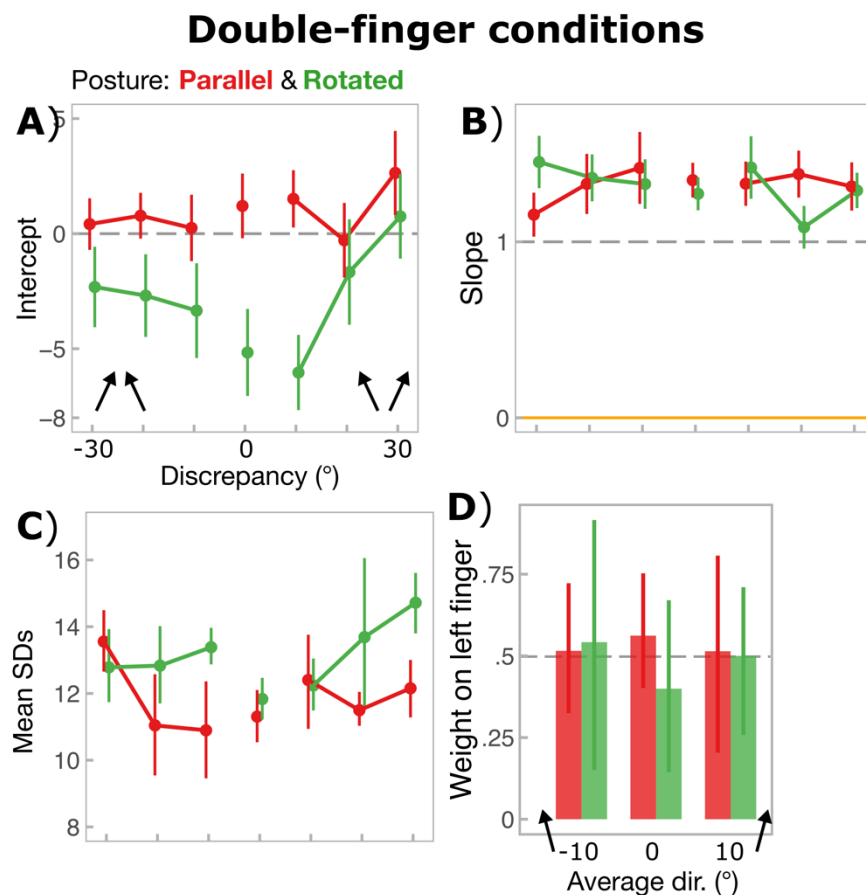


**Figure 5.4. Experiment 6: effect of discrepancy on averaging performance and weighting of component directions during averaging.** **A)** Intercept values as a function of discrepancy. The points correspond to group-level values, estimated from single-subject regressions fit to double-finger conditions, but separately to each discrepancy level (x axis). Error bars correspond to SEM. Discrepancy of 0 (when component directions were identical) is included in the plots for illustrative purposes, but was not included in the analysis, because discrepancy was factored into sign of discrepancy (negative discrepancy, when directions converged vs. positive discrepancy, when directions diverged) and level of discrepancy (30° vs. 20° vs. 10°). **B)** Slope values as a function of discrepancy; annotations are the same as for panel **A**. **C)** Unbiased SD values for repeated estimations of identical trials as a function of discrepancy (x axis). SDs were calculated for each average direction separately, but for simplicity data was averaged across average directions to show the mean SDs for each discrepancy. Annotations same as for panel **A**. **D)** Weight assigned to the left index finger during averaging. The right panel shows the weighting data as a function of average direction, while the left panel shows the same data pooled across average directions and as a function of discrepancy. Weight of 0.5 meant that the directional information from both fingers was weighted equally. In all panels, red traces reflect averaging when both hands were parallel, while green traces reflect averaging when the right hand was rotated leftward.



## 5.4. Discussion

Somatosensory processing of skin-based input provides a representation of objects as they impinge on the skin. But to successfully interact with the external environment, and enable multi-sensory integration, skin-based input needs to be translated into a common (external) reference frame. By adapting our existing paradigm to include a postural change of one of the hands, this chapter examined whether bimanual multi-touch motion integration can resolve the conflict between skin-based and external reference frames. Because participants needed to report the direction of the tactile stimulation by visuomotor adjustment of a pointer device, successful performance required them to account for the postural change of the hand, by remapping the rotated finger midline to the external principal axis of the probe's movement. If the remapping process were flawless, change of posture should not have influenced directional judgements. Our results show that, while postural information was considered during directional estimation, it was over-compensated for, resulting in significant but small bias towards the postural rotation. Importantly, the bias that resulted from the averaging of inputs from the two hands (one of which was rotated) was equivalent to the linear combination of biases related to each component. This points to a possibility that the averaging process is independent from the remapping of component directions. In other words, average percept is based on 'remapped' component directions.

### 5.4.1. *Remapping coupled with postural over-compensation*

In the parallel conditions, the hands and fingers were straight, so the finger midline was aligned with the principal axis of the motion of the probe ( $0^\circ$ ). In other words, the skin-based reference frame was aligned with the external reference frame, and direction judgement could, in principle, be successfully derived using either frame of reference. In the rotated conditions, the right hand was rotated by  $45^\circ$  counterclockwise, so the skin-based reference frame was put into conflict with the external frame. The analysis of intercepts showed that postural change had an attracting effect on motion judgements, biasing them towards the hand rotation. That is, when the hand was rotated and the finger midline was now at  $45^\circ$  instead of  $0^\circ$  as in the parallel condition, participants estimated the directions of probe's movement according to the new finger midline, and not according to the optimal remapped midline that should have remained at  $0^\circ$ . When participants judged component directions from each finger separately, the judgements on the rotated finger showed a statistically significant counterclockwise bias of  $8^\circ$ .

However, the bias was considerably smaller than the actual rotation of the hand. There are three explanations for this. First, participants may have underestimated the extent of the hand rotation. This could be because the hand was rotated by the experimenter and participants

could not see or move their hands throughout the experiment. Second, and more speculative explanation is that remapping process could not be completed leaving a small bias in the judgements. Remapping is known to take time to occur. Studies on crossed-hand paradigm have found that biased (or skin-based) performance occurs when stimuli need to be integrated with the external reference frame within the first 170 ms (Azañón & Soto-Faraco, 2008) or 300 ms (Yamamoto & Kitazawa, 2001). At longer integration intervals performance stabilises, and at 1.5 s participants make only few errors as the remapping can be successfully completed (Yamamoto & Kitazawa, 2001). Our trajectories moved for 1 s, which may have given time for remapping to occur, but not to be completed perfectly, thus, resulting in a significant but less than a complete bias. An interesting manipulation would be to vary the speed of probe's motion. The prediction would be that at faster speeds a larger bias should emerge, which would gradually disappear as the movements become slower, allowing remapping to be completed.

The third explanation is related to the framework proposed by Heed et al. (2015) and Badde & Heed (2016), whereby the skin-based spatial representation is not lost after remapping. Rather, tactile spatial perception relies on a combination of several reference frames, which need to be optimally integrated for optimal perception. Thus, in a case, where reference frames are in conflict (as in our rotated hand condition), the brain needs to resolve the conflict by allocating corresponding weights to either frame. Thus, the significant – but small – bias in our task may have occurred due to suboptimal weighting of the conflicting frames. The brain may have considered both frames, resulting in a reduction of bias relative to actual postural change, but still could not estimate the correct weighting. Weighting is known to vary across time. For example, during an experiment with an abnormal posture, participants were found to gradually recover optimal performance (Azañón et al., 2015), which could have been due to gradual adjustment of weights assigned to each spatial frame. Because we characterised participants' performance based on intercepts and slopes of linear fits that required the whole dataset, we could not look at whether the bias changed with the progression of the experiment. Considering only estimate errors would not have allowed to dissociate between bias and insufficient sensitivity. Therefore, the explanation based on reference frame weighting remains speculative.

#### *5.4.2. Averaging is independent from remapping*

The bias persisted when component directions had to be averaged across rotated and parallel bimanual fingers. Importantly, the bias in average judgements was smaller than that on the rotated finger alone and was equal to the linear mean of biases on both fingers. This suggests a serial and relatively independent processing, whereby the “remapped” (or partly remapped) representations of the probe's motion direction anchored to each finger were then aggregated to derive the unified representation of both probe's motion direction. **Figure 5.5** illustrates this

process. A consideration is that reference frame integration is believed to depend on the context of the resulting spatial percept (Badde & Heed, 2016), yet in the present study the judgement was made about an external object by adjusting the direction of a visual arrow. As such, the context of the current study required the predominance of the external frame. Future studies could control the context of motion perception by instructing participants to either focus on the moving probe or on the resulting path across the skin and examine whether these instructions modulate the relative dominance of either frame.

In terms of noise, there seemed to be two separate noise sources introduced, one during component direction estimation, and another during or after aggregation. Increased noise in estimating component directions, when those were from rotated hand could be due to the integration between activation on the skin and postural input concerning the hand rotation. Aggregating two estimates should lead to reduction of noise given that the estimates are independent (Zohary et al., 1994; Averbek et al., 2006; Alvarez, 2011). This has been the case in previous bimanual experiments in **Chapters 3 and 4**, where variability in average estimate was reduced compared to the mean variability of component direction estimates. In this experiment, there was a trend towards this relationship when both hands were parallel, but the effect did not reach statistical significance. The lack of statistical effect could be due to a larger inter-individual variability: a subset of participants with low precision was noted in **Figure 5.3B**. Interestingly, increased variability for estimates from the rotated finger were also present for average direction estimates when component directions were delivered to the parallel and rotated fingers. Even if direction estimation from a rotated finger introduced additional noise, the optimal averaging process in **Figure 5.5** should have reduced the effects of that noise. The fact that average estimate noise was similar to the noise from the rotated finger suggests that some additional noise may have entered the aggregation process depicted in **Figure 5.5**.

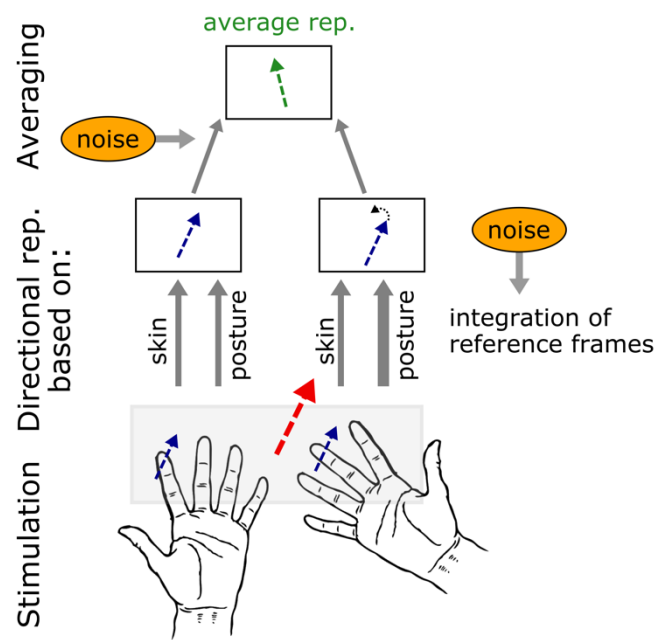


**Figure 5.5. Schematic illustration of multi-touch integration given conflicting spatial frame of reference.** Blue arrows indicate the motion direction across the two fingers and the red arrow indicates the actual average direction of the object. Perception of component directions (blue arrows in boxes) arises from integration between skin-based and postural frames of reference. According to Heed et al. (2015) biases in perception can arise from suboptimal weighting of reference frames. Our results show that when hand was rotated perceived directions were slightly biased towards the rotation of the posture, which means that posture could not be sufficiently down-weighted. Skin-based and postural reference frame integration could give rise to additional noise in direction estimation. The resulting representations (one accurate and the other biased) are then aggregated with equal weights to estimate the average direction of the object. Note that two separate noise sources are introduced, one during component direction estimation, and another during or after aggregation.

#### 5.4.3. Bias in aggregation arose from components that were less discrepant

Interestingly, further analysis of averaging conditions revealed that postural bias in the rotated condition was contingent upon the discrepancy between the component directions. Specifically, significant bias emerged when the discrepancy was small, but it almost disappeared, when discrepancy became larger. The effect of discrepancy on bias fits well with Badde and Heed's (2016) theory of weighting multiple reference frames, because they argue that the relative weighting will depend on context. For example, they argue that if the main focus is on the body, the skin-based frame will be weighted higher, whereas if the focus is an external object, the external object-based frame should acquire more weight. Our results indirectly suggest that reference frame weighting may also depend on the discrepancy between direction cues. Discrepancy between two cues may inform the brain about the source of the individual cues; a small discrepancy could indicate a single source, whereas a large discrepancy could be inferred as two separate sources. Thus, when participants perceived the two probes as clearly two separate objects it may have helped them to distinguish the probe-based frame, and thus assign it appropriate weight, leading to less biased average motion perception. However, this explanation remains a mere speculation.

## 5.5. Conclusion

In sum, the present experiment, consistent with previous studies (Rinker & Craig, 1995; Pei et al., 2014; Chen et al., 2020), showed that posture influences direction perception. In particular, we provide evidence for a remapping process where postural change is over-compensated. This means that an attempt is made to remap directional input and account for postural change, but posture still exerts an excessive influence. Importantly, we show that averaging likely occurs on the “remapped” component directions. This means that multi-touch integration, at least in our task, where an average motion direction needs to be extracted, may occur at processing levels after proprioceptive input is integrated with the skin-based representation. Further neuroimaging or EEG studies combined with the present paradigm would uncover the levels of processing that are involved in multi-touch integration that requires remapping. Transforming skin-based tactile input into an external reference frame is crucial for multi-sensory integration that requires a common frame of reference. The next chapter will present a paradigm to examine such multi-sensory integration between tactually felt and visually perceived motion direction.

## **Chapter 6: Integrating directional information between touch and vision**

This chapter examined another way in which tactile motion spatiality can be conveyed. Instead of perceiving a spatiotemporal path across the skin, participants were asked to discriminate the direction of a translational force applied to the skin via skin stretch. We show that directional information from tactile force could be optimally integrated with visually perceived direction of optical flow in order to better inform the direction of “heading” in a virtual reality setting. In contrast to previous multisensory integration studies that have mainly focussed on the effects of reliability of visual input, we examined the relative contributions of both visual and tactile reliabilities on visual-tactile integration. In order to implicitly quantify the sensation of heading, we continuously measured the postural instability (or body sway) of participants. First, we found that tactile information, when reliable, enhanced combined performance, especially when visual input is noisy. It potentially did so through a stronger entrainment to the sensation of self-motion as measured by body sway. Second, noise in the tactile signal was more detrimental than noise in the visual stimulus, and corrupted combined information even when reliable visual input was available. Although, our results may be inconclusive due to a small sample size and considerable inter-individual differences in how participants responded to our stimuli, they raise several considerations for future multisensory studies that seek to elucidate the specific role of touch, and for haptic interface design.

## 6.1. Introduction

### 6.1.1. *Encoding translational force*

Previous chapters have described tactile motion direction perception from stimulating a series of spatially separated mechanoreceptors over time. Such stimulation involves an application of a moving normal force along the skin. However, there is another widely employed way of producing tactually perceived motion – through applying one-directional force to a fingertip via a handheld haptic device. The main advantage of using translational force to convey motion direction is its intuitive application as a navigational tool for visually impaired or as a lifelike feedback in virtual reality. For instance, by creating illusory sensation of one-directional translational force, a non-grounded handheld portable device called *BuruNavi* (for details see: Amemiya et al., 2005; Amemiya & Gomi, 2012; 2014; 2016) can create a sensation of being pulled towards the force's direction. This is somewhat equivalent to following a guide dog.

In addition, force-feedback haptic devices like *PHANToM* (Tan et al., 2006; Barbagli et al., 2006) can be used to augment virtual interactions by producing pulling sensations as if something is guiding you by the hand. The disadvantage of pulling force-based directional input is the engagement of proprioceptive input, as participants are often inclined to move their limb with the force. Indeed, active movement has been found to significantly improve perception of force's direction (Amemiya & Gomi, 2016). Co-occurring proprioceptive displacement makes it difficult to dissociate purely somatosensory contribution to pulling direction from additional contributions of proprioceptive and motors systems.

Nevertheless, if it is assumed that the stimulated hand is fixed, a stimulus that produces pulling force to a fingertip gives rise to a sensation of direction by pulling and stretching the skin. Such skin pull may lead to microslips along the skin, but it generally should not lead to spatiotemporal activation across the surface of the skin like a continuously moving stimulus. The direction of a stimulus that continuously moves across the skin with a normal constant force is encoded mainly by converging input from SA1 and RA afferents, whose properties convey sustained force and spatial discontinuities, respectively (see **section 1.1.3**). In contrast, skin stretch, or skin pull, is believed to mainly engage SA2 afferents (Vallbo & Johansson, 1978; Olausson, Wessberg, & Kakuda, 2000). Olausson et al., (1998) showed that skin pull direction without spatiotemporal activation on the skin (by pulling a pin glued to the skin surface) was perceived for movements as small as 0.13 mm. Such movements are barely detectable by vision. Direction perception was retained when the surrounded skin was anaesthetized, suggesting that skin stretch direction can be encoded from receptors that are more than 15 cm away from the actual stretch location. This fits well with the properties of SA2 afferents, which are known to

be spatially diffused. In fact, microneurography showed that skin stretch influenced the activity of SA2 receptors located about 10 cm away from the point of stimulation (Olausson, Kakuda, & Wessberg, 1996). Thus, perception of skin stretch direction seems to be functionally different from perception of a spatiotemporal tactile motion stimulus, yet both can convey tactile spatiality and not just intensity (i.e., force intensity). Therefore, forces that stretch the skin could potentially be used for communicating and perceiving spatial direction.

### *6.1.2. Experience of heading*

Direction of self-motion that distinguishes, which way we are moving in the environment, arises mainly from the vestibular system that encodes the linear acceleration of the head and the body (Fernandez & Goldberg, 1976a,b,c; Gu et al., 2007). Visual information provides a strong context for self-motion. Specifically, a dynamic movement of visual surroundings (i.e., optic flow) provides information about self-motion in relation to visual surroundings (Warren et al., 2001; Lappe et al., 1999). In optic flow, visual motion in an optical array expands radially from a single point, known as the “focus of expansion” (FOE), which has an important role in heading perception (Gibson, 1954). FOE changes along with changes of agent’s movement direction to reflect the new heading direction. Extensive research has been done on elucidating the integration between vestibular and visual signals during perception of heading (for review see Angelaki et al., 2011). Interestingly, optic flow alone can elicit the illusion of self-motion (Berthoz et al. 1975; Dichgans & Brandt, 1973; 1978). Indeed, action stimulators, such as flight stimulators, but also immersive games use optic flow to create an illusion of heading. In Chapter 1, we noted that there is a growing interest in ways to use the tactile sense to augment visual experience to make the sensation of movement more intense and precise.

When participants experience optical flow without actual self-motion, the flow stimulus is known to still modulate postural responses such as stability (Raffi et al., 2014, 2017; Raffi & Piras, 2019; Piras et al., 2018). Changes in postural stability or ‘body sway’ can be measured with a force platform that detect changes in participants’ center of pressure (COP) that reflects the movement of the body’s center of gravity (Luo et al., 2018; Guerraz et al., 2001). For instance, Piras et al. (2018) observed that COP was larger during optical flow and followed the direction of the flow (right or left), reflecting direction-specific body sway. Therefore, COP measure is a useful way to quantify the sensation of heading and resulting postural sway without an actual movement (see **Figure 6.1**). COP can be considered a ‘no-report’ behavioural readout of how total stimulation affect heading. We measured COP for each participant in all conditions. We expected both visual and tactile stimuli to result in a forward and stimulus-direction-specific sway, indicating a postural response of ‘heading’. Importantly, if integration between tactually and visually perceived directional stimuli enhanced the experience of heading, one should



expect a greater sway during the combined conditions compared to unisensory conditions, reflecting a stronger entrainment.

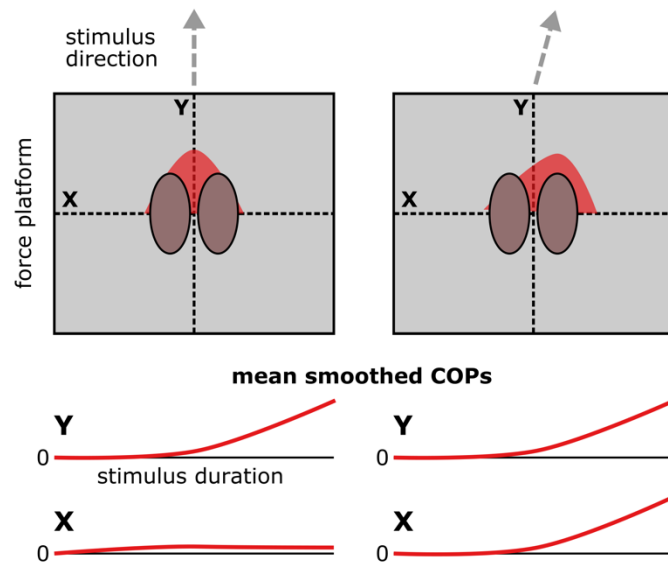


**Figure 6.1. Illustration of the COP as a function of a stimulus direction.** Participant is standing on the force platform that measures the modulations in center of pressure (COP) along two dimensions: y and x. When there is a stimulus that is heading straight forward, COP should show a forward sway of the body (red area on force platform). Magnitude of the forward-backward body sway can be extracted from y dimension. When the stimulus starts to head rightward, in addition to a forward sway, participants should show a direction-specific sway, which can be extracted from x dimension. Lower plots illustrate smoothed mean COP values (red line) as a function of time (i.e., stimulus duration). COP along y and x dimension are plotted separately. When the stimulus heads forward without rightward-leftward deviation, only COP along y dimension is informative, showing a gradual forward sway. When the stimulus deviated to the right, both dimensions are relevant, showing both a gradual forward sway and a gradual rightward sway.

### 6.1.3. Contribution of tactually acquired input on visual perception

The exact way in which information from touch and vision interact is still relatively unclear. One line of evidence suggests a consistent visual dominance over touch, when the information from the two modalities is competing. For example, there seems to be a compulsory redirection of attention to visual distractors, even when those are detrimental for the tactile task (Suzuishi, Hidaka, & Kuroki, 2020; Wani, Convento, & Yau, 2021; Craig, 2006; Bensmaia et al., 2006; Merz et al., 2020). Bensmaia et al. (2006) demonstrated that a visual distractor that moved in the same direction as a tactile motion stimulus enhanced the perception of tactile speed. But, when the visual distractor moved in the opposite direction, the effect was more complex: the enhancement effect was either reduced, eliminated or reversed. Importantly, the speed enhancement effect was only present when motion in both modalities started in synchrony. Thus, according to this study, when information from touch and vision is related to the same source, vision seems to modulate the perception of tactile spatial features. However, because participants were never asked to judge the visual stimulus, the authors could not

estimate whether the effect was solely unidirectional from vision to touch, or whether tactile information itself could influence visual percept.

Another line of studies has attempted to characterise the effect of tactile information on vision. In a visual tilt illusion, orientation of a central grating is biased by the orientation of the grating in the surround. Pérez-Bellido, Pappal, & Yau (2018) showed that when participants saw the gratings and touch equivalent gratings, the visual tilt illusion was greater compared to when they only saw the gratings. This result demonstrated that tactile information could facilitate visual processing at a relatively low-level of processing. Yet, a widespread belief is that touch could facilitate vision only when visual information is already compromised. In Pérez-Bellido et al.'s study visual stimulus needed to be corrupted with a lot of noise (96% white noise) to get a reliable tactile influence. Bresciani, Dammeier, & Ernst (2006) showed that, temporal information in touch (i.e., sequence of taps) had a stronger influence on visual temporal processing (i.e., sequence of flashes) than vice versa. However, that could be explained by the fact that participants were already better at estimating sequences of taps than sequences of flashes. Thus, while one would generally expect visual dominance over touch, touch would seem to influence vision when tactually acquired information if it were more reliable than visually acquired information. However, because vision is generally believed to be superior to touch in conveying spatial information, one would expect tactually acquired spatial information (i.e., directional input) to make only minimal contribution to the overall perception of 'heading'.

In order to test whether two concurrent sensory cues are integrated and not merely co-occurring, the maximum-likelihood estimation rule (MLE) is a popular framework to use. According to MLE, redundant sensory cues are combined linearly in a statistically optimal manner, so that reliability (inverse variance) of the integrated estimate is lower than each individual estimate, and individual estimates are integrated by assigning relative weights to each cue based on their reliability (Ernst & Bühlhoff, 2004; Angelaki, Gu, & DeAngelis, 2009). Integration that is near such optimality has been found across many modalities (Ernst & Banks, 2002; Alais & Burr, 2004; Landy & Kojima, 2001). However, visual-tactile integration studies have almost exclusively focussed on the varying properties of the visual stimulus paired with an unmanipulated tactile stimulus (e.g., Ernst & Banks, 2002; Hillis et al., 2002). The common result is that visual and tactile information can be optimally integrated, and that touch has a larger contribution on the integrated percept when vision is corrupted by noise (Ernst & Banks, 2002). However, by neglecting the specific effect of varying reliability of a tactile signal, the manner in which tactile information can affect tactile-visual integration remains unclear.

In order to fill this gap, the present experiment directly probed the contribution of tactile stimuli to the combined percept by not only varying the noise level of the visual stimulus,

but also by manipulating whether the tactile stimulus was a reliable source of information or not. Both modalities, even when they were corrupted by noise, provided congruent directional information. Thus, if participants engaged in optimal integration, their combined percept should have always exceeded the corresponding component signals, even when both were noisy. Importantly, the design allowed us to examine whether changing reliability in each modality influenced the integrated estimate over and above the information provided by the other modality (i.e., the noise manipulation was applied to each modality independently, rather than to just one modality as most previous integration studies have done).

## 6.2. Methods

### 6.2.1. Participants

Sixteen participants were recruited to take part in the experiment. However, the data of seven of those participants produced psychometric plots that showed either negative or nonlinear slopes (see **Appendix A** for individual psychometric fits of excluded and included participants). Because their data could not yield reliable measures, it was excluded from the final analysis. Thus, the final sample was composed of the remaining nine participants (mean age 32; 6 women, reportedly all right-handed). The procedures were approved by the local ethical committee of NTT Communication Science Laboratories.

### 6.2.2. Apparatus and experimental set-up

**Figure 6.2A** shows the experimental set-up. Participants were standing on a force platform to continuously measure their center of pressure (or ‘body sway’). The tactile stimulus was a sudden pulling force produced by a haptic device (Phantom premium 1.5 A, Geomagic Inc.), which participants held between the right index finger and the right thumb. The magnitude of the force was set to 0.6 N, so that force was strong enough to perceive different directions, but weak enough to not induce any sudden body movements. Participants were told that the force device will “lightly pull your hand in different directions” and that they should “hold the device in a tight grip, so it won’t fall off your hand when it pulls you” and that “it is OK if you move your hand slightly, but please don’t let it move with the device too much”. The force stimulus lasted for 1s with first and last 100ms serving as force ramp-up and ramp-down to make the pulling gradual rather than jerky.

The visual stimulus was delivered via virtual reality (VR) goggles (HTC VIVE PRO; <https://www.vive.com/us/product/vive-pro/>) that participants were wearing. The default environment was a field of 100 white dots against a black background with a red fixation point (**Figure 6.2B**). While the environment was fixed, the red fixation point moved relative to the

head position. This helped participants keep their head straight during the experiment by aligning the red dot to the center of the dot field. The sensation of a directional movement was created by contracting the white dots to the center of the field depending on the specific direction (similar to optical flow). Thus, a sensation of moving straight ( $0^\circ$ ) was created by contracting the dots into the center of the field, while a sensation of moving slightly to the right (e.g.,  $10^\circ$ ) was created by displacing the center of contraction to the right of the center of the field. Because piloting indicated that perceiving visual motion direction was relatively easy, we manipulated visual stimulus parameters to equate the performance with force perception. First, we reduced the lifetime of moving dots to 1ms and reduced the coherence of dot motion to 60%. This means that 40% of dots were moving in random directions.

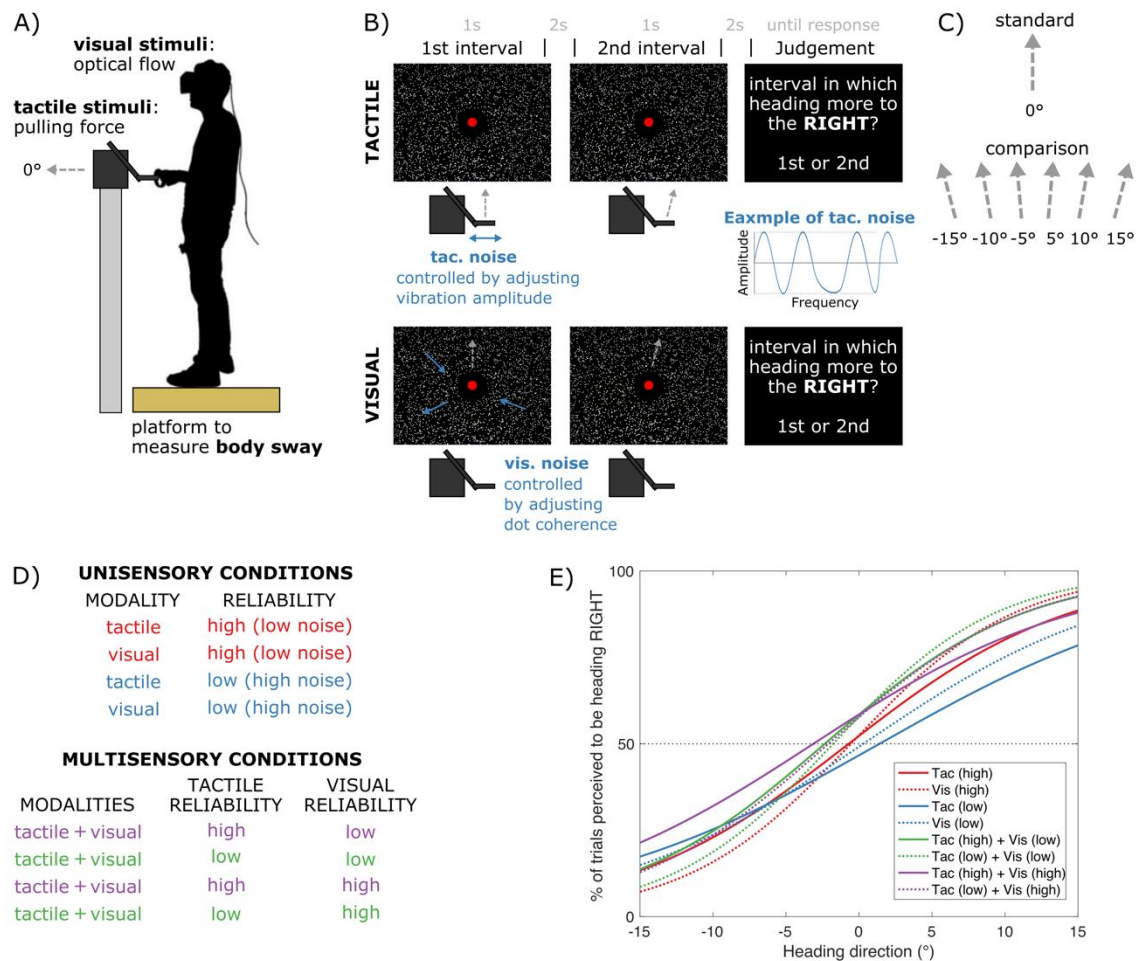


**Figure 6.2. Experiment 7: methods.** **A)** Experimental set-up. **B)** Examples of unisensory conditions. The upper panel shows tactile-only condition, where a tactile stimulus pulled participant forward in a specific direction. Noise in the directional information was produced as a sinusoid-like vibration in the tactile stimulus, but with a random frequency. The noise level was controlled by adjusting the amplitude of the vibration, as shown in the example. The lower panel shows visual-only condition, where white dots contracted towards the center in a specific direction to produce a sensation of being pulled. The noise level of visual directional information was controlled by increasing the percentage of randomly moving incoherent dots. By combining unisensory conditions with different noise levels, we could produce four different combinations of multisensory conditions shown in **D)**. **C)** Stimulus directions. Standard was always straight ahead ( $0^\circ$ ), and comparison interval could contain any of the comparison directions.

Whether standard was presented in the 1<sup>st</sup> or 2<sup>nd</sup> interval was randomised. **D)** All eight experimental conditions. Reliability condition is high when noise in that modality was low, and it is low when noise was set to degrade performance below 60% correct in the pre-experimental staircase (set for each participant individually). **E)** Group-level psychometric curves across 9 participants for each condition. Individual psychometric curves are shown in Appendix A.

### 6.2.3. Task design

The task was to judge the direction of motion between two stimuli presented in sequential intervals. To do so, participants had to report in which interval the stimulus headed more to the right (**Figure 6.2B**). The comparison was always made against a standard stimulus (0°), which was randomly presented either in the first or the second interval. The comparison stimulus (**Figure 6.2C**) moved either left (negative directions) or right (positive directions) from the standard with varying levels of discrepancy from the standard (5°, 10°, 15°).

The experiment was performed in 8 blocked conditions shown in **Figure 6.2D**. Four of these were unisensory conditions, whereby directional input was presented only via visual or tactile stimulus. These four conditions were in turn divided into high or low reliability conditions, whereby the information presented was either with low noise (high reliability) or corrupted by large amount of noise (low reliability). The upper panel of **Figure 6.2B** shows the tactile-only condition. In that condition, visual input was the default environment with no motion among the dots. At the start of the trial, the force device moved participants' hand into the starting position (at the body midline). Participants were required to keep their head straight (red fixation dot aligned with the center of the field). Then, the force device would lightly pull the hand in a pre-specified direction (1st interval), it will stop for 2 s, and then pull it in another pre-specified direction (2nd interval), after which participants made their judgement by pressing the corresponding key on a mouse that was held in their other left hand. Note that the hand was not moved to its starting position prior to the 2nd interval to not provide any additional proprioceptive feedback. After the judgement, the hand was moved to the starting position and the next trial began.

Tactile input was made noisy by adding a left-right vibration. The vibration was created as a sinusoid at a varying frequency between 3 to 13 Hz; the noise level was controlled by adjusting the amplitude of that vibration (as shown in an example in **Figure 6.2B**). In the high reliability condition [tac(high)], the vibration force was set to 0.1 N. In the low reliability condition [tac(low)], the vibration amplitude was determined by a staircase procedure prior to the main experiment. Specifically, before the experiment, participants had two practice blocks per unisensory condition. In the first practice block, they performed high reliability trials until their performance level stabilised at 80% correct. In the second practice block, the amplitude of the vibration increased in a staircase procedure making the tactile input noisier, until the

performance level fell to 60% correct. The mean amplitude of noise vibrations in low reliability conditions was  $6.5 \pm 2.3$  N across participants.

The lower panel of **Figure 6.2B** shows the visual-only condition. In that condition, the hand was moved to the same starting position as in tactile-only trials, but no pulling force was applied, and the hand remained fixed for the duration of the trial. When the trials started, the white dot field started to contract towards the pre-defined FOE (“focus of expansion”) (1st interval), then stopped for 2 s, and then contracted again towards another FOE (2nd interval). Note that instead of using expanding dot flow, we used contracting flow. Normally, an expanding optic flow creates a sensation of moving forward, whereas contracting flow induces a sensation of backward movement (Raffi & Piras, 2019). However, in our virtual reality setting, the expanding flow pushed participants backward, possibly due to a sensation that the dots moved *at* the participant. When we piloted the contracting flow, whereby dots arrived from behind the participant and move towards the FOE, the sensation was of moving “into a tunnel”. Thus, we used contracting flow in our experiment. Although such flow is not traditionally related to heading forward, ‘heading’ direction could still be extracted. The central area of the visual display was occluded by a black rectangle, so that participants could judge the direction of ‘heading’ by changes in FOE position (i.e., where dots moved), but needed to consider the motion in the surrounding dots, while fixating at the centre of the rectangle. Importantly, such heading sensation based on peripheral flow is considered to be more important than focussing on central visual field (Raffi & Piras, 2019).

The level of noise in the visual stimulus was controlled by adjusting the number of incoherent dots (dots that moved in a random direction). In the high reliability condition [vis(high)], coherence was set to 60% (40% of dots incoherent). In the first practice block, participants performed high reliability trials until their performance stabilised at 80% correct. In the second practice block, the number of incoherent dots gradually increased until the performance fell to 60% correct. The resulting level of incoherence was used for the low reliability condition [vis(low)]. The mean dot coherence level in low reliability conditions was  $29 \pm 11$  % across participants.

The remaining four conditions were multisensory conditions, whereby directions information was provided simultaneously via tactile and visual input. This means that pulling and the movement of dots began synchronously. Importantly, the directional information was always identical between the tactile and visual input with no conflict trials. This means that participants should have always benefitted from multisensory conditions if they integrated the input in an optimal manner. However, the relative reliability of each sensory input was independently modulated, so the multisensory conditions were divided into 1) when input from

touch was reliable, but visual input was noisy [tac(high)+vis(low)]; 2) when input from both modalities was noisy [tac(low)+vis(low)]; 3) when input from both modalities was reliable [tac(high)+vis(high)]; and 4) when input from touch was noisy, but visual input was reliable [tac(low)+vis(high)]. This resulted in 2 (tactile reliability: high vs. low) – by – 2 (visual reliability: high vs. low) factorial design, where effect of reliability in each modality could have been evaluated over and above the reliability in the other modality.

Each condition had 48 trials (4 trials for -15° comparison, 8 for -10°, 12 for -5°, 12 for 5°, 8 for 10°, and 4 for 15°). The order of conditions was randomised for each participant. The experiment was performed in two 1h sessions on the same day with a break in-between. Half of the trials from each condition were performed in the 1st session. In the 2nd session, the order of conditions was reversed, and the remaining trials were completed. In that way, we tried to balance out the fatigue effects, as the conditions that were performed last in the 1st session, were performed first in the 2nd session.

#### 6.2.4. Behavioral analysis

**Figure 6.2E** shows the group-level psychometric curves fitted to individual data across all 8 conditions. Adjusted  $R^2$  showed sufficient fit to data in all conditions (Table 6.1; range = 0.6 to 0.9 across conditions). Two main measures were extracted from the psychometric functions: just noticeable difference (JND) and point of subjective equality (PSE). JND corresponds to the smallest discrepancy between comparison and standard direction, at which participants could discriminate between them. In the MLE framework, JND is inversely related to the cue's perceptual reliability, and thus reflects the uncertainty (or standard deviation) in the information provided by the cue (Ernst & Banks, 2002; Rohde et al., 2016). PSE corresponds to the discrepancy between comparison and standard direction, at which participants are equally likely to select the standard or the comparison directions as the right-most direction. In designs, where a conflict is induced between modalities in multisensory conditions, PSE informs about the perceptual bias towards one or the other modality. Because in the current experiment we were mainly interested in the effects of sensory noise, no conflict trials were included. Thus, PSE, in our case, merely informed whether there was some general bias in the data (i.e., an overall deviation from 0°).

**Table 6.1:** Experiment 7: measures from psychometric fits

Condition: modality (reliability)	JND (mean ± sd)	PSE	R <sup>2</sup> adj
tac (high) + vis (high)	6.3 ± 3.0	-1.8 ± 2.3	0.9 ± 0.1
tac (high) + vis (low)	7.5 ± 2.2	-2.5 ± 3.4	0.8 ± 0.1
vis (high)	7.6 ± 7.8	-0.8 ± 2.6	0.8 ± 0.3
tac (low) + vis (high)	8.1 ± 5.3	-2.2 ± 1.7	0.8 ± 0.2
tac (high)	8.7 ± 3.0	-0.7 ± 1.9	0.8 ± 0.1
vis (low)	10.4 ± 4.6	0.7 ± 4.9	0.7 ± 0.2
tac (low)	13.6 ± 7.1	1.5 ± 3.9	0.7 ± 0.2
tac (low) + vis (low)	14.0 ± 13.9	-5.3 ± 6.7	0.6 ± 0.4

Note: Conditions ordered from the smallest mean JND to the highest, n = 9

First, we examined the performance in the unisensory conditions with a 2 (modality: tactile vs. visual) – by – 2 (reliability: high vs. low) repeated-measures ANOVA (rmANOVA) to check the difference between modalities and the effect of the reliability manipulation. Normality assumption was checked with Shapiro-Wilk test on the residuals of the model fit. There was no evidence for normality violations when modelling JND ( $p = .06$ ) and PSE ( $p = .64$ ) values.

Next, based on the unisensory JNDs, we calculated the predicted performance in the multisensory conditions according to the MLE framework. Specifically, according to the MLE rule, the brain weights the input from multiple modalities so that uncertainty  $\sigma^2$  (or variance) of a multisensory estimate is minimised:

$$\sigma_{tac+vis,PR}^2 = \frac{\sigma_{tac}^2 \times \sigma_{vis}^2}{(\sigma_{tac}^2 + \sigma_{vis}^2)} \quad (6.1)$$

JND corresponds to  $\sqrt{2}$  times the standard deviation of the underlying estimator. Thus, given the unisensory JNDs, the predicted JND can be calculated by rewriting equation 6.1:

$$JND_{tac+vis,PR} = \sqrt{\frac{JND_{tac}^2 \times JND_{vis}^2}{(JND_{tac}^2 + JND_{vis}^2)}} \quad (6.2)$$

This allowed us to characterise multisensory integration in three ways. First, by comparing the actual JND to the mean JND between corresponding unisensory conditions, we could test whether the multisensory cues were integrated. If the cues were integrated, then multisensory JND should be at least lower than the combined unisensory JND. Second, by comparing the actual multisensory JND to the JND predicted by MLE rule (equation 6.2), we could test whether the integration was truly optimal, at least in a Bayesian optimal sense. Third, by employing a 2 (tactile reliability: high vs. low) – by – 2 (visual reliability: high vs. low) rmANOVA we could evaluate whether integration optimality varied across multisensory conditions. Shapiro-Wilk test showed no significant normality violation for the integration index



( $p = .49$ ) but did show a slight deviation for optimality index ( $p = .03$ ). However, as in previous chapters, we adhered to parametric ANOVA due to its robustness against non-normality.

### 6.2.5. Body sway analysis

While the above analysis informs us about explicit directional judgements, we used body sway as an implicit postural response to the directional information, which reflects the experience of heading. Throughout the experiment, the force platform was measuring changes in participants' center of pressure (COP). Raw data was collected from 8 force channels. An additional trigger channel recorded the start time of each stimulus interval (two intervals on each trial: one containing the standard and the other containing the comparison direction). Interval-locked epochs of 1200 ms were then extracted from 200 ms before the start of the interval to 1 s into the interval, which is how long the directional stimulus was presented for. A custom MATLAB code was used to calculate, for the interval-locked raw data, the force and moment displacement along x, y, and z directions on the platform, and the resulting displacement of COP along the y direction (forward vs. backward) and x direction (leftward vs. rightward). The epochs were coded according to 1) performed condition, 2) whether the interval contained the standard or the comparison direction, 3) the specific comparison direction, and 4) whether that trial was followed by a correct or incorrect response. Epoched data was then filtered with a fourth order zero-lag Butterworth low-pass filter, whose cut-off frequency was set to 5 Hz, because we were mainly interested in the slow changes of posture.

COP displacements reflect overall change in posture relative to a baseline (i.e., no change). It is mainly determined by the large low-frequency components and thus describes slow postural adjustments. In addition, velocity of COP signal can be calculated to characterise the rate of COP displacement (Luo et al., 2018). We calculated continuous COP velocity in x and y direction as a time derivative of the COP signal:

$$COP_{vel,x} = \frac{COP_{x,t+1} - COP_{x,t}}{t_{change}} \quad (6.3)$$

$$COP_{vel,y} = \frac{COP_{y,t+1} - COP_{y,t}}{t_{change}} \quad (6.4)$$

where COP displacement between two subsequent time points ( $t$ ) is divided by the interval of the displacement ( $t_{change}$ ), which, in our case, was 0.5 ms. All variables of COP in each epoch were then baseline-corrected by subtracting the first 200 ms (before the interval started). To detect outlier COP trials, MATLAB internal function "isoutlier" was used on COP displacement. The mean COP in x and y direction was calculated across the whole time-window (-200 to 1000ms) for each condition and each directional stimulus (including standard), and epochs

where mean COP was more than 3 SDs were identified and excluded from further analysis. On average, we excluded  $1.6 \pm 1.9$  % of COP epochs that accompanied comparison intervals and  $10.1 \pm 5.1$  % that accompanied standard intervals.

To illustrate the COP signal, **Figure 6.3** shows trial-wise and mean COP displacement and velocity of one representative participant when performing three conditions: tactile-alone, visual-alone, and tactile-visual together, all under high reliability. Comparison trials were averaged into left ( $-15^\circ$ ,  $-10^\circ$ ,  $-5^\circ$ ) and right ( $15^\circ$ ,  $10^\circ$ ,  $5^\circ$ ) stimulus directions. COP displacement in y-dimension describes forward and backward postural adjustment with velocity indicating the rate of that adjustment. The expectation was that all stimuli should produce a forward sway, indicating a postural response of 'heading'. Indeed, that seemed to be the case for tactile-only and combined tactile-visual condition, but not in visual-only condition, where a brief backward sway was apparent instead. The velocity profile shows that this backward movement was much more rapid than the gradual sway seen in other conditions. The group-level y-dimension sway data (**Figure 6.7**) shows that this pattern seemed to be consistent across the group and was also present to a smaller extent during noisy visual stimuli. The important thing to note is that for all combined conditions a gradual forward sway was apparent. In addition to forward and backward sway, COP displacement in x-dimension reflects the stimulus-direction specific postural movement in rightward or leftward direction. The expectation was that postural adjustment pattern during right versus left stimulus would lead to diverging sway patterns as shown in the combined condition in **Figure 6.3**. That is, a visual or tactile stimulus implying a leftward direction would lead to postural sway to the left, while a visual or tactile stimulus implying a rightward direction would lead to postural sway to the right. The leftward-rightward sway seemed to be less strong than the forward-backward one.

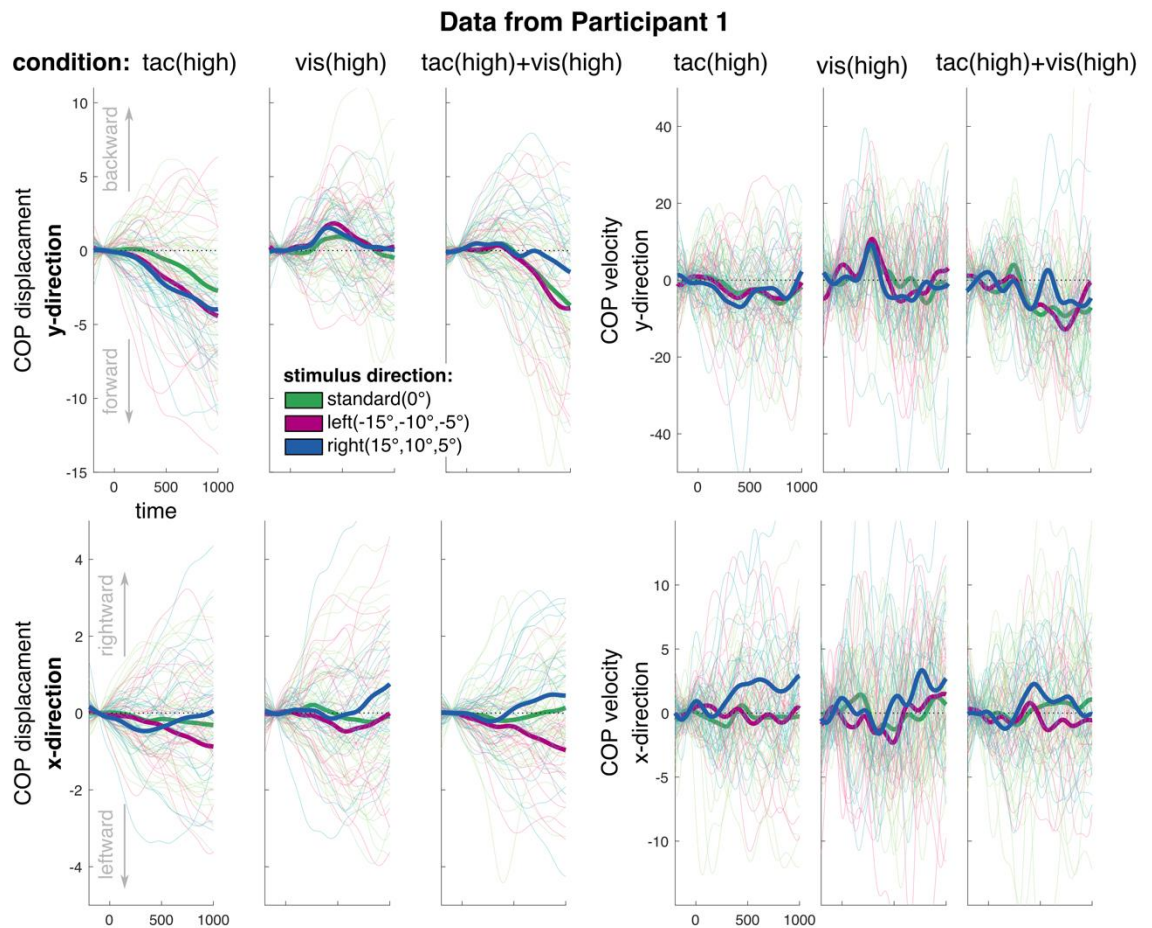


**Figure 6.3. Experiment 7: body sway data from one representative participant.** To illustrate epoched COP data across trials, one participant was selected. Data is illustrated from three conditions: tactile-only, visual-only, combined tactile-visual; all conditions from high reliability levels. Left-side panels show COP displacement, while right-side panels show the corresponding velocity of the displacement. Upper panels show the COP displacement along the y axis which correspond to forward vs. backward movement, while lower panels show displacement along the x axis which correspond to rightward vs. leftward body sway. Colors refer to stimulus direction. Left (-15°, -10°, -5°) directions are all coded as purple, right (15°, 10°, 5°) directions are all coded as blue, and standard (0°) directions are coded as green. The bold lines show the mean COP signal for all standard directions and pooled left and right comparison directions.

To quantify these qualitative observations, we extracted the mean COP displacement and velocity measures in the 200 to 1000 ms time-window after stimulus onset for each condition and stimulus direction. The time-window start time was determined by plotting COP displacement in y-dimension averaged across all directions, conditions, and participants (see **Appendix A**), and by looking at when COP started to diverge from 0, which was approximately 200 ms after the onset of the stimulus. Because each specific comparison direction had a different number of trials, we averaged the comparison data into left (-15°, -10°, -5°) and right (15°, 10°, 5°) directions, as shown in **Figure 6.3**. Our predictions were in regard to COP displacement. Thus, the mean velocity was not analysed further.

First, we predicted that mean y-dimension COP displacement (forward-backward sway) to significantly deviate from 0 during all stimulus directions (tested with one-sample t-tests against 0), indicating occurrence of forward or backward sway. Second, in x-dimension

(leftward-rightward sway), we expected the mean COP during rightwards vs. leftward stimuli to significantly differ, indicating occurrence of body sway that was sensitivity to directional input. For this we calculated this difference and compared it to 0 with one-sample t-test. Multiple comparisons were Bonferroni-corrected. These two predications test whether there was an implicit postural response. Next, we examined whether both types of sway varied across unisensory conditions with a rmANOVA that coded for modality (tactile, visual), reliability (high, low), and stimulus direction (standard, left, right). Then, we examined both types of sway across multisensory conditions as coded by tactile reliability (high, low), visual reliability (high, low) and direction (standard, left, right). In analysing x-dimension sway only left and right stimulus directions were included. Finally, we examined whether postural sway varied across multisensory and corresponding unisensory conditions. We hypothesised that multisensory conditions may result in greater sway that could index a stronger experience of 'heading'.

Last, we explored whether the postural sway was merely epiphenomenal or whether it also affected task performance. We divided trials into whether they resulted in correct or incorrect perceptual judgement response, prior to averaging across stimulus directions. **Figure 6.4** illustrates the mean forward-backward COP displacement across trials as a participant progressed through experimental blocks of two conditions, along with the outcome of the trial. Although, no clear pattern immediately emerged, we questioned whether participants may use postural feedback as an additional cue for discerning stimulus direction. For the analysis, we ran the same rmANOVAs, but added response (correct, incorrect) as an additional variable. The only difference was that in the forward-backward sway, we averaged left and right direction trials into comparison trial group, so direction factor was comparison vs. standard.

### Forward-backward sway as Participant 1 progresses through trials

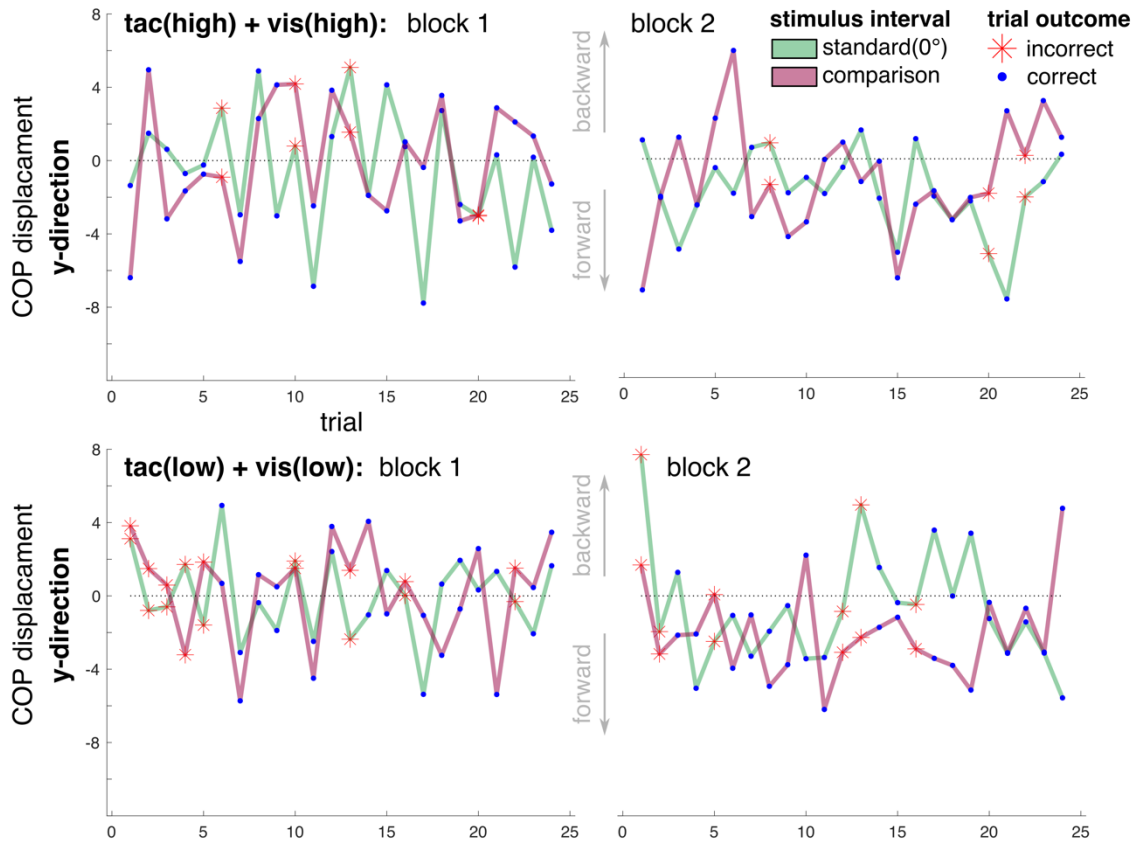


**Figure 6.4. Experiment 7: Mean forward-backward COP across trials as a participant progressed through the experimental blocks, along with the outcome of the trial.** Each data point corresponds to the mean COP displacement in the 200 to 1000 ms time-window after stimulus onset in the corresponding trial. The data is shown across two conditions, where behavioral performance was highest (reliable touch combined with reliable vision) and where it was lowest (unreliable touch combined with unreliable vision). On each trial, one stimulus interval contained the standard direction (0°; green line) and the other comparison direction (pink line), which could have been either right (15°, 10°, 5°) or left (-15°, -10°, -5°). The symbols indicate the outcome of the trial, whether it resulted in correct response (blue dot) or incorrect response (red asterisk). Each experimental condition was performed in two blocks of 24 trials

## 6.3. Results

### 6.3.1. Can people perceive direction from force and optical flow?

#### 6.3.1.1. Explicit behavioural response

Figure 6.5 shows the group-level JND and PSE results for unisensory conditions. rmANOVA yielded a significant main effect of reliability on JND ( $F(1,8) = 6.0, p = .04, np^2 = .43$ ;  $BF^{01} = .3 \pm 1.1\%, BF_{incl} = 2.8$ ) with overall higher JND in low (mean JND = 12.0, SD = 6.0) compared to high (mean JND = 8.1, SD = 5.8) condition. Although, JNDs seemed to be lower in the visual condition, the main effect of modality was non-significant ( $F(1,8) = 2.3, p = .17, np^2 = .22$ ;  $BF^{01} = 1.5 \pm 1.6\%, BF_{incl} = .7$ ) and neither was the interaction ( $F(1,8) = 0.4, p = .55, np^2 = .05$ ;  $BF^{01} = 2.0 \pm 1.1\%, BF_{incl} = .7$ ). This suggests that reliability manipulation worked equally in both modalities. Similar analysis was conducted for PSE. Although the figure suggests a difference between high

and low reliability conditions in both modalities, the main effect of reliability did not reach statistical significance ( $F(1,8) = 3.6$ ,  $p = .09$ ,  $np^2 = .31$ ;  $BF^{01} = .9 \pm 1.7\%$ ,  $BFincl = .8$ ). Other effects were far from statistical significance ( $p$  values:  $.69$  and  $.81$  for main effect of modality and interaction, respectively). Overall, PSE values tended to be close to 0 indicating no significant biases, and there was too much inter-individual variability to detect statistically significant results. Overall, this suggests that direction input could be perceived with precision of approximately  $8^\circ$  both via touch-alone and vision-alone, given that inputs were not corrupted by noise. Perception lowered to approximately  $12^\circ$  with introduction of noise.

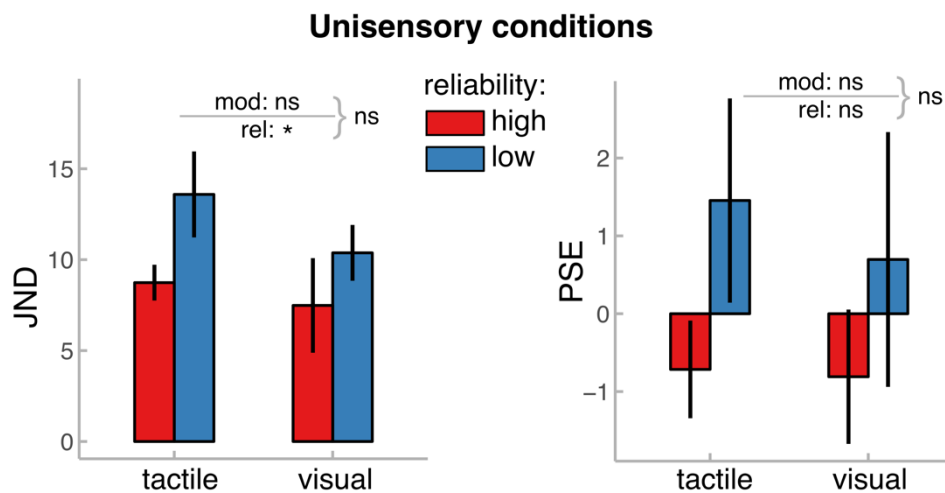


**Figure 6.5. Experiment 7: Unisensory behavioural performance.** JND and PSE of unisensory conditions with either high (red) or low (blue) reliability. Annotations on the lines show statistical significance of main effects, annotation next to the line shows interaction ( $* p < .05$ ).

### 6.3.1.2. Implicit postural response

**Figure 6.6** shows the group-level COP displacement along the forward-backward and rightward-leftward dimensions for all conditions (including multisensory conditions). **Figure 6.7A,C** shows the mean COP displacement within the stimulus interval time-window across all conditions, and **Table 6.2** shows the statistics of the mean COP displacement against the baseline, 0.

The forward-backward sway reflects a general direction-independent entrainment to the stimulation. In unisensory conditions, tactile pulling produced a significant forward sway (t-tests against 0; see **Table 6.2**). In visual-only conditions, the backward sway was statistically significant for all directions when vision was reliable, and during standard stimulus intervals when vision was noisy. ANOVA yielded a significant effect of modality ( $F(1,8) = 60.1$ ,  $p < .001$ ,  $np^2 = .88$ ), signifying the differing forward vs. backward sway pattern during tactile vs. visual stimuli. The interaction between modality and direction was also significant ( $F(2,16) = 9.0$ ,  $p = .004$ ,  $np^2 = .53$  –  $p$  value Greenhouse corrected due to non-sphericity). Follow-up Bonferroni-

corrected pairwise tests showed significant difference between left/right vs. standard direction during tactile stimuli (both  $p$  values = .02), with greater sway for comparison stimuli, but no such difference was present in visual-only conditions ( $p$  values: 1.0 and .4 for left and right stimulus against standard, respectively). Interestingly, forward-backward sway did not differ across reliability levels ( $F(1,8) = .59$ ,  $p = .46$ ,  $np^2 = .07$ ), indicating that it was similar even when corresponding input was corrupted by noise.

While forward-backward sway reflects general entrainment, rightward-leftward sway represents direction-specific postural response to the stimulus directions. **Table 6.3** shows  $x$ -dimension sway for each direction. However, because some sway is already present, when stimulus was standard, instead of comparing sway during left and right directions to 0, we first took the absolute difference between sway during left and right directions and compared that difference to 0. This can be better seen in **Figure 6.7C**. Except when tactile input was corrupted by noise ( $p = .02$  – does not survive Bonferroni-correction), all other conditions showed a significant divergence: touch with high reliability ( $p = .003$ ,  $d = 1.4$ ), vision with high reliability ( $p = .002$ ,  $d = 1.5$ ), and vision with low reliability ( $p < .001$ ,  $d = 2.5$ ). ANOVA analysis on the rightward-leftward divergence did not yield an effect of modality ( $F(1,8) = 4.2$ ,  $p = .07$ ,  $np^2 = .35$ ;  $BF^{01} = .7 \pm 2.9\%$ ,  $BF_{incl} = .5$ ) or reliability ( $F(1,8) = .51$ ,  $p = .50$ ,  $np^2 = .06$ ;  $BF^{01} = .4 \pm 84.1\%$ ,  $BF_{incl} = .9$ ). The interaction was also non-significant ( $F(1,8) = .69$ ,  $p = .43$ ,  $np^2 = .08$ ;  $BF^{01} = 1.7 \pm 2.4\%$ ,  $BF_{incl} = .2$ ). This suggests that postural response implicitly followed stimulus directions to a similar extent in all conditions. However, note that the significant divergence is likely due to a strong response to the left stimulus (see **Figure 6.7**).

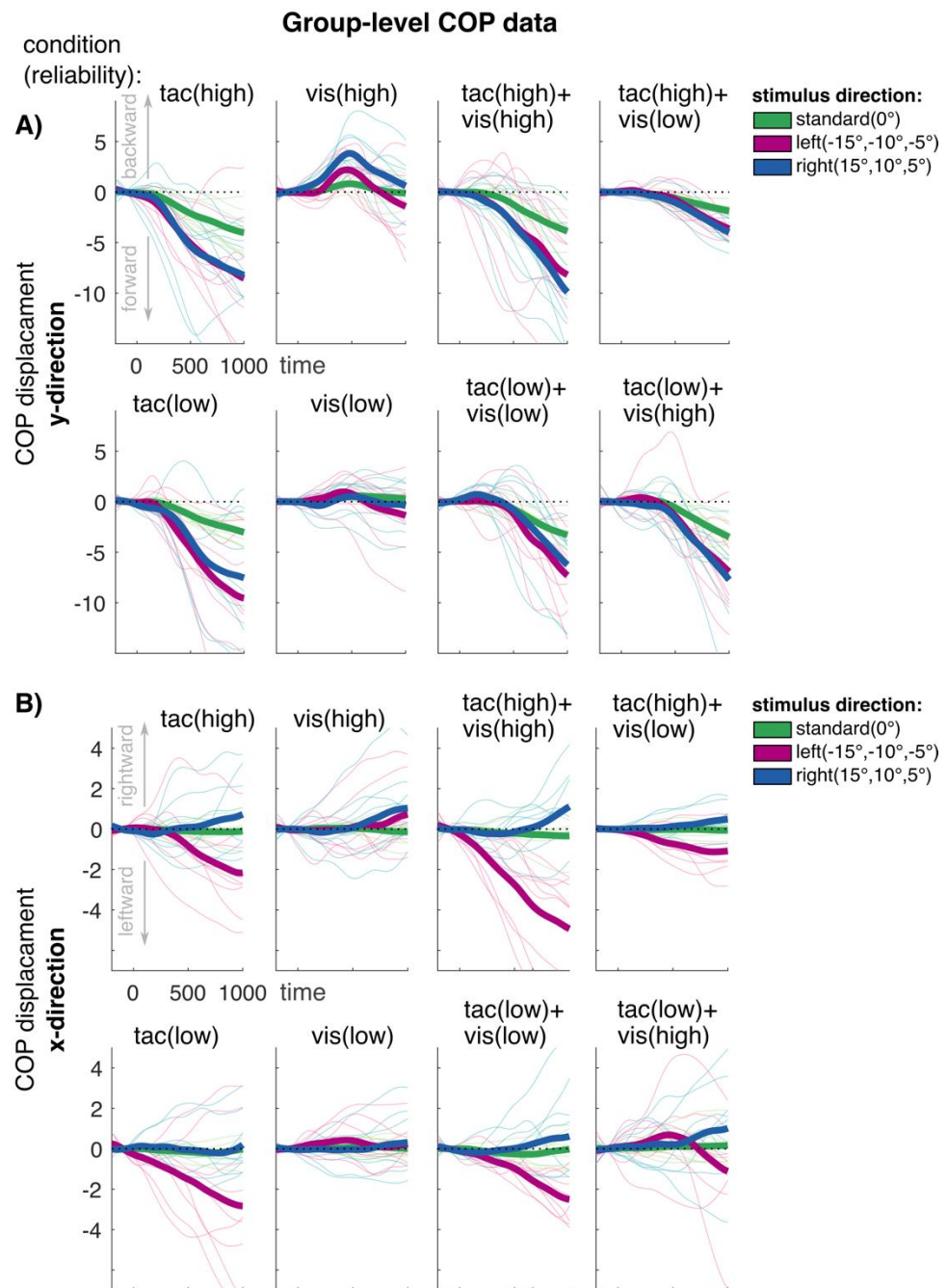


**Figure 6.6. Experiment 7: group-level body sway data.** **A)** COP displacement along the y axis, which corresponds to forward vs. backward movement. **B)** COP displacement along the x axis, which corresponds to rightward vs. leftward body sway. The COP signal was averaged for each stimulus direction across the repeated trials. For clarity, COP signal shown here was further averaged across specific directions into standard (0°), left (-15°, -10°, -5°), and right (15°, 10°, 5°) directions (coded by green, purple and blue colors, respectively). Each thin line corresponds to averaged data for one participant for that averaged direction (n= 9 for each direction). The bold line corresponds to the group mean.



**Table 6.2:** Experiment 7 mean COP displacement

Condition	Direction	y-dir. (forward-backward)		x-dir. (rightward-leftward)	
		mean $\pm$ SD	t-test against 0: $t(d)$	mean $\pm$ SD	t-test against 0: $t(d)$
tac(high)	0° (standard)	-2.3 $\pm$ 1.2	0(-1.9) <sup>†</sup> *	-.1 $\pm$ .4	-.7(-.2)
	left	-4.4 $\pm$ 2.7	-5(-1.7)*	-.7 $\pm$ 1.4	9(-.5) <sup>†</sup>
	right	-4.9 $\pm$ 3.8	-3.8(-1.3)*	.04 $\pm$ 1.5	.1(.03)
vis(high)	0°	.2 $\pm$ 1.4	.4(.1)	.2 $\pm$ .5	1.1(.4)
	left	1.3 $\pm$ 1.5	2.6(.9)*	.2 $\pm$ 1.1	.5(.2)
	right	2.0 $\pm$ 1.5	3.9(1.3)*	.1 $\pm$ 1.6	.2(.07)
tac(low)	0°	-1.7 $\pm$ .9	-5.5(1.8)*	-.2 $\pm$ .3	-2.3(-.8)*
	right	-4.9 $\pm$ 4.6	-3.2(-1.1)*	-1.4 $\pm$ 2.9	-1.4(-.5)
	left	-4.4 $\pm$ 4.0	-3.3(1.1)*	-.1 $\pm$ 1.4	-.3(-.1)
vis(low)	0°	.4 $\pm$ .4	44(1.0) <sup>†</sup> *	.003 $\pm$ .3	.03(.01)
	left	-.2 $\pm$ 2.7	27(-.1) <sup>†</sup>	.4 $\pm$ .8	1.5(.5)
	right	.2 $\pm$ 1.8	.4(1.5)	.07 $\pm$ 1.1	0.2(.07)
tac(high) + vis(high)	0°	2.0 $\pm$ 1.3	-4.2(1.4)*	.003 $\pm$ .7	.01(.004)
	left	4.6 $\pm$ 3.6	-2.9(1.0)*	-2.0 $\pm$ 1.5	-4.0(-1.3)*
	right	3.9 $\pm$ 3.8	2(-.9) <sup>†</sup> *	.6 $\pm$ 1.1	1.6(.5)
tac(high) + vis(low)	0°	1.2 $\pm$ .6	-5.7(-1.9)**	-.05 $\pm$ .3	-.4(.1)
	left	1.8 $\pm$ 1.0	-3.4(-1.2)*	-.9 $\pm$ .9	5(-.9) <sup>†</sup> *
	right	2.3 $\pm$ .9	-7.2(2.4)**	.3 $\pm$ .6	1.5(.5)
tac(low) + vis(high)	0°	1.4 $\pm$ .8	-3.6(-1.2)*	.1 $\pm$ .7	.4(.1)
	left	2.7 $\pm$ 1.1	-2.9(1.0)*	-.2 $\pm$ 1.2	-.5(-.2)
	right	3.5 $\pm$ 2.1	-3.9(1.3)*	.3 $\pm$ 1.4	.7(.2)
tac(low) + vis(low)	0°	1.5 $\pm$ .8	-5.0(1.8)*	-.2 $\pm$ .5	-1.4(-.5)
	left	3.3 $\pm$ 1.8	-2.6(.9)*	-1.1 $\pm$ .8	-4.3(-1.4)*
	right	3.3 $\pm$ 2.5	-.7(.5)	-.4 $\pm$ .8	-1.4(-.5)

\*p < .05, \*\*p < .001. x<sup>†</sup> indicate the sign test (V), which was used instead of t-test, due to non-normality. Each condition contains n = 9.

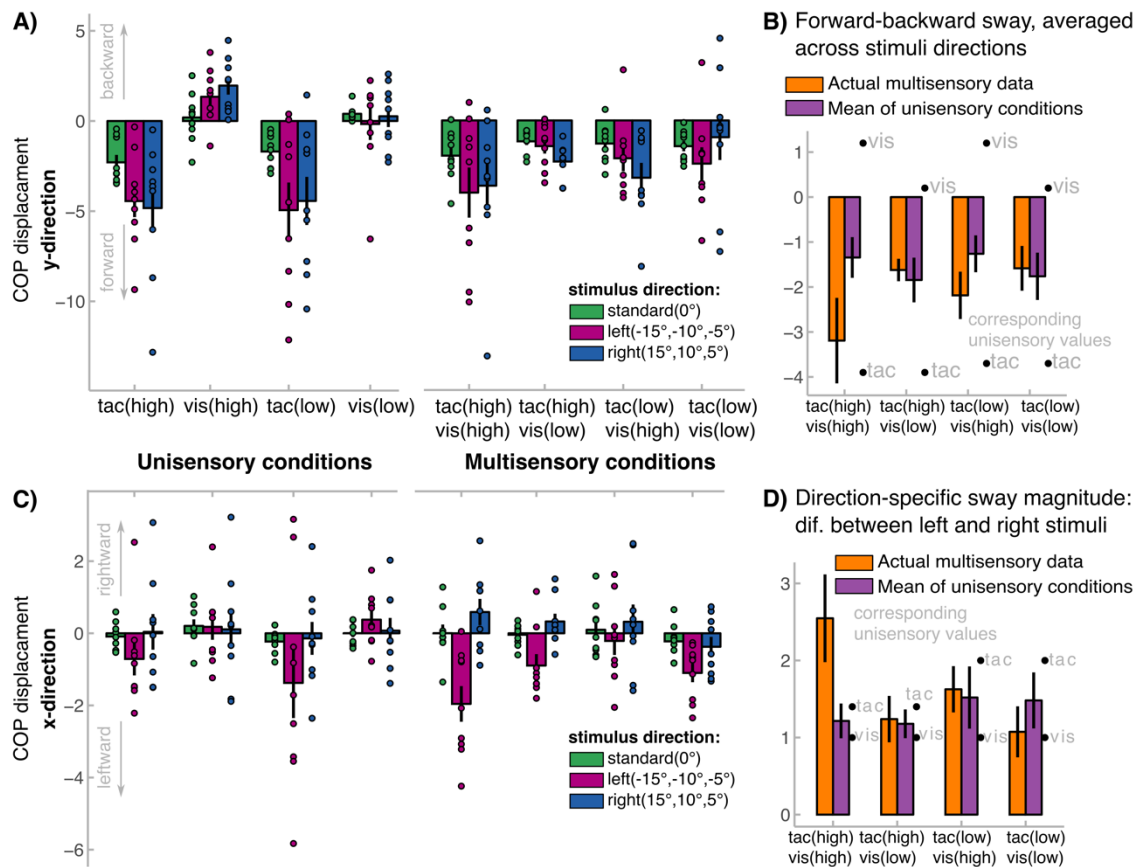


**Figure 6.7. Experiment 7: mean COP displacement in all conditions.** **A)** shows the COP displacement along the y-axis which correspond to forward (negative) vs. backward (positive) movement. **C)** shows displacement along the x-axis which correspond to leftward (negative) vs. rightward (positive) body sway. COP signal was averaged across specific directions into standard (0°), left (-15°, -10°, -5°), and right (15°, 10°, 5°) stimuli, which is coded by green, purple and blue colors, respectively. Dots represent individual participant data. **B)** shows the overall forward-backward sway (averaged across standard, left, and right directions) for each multisensory condition (orange) and mean of unisensory conditions (purple); overlaid dots represent overall sway in corresponding unimanual conditions that made up the mean data. **D)** shows the direction-specific sway magnitude with same annotations as in **B)**. To get these values, the absolute difference in x-dimension sway was calculated between left and right stimuli. Larger values reflect greater divergence in sway between left and right stimuli, and thus greater overall direction-specificity in postural sway.

### 6.3.2. Is there integration at the level of explicit perception?

To examine whether tactile and visual cues were integrated, we calculated the JND difference between actual multisensory performance and mean performance under the corresponding unisensory conditions (**Figure 6.8 lower left panel**). One-sample t-tests against 0 showed that no condition was significantly different from 0 (when both reliable:  $t(8) = 1.70$ ,  $p = .13$ ,  $d = .57$ ; when touch was reliable, but vision noisy:  $t(8) = 1.88$ ,  $p = .10$ ,  $d = .63$ ; when touch was noisy, but vision was reliable:  $t(8) = 1.19$ ,  $p = .27$ ,  $d = .40$ ; when both were noisy:  $t(8) = -.42$ ,  $p = .68$ ,  $d = -.14$ ). This suggests that even when both inputs were noisy, combined performance was at least as good as the unisensory performance. However, note that no conditions led to differences greater than 0, suggesting that the benefit from multisensory presentation was not substantial, although **Figure 6.8** shows that multisensory performance tended to be at least better than each unisensory condition, specifically when tactile input was reliable. RmANOVA

with factors tactile reliability (high, low) and visual reliability (high, low) yielded did not show a significant effect of tactile reliability ( $F(1,8) = .57, p = .47, np^2 = .07; BF^{01} = 2.6 \pm 1.2\%, BF_{incl} = .3$ ) nor of visual reliability ( $F(1,8) = .90, p = .37, np^2 = .10; BF^{01} = 2.0 \pm .9\%, BF_{incl} = .4$ ), and also no interaction ( $F(1,8) = 1.0, p = .35, np^2 = .11; BF^{01} = 1.5 \pm 5.3\%, BF_{incl} = .3$ ). This means that no significant difference was apparent between multisensory conditions, and that reliability in one modality did not modulate performance over and above the other modality. However, note that due to a small sample, the absence of effects could be due to insufficient statistical power. Indeed, the Bayes factor shows insufficient evidence, at least for the interaction.

Next, to determine whether that integration was Bayes optimal, we compared actual JNDs to predicted JNDs based on the MLE rule (**Figure 6.8 lower right panel**). One-sample t-tests against 0 showed that no condition was significantly different from 0 (when both reliable:  $t(8) = -.42, p = .68, d = -.14$ ); when touch was reliable, but vision noisy:  $t(8) = -1.0, p = .34, d = -.34$ ; when touch was noisy, but vision was reliable:  $t(8) = 1.19, p = .27, d = .40$ ; when both were noisy:  $t(8) = -1.6, p = .14, d = -.55$ ). This suggests that in all conditions, integration did not deviate from optimality, even when both cues were corrupted by noise. ANOVA analysis did not show a significant effect of tactile reliability ( $F(1,8) = 1.9, p = .20, np^2 = .19; BF^{01} = 1.4 \pm .9\%, BF_{incl} = .6$ ) nor of visual reliability ( $F(1,8) = 1.0, p = .34, np^2 = .11; BF^{01} = 2.0 \pm 5.7\%, BF_{incl} = .4$ ), and no interaction ( $F(1,8) = .66, p = .44, np^2 = .07; BF^{01} = 1.8 \pm 3.0\%, BF_{incl} = .3$ ). Again, these results suggest no difference in integration optimality between conditions. However, the Bayes factors indicate a lack of statistical power to derive definite inferences.

## Multisensory conditions and predictions for integration

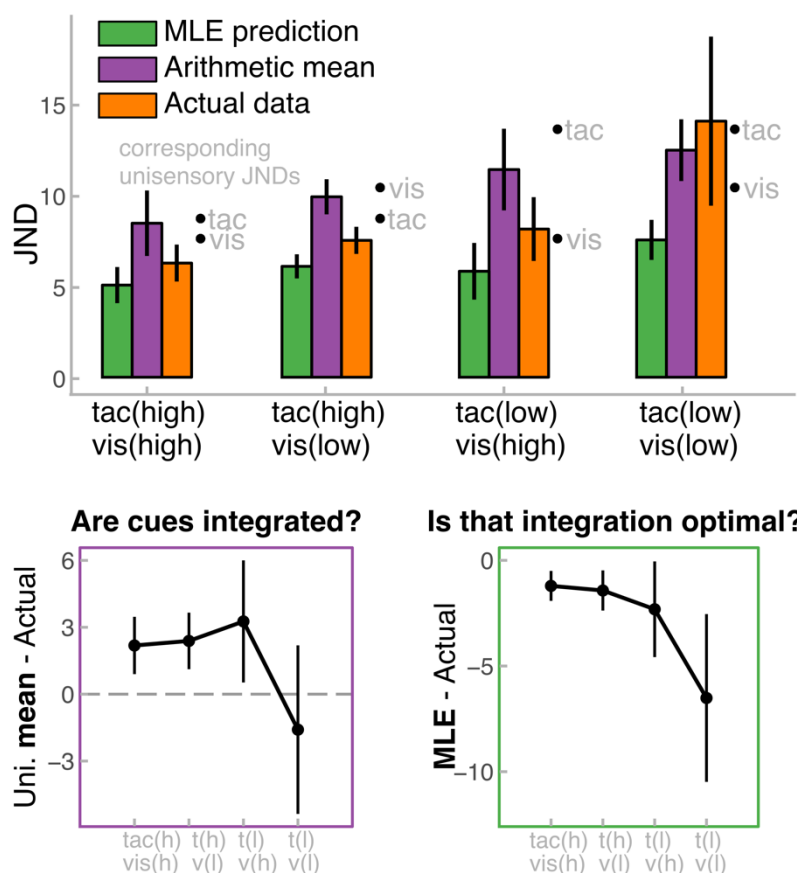


**Figure 6.8. Experiment 7: Multisensory behavioural results and predictions for integration.** Upper panel shows JNDs of each multisensory condition (orange) against the JNDs that would have been predicted, if participants integrated the two cues (arithmetic mean of unisensory JNDs; purple) and if they performed the optimal integration of the unisensory cues according to the MLE rule (green). Corresponding unisensory JNDs (black overlay dots) are also shown. In lower panels, the left panel shows the difference between arithmetic mean of unisensory JNDs and actual empirical multisensory JNDs. If some integration took place, the difference needs to be at least 0 or greater than 0. The right panel shows the difference between MLE prediction and empirical data. If integration was near-optimal, the difference should not be different from 0.

### 6.3.3. Is there integration at the level of implicit postural response?

First to ensure that body sway was present in multisensory conditions, we ran the same preliminary one-sample t-tests as for unisensory conditions. For forward-backward sway, most multisensory conditions produced a significant forward sway (except for right stimulus when both modalities were noisy; **Table 6.2**). For rightward-leftward sway, all conditions showed significant divergence between sway during rightward and leftward stimulus directions, except when both modalities were corrupted by noise ( $p = .01$  – did not survive Bonferroni-correction; other  $p$  values:  $< .001$ ,  $.002$ , and  $.003$ ).

Next, to examine whether forward sway increased in multisensory conditions, we compared COP displacement in combined condition to the mean of corresponding unisensory

conditions (**Figure 6.7B**). For ease, we first averaged the three stimulus direction groups, because the pattern of direction differences was similar for unisensory and multisensory conditions. We took the difference in four multisensory conditions and compared it to 0. However, no multisensory condition showed a greater forward-backward sway (when both reliable:  $t(8) = -.42$ ,  $p = .68$ ,  $d = -.14$ ; when touch was reliable, but vision noisy:  $t(8) = -.43$ ,  $p = .68$ ,  $d = -.14$ ; when touch was noisy, but vision was reliable:  $t(8) = 2.2$ ,  $p = .06$ ,  $d = .74$ ; when both were noisy:  $t(8) = -.31$ ,  $p = .77$ ,  $d = -.10$ ). This suggests that general entrainment was similar across multisensory and unisensory conditions. Indeed, looking back at **Figure 6.7B**, forward sway was always greater when only touch was presented. Interestingly, in multisensory conditions the backward sway seen in visual-only conditions disappeared, suggesting some contribution from tactile input. We also compared the extent of forward sway between multisensory conditions with one-way rmANOVA coding for four conditions, but it did not show a significant effect ( $F(3,24) = 2.1$ ,  $p = .13$ ,  $np^2 = .21$ ;  $BF^{01} = .7 \pm 3.5\%$ ,  $BF_{incl} = 1.4$ ).

For direction-specific sway, we compared the rightward-leftward direction divergence in multisensory conditions to the average one in corresponding unisensory conditions (**Figure 6.7D**). Although, when both cues were reliable the direction-specific sway seemed greater than sway during unisensory conditions, the effect did not survive Bonferroni correction ( $t(8) = -2.8$ ,  $p = .02$ ,  $d = -.95$ ). Difference in other conditions was far from statistical significance (when touch was reliable, but vision noisy:  $t(8) = -.17$ ,  $p = .87$ ,  $d = -.06$ ; when touch was noisy, but vision was reliable:  $t(8) = -2.17$ ,  $p = .87$ ,  $d = -.06$ ; when both were noisy:  $t(8) = 92$ ,  $p = .38$ ,  $d = .31$ ). This suggests that at least for the current sample, postural response did not significantly increase during multisensory presentation. In terms of differences across multisensory conditions, one-way rmANOVA did not yield a significant effect of condition ( $F(3,24) = 2.3$ ,  $p = .10$ ,  $np^2 = .22$ ;  $BF^{01} = 1.1 \pm .6\%$ ,  $BF_{incl} = .9$ ).

#### 6.3.4. Does extent of body sway contribute to explicit perception?

Finally, **Figure 6.9** illustrates the mean COP displacement as a function of trial outcome (whether participant was correct or not). For forward-backward sway (**Figure 6.9A**), we did not find an effect of response ( $F(1,8) = 0.1$ ,  $p = .83$ ,  $np^2 = .01$ ,  $BF^{01} = 5.7 \pm 1.1\%$ ,  $BF_{incl} = .05$ ) or any interactions with response (all  $p$  values:  $.2 < p < .96$ ) in unisensory conditions. Interestingly, in combined conditions, the main effect of response was significant ( $F(1,8) = 6.7$ ,  $p = .03$ ,  $np^2 = .46$ ,  $BF^{01} = .7 \pm 2.3\%$ ,  $BF_{incl} = 3.1$ ), suggesting that, in general, forward sway was greater prior to a correct response (mean COP =  $-2.3$ ,  $SD = 1.9$ ) than prior to an incorrect response (mean COP =  $-1.6$ ,  $SD = 2.5$ ). However, this effect was not substantial. There was also a significant interaction between response and multisensory condition ( $F(3,24) = 4.1$ ,  $p = .02$ ,  $np^2 = .34$  –  $p$  value Greenhouse-corrected). Bonferroni-corrected follow-up pairwise tests showed a significant

effect of response only when reliable tactile input was combined with noisy visual input ( $p < .001$ ; other  $p$  values:  $.5 < p < .84$ ). For direction-specific rightward-leftward sway (**Figure 6.9B**), we focused on the interaction between stimulus direction and response, because a stronger direction-specific rightward-leftward sway could be preceding a correct response. However, this interaction was not statistically significant in unisensory conditions ( $F(1,8) = 3.3$ ,  $p = .11$ ,  $np^2 = .29$ ); no higher-order interaction reached significance level (all  $p$  value:  $.17 < p < .96$ ). Similarly, the interaction in combined conditions was non-significant ( $F(1,8) = .80$ ,  $p = .40$ ,  $np^2 = .09$ ), and that interaction did not vary across combined conditions ( $F(3,24) = 1.2$ ,  $p = .33$ ,  $np^2 = .13$ ).

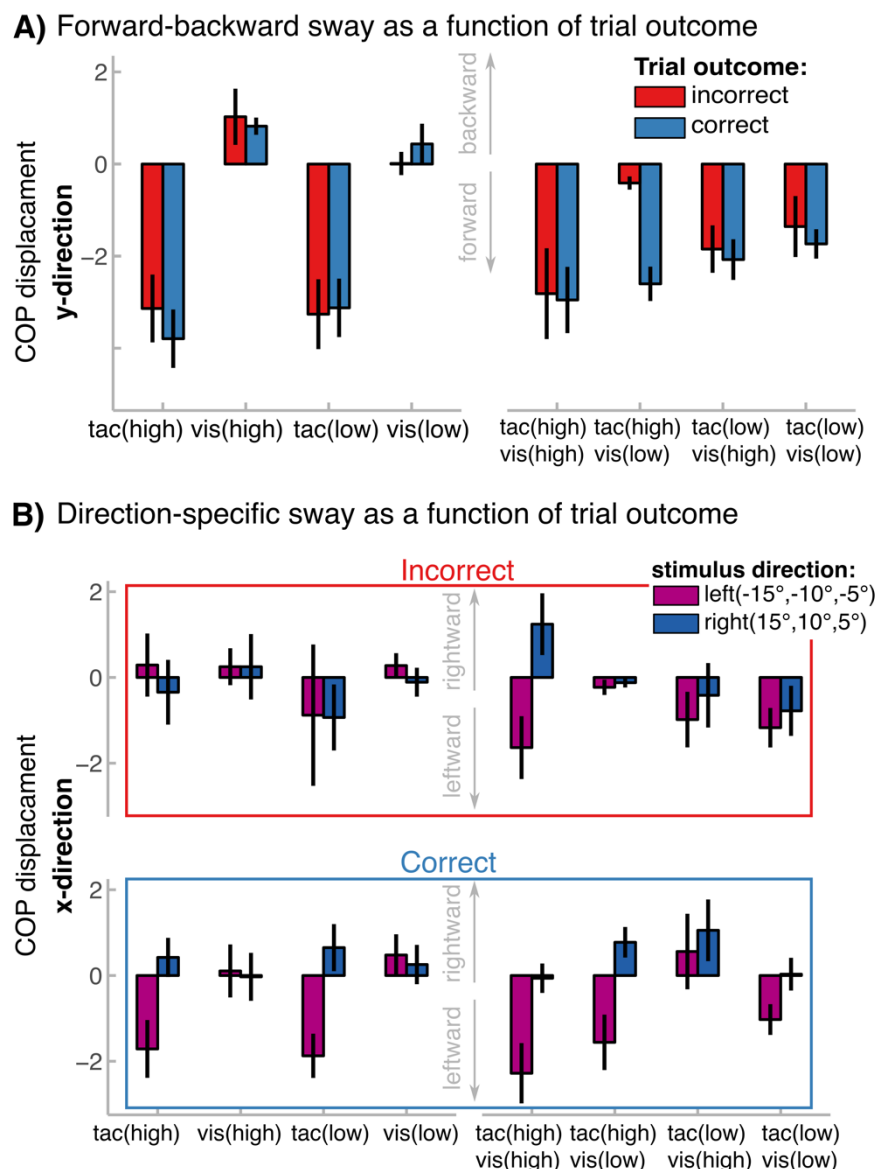


**Figure 6.9. Experiment 7: mean COP displacement as a function of trial outcome.** **A)** shows the mean forward (negative) vs. backward (positive) COP displacement preceding either correct (blue) or incorrect (red) response. Each bar contains mean COP displacement averaged across stimulus directions. **B)** shows the mean leftward (negative) vs. rightward (positive) COP displacement.

## 6.4. Discussion

In this experiment, we examined the integration between tactually and visually perceived directional information, and how it modulates the sensation of ‘heading’ by measuring body sway. Different levels of noise (low noise and high noise) were added to each sensory input in order to modulate the input’s perceptual reliability. The noise manipulation significantly degraded direction perception, both when directions were presented as visual optic expansion, or as tactile force directions from a handheld device. Pairing inputs from vision and touch with different levels of noise in each modality, allowed examining whether participants could integrate the two sources of directional information, and how closely to optimal integration they did so. We drew on the standard theory of multisensory integration, that more reliable, less noisy inputs make a greater contribution to integration than less reliable, more noisy inputs. Four different multisensory conditions were presented. Two had reliable tactile input (low noise) paired with either reliable visual input or noisy visual input. The other two, had noisy tactile input presented with reliable visual input or noisy visual input. Optimal integration predicts that in all combined cases, perception increases over conditions where only one of corresponding inputs is presented in isolation (Ernst & Banks, 2002; Rohde et al., 2016). This prediction suggests that observers are able to benefit from multiple sources of information, either by accounting for the noisy input with the reliable source, or by integrating two noisy inputs to reduce the noise in the combined percept (Ernst & Bühlhoff, 2004).

### 6.4.1. *Reliable touch improves explicit perception of ‘heading’*

We compared the actual performance with combined cues to the performance that was predicted by the MLE rule based on unisensory data. The statistical analysis did not detect any significant differences, suggesting near-optimal performance in all conditions. Neither did it detect any difference in the actual performance between the multisensory conditions. Caution is required in interpreting these null results because of a small sample size, which after excluding compromised data (psychometric plots that showed either negative or nonlinear slopes; see **Appendix A**), reduced from 15 participants to nine. Inspection of the actual group-level data in **Figure 6.8** points to some possible idiosyncratic performance patterns.

Unsurprisingly, performance seemed to be best when both inputs were reliable (with low noise). Combined estimates seemed to be more precise than unisensory estimates alone, indicating that the two directional cues were fully integrated to improve performance (indeed that was shown by statistical analysis in **section 6.3.2**). However, there was a large inter-individual variability in how multisensory conditions compared to the performance under unisensory conditions. **Figure 6.10** shows individual JNDs for all multisensory conditions and the

corresponding unisensory conditions. Interestingly, input from touch sometimes enhanced combined performance and sometimes worsened it. The individual plots are coded green when adding tactile input in the multisensory condition improved performance above performance with vision alone (*enhancement by touch*), and coded red, when combined performance was below performance with vision alone (*interference by touch*). Note that these effects are only valid when vision was the more precise source of information, because then touch influenced performance over and above vision.

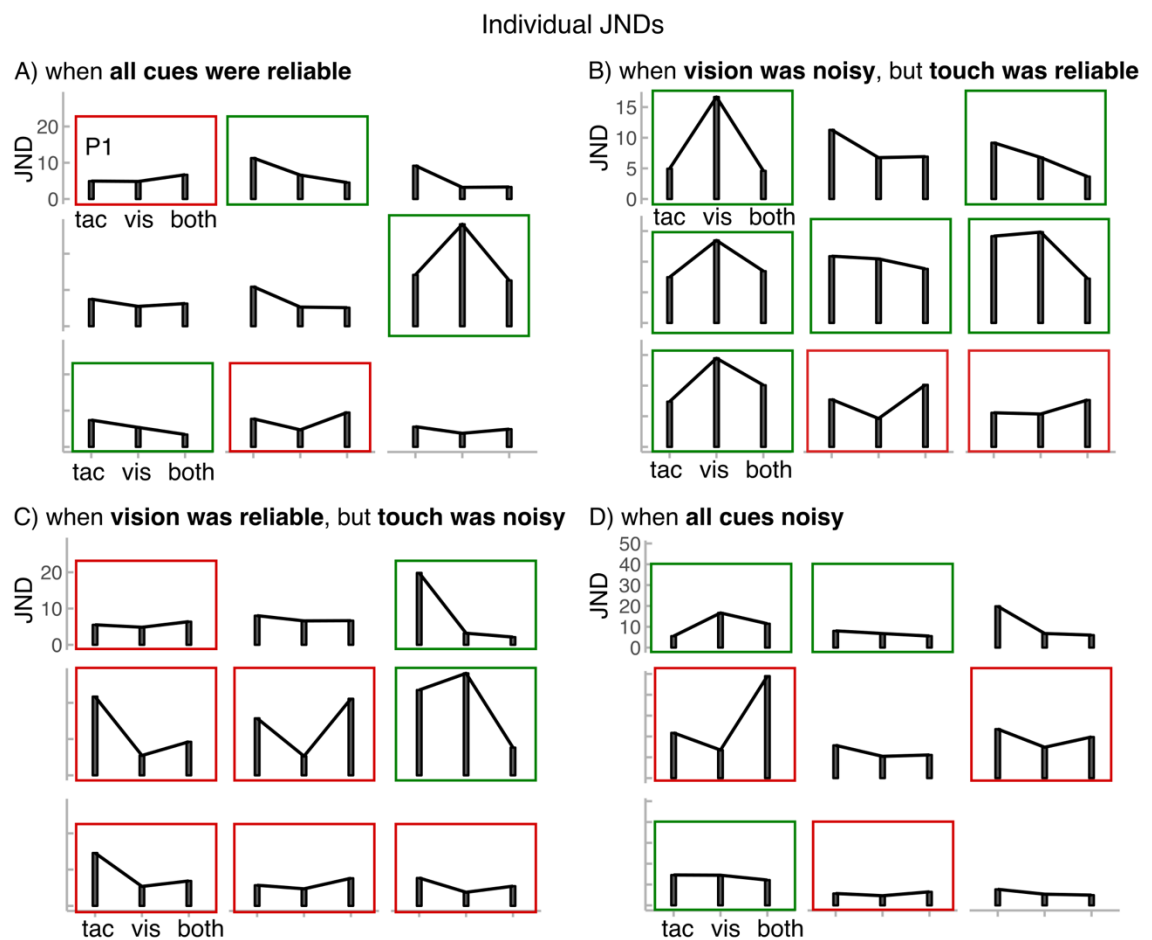


**Figure 6.10. Experiment 7: individual JNDs.** **A)** when all cues were reliable (i.e., had low noise). **B)** when vision was noisy, but touch was reliable. **C)** when vision was reliable, but touch was noisy. **D)** when all cues were noisy. Each subplot shows individual participant JND in tactile-only, visual-only, and combined condition. Green boxes indicate participants for whom combined condition led to performance increase that was above visual-only condition (*enhancement by touch*). Red boxes indicate participants for whom combined condition resulted in performance decrease that was below visual-only condition (*interference by touch*).

When both cues were reliable (**Figure 6.10A**), three participants showed a fully integrated percept, whereby combined JNDs were lower than both of the unisensory JNDs (green outline). This is considered a hallmark of integration (Ernst & Banks, 2002; Rohde et al., 2016), since the combined performance is better than the best unisensory performance. Except



in one of those participants, touch enhanced combined performance above that in the vision-only condition. In other participants, combined performance tended to be at the level of the more precise modality. Thus, in those participants, co-occurrence of two signals was not disadvantageous, but it was unclear whether the two signals were truly integrated or rather participants could rely on the more precise signal.

Reliable tactile information also improved combined performance when visual stimulus was corrupted by noise. **Figure 6.10B** shows that in majority of participants JNDs in the multisensory condition were lower than JNDs in visual-only condition, suggesting that reliable touch was successfully used to counteract the noise in the visual stimulus. In two of these participants (red boxes), combined performance was worse than the performance with the better unisensory condition (in this case with touch), suggesting that noisy visual stimulus had an interfering effect. Results of this condition, thus, indicates that when vision was compromised touch tended to enhance combined performance, in agreement to the common view that touch can enhance visually perceived stimuli especially when it is already less reliable (Lunghi, Binda, & Morrone, 2010; Lunji, Lo Verde, & Alias, 2017; Pérez-Bellido et al., 2018).

An important consideration for the facilitatory effect of tactile input is that the translational force stimulus that should have provided directional information through skin stretch, could have also engaged proprioceptive feedback from slight hand movements towards the direction of the force. Proprioceptive input could have improved the perception of force direction. We did not record the start and end position of the force device during the stimulus intervals. Thus, we cannot account for the possible proprioceptive contribution. Some reassurance comes from an earlier study by Tan and colleagues (2016) who employed a similar force device to measure perception of force direction. They did not find that the displacement of the hand during force stimulation was significantly related to the mean thresholds for force direction discrimination. Moreover, forward body sway, which indexed body movement was similar across reliable and noisy tactile-only conditions, yet only reliable touch led to improved multisensory performance.

#### **6.4.2. Noisy tactile input interferes with perception of 'heading'**

Interestingly, as shown in individual data presented in **Figure 6.10C**, when noisy touch was paired with reliable vision, thresholds for combined direction estimates consistently dropped below the thresholds acquired from reliable vision alone. This suggests that when touch was corrupted by noise, participants could not balance out that noise with reliable information for visual input. In other words, noisy touch had an *interfering* effect on vision. It is notable that noisy vision did not possess such an interfering influence, as in the condition where participants

combined reliable touch with noisy vision, only two participants showed combined thresholds that were above thresholds for tactile-only stimuli. This means that there was something about tactile noise that made integration difficult, and also made additional tactile input disadvantageous.

In the literature, it has been shown that in situations where task irrelevant tactile distractors need to be ignored to attend to visual targets, selective attention often fails, and participants cannot disengage from distracting tactile information, leading to an erroneous task performance (Spence & Walton, 2005; Ossandón, König, & Heed, 2015). However, such errors, when modalities are reversed (participants need to ignore vision and focus on touch), have been found to be even larger (Spence, Pavani, & Driver, 2004). Accordingly, if participants could not appropriately discern directional input from the added noise and considered noisy inputs as distracting, noisy vision should have had a larger interfering effect on the combined percept. Yet, some studies have observed larger distractor effects from touch on vision than vice versa. Specifically, Guest and Spence (2003) showed that in roughness perception, tactually felt roughness biased visually perceived texture, but visually perceived roughness did not have the same interfering effect on tactile perception. This suggests that depending on the nature of the stimulus quality that is being estimated, distracting input from touch or vision can have different detrimental effects.

One should consider that in the present experiment, noise seemed to be already more detrimental for tactile compared to visual discrimination, although the effect was not significant. Given the small sample size, Bayes factor did not reach sufficient evidence for the absence of that effect, pointing to possible lack of statistical power. As a consequence, whether touch can have a special interfering effect when judging spatial direction remains inconclusive. This effect would be highly surprising given the visual dominance in spatial processing. Yet, it could be related to the fact that dynamic stimulus, such as continuous translational force can have a greater entraining than dynamic visual stimuli. This entrainment component can be examined by analysing body sway data.

#### ***6.4.3. Implicit postural response mainly arises due to tactile input***

Reliable forward sway was always present for tactile force stimulation. However, interpretation of our sway data is complicated by the fact that instead of a gradual forward sway seen in tactile-only condition, the visual stimulus resulted in a brief backward deflection, which was consistent across participants. This backward deflection could reflect either a rapid postural control mechanism, whereby participants wanted to avoid forward movement, or a startle in response to the sudden move of the visual dots. One reason we employed contracting flow

instead of traditional expanding flow, was because expanding flow resulted in a sudden backward movement due to a startle response. We then employed contracting flow, as then, the dots moved from behind the participant and not towards them. As such, contracting flow created a sensation of moving “into a tunnel”. The persistence of the backward sway for contracting flow was unexpected, but presumably indicates a non-specific withdrawal response, rather than a spatially-guided entrainment of postural movement.

One speculation is that participants trusted pulling force more than the “pulling” visual sensation. Imagine being on skates blindfolded and somebody pulls you by the hand, following that hand does not seem particularly scary. Now imagine that instead of a pulling hand, you perceive a visual input that pulls you forward despite you being unable to actually see what is in front of you. Following that almost “hallucinatory” sensation seems much scarier than following somebody’s concrete guidance (i.e., pulling by a hand). Thus, to resist such uncertain pulling you might jerk backwards. The data (**Figure 6.4**) showed that backward deflection seemed larger when visual directional input was not corrupted by noise, although the effect of reliability did not reach statistical significance. This suggests that backward deflection was related to the availability of directional input. That is, when participants clearly perceived a heading direction, they were more likely to “resist it” with a backward motion. This may also explain why, when visual input was combined with tactile pulling, no backward deflection occurred, as a “trustworthy pulling guide” was present. In order to elucidate whether this backward deflection was due to the peculiarity of the VR environment, a replication with non-VR optical flow stimulus would be useful.

Despite the consistent backward deflection during visual stimulation, combined conditions always resulted in a significant forward sway, but to a no greater extent than with the tactile-only condition. Interestingly, in the combined condition, where tactile information was more likely to have an enhancing effect on overall performance (condition where reliable touch was paired with noisy vision), extent of the forward sway predicted trial outcome. There was significantly less sway prior to an incorrect response. This suggests that enhancing effect of touch may have arisen from stronger general entrainment to the stimulation. Note that forward-backward sway did not contain actual directional information, but merely showed a general heading response. Interestingly, in the condition, where touch seemed to have the strongest interfering effect, no such response distinction occurred. This suggests that the interfering effect was unlikely due to a stronger entrainment.

In contrast to forward-backward sway, direction-specific sway can reveal whether there was an implicit postural response that distinguished between stimuli. Indeed, all conditions showed a divergent sway pattern for right vs. left stimuli. However, this divergence may have

occurred due to stronger sway during leftward stimuli, and thus the presence of reliable direction-specific sway is less clear. One consideration is that direction-specific body sway response has been found to be larger when gaze is shifted towards the direction of “heading” (Piras et al., 2018), implying that eye movements are more important for inducing the body sway than directional stimuli alone. Because we asked participants to fixate at the centre of the screen (red fixation dot) in order to control for eye movements, our data may have underestimated the true potential of the directional stimuli to induce the postural sway. Importantly, combined stimulation did not reliably induce a greater direction-specific sway relative to unisensory conditions. Only when both cues were reliable was the effect close to significance.

## **6.5. Conclusion**

In conclusion, we show that participants can encode the direction of translational force applied to the skin via skin stretch, adding to previous studies that have employed a similar stimulation protocol (Barbagli et al., 2006; Tan et al., 2006). However, future studies should carefully control the proprioceptive input by measuring the start and end position of the impacted body part (Tan et al., 2006), as it remains unclear whether our tactile stimulus was purely tactile or involved a proprioceptive component. Importantly, our design allowed us to distinguish the specific contributions of touch and vision as we artificially modulated the relative reliability of each input under the multisensory conditions. Consistent with previous findings, we observed facilitatory effects of tactile information on explicit heading perception, when it was reliable, and when it was paired with noisy visual input. This finding adds to the growing interest of using tactually acquired information to augment visual spatial experience and further validates the value of touch in compensating unreliable visual input. This could point to a potential use of tactile interfaces for safer driving in environments where vision can be compromised due to weather conditions (Gallace and Spence, 2014, chapter 10).

However, noise in the tactile signal was more detrimental than noise in the visual stimulus as it could corrupt combined percept even when reliable visual input was available. Thus, when designing tactile interfaces, the reliability of the tactile signal needs to be carefully controlled, as noisy input can have adverse effects on perception even when concurrent reliable visual input is available. This is particularly important because visual dominance theories often suggest that irrelevant tactile distractors have a smaller effect on visual processing than visual distractors have on tactile processing (Eimer and Driver, 2000). This has led to an assumption that haptic cues always help visual processing and rarely interfere with it (Hale and Stanney, 2004). Our results show that potentially distracting touch can have adverse effects of performance even when reliable information is available in the visual modality.

Our experiment sought to induce a sensation of self-motion or heading. This is exactly what immersive action stimulators seek to achieve. We used body sway as an implicit measure of heading sensation and found that availability of information from both modalities resulted in stronger bodily response, especially when both inputs were reliable. However, the bodily response was mainly mediated by touch and not vision. This may be related to a postural control mechanism during VR stimulation without accompanying touch, due to uncanniness of the VR stimulation. Thus, future studies should further investigate the experience of illusory self-motion acquired via VR interface. If it is true that dynamic visual input in VR may give rise to unexpected postural responses, then our results suggest that adding continuous haptic feedback may counteract those responses.

## Chapter 7: Final discussion

There has been a growing interest in examining the ability to selectively attend to a single tactile element among distracting stimulations, revealing various interactions between competing inputs (e.g., Rhaman & Yau, 2019). The present thesis shifted the focus from selective attention to processing multiple stimulus elements to explicitly integrate them into an overall tactile percept (multi-touch integration). Specifically, we examined participants' ability to average two moving tactile stimuli of varying discrepancy. We began by showing that the attempt to integrate rather than discriminate between two inputs delivered to adjacent fingers modulated the early levels of somatosensory processing, potentially allowing for the convergence of to-be-integrated inputs (**Chapter 2: Brain mechanism of multi-touch aggregation**). Next, we examined various sensory and cognitive factors that could affect this integration mechanism. We showed that the aggregation ability was mainly constrained by a hemispheric factor that led to different patterns of performance between unimanual and bimanual aggregation (**Chapter 3: Multi-touch aggregation within- and between-hands**). It was unconstrained by the general level of discrepancy between the component inputs and by the somatotopic relationship between the stimulated fingers (**Chapter 4: Multi-touch aggregation beyond somatotopy**). It even incorporated the proprioceptive input related to each hand (**Chapter 5: Effect of posture on bimanual multi-touch perception**), implying a relatively high-level serial process. The final experiment of this thesis (**Chapter 6: Integrating directional information between touch and vision**) emphasised the importance of the reliability of tactile input over and above the reliability of visually acquired information in visual-tactile integration.

## 7.1. Task context shapes somatosensory processing to allow for convergence of inputs for multi-touch perception

Based on previous research on tactile motion processing, motion direction seems to be largely encoded in area 1 of S1. This has been found in neurophysiological recordings from monkeys (Pei et al., 2011) and also TMS study on human participants, whereby disruption to S1 affected performance on a motion discrimination task (Amemiya et al., 2017). The main purpose of this thesis was to examine whether multiple spatiotemporal inputs can be processed and integrated. Integration between two directional inputs delivered to spatially segregated regions of the skin surface would need to be ‘brought together’ to be combined. By ‘brought together’, we mean that cortical activation specific to each component direction needs to converge at some processing level to represent their combined feature.

It is known that each area of S1 is organised in columns that receive projections from restricted area of the skin. This means that adjacent fingers tend to project to adjacent cortical columns of S1 (Merzenich et al., 1978; Blankenburg et al., 2003). Activity within those columns seems to be correlated, with strength of correlations following the somatotopic distance between body parts (Reed et al., 2008). At the same time, simultaneous stimulation of two fingers leads to suppressive interaction that also follows the somatotopic organisation of the fingers as measured with EEG (Severens et al., 2011). Thus, it seems that inhibitory and excitatory interactions exist between the adjacent cortical columns. Integrated perception, as a result of multi-finger stimulation, must then arise from the balance between the inhibitory and excitatory interactions (**Figure 7.1**).

The majority of previous research has focussed on how this competition may be resolved by selective attention. Indeed, normalization models, which have been successfully applied to tactile perception (Brouwer et al., 2015), show how attentional mechanisms can resolve conflicts between competing inputs (Reynolds & Heeger, 2009; Rahman & Yau, 2019). Normalization models do not typically involve the explicit mechanism of inhibition, but they result in similar net effects as the response of a single unit is divided by the response of a population. However, under conditions of divided attention, whereby two inputs need to be explicitly considered, attentional effects may not be the factor that could resolve the inhibitory-excitatory competition. In **Chapter 2**, participants were presented with identical component motion trajectories across two adjacent fingers. They were asked to perform two different tasks that required divided attention. That is, in both tasks, participants had to select both components, but perform different computations on them. In the discrimination task, they had to contrast the directions to estimate their angular difference, whereas in the integration task,

they had to combine them to estimate their angular average. Our results indicate that the task context modulated the interaction between digit representations within early somatosensory cortex (as indicated by P40 EEG component over somatosensory electrodes). In other words, task context could have served as a top-down signal that adjusted the inhibitory links within neural circuitry of somatosensory system, increasing inhibition for discrimination while decreasing it for integration (**Figure 7.1**).

The importance of that study lays in its potential to shift the focus in tactile research from the selectivity and acuity to considering the integrative capacity of the tactile system, and to divided attention rather than selective attention. While previous studies on selectivity have revealed largely suppressive interactions between simultaneously presented tactile inputs (i.e., masking effects; Sherrick, 1964; von Békésy, 1967; Gilson, 1968), implying that two inputs may not be represented simultaneously, we show that appropriate task context (i.e., extracting overall tactile feature) allows for convergence of inputs. Future studies will need to validate our current findings. First, an improved design should better balance task performance to ensure that increased suppression in the discrimination task is not due to a greater effort due to task difficulty. Second, including additional non-adjacent finger conditions would help to ensure that the mechanism we have described is in fact inter-cortical inhibition. Particularly, when non-adjacent fingers are stimulated, overall suppression should be lower in both tasks, as inter-cortical inhibition weakens with somatotopic distance. Third, additional tasks requiring selective attention (e.g., one component needs to be ignored) would demonstrate whether the balance between integration and suppression is indeed a process that shifts according to the task requirements.

Nevertheless, what is important is that we have shown that somatosensory processing allows for controllable convergence of inputs across discontinuous body regions that is required for any multi-touch integration to occur. However, while convergence is a sensory requirement for multi-touch integration, there is also a cognitive requirement – the attentional capacity to process two tactile spatiotemporal inputs delivered in parallel. In order to examine both sensory and cognitive factors, four separate experiments were conducted in **Chapters 3 and 4**.



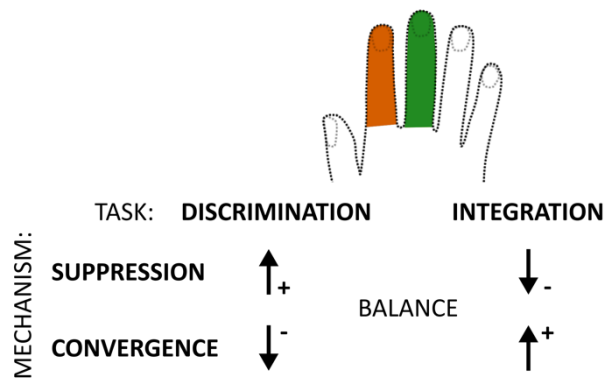


**Figure 7.1. Processing differences between discrimination and integration.** In Chapter 2, participants had to attend to the component direction on both fingers, but in the discrimination task they had to report the directional difference between them, whereas in the integration task the directional average between them. If the tactile directions on the fingers are encoded by separate populations of directionally-tuned neurons in digit-specific cortical columns, then there are two competing ‘forces’ that contribute to multi-touch perception: integrative convergence and suppressive interaction. Intuitively, discrimination would benefit from stronger suppression, whereby the difference between inputs becomes more salient. In contrast, integration would benefit from stronger convergence that would convey what is common between the inputs.

## 7.2. Multi-touch integration is shaped by cognitive rather than somatotopy-based factors

Chapters 3 and 4 contrasted the ability to integrate two tactile spatiotemporal inputs at different somatotopic distances and by engaging the inter-hemispheric exchange of information. **Figure 7.2** illustrates the multi-touch conditions that were tested. As mentioned above, the two sensory factors that may influence multi-touch perception is the convergence of inputs (integration of information) and suppression of inputs (inhibitory links between digit representations). **Chapter 2** showed that during integration the inhibitory links are released allowing for greater convergence of the inputs. However, convergence should be greater for representations that have stronger lateral connections, which in S1 seem to follow somatotopic organisation of cortical columns. Thus, one could expect integrative ability to be affected by somatotopic distance between to-be-averaged fingers.

However, our results showed no evidence for somatotopically-defined modulations either for the unimanual integration (adjacency between fingers) and bimanual integration (homology between fingers). Instead, the main difference in performance seemed to lie in averaging across either unimanual or bimanual fingers, regardless of specific fingers stimulated. This difference may be related to the attentional capacity to process two inputs in parallel (attentional resources), which based on our results, seems to improve for bimanual integration. Therefore, our findings suggest that multi-touch integration, at least in spatiotemporal domain, requires higher levels of convergence. Accordingly, task context modulates early somatosensory

processing to allow for convergence of peripheral inputs across spatially segregated skin regions, but the integrated percept itself begins to arise when those inputs are processed by processing levels that are no longer constrained by the specific skin regions stimulated. An intuitive candidate area for such processing is S2, where neurons are shown to encode properties of an object impinging on multiple fingers regardless of the exact fingers that have been touched (Fitzgerald et al., 2006a,b). S2 is known to compromise dense bilateral connections that would allow input transfer between two hands (Iwamura, Iriki, & Tanaka, 1994).

It is important to note that postulating that the main driver for the present multi-digit integration task is the degree of attentional resources does not automatically imply a higher post-somatotopic level of processing. This is because some studies have observed fine-grained somatotopic gradients of attention at the level of S1 (Kida, Takanka, & Kakigi, 2018; see Johansen-Berg & Lloyd, 2000 for a review). However, this attentional effect is not the same as the 'attentional resource' mechanism that we postulate here, whereby inter-hemispheric processing may provide separate pools of processing resources. Rather, it may indicate the strength of 'spatial attention', which may be reduced for greater somatotopic (or spatial) distances (e.g., Rahman & Yau, 2019). Given that our results did not show somatotopic distance effects on either unimanual or bimanual integration, early somatotopically-defined attentional effects are unlikely to be significant contributors to our results. Attentional effects at the higher levels of somatosensory processing (e.g., S2) have been found to be more coarse-grained with less defined finger representation boundaries (Kida et al., 2018) fitting the absence of somatotopic effects in the present results.

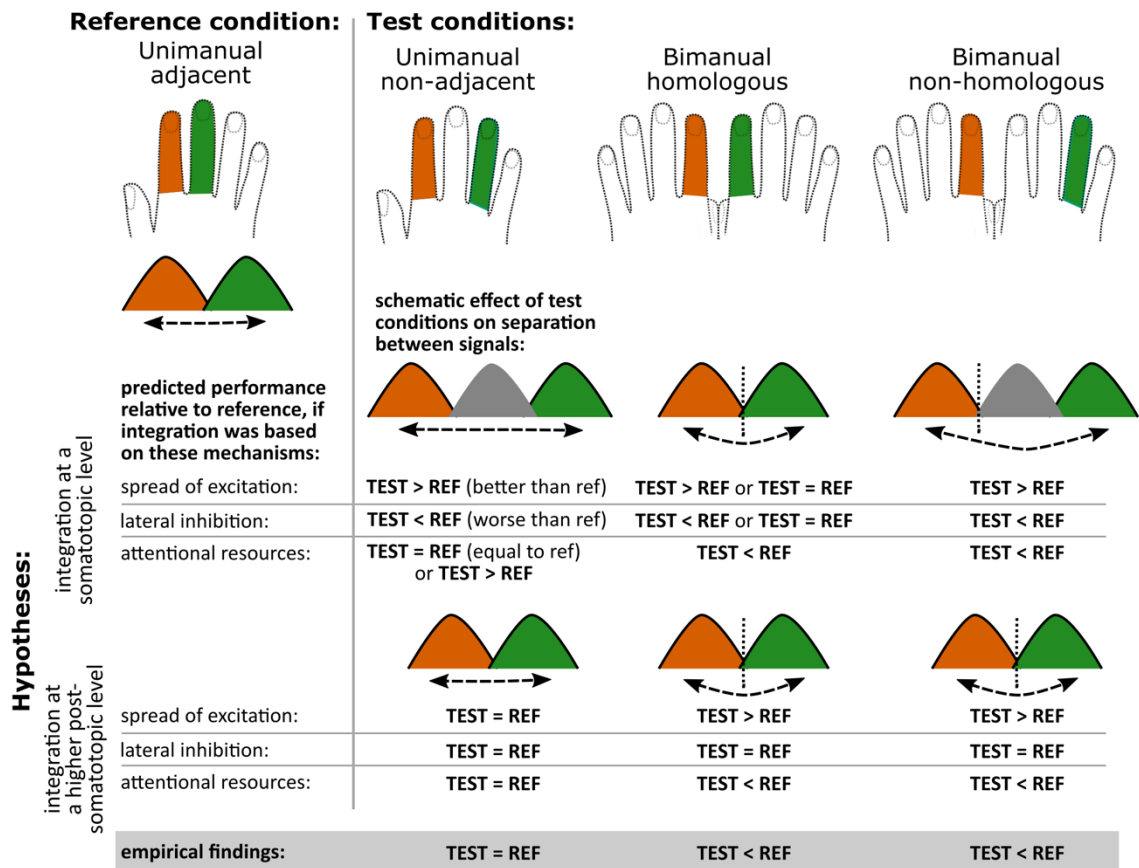


**Figure 7.2. Sensory and cognitive factors that were predicted to affect multi-touch processing.** The figure illustrates the representative multi-touch conditions tested in **Chapters 3 and 4**. The predicted results are shown relative to the unimanual adjacent condition. We can distinguish between two hypothesised levels of integration: at the somatotopic level or at the higher post-somatopic level. We can also distinguish between three mechanisms that may affect integration: spread of excitation (improves integration), degree of lateral inhibition (degrades integration), and degree of attentional resources (improves integration). If integration is driven by a somatotopic mechanism, somatotopic distance should decrease both spread of excitation and strength of lateral inhibition, leading to differences between the unimanual adjacent reference condition, and the unimanual non-adjacent test condition, in particular. However, because **Chapter 2** showed that inhibition might be reduced during multi-touch integration, spread of excitation might be a more relevant factor, in which case, performance might decrease for increased somatotopic distances, where information needs to converge through larger somatotopic distances (the length of the black dashed arrow). Note that the prediction for bimanual homologous condition is contingent upon whether the integration can occur based on early bilateral RFs or by engaging inter-hemispheric transfer, which could incur additional processing costs. ‘Attentional resources’ refers to the cognitive cost of processing two inputs in parallel. While it remains uncertain whether attentional resources can vary across somatotopic distances (see text for discussion), it is more established that it may either incur additional costs or reduce costs when stimuli are delivered bimanually – depending on whether attentional constraints are hemispheric or not. We hypothesised that a bimanual condition relieves attentional pressures if the resource limitation is hemispheric. If integration is not dependent on somatotopic mechanisms, the only difference is between unimanual vs. bimanual processing. The overall pattern of results in the thesis supports the hypothesis that integration seems to occur at higher levels of processing, which are no longer constrained by somatotopic organisation of stimulated fingers. In addition, we show that bimanual processing seems to incur benefits rather than costs.

Two previous studies that have explicitly examined the aggregation between simultaneously presented tactile inputs both involved intensity judgements (Walsh et al., 2016; followed-up by Cataldo et al., 2019) and the frequency domain (Kuroki et al., 2017). Both studies found evidence for salience-based interpolation, whereby the aggregated percept resulted from

weighted average of component inputs, but with more weight assigned to the more intense input. Kuroki et al. did not examine somatotopic modulations but did find that aggregation occurred for bimanually presented inputs and was not constrained by the fact that component frequencies activated distinct sensory channels. Thus, Kuroki et al. argued that convergence of frequencies occurred at higher levels of processing beyond S1. Walsh et al. found that saliency-based bias in aggregation occurred regardless of adjacency between fingers within unimanual aggregation, but was abolished during bimanual aggregation, whereby participants were able to account for discrepant intensities leading to more accurate aggregate representations. They reached the conclusion that aggregation occurs at more central levels within each hemisphere.

Our results contribute to these findings in two important ways. First, saliency is not the only strategy that is used by participants to resolve integration under limited attentional resources. Specifically, while intensive quality of touch is important, our paradigm kept the intensity constant and only modulated the extensive spatial aspect of tactile inputs. While we found clear weighting biases in the unimanual conditions, which were absent in the bimanual conditions, these biases were modulated by the overall direction of the components. We were able to explain those modulations by applying a direction- and context-based normalization model. Our model assumed that spatial properties experienced by a single hand are more likely to be related to a single object, whereas spatial properties experienced by two hands do not need to necessarily reflect a single object. This would give rise to a strong object-prior in the unimanual tactile spatial processing, which would lead to specific prioritisation of the more relevant component (in our case, the component on “virtually leading finger”).

This model gives rise to intriguing predications, whereby even discrepant inputs presented within a single hand may be processed within the constraint of pre-existing object priors. However, the model was designed post hoc, so future studies would need to directly manipulate the theoretical constructs of the ‘single-object-prior’. For example, bimanual averaging could be performed under two visual conditions: in one, a single object is shown above the stimulated fingers, while in the other, two separate objects. A difficulty with this design is that the visual stimuli cannot move as judgements could then be made based on visual motion, so merely presenting a stationary object may not be enough for participants to bind the component directions with the visual representation.

Second, our results point to the importance of noise associated with the aggregation of component inputs. Particularly, we showed that bimanual averaging results in less noisy (more precise) aggregate representation relative to encoding each component in isolation. This result was consistent across Chapters 3 and 4 but did not reach significance in **Chapter 5**. Thus, although the result could imply stronger interdependence of component inputs represented

within each hemisphere, which is consistent with neurophysiological recordings that show positive correlations within neurons across the whole hemisphere (Cohen & Maunsell, 2009; Reed et al., 2008), further designs explicitly tapping into noise factors affecting stimulus aggregation should be conducted, preferably combined with EEG. In the current thesis, we were interested in broadly characterising the averaging ability of tactile spatiotemporal inputs, which has not been done before. Thus, we used a wide distribution of components at the expense of repetition. This approach could have reduced the sensitivity of the SD analysis. We attempted to balance for this by using unbiased SD analysis, which should be less dependent on number of repetitions. However, future study should take a smaller range of discrepancies (e.g., 0° (identical), 15° (small discrepancy), and 30° (large discrepancy)) and increase repetitions of identical components to at least 20 (in comparison to ~7 in the current design). Correlated activity is believed to give rise to fluctuations in somatosensory rhythms whose inter-hemispheric phase coherence can be analysed with EEG (Andrew & Pfurtscheller, 1999; Kilner et al., 2003). Thus, combining the current unimanual vs. bimanual averaging paradigm with coherence measures of cortical oscillatory activity would elucidate whether changes in precision measures are indeed related to inter-hemispheric dependence.

### **7.3. Multi-touch integration occurs on “remapped” component representations**

The strength of the averaging paradigm presented in this thesis is its ability to dissociate between sensitivity to changes in directional inputs (slopes of fitted regressions) and the reference to which the directional inputs were anchored to (intercepts of fitted regressions). The analysis of intercepts became especially important in **Chapter 5**, where posture of one of the hands in bimanual averaging was rotated, which put probe-based and finger-based reference frames into conflict. Changes in intercept values informed us whether postural information was integrated during perception of directions and their aggregation, independent of changes in sensitivity. Our results showed that postural change exerted an attracting influence on directional judgements, indicating that participants did consider postural information, but in a biased manner. Importantly, the pattern of results during averaging condition suggested that averaging was performed on “remapped” component directions. This contributes to the abovementioned view that multi-touch integration results from convergence at higher levels of processing. In this case, once the proprioceptive information about posture of each stimulated finger has been considered. The region believed to integrate tactually acquired input with proprioceptive input about the state of the body is PPC (posterior parietal cortex; Andersen, 1995; Azañón et al., 2010; Sakata et al., 1973).

Interestingly, both Walsh et al. (2016) and Kuroki et al. (2017) examined the bimanual aggregation ability as a function of separation between the two hands, which is believed to engage proprioceptive input, and did not find an influencing effect. Both argued that this result suggested that aggregation occurs before that incorporation of proprioceptive input. However, hand separation could also indicate the pressures on attentional mechanisms (Rahman & Yau, 2019), and a more direct test of proprioceptive contribution is to induce a conflict between frames of reference as done in Chapter 5. The fact that when one hand was rotated and induced a bias into the component perception, averaging two components – one parallel and another rotated – resulted in a bias that was the mean of the component biases, implies that aggregation could not have occurred at any processing level before the components were ‘remapped’. Aggregation across the rotated and parallel hands incurred additional costs on performance in terms of noise. This means that remapping was a computationally demanding process, at least in a laboratory task like ours.

Relatedly to the current results, in a study by Kitada et al. (2003) either one cylinder was moved across two adjacent fingers (single object) or two separate cylinders were moved on each finger (separate objects), either in the same or opposite directions. fMRI data showed that S1 and S2 were more active when a single cylinder was moved compared to when two cylinders moved across the fingers, but the activity did not distinguish whether the movement was in the same or opposite directions, suggesting that these areas may not be where a percept of a single object arises. Instead, they found that PPC was involved in differentiating whether the stimulations could be bound together into a single object. Strangely, PPC was more activated for separate stimulations relative to a single moving stimulus. The authors speculated that PPC may be engaged when the integration across fingers is required.

#### **7.4. Limitations and future directions of the current multi-touch paradigm**

This thesis began by arguing that while motor and visual systems undoubtedly contribute to perception of spatiality of touch, the somatosensory system itself can produce spatial representation from skin stimulation. In other words, just as vision has a visual field in relation to which spatiality of visual stimuli is conveyed, so does touch have a tactile field, in relation to which spatial relationships are determined (for more detail see Haggard et al., 2007; Serino et al., 2008; Fardo et al., 2018). Yet by asking participants to estimate the average direction between spatiotemporal trajectories on the skin, we may have been requiring participants to engage in a higher level of abstraction, which may not be the case for estimating overall object movement in real haptic experience.

Moreover, because we used a visual response (participants had to respond by rotating a visual pointer), we may have already required participants to represent the skin-based trajectories in external space, abstracted away from the skin-based RF activation. The question of whether spatial perception is unimodal at all is a topic of a large debate (e.g., Spence, 2007). Indeed, spatial representation of touched and viewed objects or scenes is often considered amodal (Wolbers et al., 2011). An interesting study would be to examine whether participants could as easily average a tactile trajectory on one finger with a visual dot moving on the screen above the other finger. If there is no performance cost of tactile-visual averaging relative to tactile-tactile averaging, the aggregation task may probe the amodal spatial representation.

Another question is whether there is a way to tap into somatosensory skin-based representation of space without engaging the higher-level abstraction. We could have employed a paradigm, where participants had to compare the average direction of a pair of component stimulations to the average direction of another pair of component stimulations, either presented sequentially or to different hands. This would have removed the visual response. However, even then the question remains whether the directions would not be automatically represented in some higher-level abstract form, and then compared. The EEG study in Chapter 2 showed that task context modulated relatively early somatosensory evoked response, implying that somatosensory processing was implicated during the task. However, the EEG response was measured to the electrical shocks prior to the motion stimulation to reveal the preparatory tuning of somatosensory circuitry. Due to the dynamic and light nature of the motion stimulation (the probes only lightly touched participants' fingerpads), a reliable EEG response to the spatiotemporal stimuli could not be distinguished. Moreover, the poor spatial resolution of EEG may not be appropriate to elucidate the processing level at which the tactile spatial information was represented.

Thus, future studies should employ fNIRS recording method (functional near-infrared spectroscopy), which provides a similar (but slightly poorer) spatial resolution as fMRI but could be performed in same conditions as EEG. Because our tactile motion stimulus is relatively slow (1s) and can be even reduced in speed, it would be ideal to detect slow deflections in fNIRS signal. Importantly, the present multi-touch integration framework would allow one to determine the neural signal (early somatosensory cortex, PPC, visual cortex, or frontal regions) that can best predict the trial-by-trial changes in performance. First, one could elucidate which neural substrate can encode the trial-by-trial error in average direction estimation. Second, in the case of a bimanual task, one could determine the level of hemispheric fluctuations that encodes the trial-by-trial weight assigned to one of the fingers (cannot be done in unimanual task due to difficulty in distinguishing between finger representation at the neural level).

Another way would be to use TMS to disrupt processing at either visual, somatosensory, or parietal cortices, and examine how this disruption influences perception of component directions and perception of their corresponding average.

## **7.5. Reliability of tactile spatial input affects visual-tactile integration**

Augmenting and supporting visual processing with tactile input is becoming increasingly desirable (for review see Hale & Stanney, 2004; Gallace & Spence, 2014). Indeed, people appear to integrate visual and tactile information arising from a same source in a Bayesian optimal manner by weighting visual modality based on its reliability (Ernst & Banks, 2002). Yet seemingly no study on visual-tactile integration has manipulated the reliability of tactile input. Because vision is believed to generally dominate spatial perception, it is assumed that adding tactile input could enhance visual processing, but never interfere with it (Hale & Stanney, 2004). The visual-tactile spatial integration experiment in **Chapter 6**, indeed showed that when tactually perceived force direction was not corrupted by noise (it was reliable), it tended to be optimally integrated with the direction of the optical flow and enhanced the perception of heading direction.

However, when tactile input was corrupted by noise it tended to interfere with visual processing, even when visual input provided reliable directional information. That is, rather than just being discounted and not integrated, noisy tactile input degraded the performance under the multisensory conditions. The reason for this interference effects remains unclear. One could argue that touch leads to a stronger entrainment. However, implicit direction-specific postural response did not vary between tactile and visual input, and indeed was lower when touch was noisy. Moreover, body sway did not vary across multisensory conditions. However, due to a small sample size, null results should be interpreted with caution, and further studies with a bigger sample may be needed to elucidate the postural response pattern.

It is notable that even when touch was noisy it still provided directional input, and when noisy tactile input was presented without visual input, participants were able to distinguish the directions, albeit less reliably. Thus, the interfering effect of tactile noise during multisensory conditions could have been due to attentional overload, whereby noise elicited by the tactile device grabbed attention from the visual input and degraded directional judgements. This is in contrast to studies that have shown that tactile distractors have negligible effect on visual processing (e.g., Eimer & Driver, 2000; but see Guest & Spence, 2003). Present findings could be due to the nature of the tactile noise, which was a vibration of the device at changing frequency. Such dynamic distraction could have been better at grabbing attention than simple task-irrelevant tactile taps presented during visual processing in a lot of previous studies (e.g., Spence, Pavani, & Driver, 2004). Yet, such distracting vibration would be the most common



source of noise in tactile interfaces. For example, if a tactile interface is used during driving at the back of the seat, there will be a lot of irrelevant vibration between the interface and agent's body. The results of the present study suggest that such noise needs to be carefully controlled or one risks a "helpful" tactile interface to become harmful.

## **7.6. Final conclusion and practical implications**

The fact that across six experiments participants could perceive the movement direction of two discrepant tactile stimuli presented to different non-adjacent and even to bimanual fingers in order to average them into their overall direction, stands in stark contrast to the severe limitations of tactile processing capacity that are widely discussed in the tactile perception literature. These severe processing limits are often used to criticise attempts at tactile interfaces that should supplement or replace visual processing. Indeed, ambitious attempts at producing complex spatial images onto the skin of participants, to create an equivalent of a "tactile TV" have proven generally unsuccessful (Collins, 1970; Bach-Y-Rita et al., 1969; Bach-Y-Rita & Kercel, 2003). Of course, spatial resolution of tactile peripheral afferents is already poor relative to the retina (Loomis, Klatzky, & Giudice, 2012; Cho et al., 2016), thus any attempt at re-creating visual images on the skin will inevitably fall short.

Apart from peripheral mechanisms, the cognitive capacities of tactile processing to augment vision have also been considered rather bleak (Spence, 2014). Most notably, it is widely believed that the 'field of view' (FOV) in touch is limited to a single finger (i.e., when exploring raised line drawings; Loomis, Klatzky, Lederman, 1991; Pawluk, Adams, & Kitada, 2015), and that information uptake does not substantially increase even when multiple fingers are used (Klatzky et al., 1993). In vision, large FOV allows instant perceptual organisation and object recognition via parallel processing. Single-finger FOV in touch suggests that information needs to be pieced together serially and retained in memory to represented unified perceptual patterns and objects. Spence & Gallace (2007) and Gallace & Spence (2014) also highlight constraints in parallel processing, emphasising the inability to count multiple stimuli dispersed across the body (Gallace et al., 2006).

It is true that spatial integration in touch is inferior to that in vision, which makes it difficult to perceive rich 'images' presented to the skin. It is also true that daily haptic interactions normally involve touching one object at the time, but this is similar to gazing at one part of a visual scene at the time. The results of this thesis, however, strongly suggest that tactile FOV can be extended to two fingers, even when the input on those two fingers is discrepant. Although we never asked participants to report only one of the component directions during the averaging conditions, our weight allocation analysis reveals that participants were

processing information from both digits rather than selectively attending to only one (see Cataldo et al., 2019, who showed that individual intensity inputs could be perceived during aggregation). Thus, our multi-touch averaging paradigm opens up new avenues for examining the maximum number of independent inputs that can be perceived by touch, similarly to ensemble perception studies done in vision (Whitney & Yamanashi Leib, 2017). Interestingly, our results demonstrated a superiority of using bimanual fingers in integrating two discrepant inputs. Indeed, proficient Braille readers often make use of both hands to process distinct information simultaneously in order to integrate Braille patterns more efficiently (Bertelson, Mousty, & D'alimonte, 1985).

Apart from providing reliable input to the skin, tactile interfaces need to convey information about external environments. That is, if a tactile interface produces a pattern of stimulation across the skin, the pattern must be attributed to something that is in external space rather than on the skin. This transformation from skin-based coordinate space into external coordinates is often called remapping (Heed et al., 2015). Our findings indicate that spatiotemporal inputs felt on the skin could be remapped into external coordinates. This is because when posture of the hand was changed, participants could still largely account for the postural change when estimating the directions, albeit not fully. Importantly for practical implications, the remapping process introduced additional noise both for estimating the component directions and when integrating the remapped components, implying that it was a computationally costly process. Given that any stimulation across the skin would face the requirement of remapping, engineers of tactile interfaces should consider those costs. Remapping is not a concern for devices that produce directional input from the body midline, like a translational force input employed in **Chapter 6**. We show that force direction can be perceived with a remarkable precision ( $\sim 8^\circ$ ), and indeed it can be integrated with the direction of optical flow. However, engineers should be aware of the noise inherent in both the tactile interface and the tactile processing pathway, which can have adverse effects even when presented along reliable visual cues.

Taken together, the inclusion of models of multi-touch integration into the classical focus on tactile acuity would have important implications for tactile interface design. Not only do we show that multi-touch spatial integration is possible, despite tactile processing constraints, but we also provide a paradigm to examine the factors that could affect this integration. In our case, multi-touch spatial integration incorporated proprioceptive input, was unconstrained by the somatotopic distance between fingers and was equally unconstrained by the spatial discrepancy between the component inputs. But it was modulated by hemispheric or within-between hands factors. Namely, employment of processing resources of both

hemisphere (or both hands) may overcome hemispheric (or within-hand) processing limitations. Finally, we emphasise the need of including tactile reliability manipulations when examining visual-tactile integration. Instead of relying on the assumption that vision will provide the dominant input, our data suggests that the distinct nature of tactile signal, tactile noise, and tactile sensation itself needs to be further characterised.

## References

- Alais, D., & Burr, D. (2004). The ventriloquist effect results from near-optimal bimodal integration. *Current biology*, 14(3), 257-262.  
<https://doi.org/10.1016/j.cub.2004.01.029>
- Allen, M., Poggiali, D., Whitaker, K., Marshall, T. R., & Kievit, R. A. (2019). Raincloud plots: a multi-platform tool for robust data visualization. *Wellcome open research*, 4.  
[10.12688/wellcomeopenres.15191.1](https://doi.org/10.12688/wellcomeopenres.15191.1)
- Allison, T., McCarthy, G., Wood, C. C., Darcey, T. M., Spencer, D. D., & Williamson, P. D (1989). Human cortical potentials evoked by stimulation of the median nerve. II. Cytoarchitectonic areas generating short-latency activity. *Journal of Neurophysiology*, 62(3), 694–710. <https://doi.org/10.1152/jn.1989.62.3.694>
- Alloway, K. D., Rosenthal, P., & Burton, H. (1989). Quantitative measurement of receptive field changes during antagonism of GABAergic transmission in primary somatosensory cortex of cats. *Experimental Brain Research*, 78, 514–532.
- Alsius, A., Navarra, J., Campbell, R., & Soto-Faraco, S. (2005). Audiovisual integration of speech falters under high attention demands. *Current Biology*, 15 (9), 839–43.  
<https://doi-org.libproxy.ucl.ac.uk/10.1016/j.cub.2005.03.046>
- Alvarez, G. A. (2011). Representing multiple objects as an ensemble enhances visual cognition. *Trends in Cognitive Sciences*, 15(3), 122–131.  
<https://doi.org/10.1016/j.tics.2011.01.003>
- Amemiya, T., & Gomi, H. (2012). Directional torque perception with brief, asymmetric net rotation of a flywheel. *IEEE transactions on haptics*, 6(3), 370-375.  
<https://doi.org/10.1109/TOH.2012.38>
- Amemiya, T., & Gomi, H. (2014, June). Distinct pseudo-attraction force sensation by a thumb-sized vibrator that oscillates asymmetrically. In *International Conference on Human Haptic Sensing and Touch Enabled Computer Applications* (pp. 88-95). Springer, Berlin, Heidelberg.
- Amemiya, T., & Gomi, H. (2016). Active manual movement improves directional perception of illusory force. *IEEE transactions on haptics*, 9(4), 465-473.  
<https://doi.org/10.1109/TOH.2016.2587624>
- Amemiya, T., Ando, H., & Maeda, T. (2005, March). Virtual force display: Direction guidance using asymmetric acceleration via periodic translational motion. In *First Joint Eurohaptics Conference and Symposium on Haptic Interfaces for Virtual Environment and Teleoperator Systems. World Haptics Conference* (pp. 619-622). IEEE.  
<https://doi.org/10.1109/WHC.2005.146>
- Amemiya, T., Beck, B., Walsh, V., Gomi, H., & Haggard, P. (2017). Visual area V5/hMT+ contributes to perception of tactile motion direction: a TMS study. *Scientific reports*, 7(1), 1-7. <https://doi.org/10.1038/srep40937>
- Andres, F. G., Mima, T., Schulman, A. E., Dichgans, J., Hallett, M., & Gerloff, C. (1999). Functional coupling of human cortical sensorimotor areas during bimanual skill acquisition. *Brain*, 122(5), 855-870.
- Andrew, C., & Pfurtscheller, G. (1999). Lack of bilateral coherence of post-movement central beta oscillations in the human electroencephalogram. *Neuroscience Letters*, 273(2), 89–92. [https://doi.org/10.1016/S0304-3940\(99\)00632-1](https://doi.org/10.1016/S0304-3940(99)00632-1)
- Angelaki, D. E., Gu, Y., & DeAngelis, G. C. (2009). Multisensory integration: psychophysics, neurophysiology, and computation. *Current opinion in neurobiology*, 19(4), 452-458.
- Angelaki, D. E., Gu, Y., & DeAngelis, G. C. (2011). Visual and vestibular cue integration for heading perception in extrastriate visual cortex. *The Journal of physiology*, 589(4), 825-833.

- Angelucci, A., Bijanzadeh, M., Nurminen, L., Federer, F., Merlin, S., & Bressloff, P. C. (2017). Circuits and Mechanisms for Surround Modulation in Visual Cortex. *Annual Review of Neuroscience*, 40(1), 425–451. <https://doi.org/10.1146/annurev-neuro-072116-031418>
- Arslanova, I., Wang, K., Gomi, H., & Haggard, P. (2021). Somatosensory evoked potentials that index lateral inhibition are modulated according to the mode of perceptual processing: comparing or combining multi-digit tactile motion. *Cognitive Neuroscience*, 1-13. <https://doi.org/10.1080/17588928.2020.1839403>
- Arslanova, I., Takamuku, S., Gomi, H., & Haggard, P. (2021). Sensory and cognitive factors affecting multi-digit touch: a perceptual and modeling study. *bioRxiv*. <https://doi.org/10.1101/2021.02.25.432852>
- Averbeck, B. B., Latham, P. E., & Pouget, A. (2006). Neural correlations, population coding and computation. *Nature Reviews Neuroscience*, 7(5), 358–366. <https://doi.org/10.1038/nrn1888>
- Azañón, E., & Soto-Faraco, S. (2008). Changing reference frames during the encoding of tactile events. *Current biology*, 18(14), 1044-1049. <https://doi.org/10.1016/j.cub.2008.06.045>
- Azañón, E., Longo, M. R., Soto-Faraco, S., & Haggard, P. (2010). The posterior parietal cortex remaps touch into external space. *Current biology*, 20(14), 1304-1309.
- Azañón, E., Mihaljevic, K., & Longo, M. R. (2016). A three-dimensional spatial characterization of the crossed-hands deficit. *Cognition*, 157, 289-295.
- Azañón, E., Stenner, M. P., Cardini, F., & Haggard, P. (2015). Dynamic tuning of tactile localization to body posture. *Current Biology*, 25(4), 512-517. <https://doi.org/10.1016/j.cub.2014.12.038>
- Baars, B. J., & Gage, N. M. (2010). *Cognition, brain, and consciousness: Introduction to cognitive neuroscience*. Academic Press.
- Bach-y-Rita, P., & Kercel, S. W. (2003). Sensory substitution and the human-machine interface. *Trends in cognitive sciences*, 7(12), 541-546.
- Bach-y-Rita, P., Collins, C. C., Saunders, F. A., White, B., & Scadden, L. (1969). Vision substitution by tactile image projection. *Nature*, 221(5184), 963-964.
- Badde, S., & Heed, T. (2016). Towards explaining spatial touch perception: Weighted integration of multiple location codes. *Cognitive neuropsychology*, 33(1-2), 26-47. <https://doi.org/10.1080/02643294.2016.1168791>
- Badde, S., Röder, B., & Heed, T. (2019). Feeling a touch to the hand on the foot. *Current Biology*, 29(9), 1491-1497.
- Baek, J., & Chong, S. C. (2020). Distributed attention model of perceptual averaging. *Attention, Perception & Psychophysics*, 82(1), 63–79. <https://doi.org/10.3758/s13414-019-01827-z>
- Bakshi, A., & Ghosh, K. (2017). *A neural model of attention and feedback for computing perceived brightness in vision*. In Handbook of Neural Computation (pp. 487-513). Academic Press.
- Banich, M. T., & Belger, A. (1990). Interhemispheric interaction: how do the hemispheres divide and conquer a task?. *Cortex*, 26(1), 77-94.
- Barbagli, F., Salisbury, K., Ho, C., Spence, C., & Tan, H. Z. (2006). Haptic discrimination of force direction and the influence of visual information. *ACM Transactions on Applied Perception (TAP)*, 3(2), 125-135. <https://doi.org/10.1145/1141897.1141901>
- Baumgartner, G., Von der Heydt, R., & Peterhans, E. (1984). Anomalous contours: A tool in studying the neurophysiology of vision. *Experimental Brain Research*, 413-419.
- Bays, P. M., Wolpert, D. M., & Flanagan, J. R. (2005). Perception of the consequences of self-action is temporally tuned and event driven. *Current Biology*, 15(12), 1125-1128.

- Bender, M. B., Stacy, C., & Cohen, J. (1982). Agraphesthesia: a disorder of directional cutaneous kinesthesia or a disorientation in cutaneous space. *Journal of the neurological sciences*, 53(3), 531-555.
- Bensmaia, S. J., Hsiao, S. S., Denchev, P. V., Killebrew, J. H., & Craig, J. C. (2008). The tactile perception of stimulus orientation. *Somatosensory & motor research*, 25(1), 49-59. <https://doi-org.libproxy.ucl.ac.uk/10.1080/08990220701830662>
- Bensmaia, S. J., Killebrew, J. H., & Craig, J. C. (2006). Influence of visual motion on tactile motion perception. *Journal of neurophysiology*, 96(3), 1625-1637. <https://doi.org/10.1152/jn.00192.2006>
- Berardi, N., Bisti, S., Fiorentini, A., & Maffei, L. (1988). The transfer of visual information across the corpus callosum in cats, monkeys and humans: spatial and temporal properties. *Progress in brain research*, 75, 181-185.
- Bertelson, P., Vroomen, J., De Gelder, B., & Driver, J. (2000). The ventriloquist effect does not depend on the direction of deliberate visual attention. *Perception & Psychophysics*, 62(2), 321-32. <https://doi-org.libproxy.ucl.ac.uk/10.3758/BF03205552>
- Bertelson, P., Mousty, P., & D'alimonte, G. (1985). A study of braille reading: 2. Patterns of hand activity in one-handed and two-handed reading. *The Quarterly Journal of Experimental Psychology Section A*, 37(2), 235-256.
- Berthoz, A., Pavard, B., & Young, L. R. (1975). Perception of linear horizontal self-motion induced by peripheral vision (linearvection) basic characteristics and visual-vestibular interactions. *Experimental brain research*, 23(5), 471-489.
- Bertone, A., Mottron, L., Jelenic, P., & Faubert, J. (2005). Enhanced and diminished visuo-spatial information processing in autism depends on stimulus complexity. *Brain*, 128(10), 2430-2441. <https://doi.org/10.1093/brain/awh561>
- Biermann, K., Schmitz, F., Witte, O. W., Konczak, J., Freund, H.-J., & Schnitzler, A. (1998). Interaction of finger representation in the human first somatosensory cortex: A neuromagnetic study. *Neuroscience Letters*, 251(1), 13-16. [https://doi.org/10.1016/S0304-3940\(98\)00480-7](https://doi.org/10.1016/S0304-3940(98)00480-7)
- Blakemore, C., & Tobin, E. A. (1972). Lateral inhibition between orientation detectors in the cat's visual cortex. *Experimental Brain Research*, 15(4), 439-440. <https://doi.org/10.1007/BF00234129>
- Blakemore, S. J., Frith, C. D., & Wolpert, D. M. (1999). Spatio-temporal prediction modulates the perception of self-produced stimuli. *Journal of cognitive neuroscience*, 11(5), 551-559.
- Blankenburg, F., Ruben, J., Meyer, R., Schwiemann, J., & Villringer, A. (2003). Evidence for a rostral-to-caudal somatotopic organization in human primary somatosensory cortex with mirror-reversal in areas 3b and 1. *Cerebral Cortex*, 13(9), 987-993. <https://doi.org/10.1093/cercor/13.9.987>
- Boneau, C. A. (1960). The effects of violations of assumptions underlying the t test. *Psychological bulletin*, 57(1), 49.
- Braun, C., Haug, M., Wiech, K., Birbaumer, N., Elbert, T., & Roberts, L. E. (2002). Functional organization of primary somatosensory cortex depends on the focus of attention. *Neuroimage*, 17(3), 1451-1458. <https://doi.org/10.1006/nimg.2002.1277>
- Braun, C., Ladda, J., Burkhardt, M., Wiech, K., Preissl, H., Roberts, L. E. (2005). Objective measurement of tactile mislocalization. *IEEE Transactions on Biomedical Engineering*, 52, 728-735. <https://doi.org/10.1109/TBME.2005.845147>
- Bregman, A. S., Liao, C., & Levitan, R. (1990). Auditory grouping based on fundamental frequency and formant peak frequency. *Canadian Journal of Psychology/Revue canadienne de psychologie*, 44(3), 400.
- Breidbach, O., & Jost, J. (2006). On the gestalt concept. *Theory in Biosciences*, 125(1), 19-36.

- Bresciani, J. P., Dammeier, F., & Ernst, M. O. (2006). Vision and touch are automatically integrated for the perception of sequences of events. *Journal of vision*, 6(5), 2-2.
- Broadbent, D. E. (1958). CHAPTER 5—THE EFFECTS OF NOISE ON BEHAVIOUR. In D. E. Broadbent (Ed.), *Perception and Communication* (pp. 81–107). Pergamon.  
<https://doi.org/10.1016/B978-1-4832-0079-8.50007-4>
- Brouwer, G. J. , Arnedo, V. , Offen, S. , Heeger, D. J. , & Grant, A. C. (2015). Normalization in human somatosensory cortex. *Journal of Neurophysiology* , 114(5), 2588–2599. <https://doi.org/10.1152/jn.00939.2014>
- Brown, P. B., Koerber, H. R., & Millecchia, R. (2004). From innervation density to tactile acuity: 1. Spatial representation. *Brain Research*, 1011(1), 14–32.  
<https://doi.org/10.1016/j.brainres.2004.03.009>
- Brumberg, J. C., Pinto, D. J., & Simons, D. J. (1996). Spatial gradients and inhibitory summation in the rat whisker barrel system. *Journal of Neurophysiology*, 76(1), 130–140.  
<https://doi.org/10.1152/jn.1996.76.1.130>
- Burton, H., & Carlson, M. (1986). Second somatic sensory cortical area (SII) in a prosimian primate, Galago crassicaudatus. *Journal of Comparative Neurology*, 247(2), 200-220.
- Calford, M. B., & Tweedale, R. (1991). Acute changes in cutaneous receptive fields in primary somatosensory cortex after digit denervation in adult flying fox. *Journal of neurophysiology*, 65(2), 178-187. <https://doi.org/10.1152/jn.1991.65.2.178>
- Caminiti R, Borra E, Visco-Comandini F, Battaglia-Mayer A, Averbeck BB, Luppino G. (2017). Computational architecture of the parieto-frontal network underlying cognitive-motor control in monkeys. *eNeuro* 4: ENEURO.0306-16.2017.
- Canales-Johnson, A. , Billig, A. J. , Olivares, F. , Gonzalez, A. , Del Garcia, M. C. , Silva, W. , Vaucheret, E. , Ciralo, C. , Mikulan, E. , Ibanez, A. , Huepe, D. , Noreika, V. , Chennu, S. , & Bekinschtein, T. A. (2020). Dissociable neural information dynamics of perceptual integration and differentiation during bistable perception. *Cerebral Cortex* , 30(8), 4563–4580. <https://doi.org/10.1093/cercor/bhaa058>
- Cao, Y., Summerfield, C., Park, H., Giordano, B. L., & Kayser, C. (2019). Causal inference in the multisensory brain. *Neuron*, 102(5), 1076-1087.  
<https://doi.org/10.1016/j.neuron.2019.03.043>
- Carandini, M. , & Heeger, D. J. (2012). Normalization as a canonical neural computation. *Nature Reviews Neuroscience* , 13(1), 51–62. <https://doi.org/10.1038/nrn3136>
- Cardini, F., & Longo, M. R. (2016). Congruency of body-related information induces somatosensory reorganization. *Neuropsychologia*, 84, 213–221.
- Cardini, F., Longo, M. R., & Haggard, P. (2011). Vision of the Body Modulates Somatosensory Intracortical Inhibition. *Cerebral Cortex*, 21(9), 2014–2022.  
<https://doi.org/10.1093/cercor/bhq267>
- Cataldo, A., Dupin, L., Gomi, H., & Haggard, P. (2021). Sensorimotor signals underlying space perception: an investigation based on self-touch. *Neuropsychologia*, 151, 107729.  
<https://doi.org/10.1016/j.neuropsychologia.2020.107729>
- Cataldo, A., Ferrè, E. R., di Pellegrino, G., & Haggard, P. (2019). Why the whole is more than the sum of its parts: Saliency-driven overestimation in aggregated tactile sensations. *Quarterly Journal of Experimental Psychology*, 72(10), 2509–2526.  
<https://doi.org/10.1177/1747021819847131>
- Chen, L. M., Friedman, R. M., & Roe, A. W. (2003). Optical imaging of a tactile illusion in area 3b of the primary somatosensory cortex. *Science*, 302(5646), 881-885.
- Chen, Y. P., Yeh, C. I., Lee, T. C., Huang, J. J., & Pei, Y. C. (2020). Relative posture between head and finger determines perceived tactile direction of motion. *Scientific reports*, 10(1), 1-13. <https://doi.org/10.1038/s41598-020-62327-x>

- Cho, Y., Craig, J. C., Hsiao, S. S., & Bensmaia, S. J. (2016). Vision is superior to touch in shape perception even with equivalent peripheral input. *Journal of neurophysiology*, 115(1), 92-99. <https://doi.org/10.1152/jn.00654.2015>
- Chu, M. W., Li, W. L., & Komiyama, T. (2016). Balancing the robustness and efficiency of odor representations during learning. *Neuron*, 92(1), 174-186. <https://doi.org/10.1016/j.neuron.2016.09.004>
- Clifford, C. W. G. (2014). The tilt illusion: Phenomenology and functional implications. *Vision Research*, 104, 3-11. <https://doi.org/10.1016/j.visres.2014.06.009>
- Cline, E. (2018). *Ready player one*. Michel Lafon.
- Cohen YE, Cohen IS, Gifford GW. (2004). Modulation of LIP activity by predictive auditory and visual cues. *Cereb Cortex*. 14: 1287-1301.
- Cohen, M. R., & Maunsell, J. H. R. (2009). Attention improves performance primarily by reducing interneuronal correlations. *Nature Neuroscience*, 12(12), 1594-1600. <https://doi.org/10.1038/nn.2439>
- Collins, C. C. (1970). Tactile television-mechanical and electrical image projection. *IEEE Transactions on man-machine systems*, 11(1), 65-71.
- Craddock, M., Poliakoff, E., El-Deredy, W., Klepousniotou, E., & Lloyd, D. M. (2017). Pre-stimulus alpha oscillations over somatosensory cortex predict tactile misperceptions. *Neuropsychologia*, 96, 9-18.
- Craig, J. C. (1985). Attending to two fingers: Two hands are better than one. *Perception & psychophysics*, 38(6), 496-511. <https://doi.org/10.3758/BF03207059>
- Craig, J. C. (2003). The effect of hand position and pattern motion on temporal order judgments. *Perception & Psychophysics*, 65(5), 779-788. <https://doi.org/10.3758/BF03194814>
- Craig, J. C. (2006). Visual motion interferes with tactile motion perception. *Perception*, 35(3), 351-367.
- Culbertson, H., Schorr, S. B., & Okamura, A. M. (2018). Haptics: The present and future of artificial touch sensation. *Annual Review of Control, Robotics, and Autonomous Systems*, 1, 385-409.
- Deafblind. (n.d.). *Communication*. <https://deafblind.org.uk/information-advice/living-with-deafblindness/communication/>
- DeAngelis, G. C., Robson, J. G., Ohzawa, I., & Freeman, R. D. (1992). Organization of suppression in receptive fields of neurons in cat visual cortex. *Journal of Neurophysiology*, 68(1), 144-163. <https://doi.org/10.1152/jn.1992.68.1.144>
- Delhaye, B. P., Long, K. H., & Bensmaia, S. J. (2011). Neural basis of touch and proprioception in primate cortex. *Comprehensive Physiology*, 8(4), 1575-1602. <https://doi-org.libproxy.ucl.ac.uk/10.1002/cphy.c170033>
- Delhaye, B. P., O'Donnell, M. K., Lieber, J. D., McLellan, K. R., & Bensmaia, S. J. (2019). Feeling fooled: Texture contaminates the neural code for tactile speed. *PLoS biology*, 17(8), e3000431. <https://doi.org/10.1371/journal.pbio.3000431>
- Delorme, A., & Makeig, S. (2004). EEGLAB: An open source toolbox for analysis of single-trial EEG dynamics including independent component analysis. *Journal of Neuroscience Methods*, 134(1), 9-21. <https://doi.org/10.1016/j.jneumeth.2003.10.009>
- Dempsey-Jones, H., Harrar, V., Oliver, J., Johansen-Berg, H., Spence, C., & Makin, T. R. (2016). Transfer of tactile perceptual learning to untrained neighboring fingers reflects natural use relationships. *Journal of Neurophysiology*, 115(3), 1088-1097.
- Dempsey-Jones, H., Themistocleous, A. C., Carone, D., Ng, T. W., Harrar, V., & Makin, T. R. (2019). Blocking tactile input to one finger using anaesthetic enhances touch perception and learning in other fingers. *Journal of Experimental Psychology: General*, 148(4), 713.
- Descartes, R. (1998). *Descartes: The world and other writings*. Cambridge University Press.



- Desimone, R., & Duncan, J. (1995). Neural mechanisms of selective visual attention. *Annual review of neuroscience*, 18(1), 193-222.
- DiCarlo, J. J., Johnson, K. O., & Hsiao, S. S. (1998). Structure of Receptive Fields in Area 3b of Primary Somatosensory Cortex in the Alert Monkey. *Journal of Neuroscience*, 18(7), 2626–2645. <https://doi.org/10.1523/JNEUROSCI.18-07-02626.1998>
- Dichgans, J., & Brandt, T. (1973). Optokinetic motion sickness and pseudo-Coriolis effects induced by moving visual stimuli. *Acta otolaryngologica*, 76(1-6), 339-348.
- Dichgans, J., & Brandt, T. (1978). Visual-vestibular interaction: Effects on self-motion perception and postural control. In *Perception* (pp. 755-804). Springer, Berlin, Heidelberg.
- Drew, P. J., & Feldman, D. E. (2007). Representation of moving wavefronts of whisker deflection in rat somatosensory cortex. *Journal of neurophysiology*, 98(3), 1566-1580. <https://doi.org/10.1152/jn.00056.2007>
- Driver, J. (1996). Enhancement of selective listening by illusory mislocation of speech sounds due to lip-reading. *Nature*, 381 (6577), 66–8. <https://doi-org.libproxy.ucl.ac.uk/10.1038/381066a0>
- Driver, J., & Grossenbacher, P. G. (1996). Multimodal spatial constraints on tactile selective attention. In *Attention and performance 16: Information integration in perception and communication* (pp. 209–235). The MIT Press.
- Driver, J., & Spence, C. (1998). Attention and the crossmodal construction of space. *Trends in cognitive sciences*, 2(7), 254-262.
- Duncan, J., Martens, S., & Ward, R. (1997). Restricted attentional capacity within but not between sensory modalities. *Nature*, 387 (6635), 808–10. <https://doi-org.libproxy.ucl.ac.uk/10.1038/42947>
- Dykes, R. W., Landry, P., Metherate, R., & Hicks, T. P. (1984). Functional role of GABA in cat primary somatosensory cortex: Shaping receptive fields of cortical neurons. *Journal of Neurophysiology*, 52(6), 1066–1093. <https://doi.org/10.1152/jn.1984.52.6.1066>
- Eimer, M., & Driver, J. (2000). An event-related brain potential study of cross-modal links in spatial attention between vision and touch. *Psychophysiology*, 37(5), 697-705.
- Ernst, M. O., & Banks, M. S. (2002). Humans integrate visual and haptic information in a statistically optimal fashion. *Nature*, 415(6870), 429-433. <https://doi.org/10.1038/415429a>
- Ernst, M. O., & Bühlhoff, H. H. (2004). Merging the senses into a robust percept. *Trends in Cognitive Sciences*, 8(4), 162–169. <https://doi.org/10.1016/j.tics.2004.02.002>
- Evans, P. M., & Craig, J. C. (1991). Tactile attention and the perception of moving tactile stimuli. *Perception & psychophysics*, 49(4), 355-364.
- Fairhurst, M. T., Travers, E., Hayward, V., & Deroy, O. (2018). Confidence is higher in touch than in vision in cases of perceptual ambiguity. *Scientific reports*, 8(1), 1-9.
- Fardo, F., Beck, B., Allen, M., & Finnerup, N. B. (2020). Beyond labeled lines: A population coding account of the thermal grill illusion. *Neuroscience & Biobehavioral Reviews*, 108, 472-479. <https://doi.org/10.1016/j.neubiorev.2019.11.017>
- Fardo, F., Beck, B., Cheng, T., & Haggard, P. (2018). A mechanism for spatial perception on human skin. *Cognition*, 178, 236-243. <https://doi.org/10.1016/j.cognition.2018.05.024>
- Faul, F., Erdfelder, E., Buchner, A., & Lang, A. G. (2009). Statistical power analyses using G\* Power 3.1: Tests for correlation and regression analyses. *Behavior research methods*, 41(4), 1149-1160. <https://doi.org/10.3758/BRM.41.4.1149>
- Feldman, D. E., & Brecht, M. (2005). Map plasticity in somatosensory cortex. *Science*, 310(5749), 810-815.
- Fernandez, C., & Goldberg, J. M. (1976a). Physiology of peripheral neurons innervating otolith organs of the squirrel monkey. I. Response to static tilts and to long-duration centrifugal force. *Journal of neurophysiology*, 39(5), 970-984.

- Fernandez, C., & Goldberg, J. M. (1976b). Physiology of peripheral neurons innervating otolith organs of the squirrel monkey. II. Directional selectivity and force-response relations. *Journal of neurophysiology*, 39(5), 985-995.
- Fernandez, C., & Goldberg, J. M. (1976c). Physiology of peripheral neurons innervating otolith organs of the squirrel monkey. III. Response dynamics. *Journal of neurophysiology*, 39(5), 996-1008.
- Ferrè, E. R., Sahani, M., & Haggard, P. (2016). Subliminal stimulation and somatosensory signal detection. *Acta Psychologica*, 170, 103–111.  
<https://doi.org/10.1016/j.actpsy.2016.06.009>
- Fiori, F., & Longo, M. R. (2018). Tactile distance illusions reflect a coherent stretch of tactile space. *Proceedings of the National Academy of Sciences*, 115(6), 1238-1243.
- Fitzgerald, P. J., Lane, J. W., Thakur, P. H., & Hsiao, S. S. (2006a). Receptive Field Properties of the Macaque Second Somatosensory Cortex: Representation of Orientation on Different Finger Pads. *Journal of Neuroscience*, 26(24), 6473–6484.  
<https://doi.org/10.1523/JNEUROSCI.5057-05.2006>
- Fitzgerald, P. J., Lane, J. W., Thakur, P. H., & Hsiao, S. S. (2006b). Receptive Field (RF) Properties of the Macaque Second Somatosensory Cortex: RF Size, Shape, and Somatotopic Organization. *Journal of Neuroscience*, 26(24), 6485–6495.  
<https://doi.org/10.1523/JNEUROSCI.5061-05.2006>
- Foeller, E., Celikel, T., & Feldman, D. E. (2005). Inhibitory Sharpening of Receptive Fields Contributes to Whisker Map Plasticity in Rat Somatosensory Cortex. *Journal of Neurophysiology*, 94(6), 4387–4400. <https://doi.org/10.1152/jn.00553.2005>
- Foeller, E., Vater, M., & Kössl, M. (2001). Laminar Analysis of Inhibition in the Gerbil Primary Auditory Cortex. *JARO: Journal of the Association for Research in Otolaryngology*, 2(3), 279–296. <https://doi.org/10.1007/s101620010069>
- Forss, N., Jousmäki, V., & Hari, R. (1995). Interaction between afferent input from fingers in human somatosensory cortex. *Brain Research*, 685(1), 68–76.  
[https://doi.org/10.1016/0006-8993\(95\)00424-O](https://doi.org/10.1016/0006-8993(95)00424-O)
- Forster, B., & Eimer, M. (2004). The attentional selection of spatial and non-spatial attributes in touch: ERP evidence for parallel and independent processes. *Biological psychology*, 66(1), 1-20.
- Freides, D. (1974). Human information processing and sensory modality: Cross-modal functions, information complexity, memory, and deficit. *Psychological bulletin*, 81(5), 284.
- Friedman, A., & Polson, M. C. (1981). Hemispheres as independent resource system: Limited-capacity processing and cerebral specialization. *Journal of experimental psychology: Human perception and performance*, 7(5), 1031.
- Friston, K., Rigoli, F., Ognibene, D., Mathys, C., Fitzgerald, T., & Pezzulo, G. (2015). Active inference and epistemic value. *Cognitive neuroscience*, 6(4), 187-214. <https://doi-org.libproxy.ucl.ac.uk/10.1080/17588928.2015.1020053>
- Fulkerson, M. (2014). *The first sense: A philosophical study of human touch*. MIT Press.
- Fulkerson, M. (2020). Touch. *Stanford Encyclopedia of Philosophy*.  
<https://plato.stanford.edu/entries/touch/>
- Gallace, A., & Spence, C. (2011). To what extent do Gestalt grouping principles influence tactile perception?. *Psychological bulletin*, 137(4), 538. <https://doi.org/10.1037/a0022335>
- Gallace, A., & Spence, C. (2014). *In touch with the future: The sense of touch from cognitive neuroscience to virtual reality*. OUP Oxford.
- Gallace, A., Tan, H. Z., & Spence, C. (2006). Numerosity Judgments for Tactile Stimuli Distributed over the Body Surface. *Perception*, 35(2), 247–266.  
<https://doi.org/10.1068/p5380>

- Gandevia, S. C., Burke, D., & McKeon, B. B. (1983). Convergence in the somatosensory pathway between cutaneous afferents from the index and middle fingers in man. *Experimental Brain Research*, 50–50(2–3). <https://doi.org/10.1007/BF00239208>
- Gibson, J. J. (1937). Adaptation, after-effect, and contrast in the perception of tilted lines. II. Simultaneous contrast and the areal restriction of the after-effect. *Journal of Experimental Psychology*, 20(6), 553–569. <https://doi.org/10.1037/h0057585>
- Gibson, J. J. (1954). The visual perception of objective motion and subjective movement. *Psychological review*, 61(5), 304.
- Gibson, J. J. (1962). Observations on active touch. *Psychological review*, 69(6), 477.
- Gillmeister, H. , & Forster, B. (2012). Adverse effects of viewing the hand on tactile-spatial selection between fingers depend on finger posture. *Experimental Brain Research* , 221(3), 269–278. <https://doi.org/10.1007/s00221-012-3171-z>
- Gilson, R. D. (1969). Vibrotactile masking: Some spatial and temporal aspects. *Perception & Psychophysics*, 5(3), 176-180.
- Glass, G. V., Peckham, P. D., & Sanders, J. R. (1972). Consequences of failure to meet assumptions underlying the fixed effects analyses of variance and covariance. *Review of educational research*, 42(3), 237-288.
- Goodman, J. M., Tabot, G. A., Lee, A. S., Suresh, A. K., Rajan, A. T., Hatsopoulos, N. G., & Bensmaia, S. (2019). Postural representations of the hand in the primate sensorimotor cortex. *Neuron*, 104(5), 1000-1009.
- Gray, R., & Tan, H. Z. (2002). Dynamic and predictive links between touch and vision. *Experimental Brain Research*, 145(1), 50-55.
- Green, A. M., & Angelaki, D. E. (2010). Multisensory integration: resolving sensory ambiguities to build novel representations. *Current opinion in neurobiology*, 20(3), 353-360.
- Green, B. E. (1982). The perception of distance and location for dual tactile pressures. *Perception and Psychophysics*, 31, 315–323.
- Greenwood, J. A., & Edwards, M. (2009). The detection of multiple global directions: Capacity limits with spatially segregated and transparent-motion signals. *Journal of vision*, 9(1), 40-40. <https://doi.org/10.1167/9.1.40>
- Gu, Y., DeAngelis, G. C., & Angelaki, D. E. (2007). A functional link between area MSTd and heading perception based on vestibular signals. *Nature neuroscience*, 10(8), 1038-1047.
- Guerraz, M., Gianna, C. C., Burchill, P. M., Gresty, M. A., & Bronstein, A. M. (2001). Effect of visual surrounding motion on body sway in a three-dimensional environment. *Perception & psychophysics*, 63(1), 47-58.
- Guest, S., & Spence, C. (2003). Tactile dominance in speeded discrimination of textures. *Experimental brain research*, 150(2), 201-207.
- Gustafsson, L. (1997). Excessive lateral feedback synaptic inhibition may cause autistic characteristics. *Journal of Autism and Developmental Disorders*, 27(2), 219–223. <https://doi.org/10.1023/A:1025804226995>
- Haavik-Taylor, H., & Murphy, B. (2007). Cervical spine manipulation alters sensorimotor integration: A somatosensory evoked potential study. *Clinical Neurophysiology*, 118(2), 391–402. <https://doi.org/10.1016/j.clinph.2006.09.014>
- Haegens, S., Händel, B. F., & Jensen, O. (2011). Top-down controlled alpha band activity in somatosensory areas determines behavioral performance in a discrimination task. *Journal of Neuroscience*, 31(14), 5197-5204.
- Hagen, M. C., Franzén, O., McGlone, F., Essick, G., Dancer, C., & Pardo, J. V. (2002). Tactile motion activates the human middle temporal/V5 (MT/V5) complex. *European Journal of Neuroscience*, 16(5), 957-964.
- Haggard, P. (2006). Sensory neuroscience: from skin to object in the somatosensory cortex. *Current Biology*, 16(20), R884-R886.

- Haggard, P., & Giovagnoli, G. (2011). Spatial patterns in tactile perception: is there a tactile field?. *Acta Psychologica*, 137(1), 65-75. <https://doi.org/10.1016/j.actpsy.2011.03.001>
- Haggard, P., Cheng, T., Beck, B., & Fardo, F. (2017). Spatial perception and the sense of touch. *The Subject's Matter: Self-consciousness and the Body*, 97-114.
- Haggard, P., Christakou, A., & Serino, A. (2007). Viewing the body modulates tactile receptive fields. *Experimental Brain Research*, 180(1), 187–193. <https://doi.org/10.1007/s00221-007-0971-7>
- Hale, K. S., & Stanney, K. M. (2004). Deriving haptic design guidelines from human physiological, psychophysical, and neurological foundations. *IEEE computer graphics and applications*, 24(2), 33-39.
- Halfen, E. J., Magnotti, J. F., Rahman, Md. S., & Yau, J. M. (2020). Principles of tactile search over the body. *Journal of Neurophysiology*, 123(5), 1955–1968. <https://doi.org/10.1152/jn.00694.2019>
- Hämäläinen, H., Kekoni, J., Sams, M., Reinikainen, K., & Näätänen, R. (1990). Human somatosensory evoked potentials to mechanical pulses and vibration: contributions of SI and SII somatosensory cortices to P50 and P100 components. *Electroencephalography and clinical neurophysiology*, 75(1-2), 13-21.
- Hansson, T., & Brismar, T. (1999). Tactile stimulation of the hand causes bilateral cortical activation: a functional magnetic resonance study in humans. *Neuroscience letters*, 271(1), 29-32.
- Hari, R., Reinikainen, K., Kaukoranta, E., Hämäläinen, M., Ilmoniemi, R., Penttinen, A., ... & Teszner, D. (1984). Somatosensory evoked cerebral magnetic fields from SI and SII in man. *Electroencephalography and clinical Neurophysiology*, 57(3), 254-263.
- Harrar, V., Spence, C., & Makin, T. R. (2014). Topographic generalization of tactile perceptual learning. *Journal of Experimental Psychology: Human Perception and Performance*, 40(1), 15.
- Harrington, K., Large, D. R., Burnett, G., & Georgiou, O. (2018). Exploring the use of mid-air ultrasonic feedback to enhance automotive user interfaces. In *Proceedings of the 10th international conference on automotive user interfaces and interactive vehicular applications* (pp. 11-20).
- Harris, J. A., Harris, I. M., & Diamond, M. E. (2001a). The topography of tactile working memory. *Journal of Neuroscience*, 21(20), 8262-8269. <https://doi.org/10.1523/JNEUROSCI.21-20-08262.2001>
- Harris, J. A., Harris, I. M., & Diamond, M. E. (2001b). The Topography of Tactile Learning in Humans. *Journal of Neuroscience*, 21(3), 1056–1061. <https://doi.org/10.1523/JNEUROSCI.21-03-01056.2001>
- Head, H., & Holmes, G. (1911). Sensory disturbances from cerebral lesions. *Brain*, 34(2-3), 102-254. <https://doi.org/10.1093/brain/34.2-3.102>
- Hebb, D. O. (1949). *The organization of behavior: a neuropsychological theory*. J. Wiley; Chapman & Hall.
- Heed, T., & Azañón, E. (2014). Using time to investigate space: a review of tactile temporal order judgments as a window onto spatial processing in touch. *Frontiers in psychology*, 5, 76.
- Heed, T., Buchholz, V. N., Engel, A. K., & Röder, B. (2015). Tactile remapping: from coordinate transformation to integration in sensorimotor processing. *Trends in cognitive sciences*, 19(5), 251-258. <https://doi.org/10.1016/j.tics.2015.03.001>
- Hillis, J. M., Ernst, M. O., Banks, M. S., & Landy, M. S. (2002). Combining sensory information: mandatory fusion within, but not between, senses. *Science*, 298(5598), 1627-1630.
- Ho, H. N., Watanabe, J., Ando, H., & Kashino, M. (2011). Mechanisms underlying referral of thermal sensations to sites of tactile stimulation. *Journal of Neuroscience*, 31(1), 208-213. <https://doi.org/10.1523/JNEUROSCI.2640-10.2011>

- Howe, C. Q., & Purves, D. (2002). Range image statistics can explain the anomalous perception of length. *Proceedings of the National Academy of Sciences*, 99(20), 13184-13188.
- Hsiao, S. (2008). Central mechanisms of tactile shape perception. *Current opinion in neurobiology*, 18(4), 418-424.
- Hsieh, C. L., Shima, F., Tobimatsu, S., Sun, S. J., & Kato, M. (1995). The interaction of the somatosensory evoked potentials to simultaneous finger stimuli in the human central nervous system. A study using direct recordings. *Electroencephalography and Clinical Neurophysiology/Evoked Potentials Section*, 96(2), 135-142.  
[https://doi.org/10.1016/0168-5597\(94\)00251-9](https://doi.org/10.1016/0168-5597(94)00251-9)
- Huang, L., Treisman, A., & Pashler, H. (2007). Characterizing the limits of human visual awareness. *Science*, 317(5839), 823-825.
- Iemi, L., Busch, N. A., Laudini, A., Haegens, S., Samaha, J., Villringer, A., & Nikulin, V. V. (2019). Multiple mechanisms link prestimulus neural oscillations to sensory responses. *Elife*, 8, e43620.
- Iguchi, Y., Hoshi, Y., & Hashimoto, I. (2001). Selective spatial attention induces short-term plasticity in human somatosensory cortex. *Neuroreport*, 12(14), 3133-3136.
- Iguchi, Y., Hoshi, Y., Tanosaki, M., Taira, M., & Hashimoto, I. (2005). Attention induces reciprocal activity in the human somatosensory cortex enhancing relevant-and suppressing irrelevant inputs from fingers. *Clinical Neurophysiology*, 116(5), 1077-1087. <https://doi.org/10.1016/j.clinph.2004.12.005>
- Ishibashi, H., Tobimatsu, S., Shigeto, H., Morioka, T., Yamamoto, T., & Fukui, M. (2000). Differential interaction of somatosensory inputs in the human primary sensory cortex: A magnetoencephalographic study. *Clinical Neurophysiology*, 111(6), 1095-1102.  
[https://doi.org/10.1016/S1388-2457\(00\)00266-2](https://doi.org/10.1016/S1388-2457(00)00266-2)
- Itti, L., & Baldi, P. (2009). Bayesian surprise attracts human attention. *Vision research*, 49(10), 1295-1306. <https://doi.org/10.1016/j.visres.2008.09.007>
- Iwamura, Y., Iriki, A., & Tanaka, M. (1994). Bilateral hand representation in the postcentral somatosensory cortex. *Nature*, 369(6481), 554-556.
- Iwamura, Y., Tanaka, M., Iriki, A., Taoka, M., & Toda, T. (2002). Processing of tactile and kinesthetic signals from bilateral sides of the body in the postcentral gyrus of awake monkeys. *Behavioural brain research*, 135(1-2), 185-190.  
[https://doi.org/10.1016/S0166-4328\(02\)00164-X](https://doi.org/10.1016/S0166-4328(02)00164-X)
- Iwamura, Y., Tanaka, M., Sakamoto, M., & Hikosaka, O. (1993). Rostrocaudal gradients in the neuronal receptive field complexity in the finger region of the alert monkey's postcentral gyrus. *Experimental Brain Research*, 92(3), 360-368.
- J. Loomis, R. Klatzky, and S. Lederman, "Similarity of tactual and visual picture recognition with limited field of view," *Perception*, vol. 20, pp. 167-177, 1991.
- Jeffreys, H. 1961. *Theory of probability*, 3rd ed. New York, NY: Oxford University Press.
- Jenmalm, P., & Johansson, R. S. (1997). Visual and somatosensory information about object shape control manipulative fingertip forces. *Journal of Neuroscience*, 17(11), 4486-4499.
- Johansen-Berg, H., & Lloyd, D. M. (2000). The physiology and psychology of selective attention to touch. *Front Biosci*, 5, D894-D904.
- Johansson, R. S., & Flanagan, J. R. (2009). Coding and use of tactile signals from the fingertips in object manipulation tasks. *Nature Reviews Neuroscience*, 10(5), 345-359.  
<https://doi.org/10.1038/nrn2621>
- Johansson, R. S., & Flanagan, J. R. (2009). Coding and use of tactile signals from the fingertips in object manipulation tasks. *Nature Reviews Neuroscience*, 10(5), 345-359.
- Jones, E. G., & Powell, T. P. S. (1970). An anatomical study of converging sensory pathways within the cerebral cortex of the monkey. *Brain*, 93(4), 793-820.

- Kaas, J. H., Nelson, R. J., Sur, M., Dykes, R. W., & Merzenich, M. M. (1984). The somatotopic organization of the ventroposterior thalamus of the squirrel monkey, *Saimiri sciureus*. *Journal of comparative neurology*, 226(1), 111-140.
- Kalaska JF, Scott SH, Cisek P, Sergio LE. (1997). Cortical control of reaching movements. *Curr Opin Neurobiol* 7: 849-859.
- Kass, R. E., & Raftery, A. E. (1995). Bayes factors. *Journal of the american statistical association*, 90(430), 773-795.
- Kato, H. K., Asinof, S. K., & Isaacson, J. S. (2017). Network-Level Control of Frequency Tuning in Auditory Cortex. *Neuron*, 95(2), 412-423.e4.  
<https://doi.org/10.1016/j.neuron.2017.06.019>
- Keleş, M. F., & Frye, M. A. (2017). Object-Detecting Neurons in *Drosophila*. *Current Biology*, 27(5), 680–687. <https://doi.org/10.1016/j.cub.2017.01.012>
- Kelly, M. K., Carvell, G. E., Kodger, J. M., & Simons, D. J. (1999). Sensory Loss by Selected Whisker Removal Produces Immediate Disinhibition in the Somatosensory Cortex of Behaving Rats. *Journal of Neuroscience*, 19(20), 9117–9125.  
<https://doi.org/10.1523/JNEUROSCI.19-20-09117.1999>
- Keyson, D. V., & Houtsma, A. J. (1995). Directional sensitivity to a tactile point stimulus moving across the fingerpad. *Perception & Psychophysics*, 57(5), 738-744.
- Kida, T., Tanaka, E., & Kakigi, R. (2018). Adaptive flexibility of the within-hand attentional gradient in touch: An MEG study. *NeuroImage*, 179, 373-384.  
<https://doi.org/10.1016/j.neuroimage.2018.06.063>
- Killebrew, J. H., Bensmaia, S. J., Dammann, J. F., Denchev, P., Hsiao, S. S., Craig, J. C., & Johnson, K. O. (2007). A dense array stimulator to generate arbitrary spatio-temporal tactile stimuli. *Journal of neuroscience methods*, 161(1), 62-74.  
<https://doi.org/10.1016/j.jneumeth.2006.10.012>
- Kilner, J. M., Salenius, S., Baker, S. N., Jackson, A., Hari, R., & Lemon, R. N. (2003). Task-Dependent Modulations of Cortical Oscillatory Activity in Human Subjects during a Bimanual Precision Grip Task. *NeuroImage*, 18(1), 67–73.  
<https://doi.org/10.1006/nimg.2002.1322>
- Kiltner, K., Houborg, C., & Ehrsson, H. H. (2019). Rapid learning and unlearning of predicted sensory delays in self-generated touch. *Elife*, 8, e42888.
- Kitada, R., Kochiyama, T., Hashimoto, T., Naito, E., & Matsumura, M. (2003). Moving tactile stimuli of fingers are integrated in the intraparietal and inferior parietal cortices. *Neuroreport*, 14(5), 719-724.
- Klatzky, R. L., Loomis, J. M., Lederman, S. J., Wake, H., & Fujita, N. (1993). Haptic identification of objects and their depictions. *Perception & psychophysics*, 54(2), 170-178.
- Koffka, K. (1922). Perception: an introduction to the Gestalt-Theorie. *Psychological Bulletin*, 19(10), 531.
- Konkle, T., Wang, Q., Hayward, V., & Moore, C. I. (2009). Motion aftereffects transfer between touch and vision. *Current Biology*, 19(9), 745-750.  
<https://doi.org/10.1016/j.cub.2009.03.035>
- Kozak, M., & Piepho, H. P. (2018). What's normal anyway? Residual plots are more telling than significance tests when checking ANOVA assumptions. *Journal of Agronomy and Crop Science*, 204(1), 86-98. <https://doi.org/10.1111/jac.12220>
- Kuroki, S., Watanabe, J., & Nishida, S. (2017). Integration of vibrotactile frequency information beyond the mechanoreceptor channel and somatotopy. *Scientific Reports*, 7(1), 1–13.  
<https://doi.org/10.1038/s41598-017-02922-7>
- Kuroki, S., Watanabe, J., Kawakami, N., Tachi, S., & Nishida, S. Y. (2010). Somatotopic dominance in tactile temporal processing. *Experimental Brain Research*, 203(1), 51-62.

- Kuroki, S., Watanabe, J., Mabuchi, K., Tachi, S., & Nishida, S. Y. (2012). Directional remapping in tactile inter-finger apparent motion: a motion aftereffect study. *Experimental brain research*, 216(2), 311-320.
- Kusnir, F., Pesin, S., & Landau, A. N. (2020). Hello From the Other Side: Robust Contralateral Interference in Tactile Detection. *bioRxiv*. <https://doi.org/10.1101/2020.07.21.213751>
- Landy, M. S., & Kojima, H. (2001). Ideal cue combination for localizing texture-defined edges. *JOSA A*, 18(9), 2307-2320.
- Lappe, M., Bremmer, F., & Van den Berg, A. V. (1999). Perception of self-motion from visual flow. *Trends in cognitive sciences*, 3(9), 329-336.
- Laskin, S. E., & Spencer, W. A. (1979). Cutaneous masking. II. Geometry of excitatory and inhibitory receptive fields of single units in somatosensory cortex of the cat. *Journal of neurophysiology*, 42(4), 1061-1082. <https://doi.org/10.1152/jn.1979.42.4.1061>
- Lederman, S. J., & Klatzky, R. L. (1993). Extracting object properties through haptic exploration. *Acta psychologica*, 84(1), 29-40.
- Lederman, S. J., & Klatzky, R. L. (2004). Haptic identification of common objects: Effects of constraining the manual exploration process. *Perception & psychophysics*, 66(4), 618-628.
- Li Hegner, Y., Lee, Y., Grodd, W., & Braun, C. (2010). Comparing tactile pattern and vibrotactile frequency discrimination: a human fMRI study. *Journal of neurophysiology*, 103(6), 3115-3122. <https://doi.org/10.1152/jn.00940.2009>
- Lieber, J. D., & Bensmaia, S. J. (2019). High-dimensional representation of texture in somatosensory cortex of primates. *Proceedings of the National Academy of Sciences*, 116(8), 3268-3277. <https://doi.org/10.1073/pnas.1818501116>
- Longo, M. R., & Haggard, P. (2011). Weber's illusion and body shape: anisotropy of tactile size perception on the hand. *Journal of Experimental Psychology: Human Perception and Performance*, 37(3), 720.
- Longo, M. R., Azañón, E., & Haggard, P. (2010). More than skin deep: body representation beyond primary somatosensory cortex. *Neuropsychologia*, 48(3), 655-668. <https://doi.org/10.1016/j.neuropsychologia.2009.08.022>
- Longo, M. R., Azañón, E., & Haggard, P. (2010). More than skin deep: body representation beyond primary somatosensory cortex. *Neuropsychologia*, 48(3), 655-668. <https://doi.org/10.1016/j.neuropsychologia.2009.08.022>
- Loomis, J. M., Klatzky, R. L., & Giudice, N. A. (2012). Sensory substitution of vision: importance of perceptual and cognitive processing. *Assistive technology for blindness and low vision*, 162-191.
- Lopez-Calderon, J., & Luck, S. J. (2014). ERPLAB: An open-source toolbox for the analysis of event-related potentials. *Frontiers in Human Neuroscience*, 8, 213. <https://doi.org/10.3389/fnhum.2014.00213>
- Lotze, H. (1884). *Metaphysic: In Three Books, Ontology, Cosmology, and Psychology* (Vol. 3). Clarendon Press.
- Luck, S. J., & Vogel, E. K. (1997). The capacity of visual working memory for features and conjunctions. *Nature*, 390(6657), 279-281. <https://doi.org/10.1038/36846>
- Lunghi, C., Binda, P., & Morrone, M. C. (2010). Touch disambiguates rivalrous perception at early stages of visual analysis. *Current Biology*, 20(4), R143-R144.
- Lunghi, C., Lo Verde, L., & Alais, D. (2017). Touch accelerates visual awareness. *i-Perception*, 8(1), 2041669516686986.
- Luo, H., Wang, X., Fan, M., Deng, L., Jian, C., Wei, M., & Luo, J. (2018). The effect of visual stimuli on stability and complexity of postural control. *Frontiers in neurology*, 9, 48.
- Makin, T. R., & Bensmaia, S. J. (2017). Stability of sensory topographies in adult cortex. *Trends in cognitive sciences*, 21(3), 195-204. <https://doi.org/10.1016/j.tics.2017.01.002>

- Mancini, F., Bauleo, A., Cole, J., Lui, F., Porro, C. A., Haggard, P., & Iannetti, G. D. (2014). Whole-body mapping of spatial acuity for pain and touch. *Annals of Neurology*, 75(6), 917–924. <https://doi.org/10.1002/ana.24179>
- Mareschal, I., Morgan, M. J., & Solomon, J. A. (2010). Cortical distance determines whether flankers cause crowding or the tilt illusion. *Journal of Vision*, 10(8), 13–13. <https://doi.org/10.1167/10.8.13>
- Marr, David. *Vision: A computational investigation into the human representation and processing of visual information*. MIT press, 2010.
- Martin, M. (1992). Sight and Touch. *In The Contents of Experience: Essays on Perception* (pp. 196– 215). Cambridge UP.
- Matteau, I., Kupers, R., Ricciardi, E., Pietrini, P., & Ptito, M. (2010). Beyond visual, aural and haptic movement perception: hMT+ is activated by electrotactile motion stimulation of the tongue in sighted and in congenitally blind individuals. *Brain research bulletin*, 82(5-6), 264-270.
- Medina, J., & Coslett, H. B. (2010). From maps to form to space: Touch and the body schema. *Neuropsychologia*, 48(3), 645-654.
- Medina, J., McCloskey, M., Coslett, H., & Rapp, B. (2014). Somatotopic representation of location: evidence from the Simon effect. *Journal of Experimental Psychology: Human Perception and Performance*, 40(6), 2131.
- Melzack, R., & Wall, P. D. (1965). Pain mechanisms: a new theory. *Science*, 150(3699), 971-979.
- Meng, F., & Spence, C. (2015). Tactile warning signals for in-vehicle systems. *Accident analysis & prevention*, 75, 333-346.
- Merz, S., Meyerhoff, H. S., Frings, C., & Spence, C. (2020). Representational momentum in vision and touch: Visual motion information biases tactile spatial localization. *Attention, Perception, & Psychophysics*, 1-12.
- Merzenich, M. M., Kaas, J. H., Sur, M., & Lin, C. S. (1978). Double representation of the body surface within cytoarchitectonic area 3b and 1 in "SI" in the owl monkey (*Aotus trivirgatus*). *Journal of Comparative Neurology*, 181(1), 41-73. <https://doi.org/10.1002/cne.901810104>
- Miller, L. E., Montroni, L., Koun, E., Salemme, R., Hayward, V., & Farnè, A. (2018). Sensing with tools extends somatosensory processing beyond the body. *Nature*, 561(7722), 239-242. <https://doi.org/10.1038/s41586-018-0460-0>
- Mirabella, G., Battiston, S., & Diamond, M. E. (2001). Integration of Multiple-whisker Inputs in Rat Somatosensory Cortex. *Cerebral Cortex*, 11(2), 164–170. <https://doi.org/10.1093/cercor/11.2.164>
- Nabokov, V. (1955). *Lolita*. Paris: The Olympia Press
- Nguyen, D., Brown, J., & Alais, D. (2020). Cost of Dual-Task Performance in Tactile Perception Is Greater for Competing Tasks of the Same Type. *Perception*, 49(5), 515-538. <https://doi.org/10.1177/0301006620908778>
- Nguyen, R. H., Forshey, T. M., Holden, J. K., Francisco, E. M., Kirsch, B., Favorov, O., Tommerdahl, M. (2014). Vibrotactile discriminative capacity is impacted in a digit-specific manner with concurrent unattended hand stimulation. *Experimental Brain Research*, 232, 3601–3612. <https://doi.org/10.1007/s00221-014-4045-3>
- Norman, W. D., M. A. Jeeves, A. Milne, and T. Ludwig. "Hemispheric interactions: The bilateral advantage and task difficulty." *Cortex* 28, no. 4 (1992): 623-642.
- O'Shaughnessy, B. (1989). The sense of touch. *Australasian journal of philosophy*, 67(1), 37-58.
- Okamura, A. M. (2009). Haptic feedback in robot-assisted minimally invasive surgery. *Current opinion in urology*, 19(1), 102.
- Olausson, H., Hamadeh, I., Pakdel, P., & Norrsell, U. (1998). Remarkable capacity for perception of the direction of skin pull in man. *Brain research*, 808(1), 120-123.



- Olausson, H., Kakuda, N., & Wessberg, J. (1996). Human mechanoreceptors serving tactile directional sensibility. In *Soc. Neurosci. Abstr.* (Vol. 22, p. 1807).
- Olausson, H., Wessberg, J., & Kakuda, N. (2000). Tactile directional sensibility: peripheral neural mechanisms in man. *Brain research*, *866*(1-2), 178-187.
- Oruç, I., Maloney, L. T., & Landy, M. S. (2003). Weighted linear cue combination with possibly correlated error. *Vision research*, *43*(23), 2451-2468. [https://doi.org/10.1016/S0042-6989\(03\)00435-8](https://doi.org/10.1016/S0042-6989(03)00435-8)
- Ossandón, J. P., König, P., & Heed, T. (2015). Irrelevant tactile stimulation biases visual exploration in external coordinates. *Scientific reports*, *5*(1), 1-11.
- Overvliet, K. E., Azañón, E., & Soto-Faraco, S. (2011). Somatosensory saccades reveal the timing of tactile spatial remapping. *Neuropsychologia*, *49*(11), 3046-3052. <https://doi.org/10.1016/j.neuropsychologia.2011.07.005>
- Overvliet, K. E., Krampe, R. T., & Wagemans, J. (2012). Perceptual grouping in haptic search: The influence of proximity, similarity, and good continuation. *Journal of experimental psychology: Human perception and performance*, *38*(4), 817.
- Overvliet, K. E., Smeets, J. B., & Brenner, E. (2007). Parallel and serial search in haptics. *Perception & Psychophysics*, *69*(7), 1059-1069.
- Overvliet, K. E., Smeets, J. B., & Brenner, E. (2007). Parallel and serial search in haptics. *Perception & Psychophysics*, *69*(7), 1059-1069. <https://doi.org/10.3758/BF03193944>
- Pack, C. C., & Bensmaia, S. J. (2015). Seeing and feeling motion: canonical computations in vision and touch. *PLoS Biol*, *13*(9), e1002271.
- Pack, C. C., Livingstone, M. S., Duffy, K. R., & Born, R. T. (2003). End-stopping and the aperture problem: two-dimensional motion signals in macaque V1. *Neuron*, *39*(4), 671-680.
- Palmer, L. M., Schulz, J. M., Murphy, S. C., Ledergerber, D., Murayama, M., & Larkum, M. E. (2012). The cellular basis of GABAB-mediated interhemispheric inhibition. *Science*, *335*(6071), 989-993.
- Pascual-Leone, A., & Torres, F. (1993). Plasticity of the sensorimotor cortex representation of the reading finger in Braille readers. *Brain*, *116*(1), 39-52. <https://doi.org/10.1093/brain/116.1.39>
- Pawluk, D. T., Adams, R. J., & Kitada, R. (2015). Designing haptic assistive technology for individuals who are blind or visually impaired. *IEEE transactions on haptics*, *8*(3), 258-278.
- Pei, Y. C., & Bensmaia, S. J. (2014). The neural basis of tactile motion perception. *Journal of Neurophysiology*, *112*(12), 3023-3032. <https://doi.org/10.1152/jn.00391.2014>
- Pei, Y. C., Hsiao, S. S., & Bensmaia, S. J. (2008). The tactile integration of local motion cues is analogous to its visual counterpart. *Proceedings of the National Academy of Sciences*, *105*(23), 8130-8135. <https://doi.org/10.1073/pnas.0800028105>
- Pei, Y. C., Hsiao, S. S., Craig, J. C., & Bensmaia, S. J. (2010). Shape invariant coding of motion direction in somatosensory cortex. *PLoS Biol*, *8*(2), e1000305. <https://doi.org/10.1371/journal.pbio.1000305>
- Pei, Y. C., Hsiao, S. S., Craig, J. C., & Bensmaia, S. J. (2011). Neural mechanisms of tactile motion integration in somatosensory cortex. *Neuron*, *69*(3), 536-547. <https://doi.org/10.1016/j.neuron.2010.12.033>
- Pei, Y. C., Lee, T. C., Chang, T. Y., Ruffatto III, D., Spenko, M., & Bensmaia, S. (2014). A multi-digit tactile motion stimulator. *Journal of neuroscience methods*, *226*, 80-87. <https://doi.org/10.1016/j.jneumeth.2014.01.021>
- Penfield, W., & Boldrey, E. (1937). Somatic motor and sensory representation in the cerebral cortex of man as studied by electrical stimulation. *Brain*, *60*(4), 389-443.
- Pérez-Bellido, A., Pappal, R. D., & Yau, J. M. (2018). Touch engages visual spatial contextual processing. *Scientific reports*, *8*(1), 1-9.

- Perquin, M. N., Taylor, M., Lorusso, J., & Kolasinski, J. (2020). Directional biases in whole hand motion perception revealed by mid-air tactile stimulation. *bioRxiv*.  
<https://doi.org/10.1101/2020.04.23.058024>
- Piras, A., Raffi, M., Perazzolo, M., & Squatrito, S. (2018). Influence of heading perception in the control of posture. *Journal of Electromyography and Kinesiology*, *39*, 89-94.
- Plaisier, M. A., Tiest, W. M. B., & Kappers, A. M. (2009). One, two, three, many—Subitizing in active touch. *Acta psychologica*, *131*(2), 163-170.
- Plaisier, M. A., Tiest, W. M. B., & Kappers, A. M. (2010). Grabbing subitizing with both hands: bimanual number processing. *Experimental Brain Research*, *202*(2), 507-512.
- Pleger, B., & Villringer, A. (2013). The human somatosensory system: from perception to decision making. *Progress in neurobiology*, *103*, 76-97.
- Pruszynski, J. A., & Johansson, R. S. (2014). Edge-orientation processing in first-order tactile neurons. *Nature neuroscience*, *17*(10), 1404-1409. <https://doi.org/10.1038/nn.3804>
- Pruszynski, J. A., Flanagan, J. R., & Johansson, R. S. (2018). Fast and accurate edge orientation processing during object manipulation. *Elife*, *7*, e31200.  
<https://doi.org/10.7554/eLife.31200>
- Raffi, M., & Piras, A. (2019). Investigating the crucial role of optic flow in postural control: central vs. peripheral visual field. *Applied Sciences*, *9*(5), 934.
- Raffi, M., Piras, A., Persiani, M., & Squatrito, S. (2014). Importance of optic flow for postural stability of male and female young adults. *European journal of applied physiology*, *114*(1), 71-83.
- Raffi, M., Piras, A., Persiani, M., Perazzolo, M., & Squatrito, S. (2017). Angle of gaze and optic flow direction modulate body sway. *Journal of Electromyography and Kinesiology*, *35*, 61-68.
- Rahman, M. S., & Yau, J. M. (2019). Somatosensory interactions reveal feature-dependent computations. *Journal of Neurophysiology*, *122*(1), 5–21.  
<https://doi.org/10.1152/jn.00168.2019>
- Reed, J. L., Pouget, P., Qi, H.-X., Zhou, Z., Bernard, M. R., Burish, M. J., Haitas, J., Bonds, A. B., & Kaas, J. H. (2008). Widespread spatial integration in primary somatosensory cortex. *Proceedings of the National Academy of Sciences*, *105*(29), 10233–10237.  
<https://doi.org/10.1073/pnas.0803800105>
- Reed, J. L., Qi, H. X., & Kaas, J. H. (2011). Spatiotemporal properties of neuron response suppression in owl monkey primary somatosensory cortex when stimuli are presented to both hands. *Journal of Neuroscience*, *31*(10), 3589-3601.  
<https://doi.org/10.1523/JNEUROSCI.4310-10.2011>
- Reinacher, M., Becker, R., Villringer, A., & Ritter, P. (2009). Oscillatory brain states interact with late cognitive components of the somatosensory evoked potential. *Journal of neuroscience methods*, *183*(1), 49-56.
- Reynolds, J. H. , & Heeger, D. J. (2009). The normalization model of attention. *Neuron* , *61*(2), 168–185. <https://doi.org/10.1016/j.neuron.2009.01.002>
- Ricciardi, E., Vanello, N., Sani, L., Gentili, C., Scilingo, E. P., Landini, L., ... & Pietrini, P. (2007). The effect of visual experience on the development of functional architecture in hMT+. *Cerebral Cortex*, *17*(12), 2933-2939.
- Riggs, K. J., Ferrand, L., Lancelin, D., Fryziel, L., Dumur, G., & Simpson, A. (2006). Subitizing in tactile perception. *Psychological Science*. *17*(4), 271–272. <https://doi.org/10.1111/j.1467-9280.2006.01696.x>
- Rinker, M. A., & Craig, J. C. (1994). The effect of spatial orientation on the perception of moving tactile stimuli. *Perception & Psychophysics*, *56*(3), 356-362.
- Röder, B., Spence, C., & Rösler, F. (2002). Assessing the effect of posture change on tactile inhibition-of-return. *Experimental brain research*, *143*(4), 453-462.

- Rohde, M., van Dam, L. C., & Ernst, M. O. (2016). Statistically optimal multisensory cue integration: a practical tutorial. *Multisensory research*, 29(4-5), 279-317.
- Rouder, J. N., Morey, R. D., Speckman, P. L., & Province, J. M. (2012). Default Bayes factors for ANOVA designs. *Journal of Mathematical Psychology*, 56(5), 356-374.
- Ruben, J., Schwiemann, J., Deuchert, M., Meyer, R., Krause, T., Curio, G., ... & Villringer, A. (2001). Somatotopic organization of human secondary somatosensory cortex. *Cerebral cortex*, 11(5), 463-473.
- Rubin, P. (2019). Exclusive: A Deeper Look at the PlayStation 5. *Wired*.  
<https://www.wired.com/story/exclusive-playstation-5/>
- Saal, H. P., & Bensmaia, S. J. (2014). Touch is a team effort: interplay of submodalities in cutaneous sensibility. *Trends in neurosciences*, 37(12), 689-697.  
<https://doi.org/10.1016/j.tins.2014.08.012>
- Sachdev, R. N. S., Krause, M. R., & Mazer, J. A. (2012). Surround suppression and sparse coding in visual and barrel cortices. *Frontiers in Neural Circuits*, 6.  
<https://doi.org/10.3389/fncir.2012.00043>
- Sainburg RL, Ghilardi MF, Poizner H, Ghez C. Control of limb dynamics in normal subjects and patients without proprioception. *Journal of neurophysiology*, 73: 820-835, 1006 1995.
- Sakata, H., Takaoka, Y., Kawarasaki, A., & Shibutani, H. (1973). Somatosensory properties of neurons in the superior parietal cortex (area 5) of the rhesus monkey. *Brain research*, 64, 85-102.
- Schnitzler, A., Salmelin, R., Salenius, S., Jousmäki, V., & Hari, R. (1995). Tactile information from the human hand reaches the ipsilateral primary somatosensory cortex. *Neuroscience letters*, 200(1), 25-28.
- Schweizer, M. Maier, C. Braun, N. Birbaumer, R. (2000). Distribution of mislocalizations of tactile stimuli on the fingers of the human hand. *Somatosensory & Motor Research*, 17(4), 309-316.
- Seelke AMH, Padberg J, Disbrow E, Purnell SM, Recanzone G, Krubitzer LA. (2012). Topographic maps within Brodmann's area 5 of macaque monkeys. *Cereb Cortex* 22: 1834-1850.
- Serino, A., & Haggard, P. (2010). Touch and the body. *Neuroscience & Biobehavioral Reviews*, 34(2), 224-236. <https://doi.org/10.1016/j.neubiorev.2009.04.004>
- Serino, A., Giovagnoli, G., de Vignemont, F., & Haggard, P. (2008). Spatial organisation in passive tactile perception: Is there a tactile field?. *Acta psychologica*, 128(2), 355-360.
- Serino, A., Padiglioni, S., Haggard, P., & Làdavas, E. (2009). Seeing the hand boosts feeling on the cheek. *Cortex*, 45(5), 602-609. <https://doi.org/10.1016/j.cortex.2008.03.008>
- Severens, M., Farquhar, J., Desain, P., Duysens, J., & Gielen, C. (2010). Transient and steady-state responses to mechanical stimulation of different fingers reveal interactions based on lateral inhibition. *Clinical Neurophysiology*, 121(12), 2090–2096.  
<https://doi.org/10.1016/j.clinph.2010.05.016>
- Sherrick, C. E. (1964). Effects of Double Simultaneous Stimulation of the Skin. *The American Journal of Psychology*, 77(1), 42–53. *JSTOR*. <https://doi.org/10.2307/1419270>
- Shuler, M. G., Krupa, D. J., & Nicolelis, M. A. (2001). Bilateral integration of whisker information in the primary somatosensory cortex of rats. *Journal of Neuroscience*, 21(14), 5251-5261.
- Snyder, L. H., Batista, A. P., & Andersen, R. A. (1997). Coding of intention in the posterior parietal cortex. *Nature*, 386(6621), 167-170.
- Solomon, J. A. (2020). Five dichotomies in the psychophysics of ensemble perception. *Attention, Perception, & Psychophysics*. <https://doi.org/10.3758/s13414-020-02027-w>
- Soto-Faraco, S., & Azañón, E. (2013). Electrophysiological correlates of tactile remapping. *Neuropsychologia*, 51(8), 1584-1594.
- Soto-Faraco, S., Kvasova, D., Biau, E., Ikumi, N., Ruzzoli, M., Morís-Fernández, L., & Torralba, M. (2019). *Multisensory interactions in the real world*. Cambridge University Press.

- Soto-Faraco, S., Ronald, A., & Spence, C. (2004). Tactile selective attention and body posture: Assessing the multisensory contributions of vision and proprioception. *Perception & Psychophysics*, 66(7), 1077–1094. <https://doi.org/10.3758/BF03196837>
- Spence, C. (2014). The skin as a medium for sensory substitution. *Multisensory research*, 27(5-6), 293-312.
- Spence, C., & Gallace, A. (2007). Recent developments in the study of tactile attention. *Canadian Journal of Experimental Psychology/Revue canadienne de psychologie expérimentale*, 61(3), 196. <https://doi.org/10.1037/cjep2007021>
- Spence, C., & Walton, M. (2005). On the inability to ignore touch when responding to vision in the crossmodal congruency task. *Acta psychologica*, 118(1-2), 47-70.
- Spence, C., Pavani, F., & Driver, J. (2004). Spatial constraints on visual-tactile cross-modal distractor congruency effects. *Cognitive, Affective, & Behavioral Neuroscience*, 4(2), 148-169.
- Stephani, T., Waterstraat, G., Haufe, S., Curio, G., Villringer, A., & Nikulin, V. (2020). Temporal signatures of criticality in human cortical excitability as probed by early somatosensory responses. *Journal of Neuroscience*, 40(34), 6572–6583. <https://doi.org/10.1523/JNEUROSCI.0241-20.2020>
- Stowe, T. (2017). What is the Nintendo Switch's Haptic Feedback/ HD Rumble?. *Consoledeals*. <https://www.console-deals.com/advice/nintendo-switch-haptic-feedback-hd-rumble/>
- Sutherland, M. T., & Tang, A. C. (2006). Reliable detection of bilateral activation in human primary somatosensory cortex by unilateral median nerve stimulation. *Neuroimage*, 33(4), 1042-1054. <https://doi.org/10.1016/j.neuroimage.2006.08.015>
- Suzuishi, Y., Hidaka, S., & Kuroki, S. (2020). Visual motion information modulates tactile roughness perception. *Scientific Reports*, 10(1), 1-10.
- Talsma, D., & Woldorff, M. G. (2005). Selective attention and multisensory integration: multiple phases of effects on the evoked brain activity. *Journal of Cognitive Neuroscience*, 17 (7), 1098–1114. <https://doi-org.libproxy.ucl.ac.uk/10.1162/0898929054475172>
- Tamè, L., & Holmes, N. P. (2016). Involvement of human primary somatosensory cortex in vibrotactile detection depends on task demand. *NeuroImage*, 138, 184-196.
- Tamè, L., Azañón, E., & Longo, M. R. (2019). A conceptual model of tactile processing across body features of size, shape, side, and spatial location. *Frontiers in psychology*, 10, 291.
- Tamè, L., Braun, C., Holmes, N. P., Farnè, A., & Pavani, F. (2016). Bilateral representations of touch in the primary somatosensory cortex. *Cognitive Neuropsychology*, 33(1-2), 48-66. <https://doi.org/10.1080/02643294.2016.1159547>
- Tamè, L., Farnè, A., & Pavani, F. (2011). Spatial coding of touch at the fingers: Insights from double simultaneous stimulation within and between hands. *Neuroscience Letters*, 487(1), 78–82. <https://doi.org/10.1016/j.neulet.2010.09.078>
- Tamè, L., Moles, A., & Holmes, N. P. (2014). Within, but not between hands interactions in vibrotactile detection thresholds reflect somatosensory receptive field organization. *Frontiers in Psychology*, 5. <https://doi.org/10.3389/fpsyg.2014.00174>
- Tamè, L., Pavani, F., Papadelis, C., Farne, A., & Braun, C. (2015). Early integration of bilateral touch in the primary somatosensory cortex. *Human brain mapping*, 36(4), 1506-1523.
- Tan, H. Z., Barbagli, F., Salisbury, J. K., Ho, C., & Spence, C. (2006). Force-direction discrimination is not influenced by reference force direction (short paper). <http://hdl.handle.net/1773/34894>
- Tommerdahl, M., Simons, S. B., Chiu, J. S., Favorov, O., & Whitsel, B. (2005). Response of SI cortex to ipsilateral, contralateral and bilateral flutter stimulation in the cat. *BMC neuroscience*, 6(1), 1-14.

- Urban, N. N. (2002). Lateral inhibition in the olfactory bulb and in olfaction. *Physiology & Behavior*, 77(4), 607–612. [https://doi.org/10.1016/S0031-9384\(02\)00895-8](https://doi.org/10.1016/S0031-9384(02)00895-8)
- Vallbo, A. B., & Johansson, R. S. (1984). Properties of cutaneous mechanoreceptors in the human hand related to touch sensation. *Hum neurobiol*, 3(1), 3-14.
- Van Der Burg, E. , Olivers, C. N. L. , Bronkhorst, A. W. , & Theeuwes, J. (2008). Pip and pop: nonspatial auditory signals improve spatial visual search. *Journal of Experimental Psychology: Human Perception and Performance*, 34 (5), 1053–65. <https://doi-org.libproxy.ucl.ac.uk/10.1037/0096-1523.34.5.1053>
- Van Kemenade, B. M., Seymour, K., Wacker, E., Spitzer, B., Blankenburg, F., & Sterzer, P. (2014). Tactile and visual motion direction processing in hMT+/V5. *Neuroimage*, 84, 420-427.
- Vergassola, M., Villermaux, E., & Shraiman, B. I. (2007). ‘Infotaxis’ as a strategy for searching without gradients. *Nature*, 445(7126), 406-409. <https://doi.org/10.1038/nature05464>
- von Békésy, G. (1967). Mach band type lateral inhibition in different sense organs. *The Journal of general physiology*, 50(3), 519-532.
- Vroomen, J. , Bertelson, P. , & de Gelder, B. (2001). Directing spatial attention towards the illusory location of a ventriloquized sound. *Acta Psychologica*, 108 (1), 21–33. [https://doi-org.libproxy.ucl.ac.uk/10.1016/S0001-6918\(00\)00068-8](https://doi-org.libproxy.ucl.ac.uk/10.1016/S0001-6918(00)00068-8)
- Wacker, E., Spitzer, B., Lützkendorf, R., Bernarding, J., & Blankenburg, F. (2011). Tactile motion and pattern processing assessed with high-field fMRI. *PLoS one*, 6(9), e24860.
- Wagenmakers, E. J., Love, J., Marsman, M., Jamil, T., Ly, A., Verhagen, J., ... & Morey, R. D. (2018b). Bayesian inference for psychology. Part II: Example applications with JASP. *Psychonomic bulletin & review*, 25(1), 58-76.
- Wagenmakers, E. J., Marsman, M., Jamil, T., Ly, A., Verhagen, J., Love, J., ... & Morey, R. D. (2018a). Bayesian inference for psychology. Part I: Theoretical advantages and practical ramifications. *Psychonomic bulletin & review*, 25(1), 35-57.
- Walsh, L., Critchlow, J., Beck, B., Cataldo, A., de Boer, L., & Haggard, P. (2016). Salience-driven overestimation of total somatosensory stimulation. *Cognition*, 154, 118–129. <https://doi.org/10.1016/j.cognition.2016.05.006>
- Wani, Y. R., Convento, S., & Yau, J. M. (2020). Online and offline influences of vision on bimanual tactile spatial perception. *PsyArXiv*. [10.31234/osf.io/c28ub](https://doi.org/10.31234/osf.io/c28ub)
- Warren, W. H., Kay, B. A., Zosh, W. D., Duchon, A. P., & Sahuc, S. (2001). Optic flow is used to control human walking. *Nature neuroscience*, 4(2), 213-216.
- Watamaniuk, S. N. J., & McKee, S. P. (1998). Simultaneous encoding of direction at a local and global scale. *Perception & Psychophysics*, 60(2), 191–200. <https://doi.org/10.3758/BF03206028>
- Watamaniuk, S. N. J., Sekuler, R., & Williams, D. W. (1989). Direction perception in complex dynamic displays: The integration of direction information. *Vision Research*, 29(1), 47–59. [https://doi.org/10.1016/0042-6989\(89\)90173-9](https://doi.org/10.1016/0042-6989(89)90173-9)
- Weber, E. H. (1996). De subtilitate tactus (H. E. Ross, ). In H. E. Ross & D. J. Murray ( ), E. H. Weber on the tactile senses, 2<sup>nd</sup> ed (pp. 21–128). London: Academic Press. (Original work published 1834)
- Wehr, M., & Zador, A. M. (2003). Balanced inhibition underlies tuning and sharpens spike timing in auditory cortex. *Nature*, 426(6965), 442–446. <https://doi.org/10.1038/nature02116>
- Weinstein, S. (1968). Intensive and Extensive Aspects of Tactile Sensitivity as a Function of Body Part, Sex and Laterality. In *The Skin Senses*. Springfield, Ill: Thomas.
- Welch, R. B., & Warren, D. H. (1980). Immediate perceptual response to intersensory discrepancy. *Psychological bulletin*, 88(3), 638.
- Wertheimer, M. (1923). Untersuchungen zur Lehre von der Gestalt. II. *Psychologische forschung*, 4(1), 301-350.

- Whitney, D., & Yamanashi Leib, A. (2018). Ensemble Perception. *Annual Review of Psychology*, 69(1), 105–129. <https://doi.org/10.1146/annurev-psych-010416-044232>
- Wilimzig, C., Ragert, P., & Dinse, H. R. (2012). Cortical topography of intracortical inhibition influences the speed of decision making. *Proceedings of the National Academy of Sciences*, 109(8), 3107–3112. <https://doi.org/10.1073/pnas.1114250109>
- Wolbers, T., Klatzky, R. L., Loomis, J. M., Wutte, M. G., & Giudice, N. A. (2011). Modality-independent coding of spatial layout in the human brain. *Current Biology*, 21(11), 984–989.
- Wolman, D. (2012). The split brain: a tale of two halves. *Nature News*, 483(7389), 260.
- Yamamoto, S., & Kitazawa, S. (2001). Reversal of subjective temporal order due to arm crossing. *Nature neuroscience*, 4(7), 759–765.
- Yang, S. C. H., Wolpert, D. M., & Lengyel, M. (2016). Theoretical perspectives on active sensing. *Current opinion in behavioral sciences*, 11, 100–108. <https://doi.org/10.1016/j.cobeha.2016.06.009>
- Yau, J. M., DeAngelis, G. C., & Angelaki, D. E. (2015). Dissecting neural circuits for multisensory integration and crossmodal processing. *Philosophical Transactions of the Royal Society B: Biological Sciences*, 370(1677), 20140203. <https://doi.org/10.1098/rstb.2014.0203>
- Yau, J. M., Kim, S. S., Thakur, P. H., & Bensmaia, S. J. (2016). Feeling form: the neural basis of haptic shape perception. *Journal of neurophysiology*, 115(2), 631–642.
- Yau, J. M., Pasupathy, A., Fitzgerald, P. J., Hsiao, S. S., & Connor, C. E. (2009). Analogous intermediate shape coding in vision and touch. *Proceedings of the National Academy of Sciences*, 106(38), 16457–16462.
- Yokoi, M., Mori, K., & Nakanishi, S. (1995). Refinement of odor molecule tuning by dendrodendritic synaptic inhibition in the olfactory bulb. *Proceedings of the National Academy of Sciences*, 92(8), 3371–3375. <https://doi.org/10.1073/pnas.92.8.3371>
- Zangaladze, A., Epstein, C. M., Grafton, S. T., & Sathian, K. (1999). Involvement of visual cortex in tactile discrimination of orientation. *Nature*, 401(6753), 587–590.
- Ziat, M., Hayward, V., Chapman, C. E., Ernst, M. O., & Lenay, C. (2010). Tactile suppression of displacement. *Experimental brain research*, 206(3), 299–310.
- Zohary, E., Shadlen, M. N., & Newsome, W. T. (1994). Correlated neuronal discharge rate and its implications for psychophysical performance. *Nature*, 370(6485), 140–143. <https://doi.org/10.1038/370140a0>

## **Appendix A: Supplementary material for Chapter 6**

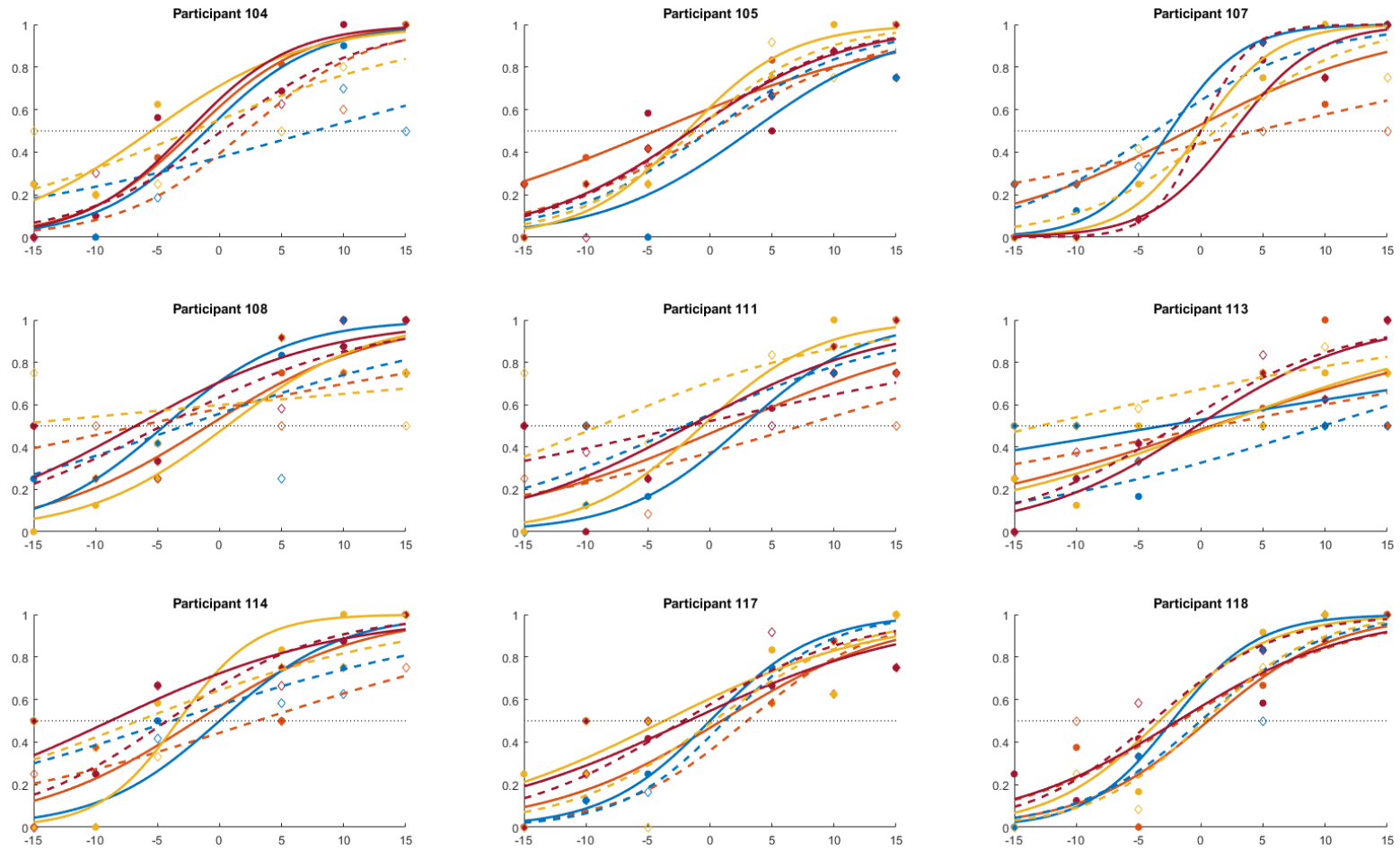


**Figure A. 1. Experiment 7: psychometric fits from included participants.** Nine participants who were included in the main analysis. Each curve corresponds to one of eight conditions, data points correspond to the mean response in the particular condition for each stimulus direction.



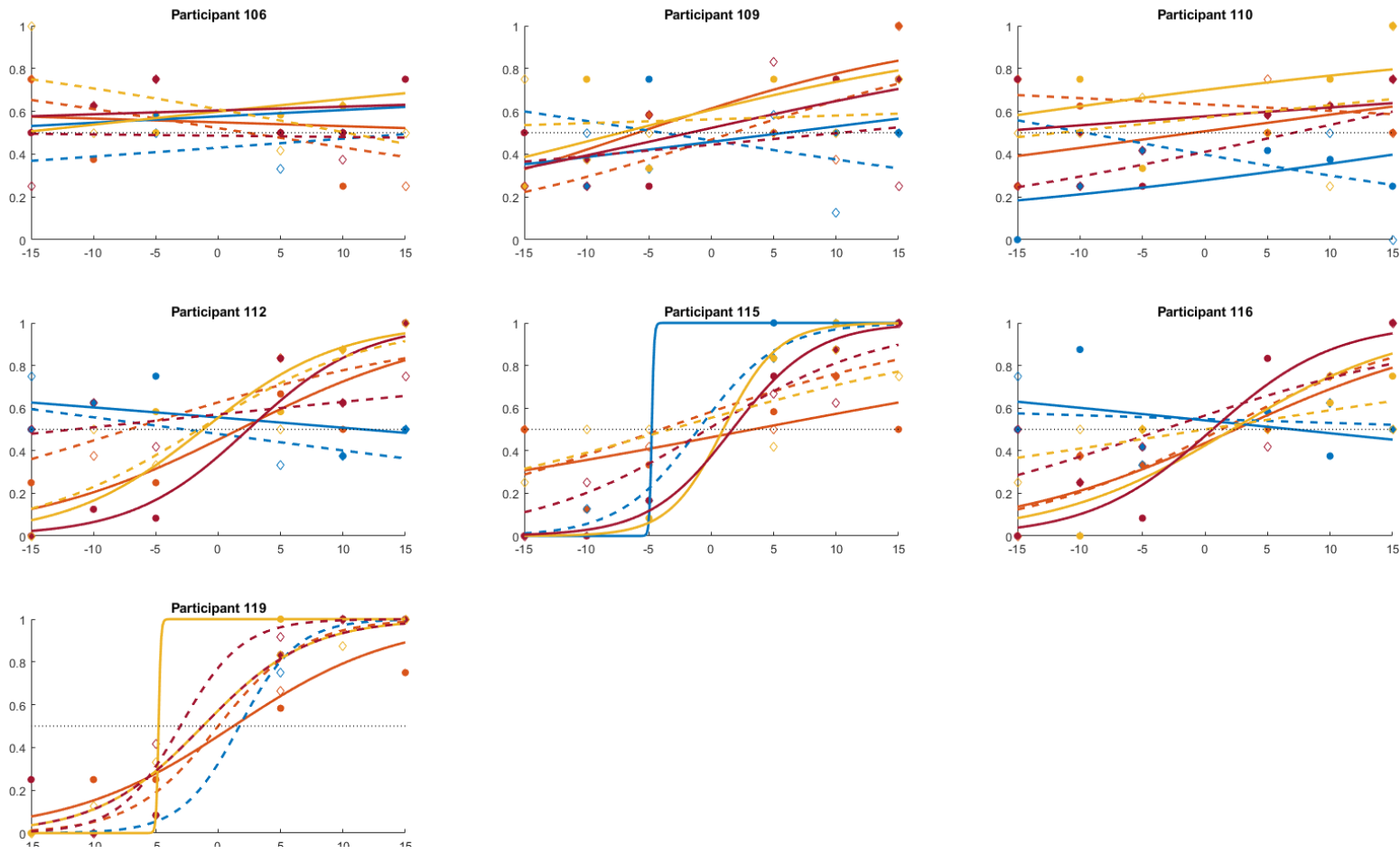


**Figure A. 2. Experiment 7: psychometric fits from excluded participants.** Seven participants who were excluded from the main analysis because the psychometric plots in at least one of eight conditions showed either negative or nonlinear slopes.

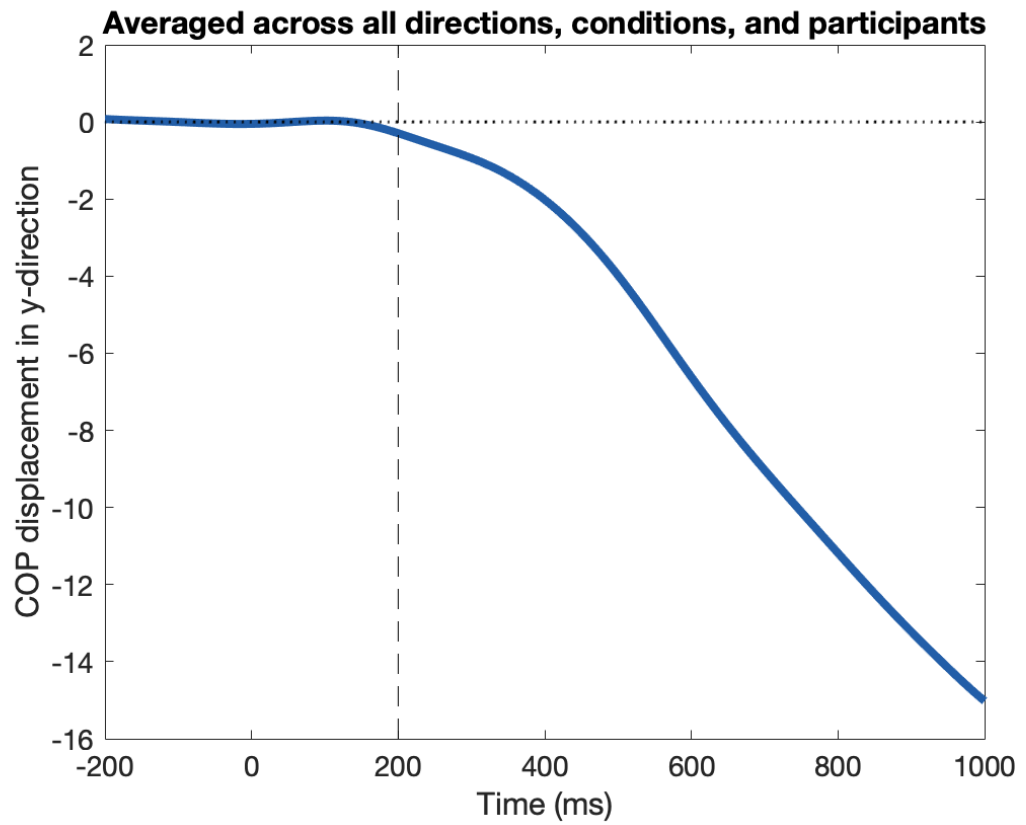


**Figure A. 3. Pooled COP in y-dimension.** COP displacement in y-dimension averaged across all directions, conditions, and participants in order to determine the start time of displacement, which was approximately 200 ms after the onset of the stimulus.